Process studies of the biological pump of carbon dioxide in the North Sea and Southern Ocean

Yann Bozec

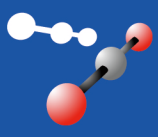

Process studies of the biological pump of carbon dioxide in the North Sea and Southern Ocean

The research reported in this thesis was carried out at the Department of Marine Chemistry and Geology of the Royal Netherlands Institute for Sea Research (NIOZ), Postbus 59, 1790 AB Den Burg, Texel, The Netherlands.

Cover Design: Monsieur Serk

Printed by: Printon Trükikoda AS

ISBN: 90 367 2358 2

RIJKSUNIVERSITEIT GRONINGEN

Process studies of the biological pump of carbon dioxide in the North Sea and Southern Ocean

Proefschrift

ter verkrijging van het doctoraat in de
Wiskunde en Natuurwetenschappen
aan de Rijksuniversiteit Groningen
op gezag van de
Rector Magnificus, dr.F. Zwarts,
in het openbaar te verdedigen op
maandag 3 oktober 2005
om 14:45 uur

door

Yann Bozec

geboren op 27 december 1977
te Morlaix, Frankrijk

Promotores:	Prof. dr ir H.J.W. de Baar Prof. dr H. Thomas
Beoordelingscommissie:	Prof. dr L. Anderson Prof. dr J.J. Middelburg Prof. dr J-P. Gattuso

à mes parents…

Contents

Chapter 1

Introduction and Objectives

The current increase of carbon dioxide (CO_2) in the atmosphere, and its possible consequences for climate change, have led to more scientific interest in the global carbon cycle. This thesis deals with the role of the oceans in the global carbon cycle, with emphasis on two key regions: the North Sea as a case study of coastal seas, and the Southern Ocean.

1. The natural and enhanced greenhouse effect

The greenhouse effect is related to the Earth's radiation balance. About 45% of the solar radiative energy incoming at the top of the atmosphere is absorbed by the surface of the Earth. The solar energy absorbed by the Earth's surface is re-emitted as infrared radiation (long-wave radiation, 8-13 μm) and about 55% of this radiative energy is absorbed in the lower atmosphere (first 10-15 km, *i.e.* troposphere) by various gases and water vapour. It is then either released as heat or re-emitted as infrared radiation towards the surface of the earth. This natural greenhouse effect by trace gases and water vapour, warms the surface of the earth and the troposphere by about 33 ^{o}C and thus maintains favourable conditions for life on the planet (without the greenhouse effect the planetary surface temperature would be -18 ^{o}C). Natural atmospheric gases such as water vapour (H_2O), carbon dioxide (CO_2), tropospheric ozone (O_3), methane (CH_4) and nitrous oxide (N_2O) as well as anthropogenic atmospheric gases such as chlorofluorocarbons (CCl_3F and CCl_2F_2), that absorb outgoing infrared radiation, are called greenhouse gases.

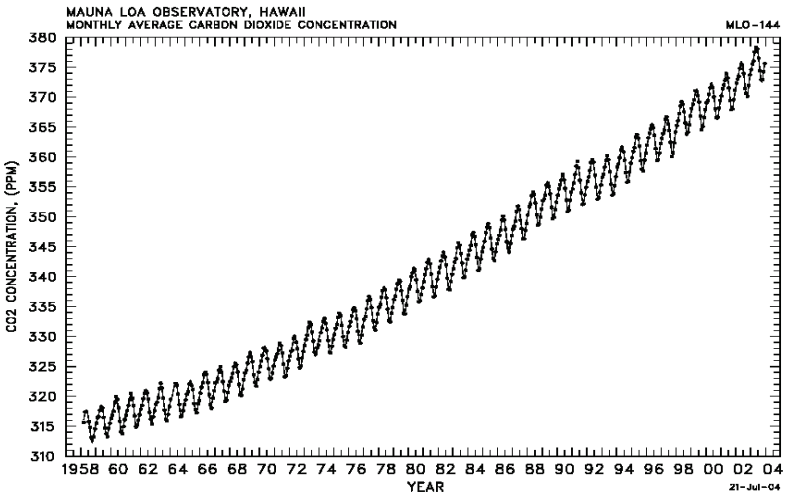

Figure 1: *Evolution of atmospheric carbon dioxide since 1958 to present at Mauna Loa site (Hawaii) from Keeling and Whorf (2004).*
Available on internet at http://cdiac.esd.ornl.gov/trends/co2/sio-mlo.htm.

In 1957 Dave C.D. Keeling from Scripps Institute of Oceanography started the well-known time series of atmospheric CO_2 measurements at Mauna Loa, Hawaii, far away from local industrial sources (Keeling, 1960). The first values of about 315 μatm were rapidly rising at a rate of ~2 μatm yr^{-1} (Keeling and Whorf, 1999). Soon, this rise was attributed to the burning of fossil fuels by mankind. Nowadays in 2005 the values are approaching 380 μatm and continue to rise (Keeling and Whorf, 2004) (Figure 1).

In order to know what the natural CO_2 was in the atmosphere before the onset of the Industrial Revolution, many efforts and approaches to reconstruct the past CO_2 have been conducted (for overview see Gammon et al., 1985). Eventually, the drilling of ice-cores at Greenland and Antarctica provided well-preserved records of CO_2 in air bubbles enclosed within the ice (Petit et al., 1997). Ice cores collected in regions with high precipitation (snow which in the upper ~0.5 m rapidly converts to ice with gas bubble enclosures) have proven that over the preceding ~1000 years, and ~10,000 years, of the Holocene, the CO_2 in air was quite constant at ~280$\pm$3 μatm (Petit et al., 1999). Then, from 1780 A.D. onwards, it increased rapidly, and from 1957 onwards, the ice core record perfectly overlaps with the Anthropocene atmospheric record of Keeling (Keeling et al., 1989). Moreover, by deep ice drilling at central Antarctica where is very little precipitation, ice cores with lower resolution but very long records were obtained, first over the past ~160,000 yr (Barnola et al., 1987), next over the past ~420,000 yr (Petit et al., 1999) and recently over the past 740,000 yr (EPICA, 2004). The first cores showed regular oscillation of atmospheric CO_2 over the well-known 100,000 yr glacial/interglacial cycle, with minima and maxima of ~190 and 290 μatm. For the recent 740,000 yr ice core, 8 complete glacial/interglacial cycles were shown (EPICA, 2004). Its air bubbles record has not yet been completely analyzed, but preliminary CO_2 results thus far confirm the oscillations and minima/maxima of the previous cores. The regular CO_2 oscillations are correlating with the temperature record as derived from stable isotope signals in the ice. This shows a minimum local temperature at the Vostok drilling site which is ~6-7 ^oC below the interglacial or "warm" periods like the modern Holocene interglacial era.

Summarizing the above, the atmospheric CO_2 value of today (~375 μatm) is ~100 μatm higher than the past 10,000 yr Holocene. This rise is the same magnitude (~100 μatm), but beyond, the regular oscillation between 190 and 290 μatm over the past >420,000 yr (Petit et al., 1999). Latter oscillation co-varying with a ~6-7 ^oC warming and cooling, there is concern that the current 100 μatm excess CO_2 will give rise to an excessive global warming of similar magnitude because of the anthropogenic enhancement of the greenhouse effect.

Currently we know that several other greenhouse gases also are increasing due to activity of mankind (CH_4, N_2O, CCl_3F and CCl_2F_2). Because of the much more important global warming effect of CO_2 compared to other increasing greenhouse gases, many investigations have been focused on the CO_2 in context of the global carbon cycle.

2. Ocean Carbon Cycle

2.1 Main reservoirs of the Global Carbon Cycle

Towards unravelling the fate of the anthropogenic CO_2 and related global warming, it is important to identify the major reservoirs involved in the natural global carbon cycle. The data presented in Table 1, mainly focus on the oceanic reservoirs and are based on the review articles by Gruber et al. (2004) and Sabine et al. (2004b).

Table 1: *Relevant reservoirs for the global carbon cycle in Peta grams of Carbon (Pg C) (1 Pg C = 1 Gt C = 10^{15} g C) for the 1980s and 1990s based on Gruber et al. (2004) and Sabine et al. (2004b). Inventories (Pg C) of DIC = Dissolved Inorganic Carbon; DOC = Dissolved Organic Carbon and POC = Particulate Organic Carbon.*

Reservoir		Pg C
Atmosphere		751
Ocean	Surface waters	915 DIC + 3 POC + 25 DOC
	Deep and intermediate waters	37195 DIC + 700 DOC
Terrestrial biosphere	Soils	3150
	Plants	650
Lithosphere	Limestone	60×10^6
	Organic carbon	15×10^6
	Recoverable fossil fuels	4×10^3

The sediment reservoirs of both limestone and organic carbon are by far the largest carbon reservoirs but on a time-scale of 100 years these carbon reservoirs are not expected to react to an additional input of atmospheric CO_2. The actual atmospheric content of 751 PgC comprises a natural background component as well as an increasing anthropogenic component. Latter is due to the airborne fraction (about 60%) of the emissions by mankind in past 200 years through net deforestation, the burning of fossil fuels and cement making (see below section 3). Among the "reactive" carbon reservoirs, the deep ocean is the largest and holds about 50 times more carbon than the atmosphere. Some 98% of this carbon in seawater is in the pool of dissolved inorganic carbon (DIC), this pool is also increasing, because part (~40%) of anthropogenic CO_2 emissions into the air is absorbed by the ocean.

2.2 Chemistry of the Dissolved Inorganic Carbon in seawater

In order to understand the role of the oceans in the carbon cycle, it is necessary to define the DIC pool in seawater. Here, based on the extensive descriptions by Skirrow, (1975); Millero (1995); DOE (1997); Zeebe and Wolf-Gladrow (2001), we define and summarize the relevant parameters of the inorganic carbon chemistry in seawater used in the different chapters of this thesis. For a recent and most detailed overview of the CO_2 system in seawater the reader should refer to Zeebe and Wolf-Gladrow (2001).
Exchange of the CO_2 gas occurs at the air-sea interface. The gaseous CO_2 reacts with the water to form the unstable carbonic acid (H_2CO_3), which further dissociates. Dissolved inorganic carbon, also called in literature total CO_2 (C_T, TCO_2) is the sum of the dissolved inorganic species in seawater:

$$DIC = [CO_2(aq)] + [H_2CO_3] + [HCO_3^-] + [CO_3^{2-}] \quad (1\text{-}1)$$

where brackets represent total stoichiometric concentrations. Direct measurement of DIC is in molar units ($\mu mol\ L^{-1}$), then converted to molality ($\mu mol\ kg^{-1}$ seawater) as to avoid density change of seawater with increasing depth (pressure) in seawater. The bicarbonate (HCO_3^-) ion constitutes about 90% of the overall DIC pool. The carbonate (CO_3^{2-}) ion is in the order of 9%, free carbon dioxide ($CO_2(aq)$) of 1% and carbonic acid of 0.001%. Since the concentration of H_2CO_3 is much smaller than that of $CO_2(aq)$, the sum of the two electrically neutral forms, carbonic acid, H_2CO_3, and aqueous carbon dioxide, $CO_2(aq)$, which are chemically not separable, is usually denoted by CO_2:

$$[CO_2] = [CO_2(aq)] + [H_2CO_3] \quad (1\text{-}2)$$

Note that this notation will be used in the following equations. This gives the following relative proportions:

$$[CO_2] : [HCO_3^-] : [CO_3^{2-}] \approx 1 : \approx 90 : \approx 9 \quad (1\text{-}3)$$

In thermodynamic equilibrium with gaseous carbon dioxide ($CO_2(g)$)

$$CO_2(g) \longleftrightarrow [CO_2] \quad (1\text{-}4)$$

the concentration of CO_2 in seawater is given by the Henry's law formula:

$$[CO_2] = K'_0\,(S,T) \times fCO_2 \quad (1\text{-}5)$$

where the solubility coefficient of CO_2 in seawater (K'_0) depends on temperature (T) and salinity (S) (Weiss, 1974) and fCO_2 (μatm) is the fugacity of CO_2. The partial pressure of CO_2 (pCO_2) can be used after correction for non-ideal behaviour of the gas mixture in the air with the fugacity coefficient γ using the following equation:

$$fCO_2 = \gamma \times pCO_2 \qquad (1\text{-}6).$$

The three inorganic carbon species in the seawater are in thermodynamic equilibrium according to the following equations:

$$CO_2 + H_2O \xleftrightarrow{K_1} HCO_3^- + H^+ \xleftrightarrow{K_2} CO_3^{2-} + H^+ \qquad (1\text{-}7)\text{-}(1\text{-}8)$$

where K_1 and K_2 are the first and second dissociation constants of carbonic acid, respectively. These equilibria are the natural buffer for the pH of seawater, which therefore is very constant ≈ 8.1 in surface waters. For the description of the carbonate system in seawater, stoichiometric equilibrium constants, which are related to concentrations, are used:

$$K_1^* = [HCO_3^-][H^+]/[CO_2] \qquad (1\text{-}9)$$

$$K_2^* = [CO_3^{2-}][H^+]/[[HCO_3^-] \qquad (1\text{-}10)$$

Stoichiometric equilibrium constants depend on T, S and pressure (p) and are conventionally denoted by a star. These two constants only apply for the pH scale, the concentration scale and the composition of the ionic medium, for which they have been determined (see for details Millero (1995)).

The above description started with the CO_2 in air and therefore would in itself be adequate if equilibration and exchange with the air would have been the major source for DIC in seawater. In reality the major source is and always has been the continuous input of DIC into the oceans by rivers from the weathering of continental limestone:

$$CaCO_3 + CO_2 + H_2O \longrightarrow Ca^{2+} + 2HCO_3^- \qquad (1\text{-}11)$$

thus bringing both dissolved $[Ca^{2+}]$ and DIC into the oceans. This is one of several reasons for introduction of the Alkalinity concept, as required for a complete understanding and description of the DIC system in seawater.

2.3 Total Alkalinity

Total Alkalinity (TA) is an essential variable for the understanding of the inorganic carbon system in seawater. When adding together the electrical charges of the cations of the strong bases (cations of fully dissociated bases such as Na^+, K^+, Ca^{2+}, Mg^{2+}) in seawater with given salinity (here taken as salinity S = 35), we come to a charge equivalent of 605.0 mmol kg^{-1}. Subtracting the charge equivalent of the anions of strong acids (Cl^-, SO_4^{2-}, NO_3^-; = 602.8 mmol kg^{-1}), we come to a difference of 2.2 mmol kg^{-1}, which is then compensated by the charges of the anions of the weak acids such as CO_3^{2-},

HCO_3^- and as $B(OH)_4^-$ and a suite of other but very minor species in common seawater. Thus, TA is defined as the equivalents of all bases that can accept a proton to the carbonic acid endpoint (close to a pH of 4.5, see Dickson, (1981)). The proton acceptors are the bases formed from weak acids with dissociation constants $K \leq 10^{-4.5}$ ($pK \geq 4.5$) at 25ºC, and proton donors are acids with dissociation constant $K > 10^{-4.5}$ ($pK < 4.5$):

$$TA = [HCO_3^-] + 2[CO_3^{2-}] + [B(OH)_4^-] + [OH^-] + [HPO_4^{2-}] + 2[PO_4^{3-}] + [SiO(OH)_3^-] +$$

$$[NH_3] + [HS^-] + 2[S^{2-}] - [H^+] - [HSO_4^-] - [HF] - [H_3PO_4] \quad (1\text{-}12)$$

One might say that in seawater, DIC (equation 1-1) keeps track of the carbon and Total alkalinity (equation 1-12) keeps track of the charges. Bicarbonate and carbonate constitutes approximately 98% of the total alkalinity, the carbonate alkalinity (CA) is defined as:

$$CA = [HCO_3^-] + 2[CO_3^{2-}] \quad (1\text{-}13)$$

In other words, when taking into account and correcting for both the borate and all the minor species in above (1-12) it is possible to derive, from the measured Total Alkalinity, the Carbonate Alkalinity (Millero, 1995). This is feasible because borate, sulphate and fluorine are proportional to salinity in ocean seawater, and the nutrients phosphate, silicate (and ammonia where present) can be measured independently.

2.4 Governance by set of four equations

The variables and equations introduced above are used for the quantitative description of the carbonate system in seawater. The mass balance for total inorganic carbon (equation 1-1), the two equilibrium conditions (equations 1-9 and 1-10) and the charge balance (1-13) together constitute four equations with six unknown variables $[CO_2]$, $[HCO_3^-]$, $[CO_3^{2-}]$, $[H^+]$, DIC and CA. As a result, when 2 variables are known, the system is determined and all other components can be calculated. Theoretically, this goal could be achieved by measuring any two of the six quantities. In practice, only $[CO_2]$ (or in fact via fCO_2), DIC, $[H^+]$ (or in fact via pH) and TA can be measured directly. Obviously it is preferable to measure the concentration of a parameter directly, rather than to calculate it from two other observed variables. For this thesis, we measured the DIC and pCO_2 directly during our cruises, using the most robust techniques with the most satisfactory accuracy and precision for the determination of these two parameters (for more details see the method parts of the different chapters of the thesis). If a parameter can not be measured directly, the choice of the two variables used in the calculation, and the inherent accuracy of the constants K_1^* and K_2^*, together determine the precision of the obtained value (Millero, 1995).

2.5 Inorganic Carbon Dynamics

Inorganic carbon dynamics depend on the combination of various processes such as biological activity, air-sea exchange, water mass mixing and temperature variations. These are superimposed on the very large background content of DIC and TA in seawater as part of the overall dissolved salt content or salinity in seawater. Here we briefly present the main processes driving the inorganic carbon system, which are discussed in this thesis.

2.5.1 Salinity

As mentioned, most of the DIC in seawater originates from the long time river input due to weathering of limestone on land. Therefore at any given place and time in the oceans, the absolute values of both DIC and TA are largely corresponding with the salinity of that seawater. Within the open oceans, the salinity is constituted from dissolved cations and anions in constant proportions, and varies only within a narrow (33-37) range. Therefore, in the central North Sea and the southern Ocean, we can focus on other change of DIC and TA, notably photosynthesis and respiration, which are of major interest for this thesis and described below. However some caution is required when in coastal seas approaching rivers (coastal areas of the North Sea) and enclosed seas, notably the Baltic Sea, or various fjords. Here one may encounter salinity well below 33. Moreover the major ion composition of any given river may deviate strongly from that of the open oceans, such that general relations of salinity with DIC and TA are not necessarily valid anymore in the region where river water is mixing with seawater. Such deviations may also be the case to lesser extent in the Baltic Sea or any given fjord.

2.5.2 Photosynthesis/Respiration

The most fundamental biological processes involved in the dynamics of dissolved inorganic carbon are photosynthesis and aerobic respiration:

$$106\ CO_2 + 122\ H_2O + 16\ HNO_3 + H_3PO_4 \xrightarrow{Photosynthesis} [(CH_2O)_{106}(NH_3)_{16}H_3PO_4]_{organic} + 138\ O_2 \qquad (1\text{-}14)$$

Equation (1-14) corresponds to photosynthesis by algae, which on average, produces organic matter with Redfield ratios, i.e. C:N:P of 106:16:1 with concomitant production of 138 O_2. During photosynthesis, 106 moles of CO_2 are consumed, corresponding to a decrease of 106 moles of DIC. Moreover, the TA increases slightly by 16 moles or equivalent due to the consumption of strong anion nitrate (NO_3^-). The overall decrease of DIC and slight increase of TA lead to adjustments within the set of 4 equations (1-1, 1-9, 1-10, 1-13) and, as a result, the $[HCO_3^-]$ and $[CO_2]$ hence fCO_2 have decreased while the $[CO_3^{2-}]$ has increased. The ensuing change in ratio of $[HCO_3^-]$ and $[CO_3^{2-}]$ furthermore controls a concomitant decrease of $[H^+]$ hence increase of the pH ($pH = -\ ^{10}\log(H+)$).

Eventually, the algal organic matter will, virtually completely, be degraded by aerobic respiration. This is the exact opposite of equation (1-14).

2.5.3 Formation/dissolution of $CaCO_3$

Formation and dissolution of calcium carbonate ($CaCO_3$) are also important processes controlling dissolved inorganic carbon dynamics. Calcification is the formation of carbonates that is biologically mediated from either planktonic (coccolithopores, foraminifera, pteropods…) or benthic (bivalves, corals, marine calcareous algae…) organisms. However, carbonates are present in various forms, calcite and aragonite. Calcite and aragonite are both calcium carbonate forms that differ in their crystallographic structure. The precipitation of $CaCO_3$ is given by the following equation:

$$Ca^{2+} + CO_3^{2-} \longleftrightarrow CaCO_3 \qquad (1\text{-}15)$$

From equation (1-15) and rearranging equations (1-7) and (1-8), we obtain the following equation:

$$Ca^{2+} + 2HCO_3^{-} \longrightarrow CaCO_3 + CO_2 + H_2O \qquad (1\text{-}16)$$

which is the inverse of the above dissolution reaction (1-11). According to the above equation (1-16), for each mole of $CaCO_3$ precipitated, one mole of CO_2 is produced. However, this CO_2 interacts through thermodynamic equilibria (equations 1-7 and 1-8) with the bases present in seawater (buffer effect), and this adjustment can be calculated exactly from the set of 4 equations, leading to the $[CO_2]$ increase being less than 1. The $[CO_2]$ increase is 0.6 mole for each mole of $CaCO_3$ precipitated, for "standard" seawater conditions. The ratio of CO_2 production to $CaCO_3$ precipitation is defined by the letter Ψ.
Carbonate dissolution is controlled by the solubility product according to:

$$CaCO_3 \overset{Ks}{\longleftrightarrow} Ca^{2+} + CO_3^{2-} \qquad (1\text{-}17)$$

where K_s is the solubility product:

$$K_s = [Ca^{2+}]_{eq} \times [CO_3^{2-}]_{eq} \qquad (1\text{-}18)$$

Equation (1-17) and (1-18) correspond to equilibrium conditions between the solid and dissolved inorganic carbon phases. The K_s is larger for calcite than for aragonite, and both dependent strongly on temperature and pressure. A convenient parameter is the degree of saturation (Ω) that is defined as the ratio of the product of the *in situ* concentrations of Ca^{2+} and CO_3^{2-} to the solubility product:

$$\Omega = ([Ca^{2+}]_{in\ situ} \times [CO_3^{2-}]_{in\ situ})/K_s \qquad (1\text{-}19)$$

Oversaturation, saturation and undersaturation with respect to calcium carbonate are defined by $\Omega>1$, $\Omega = 1$ and $\Omega<1$. These two parameters (K_s and Ω) are defined here in order to discuss the impact of increasing atmospheric CO_2 on the inorganic carbon chemistry in the ocean (see below section 4.2).

2.6 Air-Sea gas exchange

In the preceding section we considered the main parameters of the carbonate system in seawater and several processes involved in the dynamics of this system. Another key issue of dissolved inorganic carbon dynamics is the exchange of CO_2 between the atmosphere and surface waters resulting from the gradient of CO_2 across the air-sea interface.

The rate of exchange of any given gas across the surface of the sea will be driven by both the concentration difference of the gas between air and seawater, and the existing turbulence at the air-sea interface. This turbulence is directly related with the sea-state where wind velocity (both present and in preceding hours and days), swell, surface slicks, bubbles by breaking waves all play a role. The unraveling of all these various forcing on sea state hence overall turbulence is an actively pursued, yet difficult, research topic (Zemmelink, 2003). In general it is agreed that wind velocity is the major forcing of sea state and turbulence, and this is adequate for this thesis.
Gas transport across the air-sea interface is dominated by turbulence but can be parameterized following Fick's first law of molecular diffusion:

$$F = -D \times \frac{\partial C}{\partial z} \qquad (1\text{-}20)$$

where the gas flux, F (mol m^{-2} s^{-1}), is given as the product of the molecular diffusion coefficient D (m^2 s^{-1}) and the concentration gradient ($\partial C/\partial z$, mol m^{-4}) across a boundary layer.
This equation has been adapted to the air-sea exchange of CO_2 according to:

$$F = k \times ([CO_2]_{sea} - [CO_2]_{air}) = \alpha \times k \times (pCO_{2sea} - pCO_{2air}) \qquad (1\text{-}21)$$

where F is the air-sea flux of CO_2 (mol m^{-2} s^{-1}), k (m s^{-1}) is the exchange coefficient or gas transfer velocity of CO_2, α is the solubility coefficient of CO_2 (mol atm^{-1} m^{-3}), $[CO_2]_{sea}$ is the concentration of CO_2 in the bulk of mixed layer and $[CO_2]_{air}$ is the concentration of CO_2 in the atmosphere above the air-sea interface (mol m^{-3}), and pCO_{2sea} and pCO_{2air} are the respective partial pressure (atm).

For CO_2, the resistance for the exchange across the air-sea interface is mainly in the aqueous phase through a micro-layer of water where the exchange depends on molecular diffusion (Liss, 1983). Besides molecular diffusivity (D), the exchange coefficient k depends, among other processes, on turbulence at the interface. To take this into account, the Schmidt number was introduced. The Schmidt number is the ratio of

transfer coefficients for momentum and mass, which are respectively the kinematic viscosity of water ν (m^2 s^{-1}) and the molecular diffusion coefficient D of the gas in seawater:

$$Sc = \frac{\nu}{\mathrm{D}} \tag{1-22}$$

The Schmidt number depends on the given gas, the salinity and temperature. The Schmidt number for CO_2 at 20ºC is 600 in freshwater and 660 in seawater (Liss and Merlivat, 1986). Three main conceptual models for air-sea exchange of CO_2 have been developed that differ in the way they take the Schmidt number into account.

In the *Film Model* (Whitman, 1923), air-sea exchange is only limited at the air-sea interface by molecular diffusion through a perceived stagnant micro-layer of water with a constant thickness for a given set of conditions. In this model, air-sea exchange is limited by molecular diffusion and the thickness of the micro-layer, so that the exchange coefficient is proportional to molecular diffusion:

$$k \sim D \leftrightarrow k \sim Sc^{-1} \tag{1-23}$$

The *Surface Renewal Model* (Higbie, 1935; Danckwerts, 1951) is based on the film model, but the micro-layer is periodically replaced by fluid from the underlying bulk. Air-sea exchange is then limited by the rate of renewal of the micro-layer and K is given by:

$$k \sim D^{0.5} \leftrightarrow k \sim Sc^{-0.5} \tag{1-24}$$

In the *Boundary Layer Model* (Deacon, 1977) for smooth or rigid water surfaces, the gas transfer velocity K is proportional to $Sc^{-2/3}$:

$$k \sim D^{2/3} \leftrightarrow k \sim Sc^{-2/3} \tag{1-25}$$

Based on the above conceptual considerations, various field and laboratory experiments have been carried out to attempt to parameterize k as a function of wind speed. The interest of the development of theoretical and empirical relationships between k and wind speed is that air-sea fluxes can then be easily computed since wind speed is a relatively easy parameter to measure. The effect of other factors on air-sea exchange such as waves, air bubbles, surface films, heat exchange at the interface have also been investigated, although wind speed is recognised as the main forcing factor on k. Furthermore, the occurrence of some of these factors (*e.g.* waves, air bubbles) are more or less directly related to wind conditions. For an extensive review of the various field and laboratory experiments used for the parameterization of k as a function of wind speed (wind tunnel experiments, carbon balance method, the bomb ^{14}C produced method, the ^{222}Rn

deficiency method, the sulphur hexafluoride (SF_6) and ^3He deliberate tracer) see Broecker and Peng (1974); Liss (1983); Wanninkhof et al. (1985); Liss and Merlivat (1986); Frankignoulle (1988); Watson et al. (1991); Donelan and Wanninkhof (2002). Here we give the main k versus wind speed relationships obtained from the above experiments with a particular emphasis on those used in this thesis:

The Liss and Merlivat (1986) k-wind speed relationship has been deduced from deliberate tracer experiment with SF_6 at a lake (Wanninkhof et al., 1985) for wind speeds up to 13 m s^{-1} and from wind tunnel data (Broecker and Siems, 1984) at higher wind speeds. Three wind speed regimes are distinguished: a smooth surface regime (1-26), a rough surface regime (1-27) and a breaking wave regime (1-28) with the gas transfer velocity k (cm h^{-1}) and wind speed u (m s^{-1}) at a height of 10 m (Liss and Merlivat, 1986):

$$k = 0.17u \times (Sc/600)^{-2/3} \qquad u \leq 3.6 \qquad (1\text{-}26)$$

$$k = 2.85u - 9.65 \times (Sc/600)^{-0.5} \qquad 3.6 \leq u \leq 13 \qquad (1\text{-}27)$$

$$k = 5.9u - 49.3 \times (Sc/600)^{-0.5} \qquad u > 13 \qquad (1\text{-}28)$$

For the *Wanninkhof (1992) k-wind speed relationship,* Wanninkhof proposed that gas exchange shows a non linear dependence of wind speed. As a result k determined from a particular average wind speed will depend on the wind speed variability during the measurement interval. Because of the disproportionate influence of higher wind speeds on gas exchange, estimates of k over long periods with variable winds, will be somewhat higher than corresponding estimates over short time scales with steady winds. Using the ^{14}C data from Broecker et al. (1985) and Cember (1989), Wanninkhof derived the following relationship for long term averages of wind speed

$$k = 0.39u_{av}^2 \times (Sc/660)^{-0.5} \qquad (1\text{-}29)$$

where u_{av} is the long term average wind velocity at ten meter elevation. For short term, steady winds, (derived from spot measurements by ship borne anemometers and wind speeds inferred from scatterometers and radiometers) Wanninkhof suggested

$$k = 0.31u^2 \times (Sc/660)^{-0.5} \qquad (1\text{-}30)$$

The *Wanninkhof and McGillis (1999) k-wind speed relationship* is based on the results from SF_6 and ^3He tracer experiment in the north Atlantic (for winds up to 14.5 m s^{-1}) that were cross-checked with the global ^{14}C inventory in the ocean (Broecker et al., 1985). Wanninkhof and McGillis (1999) propose two formulations for short-term (1-31) and long term (1-32) wind speeds:

$$k = 0.0283u^3 \times (Sc/660)^{-0.5} \qquad (1\text{-}31)$$

$$k_{av} = [1.09u_{av} - 0.333u_{av}^2 + 0.078u_{av}^3] (Sc/660)^{-0.5} \quad (1\text{-}32)$$

where k and k_{av} are the exchange coefficients (cm h^{-1}) for respectively the short-term and long average of wind speed measured at 10 meters height.

Finally, another *k-wind speed relationship by Nightingale et al. (2000)* found a quadratic dependence between air-sea gas exchange rates obtained from deliberate tracer experiments in the southern North Sea:

$$k = (0.222u^2 + 0.333u) \times (Sc/660)^{-0.5} \quad (1\text{-}33)$$

The k-wind relationships are so far the only available parameterizations for the CO_2 exchange coefficient. No consensus has yet been achieved and the various relationships give fairly different k values, in particular at high wind speeds. Thus, in this thesis, we applied the various most widely used k-wind speed relationships mentioned above to provide a range of computed air-sea fluxes of CO_2.

3. Global anthropogenic CO_2 budgets and uptake by the Oceans

Having described the inorganic carbon chemistry and the air-sea exchange at the air-sea interface, we can now consider the role and the response of the ocean in the context of the increasing atmospheric CO_2. The increase of atmospheric CO_2 accurately measured by Keeling and others, is much less than the annual emissions from fossil fuel burning. These emissions also are known fairly accurately from the annual production statistics of the petroleum and natural gas companies, and coal mining. Similarly, the emissions due to cement production can be assessed rather precisely. However, the emissions due to land use change (notably deforestation as well as restoration of forests) are very difficult to quantify directly.

Only about half of the anthropogenically emitted CO_2 remains in the atmosphere. The atmosphere is in contact with two major carbon reservoirs: terrestrial systems and the oceans. These two reservoirs are the two most likely candidates for present-day storage of the remainder of the emitted CO_2. The rate of the net oceanic uptake of CO_2 is primarily determined by the physico-chemical equilibria of the inorganic carbon system in seawater and the renewal times of surface water, rather than by the air-sea exchange of CO_2. Large spatial and temporal variability of the air-sea exchange of CO_2 has complicated estimates of net oceanic uptake of CO_2 from direct observations. Based on such observations, Takahashi et al. (2002) estimated an ocean uptake of 2.2 Pg C yr^{-1}, applying the Wanninkhof (1992) relationship mentioned above, for a reference year of 1995.

Several independent estimates of the net oceanic uptake of CO_2 exist. During the 1970's, an extensive dataset for DIC was collected during GEOSECS (Geochemical Ocean Sections Study) and allowed the first estimates of the CO_2 anthropogenic in the ocean based on tracer separation technique (Brewer, 1978; Chen and Millero, 1979). However, it took until the 1990's before the oceanic measurement of DIC and pCO_2 were accurate enough to refine the approach for such estimates (Gruber, 1996). The large international projects such as the World Ocean Circulation Experiment (WOCE) and the Joint Global Ocean Flux Study (JGOFS) as well as many national programs have been devoted to understand and asses the ocean's role in the global carbon cycle. Thus, the large amount of now very accurate data for DIC and pCO_2 collected in the ocean during the different expeditions of the these programs allowed the scientific community to constrain, with improved accuracy, the oceanic uptake of CO_2. Based on a separation tracer concept applied to the accurate JGOFS/WOCE Ocean CO_2 survey, Sabine et al. (2004a) calculated the latest estimate of the anthropogenic CO_2 inventory of the world oceans (Table 2). Since the onset of the industrial revolution (~1800) until ~1994 the oceans have accumulated an estimated 48% of CO_2 emissions from fossil fuel burning and cement production. Over the final 20 years of the century this ocean uptake was a third of the previous 200 years, but relatively less at 31% of the emissions. By absorbing 31-48% of fossil fuel emissions, the oceans have slowed down the atmospheric CO_2 increase accordingly.

Table 2: *Anthropogenic CO_2 budget for the Anthropocene (1800 to 1994) and its most recent decades 1980-1999 from Sabine et al. (2004a).*

	CO_2 Sources and Sinks [Pg C] = [Petagram C] = [10^{15} gram Carbon]	1800-1994 [Pg C]	1980-1999 [Pg C]
	Constrained sources and sinks:		
(1)	Emissions from fossil fuel and cement production	244 $\pm$ 20	117 $\pm$ 5
(2)	Storage in the atmosphere	-165 $\pm$ 4	-65 $\pm$ 1
(3)	Uptake and storage in the oceans	-118 $\pm$ 19	-37 $\pm$ 8
	Inferred net terrestrial balance:		
(4)	Net terrestrial balance = [-(1) - (2) - (3)]	39 $\pm$ 28	-15 $\pm$ 9

4. Global change and change in the ocean

In this section, we relate the increase of pCO_2 and DIC observed in the atmosphere and the ocean, respectively, to the observed and predicted changes in these two reservoirs. A review of predictive models of climate change and of the biological and chemical changes in the ocean is clearly out of the scope of the present work, however, it is interesting to outline a few elements to emphasize the relevance of studying and improving our understanding of the global carbon cycle. Moreover, mankind and the planet have risen well outside the CO_2 versus temperature 'calibration' of past >420,000 yr, which means the CO_2-temperature correlation of the past is, on its own, not necessarily valid for the future and global climate change take place in unpredictable proportions.

4.1 Climate Change

Recently, the Intergovernmental Panel on climate Change (IPCC) reported an observed global warming over the past century (IPCC, 2001). While recognizing the complexity of the climate system, the most straightforward, hence most acceptable explanation of this observed warming is due to the rise of CO_2 in the atmosphere. This is consistent with the most recent climate models, which, when taking into account all other variations (solar cycle, volcanism, etc.), cannot reproduce the observed warming trend, unless also taking into account the anthropogenic enhancement of the natural CO_2-greenhouse mechanism by the rising CO_2 in the atmosphere (see http://www.acia.uaf.edu/). Climate models predict the most rapid global warming at high latitudes, notably in the Arctic (Hassol, 2004). The recent Arctic Climate Impact Assessment (ACIA) predicts a temperature rise of ~5-7 ^oC in 2100 in the Arctic, when the CO_2 would have risen well over 800 μatm (see http://www.acia.uaf.edu/). Arrhenius also foresaw this, one century ago: "A simple calculation shows that the temperature in the Arctic regions would rise about 8^{o}C to 9^{o}C, if the carbonic acid increased to 2.5 or 3 times its present value." Using the atmospheric CO_2 value of 296 μatm in 1896, one arrives at 740-880 μatm to achieve the 8-9^{o}C (Arrhenius, 1896).

The predictions by Arrhenius (1896) and ACIA in 2004, are major reasons for caution for the possibility of irreversible climate changes due to the global warming. Climate change over the past ~30 years has produced numerous shifts in the distribution and abundance of species and has been directly related to increasing extinction risk of several species (Thomas et al., 2004).

4.2 Change in the ocean

While contributing to about 55% of the anthropogenic enhancement of the greenhouse effect (Mackenzie, 1998), the increasing atmospheric CO_2 content has also been related to major changes in chemical and biological processes in the ocean. Although time series measurement of DIC for the ocean do not cover periods as long as for the atmosphere, increasing DIC content of seawater was reported, notably at the BATS station in the western North Atlantic (Bates et al., 2002) and at station ALOHA in the subtropical North Pacific Ocean (Keeling et al., 2004). These recently measured increases are consistent with long known physical-chemical predictions by Revelle and Suess (1957) and others. General circulation models as cited and summarized by the IPCC, indicate that surface water DIC could probably increase by 12% by the end of the century when the atmospheric CO_2 level will be over 800 ppm. The carbonate ion concentration would then decrease by almost 60% (Brewer, 1997) because of the shift in above chemical equilibria (1-4, 1-7, 1-8) of the DIC pool, which can be summarized as follows:

$$[CO_2] + [CO_3^{2-}] + H_2O \rightarrow 2[HCO_3^-] \qquad (1\text{-}34)$$

The corresponding pH drop would be about 0.4 pH units in surface waters (Caldeira and Wickett, 2003). Moreover, the actual invasion of CO_2 in the ocean has a direct impact on the horizon depth of the degree of saturation of seawater with respect to aragonite and calcite (Ω) (Feely et al., 2004).

Because the upper ocean is supersaturated with respect to all phases of $CaCO_3$, the carbonate chemistry was not previously considered as a limiting factor in biogenic calcification. However, more recently it was shown that the lesser degree of supersaturation slows down the rate of calcification in corals and coralline macroalgae (Gattuso et al., 1998a; Langdon et al., 2000; Langdon et al., 2003). In other words, at lower ambient $[CO_3^{2-}]$, the rate of bio-calcification appears to decrease accordingly.

The majority of marine calcification occurs in planktonic organisms: bio-calcification is virtually the only route, spontaneous abiotic precipitation of $CaCO_3$ is deemed to be exceptional, if occurring at all. The formation of these calcareous skeletons by marine planktonic organisms and their subsequent sinking to depth generates a continuous rain of calcium-carbonate to the deep ocean and underlying sediments. This is important in regulating marine carbon cycling and ocean-atmosphere CO_2 exchange. Here, the concept of rain rate ratio of sinking organic carbon versus inorganic (but biogenic) $CaCO_3$ is known to be very crucial in ocean carbon cycle simulation models of past, present and future oceans (Heinze et al., 1991; Zeebe and Wolf-Gladrow, 2001). It was also shown that the present invasion of CO_2 in the ocean reduced the calcite production of dominant marine calcifying phytoplankton species, thus slowing down the production of calcium carbonate in the surface ocean. This corresponds to a shift of equation (1-16) to the left and therefore constitutes a negative feedback of the increasing atmospheric CO_2 content (Riebesell et al., 2000; Zondervan et al., 2001) that would result in a diminution of the release of CO_2 from the ocean to the atmosphere between 6 an 32 PgC for the period between 1950 and 2100 (Riebesell et al., 2000). However, Armstrong et al. (2002) have derived that a downward settling flux of organic carbon is strongly coupled with the settling flux of $CaCO_3$. This "ballast effect" of $CaCO_3$ enhancing a downward flux of organic carbon may decrease, due to the diminishing production of calcite shells, such that the efficiency of the biological pump mentioned in the next section, will overall decrease as well. Thus, by less "ballast", there is a reducing of the CO_2 uptake capacity of the ocean, this by definition constituting a positive feedback of the rise of atmospheric CO_2. In other words, bio-calcification has opposing effects, chemical release of CO_2 versus carbon settling by the physical ballast, and the overall net impact on the CO_2 budget varies with subtle changes in each of these processes (Buitenhuis et al., 2001). Moreover, Tortell et al. (2002) suggested that increasing CO_2 concentrations could potentially influence competition among marine phytoplankton taxa and affect oceanic nutrient cycling.

These few examples, among others, underline the potential and poorly understood feedbacks of anthropogenic CO_2 on our climate and the chemistry and biology of the ocean. These feedbacks particularly affect the biological pump which is defined in the next section. Thus, it is of particular importance to understand the process that control this biological pump for the uptake of CO_2, in particular in regions where the uptake of CO_2 has not yet been entirely constrained (i.e the coastal seas), or where this biological pump could

be stimulated (Southern Ocean). This thesis aims at improving our knowledge and understanding of this biological pump in these two key regions.

5. Mechanism of the oceanic CO_2 pump

The net uptake of anthropogenic CO_2 takes place via two well known mechanisms: the so-called "physical pump" and the "biological pump". More recently, the "continental shelf pump", which constitutes a specific case of the biological pump has been defined. Here we briefly describe these three mechanisms for the oceanic pump of CO_2, with particular emphasis on the latter two, which are particularly investigated in the different chapters of this thesis.

5.1 The physical pump

In the North Atlantic, north of Iceland, the surface water cools down during the northern hemisphere winter. As a result it contracts, its density increases, and once the density is higher than that of the deeper water layers, the surface water sinks to greater depths. When sinking it takes along all its dissolved substances, thus dissolved CO_2. The same processes occur in the Weddell Sea during austral winter. The process of deep water formation has taken place for a very long time and the deep water has entered into the deep Indian and Pacific Oceans, where it arrives ~ 1000 years or more after it has left the surface in Arctic or Antarctic winter. Due to the higher atmospheric CO_2, the polar winter waters are nowadays taking up some more CO_2 than before industrial times, by this extra CO_2 driving the physical pump for net uptake of anthropogenic CO_2.

In temperate and tropical regions, the transfer of anthropogenic CO_2 into the deep ocean is hindered by the thermocline, acting as a barrier for mixing between the surface ocean and the deep ocean. Nevertheless, some anthropogenic CO_2 has entered and continues to enter the surface waters, and is slowly mixed down into the deep oceans. At global scale this is much less than the CO_2 uptake by above deep water formation, nevertheless it also contributes to the worldwide physical pump.

Since CO_2 has a large natural background and biogeochemical cycling, the physical CO_2 pump is not as immediately discernible as the invasion of truly anthropogenic tracers, such as the Chlorofluorocarbons (CFC's), or the excessive radioactive tritium (^3H) introduced by atomic bomb testing. The invasion of CFC's and ^3H into the oceans is a striking analogue of the physical CO_2 pump, and indeed used to quantify the latter.

5.2 The Biological pump

The natural biological pump was described, in essence, with the forward and backward reactions of equation (1-14). Before the industrial revolution, this presumably was in balance, i.e when averaging out the biological pump over one year and all oceans regions, the net exchange of CO_2 with the atmosphere due to the natural biological pump is assumed to be zero. With rising CO_2 levels, or by iron fertilization, this biological pump could be stimulated, i.e the overall biological pump gets stronger, and the net increase would be the "extra" biological pump bringing down "extra" CO_2. The iron fertilizations of High Nutrients Low Chlorophyll (HNLC) regions as a stimulus for the biological pump of CO_2, is based on the hypothesis that low concentrations of iron in these three vast oceanic regions (the Southern Ocean, the North Pacific and the Equatorial Pacific), limit the phytoplankton growth and therefore the biological pump of CO_2 (Martin and Fitzwater, 1988. Martin (1990), and more recently Markels and Barber (2001), suggested that large-scale iron fertilization of the HNLC regions would remove CO_2 from the atmosphere and would sequester it into the deep ocean. However, other parameters such as depth of the Wind Mixed Layer (WML) that induces light limitation, are deemed to be mostly responsible for the limited phytoplankton growth in HNLC regions, and might be an obstacle for the efficiency of such fertilization in HNLC regions (De Baar et al., 2005). Moreover the magnitude and duration of carbon storage remain uncertain and difficult to quantify (Gnanadesikan et al., 2003). In chapters 6 and 7 of this thesis, we will examine the potential of the stimulation of the phytoplankton growth in the Southern Ocean on the uptake of CO_2 during an iron fertilization experiment carried out during austral spring.

5.3 The Continental shelf pump

The "continental shelf pump" (Tsunogai et al., 1999) consists of a biological uptake of CO_2 in the coastal regions, which is then transported and stored for a longer period in the deeper layer of the open ocean. This continental shelf pump is of particular importance since the various assessments of the oceanic CO_2 sink (Sarmiento et al., 2000; Gruber and Keeling, 2001; IPCC, 2001; Orr et al., 2001; Thomas et al., 2001; Sarmiento and Gruber, 2002; Takahashi et al., 2002; Sabine et al., 2004a) do not take into account these fluxes in the coastal zone. Coastal and marginal seas play a key role in the global carbon cycle by linking the terrestrial, oceanic and atmospheric reservoirs (Walsh, 1991; Wollast, 1998; Andersson and Mackenzie, 2004). They occupy only 7% of the global ocean surface area but house 10-30% of the global marine production (Gattuso et al., 1998b). Moreover, the net biological community production in coastal margins, which is related to the magnitude of the CO_2 air-sea fluxes, varies from net autotrophic to net heterotrophic (Smith and Hollibaugh, 1993; Gattuso et al., 1998b; Andersson and Mackenzie, 2004; Mackenzie et al., 2004). It is therefore essential to acquire complete field datasets for DIC and pCO_2 in various coastal regions of the world, in order to quantify the overall CO_2 air-sea fluxes of these regions and the processes driving the continental shelf pump of CO_2.

In chapters 2, 3, 4 and 5 of this thesis we will test the hypothesis of a continental shelf pump of CO_2 in the North Sea and assess the mechanisms involved in this pump.

6. This thesis

6.1 Objectives

This PhD thesis was carried out in the context of increasing atmospheric CO_2 observed since the beginning of the industrial revolution, which is closely related to the concomitant CO_2 uptake by the ocean, with two major objectives: 1) To quantify this uptake by coastal seas with a case study in the North Sea 2) To assess the response of the biological pump of CO_2 to an *in-situ* iron fertilization in the Southern Ocean during austral spring.

The continental shelf pump of CO_2 in the North Sea

The work was carried out in the framework of the CANOBA program with the following objectives:
The acquisition of a complete new field dataset for the CO_2 system and related parameters for the North Sea based on four consecutive cruises, of one month each, covering every season of the year, between 2001 and 2002. The determination of the air-sea fluxes of CO_2 in the North Sea as part of the overall assessment of the CO_2 air-sea fluxes in the coastal zone. The assessment of the biological, chemical and physical processes controlling the inorganic carbon system in the North Sea. The elaboration of a comprehensive budget for carbon in the North Sea based on the dataset acquired during this thesis combined with results from precedent investigations.

Fe fertilization in the Southern Ocean

The work was carried out as part of the CARUSO program with the following objectives:
To follow the evolution of an *in-situ* iron enriched patch during a two month cruise under contrasting meteorological conditions. To determine the factors influencing the inorganic carbon uptake throughout the experiment. To relate the observed changes for inorganic carbon to the observed changes in other inorganic nutrient. To assess the potential net carbon uptake of such iron fertilization.

6.2 Outline

The chapters of this thesis have either been published in (2, 3, 5, 6, 7) or are in revision for (4) peer-reviewed journals. We kept the content of each chapters in the particular format of the journal where the article was published. Therefore, for each chapter, here a more detailed introduction completes this general introduction and describes the particular context and objectives of each article. The analytical method used is detailed in each "method" section of each chapter and the results are presented and discussed. Chapters 2, 3, 4 and 5 are focused on the continental shelf pump of CO_2 in the North Sea, whereas chapters 6 and 7 discuss the results from the EisenEx iron enrichment experiment in the Southern Ocean.

Chapter 2 focuses on the late summer distribution of the inorganic carbon in the North sea, highlighting the strong difference between the southern (≈ south of 54ºN) and the northern North Sea (54ºN-61ºN). The different processes driving the DIC and pCO_2 variations at that time of the year are assessed. The fluxes of CO_2 in both regions as well as in the whole North Sea are computed and a mechanism driving theses fluxes for that period of the year is proposed.

In **chapter 3**, based on the very large amount of continuous pCO_2 data collected during the four cruises of our CANOBA program and the wind speeds acquired during the period of observations, we compute the annual CO_2 air-sea exchange for different areas of the North Sea and the whole North Sea. We compare the results obtained with the different k-wind speed formulations given in section 2.5 and underline the importance of the late summer situation discussed in **chapter 2** for the annual CO_2 air-sea fluxes. The computed CO_2 air-sea fluxes are compared to the fluxes calculated in other coastal regions and to the latest estimates of the net oceanic uptake of CO_2, in order to highlight the significance of the coastal regions in the overall oceanic uptake of CO_2.

In **chapter 4**, we use the seasonally resolved dataset of DIC, pCO_2 and inorganic nutrients to assess the abiotic and biological processes in the whole water column of the North Sea throughout the year. The North Sea's regional variability is accounted for by using the 15-boxes scheme as proposed by the International Council for the Extrapolation of the Seas (ICES) (ICES, 1983). We use the changes in DIC due to biological processes calculated for different regions of the North Sea to assess the Net Community Production (NCP) based on inorganic carbon. This is compared to the NCP based on inorganic nutrients and previous calculation. The NCP based on inorganic carbon for every region of the North Sea is used to compute the overall NCP for the whole North Sea, thus taking into account the internal spatial variability for this parameter. The NCP estimate allows the determination of the trophic state of the North Sea, which can then be related to the annual CO_2 air-sea fluxes calculated in **chapter 3**.

In **chapter 5**, a complete carbon budget is established for the whole North Sea, based on the data collected during our cruises and previous investigations. A gross and a net budget are established in order to identify the key players of the budget. Moreover, inorganic and organic carbon budgets have been established to quantify the internal sources of dissolved inorganic carbon. Finally, this one-box carbon budget approach is use to assess the trophic sate of a larger area than in **chapter 4**.

Chapter 6 presents the evolution of DIC, in relation with the inorganic nutrients changes observed, during the course of the EisenEx iron enrichment experiment in the southern Ocean. The variations of the wind mixed layer under contrasting meteorological conditions during such experiment is related to the evolution of the uptake of CO_2. Finally, a preliminary budget of the net uptake of CO_2, based on DIC measurements is elaborated.

In **chapter 7**, a more comprehensive budget of the net uptake of CO_2, based on the fCO_2 data is established using the finalized data set of the Fe-enriched patch tracers. The same method as for the precedent iron enrichment experiment carried out in the southern Ocean (SOIREE) is applied in order to compare the net CO_2 uptake estimates in both experiments.

Finally, in **chapter 8**, results from the preceding chapters are synthesized and the implications of the research presented in this thesis are discussed in a wider context.

References

Andersson, A.J. and Mackenzie, F.T., 2004. Shallow-water oceans: a source or sink of atmospheric CO_2. Frontiers in Ecology and the Environment, 2(7): 348-353.

Armstrong, R.A., Lee, C., Hedges, J.I., Honjo, S. and Wakeham, S.G., 2002. A new, mechanistic model for organic carbon fluxes in the ocean based on the quantitative association of POC with ballast minerals. Deep-Sea Research II, 49: 219-236.

Arrhenius, S., 1896. On the influence of carbonic acid in the air upon the temperature on the ground. Philosophical Magazine, 41: 237-276.

Barnola, J.-M., Raynaud, D., Korotkevich, Y.S. and Lorius, C., 1987. Vostock ice cores provides 160,000-year record of atmospheric CO_2. Nature, 329: 402-408.

Bates, N.R., Pequignet, A.C., Johnson, R.J. and Gruber, N., 2002. A short-term sink for atmospheric CO_2 in subtropical mode water of the North Atlantic Ocean. Nature, 420: 489-493.

Brewer, P.G., 1978. Direct measurement of the oceanic CO_2 increase. Geophysical Research Letters, 5: 997-1000.

Brewer, P.G., 1997. Ocean chemistry of the fossil fuel CO_2 signal: The haline signal of "business as usual". Geophysical Research Letters, 24(11): 1367-1369.

Broecker, W.S. and Peng, T.-H., 1974. Gas exchange rates between air and sea. Tellus, 26: 21-35.

Broecker, W.S., Peng, T.-H., Ostlund, G. and Stuiver, M., 1985. The distribution of bomb radiocarbon in the ocean. Journal of Geophysical Research, 90: 6953-6970.

Broecker, W.S. and Siems, W., 1984. The role of bubbles for gas transfer from water to air at higher windspeeds: experiments in wind-wave facility in Hambourg. In: W. Brustaert and G.H. Jirka (Editors), Gas transfer at water surfaces. Reidel Publishing compagny, Dordrecht, pp. 229-238.

Buitenhuis, E.T., van der Wal, P. and De Baar, H.J.W., 2001. Blooms of *Emiliana huxleyi* are Sinks of atmospheric Carbon Dioxide: a field and Mesocosm Study derived Simulation. Global Biogeochemical Cycles, 15(3): 577-587.

Caldeira, K. and Wickett, M.E., 2003. Anthropogenic carbon and ocean pH. Nature, 425: 365.

Cember, R., 1989. Bomb radiocarbon in the Red Sea: a medium scale gas exchange experiment. Journal of Geophysical Research, 94: 2111-2123.

Chen, C.-T.A. and Millero, F.J., 1979. Gradual increase of oceanic CO_2. Nature, 373: 412-415.

Danckwerts, P.V., 1951. Significance of liquid-film coefficients in gas absorption. Industrial Engineering Chemistry, 43: 1460-1467.

De Baar, H.J.W., Boyd, P.W., Coale, K.H., Landry, M.R., Tsuda, A., Assmy, P., Bakker, D.C.E., Bozec, Y., Barber, R.T., Brzezinski, M.A., Buesseler, K.O., Boyé, M., Croot, P.L., Gervais, F., Gorbunov, M.Y., Harrison, P.J., Hiscock, W.T., Laan, P., Lancelot, C., Levasseur, M., Marchetti, A., Millero, F.J., Nishioka, J., Nojiri, Y., van Oijen, T., Riebesell, U., Rijkenberg, M.J.A., Saito, H., Takeda, S., Timmermans, K.R. and Veldhuis, M.J.W., 2005. Synthesis of 8 Iron Fertilization Experiments:

from the Iron age in the Age of Enlightenment. Journal of Geophysical Research (Oceans), in press.

Deacon, E.L., 1977. Gas transfer to and across an air-water interface. Tellus, 29: 363-374.

Dickson, A.G., 1981. An eaxact definition of total alkalinity and a procedure for the estimation of alkalinity and total inorganic carbon from titration data. Deep-Sea Research I, 28: 609-623.

DOE, 1997. Handbook of methods for the analysis of the various parameters of the carbon system in seawater, version 2.11. In: A.G. Dickson and C. Goyet (Editors). ORNL/CDIAC 74.

Donelan, M.A. and Wanninkhof, R., 2002. Gas Transfer at Water surfaces-Concepts and Issues. In: M. Donelan, W.M. Drennan, E.S. Saltzman and R. Wanninkhof (Editors), Gas transfer at water surfaces. American Geophysical Union, Washington, pp. 1-10.

EPICA, 2004. Eight glacial cycles from an Antarctic ice core. Nature, 429: 623-628.

Feely, R.A., Sabine, C.L., Lee, K., Berelson, W., kleypas, J., Fabry, V.J. and Millero, F.J., 2004. Impact of Antropogenic CO_2 on the $CaCO_3$ System in the Oceans. Science, 305: 362-366.

Frankignoulle, M., 1988. Field measurements of air-sea CO_2 exchange. Limnology and Oceanography, 33: 313-322.

Gammon, R.H., Sundquist, E.T. and Fraser, P.J., 1985. Hystory of carbon dioxide in the atmosphere. In: J.R. Trabalka (Editor), Atmospheric Carbon Dioxide and the Global Carbon Cycle. United States Department of Energy, Oak Ridge National Laboratory, Washington, DOE/ER-0239, pp. 25-62.

Gattuso, J.-P., Frankignoulle, M., Bourge, I., Romaine, S. and Buddemeier, R.W., 1998a. Effect of calcium carbonate saturation state on the calcification rate of an experimental coral reef. Global and Planetary Change, 18: 37-46.

Gattuso, J.-P., Frankignoulle, M. and Wollast, R., 1998b. Carbon and carbonate metabolism in coastal aquatic ecosystems. Annual Reviews of Ecological Systems, 29: 405-434.

Gnanadesikan, A., Sarmiento, J.L. and Slater, R.D., 2003. Effects of patchy ocean fertilization on atmospheric carbon dioxide and biological production. Global Biogeochemical Cycles, 17(2): 1050, doi: 1029/2002GB001940.

Gruber, N., 1996. An improved methode for detecting anthropogenic CO_2 in the oceans. Global Biogeochemical Cycles, 10: 809-837.

Gruber, N., Freidlingstein, P., Field, C.B., Valentini, R., Heimann, M., Richey, J.E., Lankao, P.R., Schulze, E.-D. and Chen, C.-T.A., 2004. The Vulnerability of the Carbon Cycle in the 21st Century: An Assessment of Carbon-Climate-Human Interactions. In: C.B. Field and M.R. Raupach (Editors), The global carbon cycle: integrating human, climate and the natural world. SCOPE, ISSN, Washington, D.C., pp. 45-77.

Gruber, N. and Keeling, C.D., 2001. An improved estimate of the isotopic air-sea disequilibrium of CO_2: Implications for the oceanic uptake of anthropogenic CO_2. Geophysical Research Letters, 28(3): 555-558.

Hassol, S.J., 2004. Impacts of warming Arctic: Arctic Climate Impact Assessment. Cambridge University Press. http://www.acia.uaf.edu/

Heinze, C., Maier-Reimer, E. and Winn, K., 1991. Glacial pCO_2 reduction by the world ocean: Experiments with the Hambourg Carbon Cycle Model. Paleoceanography, 6: 395-430.

Higbie, R., 1935. The role of absorption of a pure gas into a still liquid during short periods of exposure. Transactions of the American Institute of Chemical Engineering, 35: 365-373.

ICES, 1983. Flushing times of the North Sea. ICES Cooperative Research Report. 123.

IPCC, 2001. The scientific basis. In: J.T. Houghton et al. (Editors), Contribution of Working Group I to the Third Assessment Report of the Intergovernmental Panel on Climate Change. Cambridge University Press, New York, USA, pp. 881.

Keeling, C.D., 1960. The concentration and isotopic abundances of carbon doxide in the atmosphere. Tellus, 12: 200-203.

Keeling, C.D., Bacastow, R.B., Carter, A.F., Piper, S.C., Whorf, T.P., Heimann, M., Mook, W.G. and Roeloffzen, H., 1989. A three dimensional model of atmospheric CO_2 transport based on observed winds: Analysis of data. In: D.H. Peterson (Editor), Aspect of climate variability in the Pacific and the Western Americas. Geophysical monograph 55, pp. 165-236.

Keeling, C.D., Brix, H. and Gruber, N., 2004. Seasonal and long-term dynamics of the upper ocean carbon cycle at Station ALOHA near Hawaii. Global Biogeochemical Cycles, 18(GB4006, doi:10.1029/2004GB002227).

Keeling, C.D. and Whorf, T.P., 1999. Atmospheric records from sites in the SIO air sampling network. In: T.A. Boden, D.P. Kaiser, R.J. Sepanski and F.W. Stoss (Editors), Trends: A compendium of data on global change, ORNL/CDIAC., Oak Redge, Tenessee, pp. 983.

Keeling, C.D. and Whorf, T.P., 2004. Atmospheric CO_2 records from sites in the SIO air sampling network., In Trends: A compendium of data on Global Change. Carbon Dioxide Information Analysis Center, Oak Ridge National Laboratory, U.S Department of Energy, Oak Ridge, Tennessee, USA. http://cdiac.esd.ornl.gov/trends/co2/sio-mlo.htm

Langdon, C., Broecker, W.S., Hammond, D.E., Glenn, E., Fitzsimmons, K., Nelson, S.G., Peng, T.-H., Hadjas, I. and Bonani, G., 2003. Effect of elevated CO_2 on the community of an experimental coral reef. Global Biogeochemical Cycles, 17(1): 1011, doi:10.1029/2002GB001941.

Langdon, C., Takahashi, T., Sweeney, C., Chipman, D.W., Goddard, J., Marubini, F., Aceves, H., Barnett, H. and Atkinson, M.J., 2000. Effect of calcium carbonate saturation state on the calcification rate of an experimental coral reef. Global Biogeochemical Cycles, 14(2): 639-654.

Liss, P.S., 1983. Gas transfer: experiments and geochemical implications. In: P.S. Liss and W.G.N. Slinn (Editors), Air-sea exchange of gases and particle. D. Reidel Publishing Compagny, pp. 241-298.

Liss, P.S. and Merlivat, L., 1986. Air-sea gas exchange rates: Introduction and synthesis. In: P. Buat-Ménard (Editor), The Role of Air-Sea Exchange in Geochemical Cycling. D. Reidel Publishing Company, pp. 113-127.

Mackenzie, F.T., 1998. Our Changing Planet. Prentice-Hall, Englewood Cliffs, New York, 486 pp.

Mackenzie, F.T., Lerman, A. and Andersson, A.J., 2004. Past and present of sediment and carbon biogeochemical cycling models. Biogeosciences, 1: 11-32.

Markels, M. and Barber, R.T., 2001. Sequestration of CO_2 by ocean fertilization. In: N.E.T. Laboratory (Editor), First National Conference on Carbon Sequestration.

Martin, J.-M., 1990. Glacial to interglacial CO_2 change: the iron hypothesis. Paleoceanography, 5: 1-13.

Martin, J.-M. and Fitzwater, S.E., 1988. Iron deficiency limits phytoplankton growth in the northeast Pacific subarctic. Nature, 331: 341-343.

Millero, F.J., 1995. Thermodynamic of the carbon dioxide system in the oceans. Geochimica et Cosmochimica Acta, 59(4): 661-677.

Nightingale, P.D., Malin, G., Law, C.S., Watson, A.J., Liss, P.S., Liddicoat, M.I., Boutin, J. and Upstill-Goddard, R.C., 2000. In situ evaluation of air-sea gas exchange parameterizations using novel conservative and volatile tracers. Global Biogeochemical Cycles, 14(1): 373-387.

Orr, J.C., Maier-Reimer, E., Mikolajewicz, U., Monfray, P., Sarmiento, J.L., Toggweiler, J.R., Taylor, N.K., Palmer, J., Gruber, N., Sabine, C.L., Le Quéré, C., Key, R.M. and Boutin, J., 2001. Estimates of anthropogenic carbon uptake from four three-dimensional global ocean models. Global Biogeochemical Cycles, 15(1): 43-60.

Petit, J.R., Basile, I., Leruyet, A., Raynaud, D., Lorius, C., Jouzel, J., Stievenard, M., Lipenkov, V.Y., Barkov, N.I., Kudryashov, B.B., Davis, M., Saltzman, E. and Kotlyakov, V., 1997. Four climates cycle in Vostock ice core. Nature, 387: 359-360.

Petit, J.R., Jouzel, J., Raynaud, D., Barkov, N.I., Barnola, J.-M., Basile, I., Bender, M., Chappelaz, J., Davis, M., Delaygue, M., Kotlyakov, V.M., Legrand, M., Lipenkov, V.Y., Lorius, C., Pépin, L., Ritz, C., Saltzman, E. and Stievenard, M., 1999. Climate and atmospheric history of the past 420,000 years from the Vostock ice core, Antarctica. Nature, 399: 429-436.

Revelle, R. and Suess, H.E., 1957. Carbon Dioxide Exchange Between Atmosphere and Ocean and the Question of an Increase of Atmospheric CO_2 during the Past Decades. Tellus, 9: 18-27.

Riebesell, U., Zondervan, I., Rost, B., Tortell, P.D., Zeebe, R.E. and Morel, F.M.M., 2000. Reduced calcification of marine plankton in response to increased atmospheric CO_2. Nature, 407: 364-367.

Sabine, C.L., Feely, R.A., Gruber, N., Key, R.M., Lee, K., Bullister, J.L., Wanninkhof, R., Wong, C.S., Wallace, D.W.R., Tilbrook, B., Millero, F.J., Peng, T.-H., Kozyr, A., Ono, T. and Rios, A.F., 2004a. The Oceanic Sink for Anthropogenic CO_2. Science, 305: 367-371.

Sabine, C.L., Heimann, M., Artaxo, P., Bakker, D.C.E., Chen, C.-T.A., Field, C.B., Gruber, N., Le Quéré, C., Prinn, R.G., Richey, J.E., Lankao, P.R., Sathaye, J.A. and Valentini, R., 2004b. Current Status and Past Trends of the Global Carbon Cycles. In: C.B. Field and M.R. Raupach (Editors), The global carbon cycle: integrating human, climate and the natural world. SCOPE, ISSN, Washington, D.C, pp. 17-44.

Sarmiento, J.L. and Gruber, N., 2002. Sinks for anthropogenic carbon. Physics Today, 55(8): 30-36.

Sarmiento, J.L., Monfray, P., Maier-Reimer, E., Aumont, O., Murnane, R.J. and Orr, J.C., 2000. Sea-air CO_2 fluxes and carbon transport: A comparison of three ocean general circulation models. Global Biogeochemical Cycles, 14(4): 1267-1281.

Skirrow, G., 1975. The dissolved gases-carbon dioxide. In: J.P. Riley and G. Skirrow (Editors), Chemical Oceanography, 2, 2nd edition, Academic Press, pp. 1-92.

Smith, S.V. and Hollibaugh, J.T., 1993. Coastal metabolism and the ocean organic carbon balance. Reviews of Geophysics, 31(1): 75-89.

Takahashi, T., Sutherland, S.C., Sweeney, C., Poisson, A., Metzl, N., Tilbrook, B., Bates, N.R., Wanninkhof, R., Feely, R.A., Sabine, C.L., Olafsson, J. and Nojiri, Y., 2002. Global sea –air CO_2 flux based on climatological surface ocean pCO_2, and seasonal biological and temperature effects. Deep-Sea Research II, 49: 1601-1622.

Thomas, C.D., Cameron, A., Green, R.E., Bakkenes, M., Beaumont, L.J., Collingham, Y.C., Erasmus, B.F.N., de Siqueira, M.F., Grainger, A., Hannah, L., Hughes, L., Huntley, B., A.S., V.J., Midgley, G.F., Miles, L., Ortega-Huerta, M.A., Townsend-Peterson, A., Phillips, O.L. and Williams, S.E., 2004. Extinction Risk from climate change. Nature, 427: 145-148.

Thomas, H., England, M.H. and Ittekkot, V., 2001. An off-line 3D model of anthropogenic CO_2 uptake by the oceans. Geophysical Research Letters, 28(3): 547-550.

Tortell, P.D., DiTullio, G.R., Sigman, D.M. and Morel, F.M.M., 2002. CO_2 effects on taxonomic composition and nutrient utilization in an Equatorial Pacific phytoplankton assemblage. Marine Ecology Progress Series, 236: 37-43.

Tsunogai, S., Watanabe, S. and Sato, T., 1999. Is there a "continental shelf pump" for the absorption of atmospheric CO_2? Tellus, 51B: 701-712.

Walsh, J.J., 1991. Importance of continental margins in the marine biogeochemical cycling of carbon and nitrogen. Nature, 350: 53-55.

Wanninkhof, R., 1992. Relationship between wind speed and gas exchange over the ocean. Journal of Geophysical Research, 97(C5): 7373-7382.

Wanninkhof, R., Ledwell, J.J. and Broecker, W.S., 1985. Gas exchange wind speed relation measured with sulphur hexafluoride on a lake. Science, 227: 1224-1226.

Wanninkhof, R. and McGillis, W.R., 1999. A cubic relationship between air-sea CO_2 exchange and wind speed. Geophysical Research Letters, 26(13): 1889-1892.

Watson, A.J., Upstill-Goddard, R.C. and Liss, P.S., 1991. Air-sea gas exchange in rough and stormy seas measured by a dual tracer technique. Nature, 349: 145-147.

Weiss, R.F., 1974. Carbon dioxide in water and seawater: the solubility of a non-ideal gas. Marine Chemistry, 2: 203-215.

Whitman, W.G., 1923. The two-film theory of gas absorption. Chemical Metallurgy Engineering, 29: 146-148.

Wollast, R., 1998. Evaluation and comparison of the global carbon cycle in the coastal zone and in the open ocean. In: K.H. Brink and A.R. Robinson (Editors), The Sea. John Wiley & Sons, Inc., New York, pp. 213-252.

Zeebe, R.E. and Wolf-Gladrow, D.A., 2001. CO_2 in seawater: equilibrium, kinetics, isotopes, 65, Elsevier Oceanography Series, 346 pp.

Zemmelink, H.J., 2003. Dimethly Sulphide: Measuring emissions from the ocean to the atmosphere. Ph.D Thesis, Rijksuniversiteit Groningen, Groningen, 166 pp.

Zondervan, I., Zeebe, R.E., Rost, B. and Riebesell, U., 2001. Decreasing marine biogenic calcification: a negative feedback on rising atmospheric pCO_2. Global Biogeochemical. Cycles, 15(2): 507-516.

Chapter 2

The continental shelf pump for CO_2 in the North Sea– evidence from summer observations

This chapter by Yann Bozec, Helmuth Thomas, Khalid Elkalay and Hein J.W. de Baar has been published in Marine Chemistry, 93: 131-147.

Abstract

Data on the distribution of dissolved inorganic carbon (DIC) and partial pressure of CO_2 (pCO_2) were obtained during a cruise in the North Sea during late summer 2001. A 1° by 1° grid of 97 stations was sampled for DIC while the pCO_2 was measured continuously between the stations. The surface distributions of these two parameters show a clear boundary located around 54°N. South of this boundary the DIC and pCO_2 range from 2070 to 2130 µmol kg^{-1} and 290 to 490 ppm, respectively, whereas in the northern North Sea, values range between 1970 to 2070 µmol kg^{-1} and 190 to 350 ppm, respectively. The vertical profiles measured in the two different areas show that the mixing regime of the water column is the major factor determining the surface distributions. The entirely mixed water column of the southern North Sea is heterotrophic, whereas the surface layer of the stratified water column in the northern North Sea is autotrophic. The application of different formulations for the calculation of the CO_2 air-sea fluxes show that the southern North Sea acts as a source of CO_2 for the atmosphere within a range of +0.8 to +1.7 mmol m^{-2} day^{-1}, whereas the northern North Sea absorbs CO_2 within a range of -2.4 to -3.8 mmol m^{-2} day^{-1} in late summer. The North Sea as a whole acts as a sink of atmospheric CO_2 of -1.5 to -2.2 mmol m^{-2} day^{-1} during late summer. Compared to the Baltic and the East China Seas at the same period of the year, the North Sea acts as a weak sink of atmospheric CO_2. The anticlockwise circulation and the short residence time of the water in the North Sea lead to a rapid transport of the atmospheric CO_2 to the deeper layer of the North Atlantic Ocean. Thus, in late summer, the North Sea exports 2.2×10^{12} g C $month^{-1}$ to the North Atlantic Ocean via the Norwegian trench, and, at the same period, absorbs from the atmosphere a quantity of CO_2 ($0.4\ 10^{12}$ g C $month^{-1}$) equal to 15% of that export, which makes the North Sea a continental Shelf pump of CO_2.

Note: *In the present chapter, Thomas et al. (2004) refers to chapter 3 of this thesis.*

1. Introduction

Human activities have released vast amounts of the greenhouse gas carbon dioxide (CO_2) into the atmosphere by fossil fuel burning and deforestation, which corresponds to ~ 5.4 ± 0.3 petagrams of carbon per year (Pg C yr^{-1}) (1 Pg = 10^{15} g) during the 1980s. It is well established that 3.3 ± 0.1 Pg C yr^{-1} remain in the atmosphere (IPCC, 2001). The world ocean behaves as a sink estimated as 1.9 ± 0.6 Pg C yr^{-1}, and the terrestrial biosphere is assumed to trap the remaining 0.2 ± 0.7 Pg C yr^{-1} (IPCC, 2001). Since the land sink is usually considered as the closing term for the global budgeting, it is essential to reduce the uncertainties regarding the oceanic uptake of anthropogenic CO_2. The estimates of this uptake still vary significantly (Lee et al., 1998; Gruber and Keeling, 2001; Orr et al., 2001; Thomas et al., 2001). One of the reasons for this uncertainty could be that all these assessments ignore the CO_2 fluxes in the coastal oceans. Because of the small scale variability observed in these regions, it has been difficult to consider coastal seas in global

circulation models. Moreover, hitherto there has been a lack of field data on the spatial and temporal variability of dissolved inorganic carbon (DIC) and the partial pressure of CO_2 (pCO_2) for the coastal ocean.

The coastal ocean is known to house a disproportionately large fraction of the oceanic primary production of 15% to 30% (Walsh, 1991; Wollast, 1998), a contribution that is much larger than the contribution of coastal seas (7%) to the total ocean surface area. Thus, these regions strongly affect the global carbon cycle, however it has not been established yet whether they act as a sink or as a source of atmospheric CO_2 (Walsh, 1991; Smith and Hollibaugh, 1993; Kempe, 1995; Gattuso et al., 1998; Mackenzie et al., 1998; Wollast, 1998).

The North Sea has been the subject of intense investigations for many decades by several institutions, making this area one of the best understood coastal seas of the world. Very recent results by Thomas et al. (2004) showed that the North Sea acts as a sink for atmospheric CO_2 and export ≈93% of the absorbed CO_2 to the North Atlantic Ocean, therefore acting like a continental Shelf pump as described by Tsunogai et al. (1999) for the East China Sea. Thomas et al. (2004) suggested that during the late summer situation, the differences between the two biogeochemical regions with regard to the air-sea exchange of CO_2 are most prominent. A detailed investigation of the CO_2 system in this period is provided here in order to gain insight in the control mechanisms of the CO_2 air-sea exchange on the North Sea.

In the North Sea, previous investigations focused mainly on certain aspects related to the carbon cycle, e.g. primary production and the transport of organic matter within the North Sea (Postma and Rommets, 1984; Kempe et al., 1988). Pioneering investigations of the inorganic carbon cycle during summer 1986 had been done with potentiometric determination of DIC and alkalinity (Pegler and Kempe, 1988; Kempe and Pegler, 1991), upon which the alkalinity was used together with pH to calculate the pCO_2. Moreover, many other regional studies were conducted (Hoppema, 1990; Hoppema, 1991; Kempe and Pegler, 1991; Bakker et al., 1996; Frankignoulle et al., 1996a; Frankignoulle et al., 1996b; Frankignoulle et al., 1996c; Frankignoulle et al., 1998; Borges and Frankignoulle, 1999; Brasse et al., 1999; Borges and Frankignoulle, 2002; Brasse et al., 2002). However, the currently available carbon data sets for the entire North Sea still are sparse and do not allow unequivocal conclusions about the carbon cycle.

The bottom topography of the North Sea is likely to constitute the major control for biogeochemical cycling, in particular for inorganic carbon parameters: The deeper northern part reveals depths of approximately 150 m on the shelf, of 400 m in the Norwegian Channel and of 700 m in the Skagerrak (Figure 1). In the southern part (south of 54ºN) depths are less than 50 m and even less than 20 m near the coasts (Eisma, 1987). Because of the shallow conditions in the south, the water column is mixed throughout the year, while thermal stratification occurs in the northern part during summer. The spatial distribution of the carbonate system is also affected by the inorganic and organic carbon inputs from the estuaries. The southern part receives most of the freshwater inputs, notably from the rivers Rhine, Scheldt, Thames and Elbe (Figure 1). Haline stratification is an exception in the northern part and only occurs in the Norwegian Trench area and in the vicinity of river inlets with strong freshwater input.

The main aim of the present study is to verify the hypothesis of a "continental shelf pump" for the uptake of atmospheric CO_2 with subsequent transport to the open ocean. Here we present a new comprehensive study in the late summer of 2001, with improved accuracy relying on now available certified DIC standards, and direct measurements of pCO_2 which is calibrated versus certified gas mixtures. We also investigate the interactions between carbon, oxygen and nutrients in order to describe the "biological CO_2 pump". We can rely on a complete new data set with high spatial resolution for the carbonate system and related chemical, biological and physical parameters obtained during our cruise in the North Sea during late summer 2001.
In the present paper we firstly describe the surface water distribution of the inorganic carbon system and for related parameters in the North Sea. In part 4.1 we describe the different water masses, which govern these distributions. In parts 4.2 and 4.3 we will focus on the differences in carbonate chemistry between the northern and the southern North Sea, respectively. In part 4.4, we evaluate the monthly atmospheric CO_2 fluxes in both regions and assess, whether the North Sea acts as a source or a sink for CO_2 during late summer. Finally, in part 4.5 we propose a mechanism of the continental shelf pump in the North Sea.

2. Material and methods

The data were obtained during a cruise in the North Sea (18.08.2001-13.09.2001), on board R.V Pelagia. The North Sea was covered by an adapted 1° by 1° grid with 97 stations (Figure 1). This grid was specifically designed to focus on the relevant regions for biogeochemical cycles such as the Shetland and English Channels (inflow of North Atlantic water), the Skagerrak area (inflow of Baltic Sea water) and the western Scandinavian coast (outflow to the North Atlantic). The stations were also denser in the Southern Bight (Figure 1) that receives the major freshwater inputs, whereas the stations distribution was sparser in the more homogenous central North Sea.

During this cruise, a total of 745 water samples were collected at the stations and the concentrations of DIC, oxygen and nutrient as well as chlorophyll *a* (from the surface water samples), salinity and temperature were determined. In the surface waters, salinity and temperature were determined continuously from the ship's water supply as well as the pCO_2 leading to a total of 22 000 surface measurements for this parameter (Figure 1).

DIC samples from CTD casts were collected in 250 mL glass bottles, which were kept cold in the dark before measurement. The DIC concentrations were determined by the coulometric method of Johnson et al. (1993), as previously described by Stoll (1994). A new coulometric cell was prepared approximately every 12 hours and calibrated versus Certified Reference Material (CRM) (batch #52). The accuracy and the precision of the system were controlled by the repeated measurement of CRM material before and after each station. Three to four replicates were determined of each sample and of each standard with a precision better than 1 $\mu mol\ kg^{-1}$.

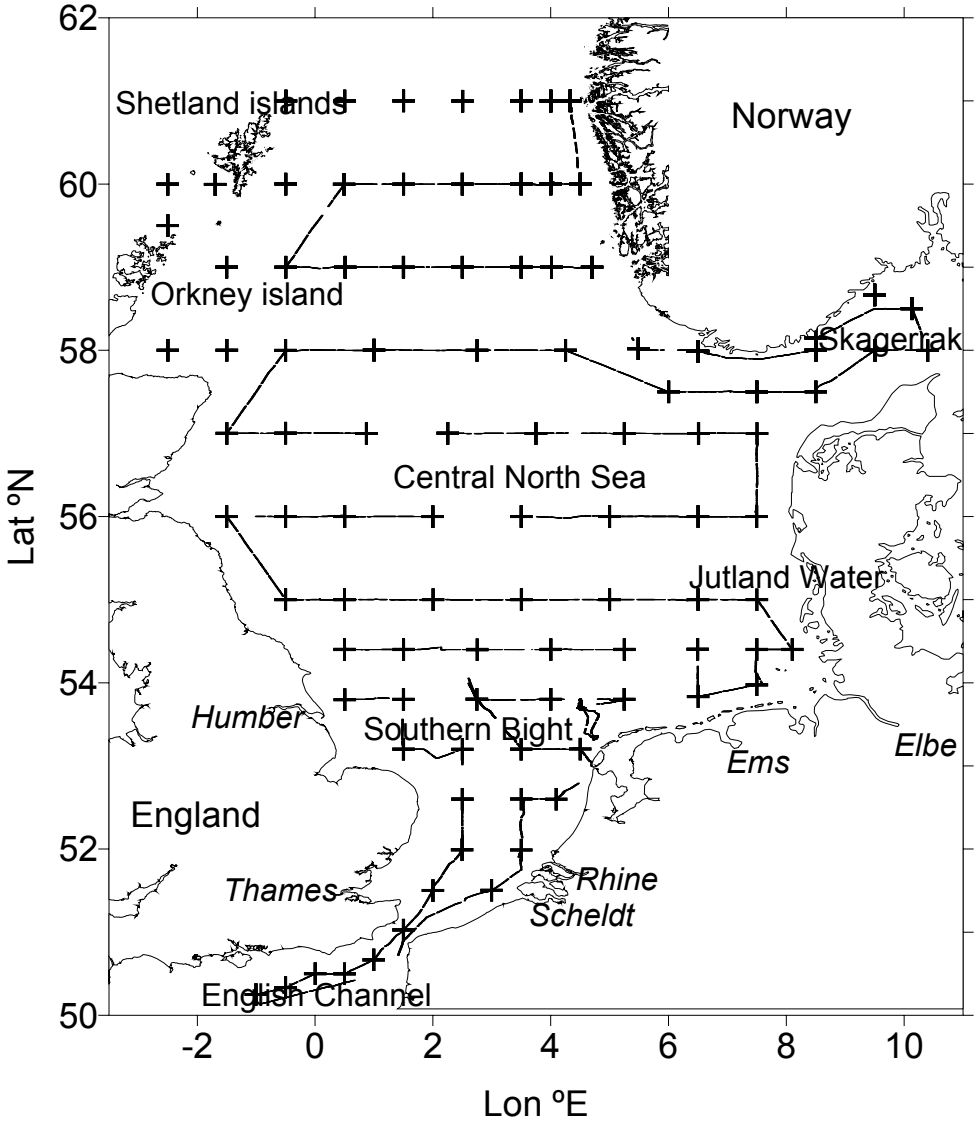

Figure 1: *Map of the study area. The North Sea was covered by an adapted 1° by 1° sampling grid of 97 stations (+). Between the stations, continuous measurements of temperature, salinity and pCO_2 were carried out (dotted line).*

The pCO_2 in the surface waters was determined using an underway system with continuous flow equilibration. The water flow from the pump was about 60 L min^{-1}, which was reduced by a bypass just before the equilibrator to 2-3 L min^{-1}. The temperature difference between the equilibrator and the surface water was less than 0.5 K, and usually 0.1 K. The detection of pCO_2 was performed by a non-dispersive infrared spectrometer, which was calibrated against *National Oceanic and Atmospheric Administration* (NOAA) standards every 24 hours. The method is described in detail by Körtzinger et al. (1996) with an estimated error of approximately 1 µatm. The atmospheric pCO_2 was sampled at the antenna platform of the ship and determined every 2 hours.

Nitrate (NO_3^-), nitrite (NO_2^-) and phosphate (PO_4^{3-}) were analysed in all samples within 10 hours after sampling, using a technicon TRAACS 800 auto-analyser according to Grasshoff et al. (1983). The standard deviation for the sum of NO_3^- and NO_2^- ($NO_{2/3}$) was ± 0.02 µM and for PO_4^{3-} ± 0.01 µM. The estimated accuracy were ± 1.5% and 3%, respectively.

The oxygen concentration was measured by the Winkler method using a potentiometric end-point determination with an estimated accuracy of ± 2 µmol kg^{-1} (± 0.5% of level of saturation). The oxygen saturation level ($\%O_2$) and the apparent oxygen utilisation (AOU) were calculated from the observed concentrations of dissolved O_2 and the concentrations of O_2 at saturation using the algorithm proposed by Weiss (1970).

The sea-surface temperature and salinity were measured continuously with an AQUAFLOW thermo-salinograph with the water intake at a depth of about 3 meters. Temperature and salinity were calibrated vs. the CTD measurements.

The concentration of chlorophyll *a* was determined from GF/F filtered samples by the fluorimetric method based on the method by Holm-Hansen et al. (1965) with a precision of ± 4%.

3. Observations

3.1. Temperature and Salinity

The continuous measurements of salinity and temperature during the cruise allowed us to plot high resolution maps of these parameters in the surface water of the North Sea. A clear gradient of decreasing temperature is present in the North Sea from the south-east to the north-west (Figure 2a). Highest temperatures between 18°C and 19.2°C were observed in the shallow southern and south-eastern area, i.e., in the coastal areas, which receive large freshwater inputs from the English, Belgian, Dutch, German, and Danish coasts. High temperatures were also observed in the Skagerrak area, where high inputs of less saline water from the Baltic Sea and from the Norwegian coast occur. Lower temperatures were observed off the Humber estuary. The northern and north-western parts were characterised by temperatures of 11°C to 15°C. These low values, especially in the Shetlands Islands Channel, indicate water input from the North Atlantic Ocean via the northern boundary of the North Sea.

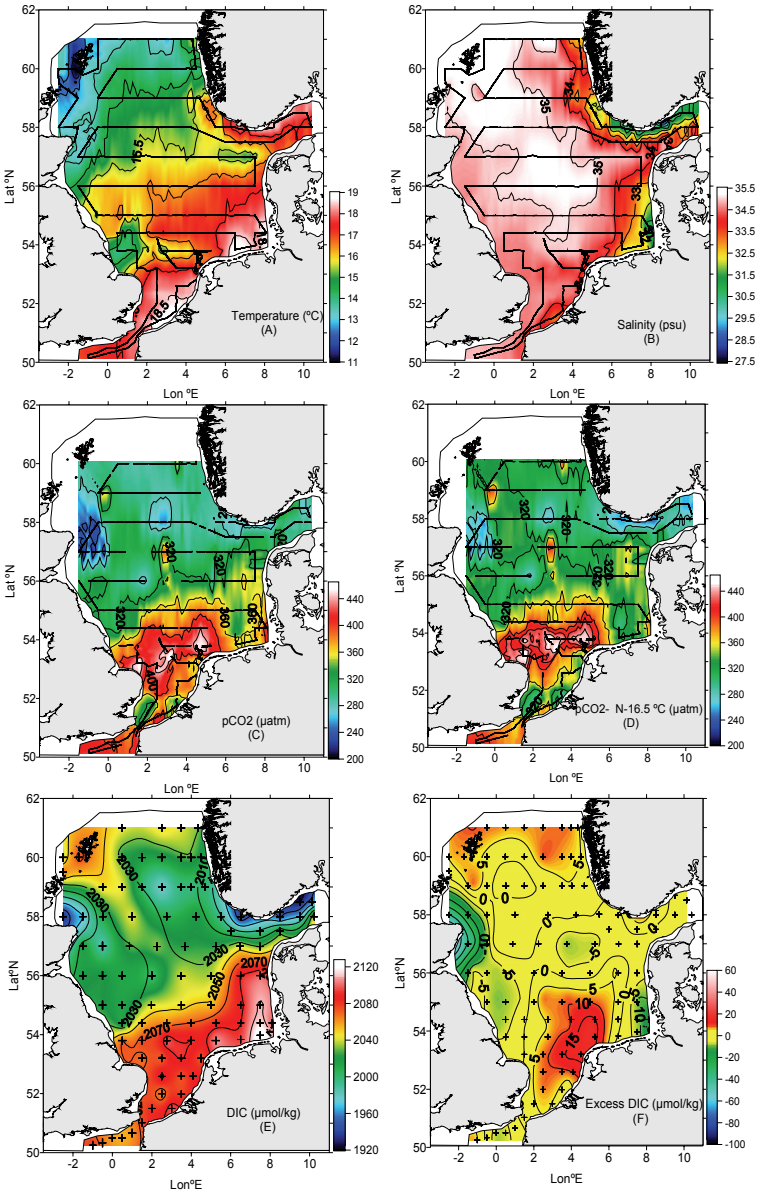

Figure 2: *Surface maps of temperature (a), salinity (b), the partial pressure of CO_2 (c), the partial pressure of CO_2 normalised to 16.5°C (d), DIC (e) and excess DIC (f). For (a), (b), (c) and (d), the black line represents the continuous measurements for these parameters. The crosses on (e) and (f) represent the sampled stations for DIC.*

West of the 4°E meridian, the North Sea is rather homogeneous in its surface salinity distribution with an average value of 34.5 (Figure 2b), except off the Scheldt estuary, where riverine water inputs resulted in a salinity of 32.8. Highest salinities (35.1) were observed close to the North Sea's boundaries with the Atlantic Ocean in the north and in the English Channel. East of the 4ºE meridian, the North Sea is characterized by lower salinity: Waters in the German Bight and in the adjacent Jutland waters had an average salinity of 32. Waters with lowest salinity of 27 were found in the Skagerrak area along the Norwegian south coast due to large inputs of less saline Baltic Sea water.

3.2. Observations of the CO_2 system and nutrients

The pCO_2 data recorded during the cruise allow us to plot the first high resolution map of pCO_2 for the North Sea in late summer (Figure 2c). Two different features of the pCO_2 distribution in the surface waters were observed, separating the North Sea in a southern and a northern region. In the south, pCO_2 was super-saturated relative to the atmosphere (atmospheric CO_2 value of 365 μatm) with values between 400 and 450 μatm. Highest values of pCO_2 were found in the German Bight and in the English Channel. The system changes from super-saturation to under-saturation in northward direction at approximately 54°N, where the North Sea becomes deeper and stratified. Thus, in the north the dominant feature was a strong CO_2 under-saturation of the surface waters with lowest values for the pCO_2 of 220 μatm observed in the Skagerrak area and the most northern region. The major features of the pCO_2 distribution remain visible after normalization of the pCO_2 values to the average temperature of 16.5°C (Figure 2d).

The DIC data show a similar pattern in surface waters (Figure 2e). Higher concentrations relative to the Central North Sea were found in the southern part with values of 2070 μmol kg^{-1} in the English Channel, 2100 μmol kg^{-1} along the Belgian, Dutch and southern English coasts, with a maximum of 2130 μmol kg^{-1} in the German Bight. High concentrations relative to the rest of the North Sea were found locally off the main estuaries: DIC concentrations were 2099, 2081, 2096, 2108 and 2130 μmol kg^{-1} for the stations off the Scheldt, Thames, Humber, Ems and Elbe estuaries, respectively. Lower concentrations were found in the northern region of the North Sea, where the DIC concentration ranged from 1930 to 2070 μmol kg^{-1}. Lowest values were found in the Skagerrak and near the Scottish coast, whereas higher concentrations relative to the rest of the northern North Sea were found at the North Atlantic Water inputs in the Shetland Channel and in the northwestern region.

The excess DIC (Figure 2f) has been calculated using the two linear regressions of Figure 3. We used the equation established for the Skagerrak area to calculate the DIC expected from a conservative mixing in the northern North Sea (54ºN-61ºN) and the equation established in the Southern Bight to calculate the DIC expected from a conservative mixing in the southern North Sea (51ºN-54ºN). The difference between the DIC measured and the DIC calculated gives the excess DIC. The surface map of excess DIC (Figure 2f) shows similar trend than the DIC surface map (Figure 2e) with positive values in the southern North Sea and small negative values in the northern North Sea.

The excess DIC allows us to identify the processes responsible for the DIC concentration observed in areas with important mixing such as the Southern Bight or Skagerrak area and will be discussed more in details in sections 4.2 and 4.3.

In late summer, at the end of the productive period the inorganic nutrients nitrate and phosphate were exhausted almost in the entire North Sea. South of 54°N the concentrations increased to 0.6 µM for $NO_{3/2}$ and 0.3 µM for PO_4^{3-}. In certain areas close to the estuaries of the rivers Thames, Scheldt, Humber and Elbe their concentrations were somewhat elevated up to 5 µM for $NO_{3/2}$ and 1 µM for PO_4^{3-}. Moreover, the areas directly affected by inputs of North Atlantic Ocean waters (English and Shetland islands Channels) show higher $NO_{3/2}$ concentration up to 3µM (Table 1).

4. Results and Discussion

4.1. Dissolved inorganic carbon versus salinity

The relationship between DIC and salinity is exploited in order to investigate the DIC water mass characteristics in the North Sea (Figure 3).

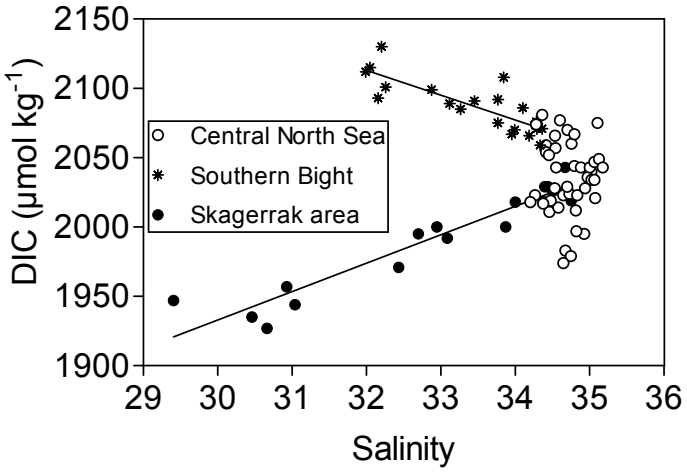

Figure 3: *Plots of surface water DIC versus salinity from CTD casts in the Central North Sea (o), Skageraak area (•) and Southern Bight (∗). Linear regression fits have the equations: DIC = -17.9S + 2685 (n = 20, r^2 = 0.7) for the Southern Bight and DIC = 20.5S + 1318 (n = 17, r^2 = 0.9) for the Skagerrak.*

In the surface waters the DIC/salinity relationship indicates the three main water masses in the North Sea, which govern the inorganic carbon distribution during late summer:

(1) The Central North Sea water, which has similar characteristics to the North Atlantic water of high salinity (≈35) and DIC concentrations between 2050 and 2070 μmol kg^{-1}.

(2) The Southern Bight water mass, which is influenced by the riverine water input from the southern English, Belgian, Dutch, German and Danish coasts. Accordingly, it has lower salinities (30-34) and high DIC concentrations compared to the central North Sea, between 2090 and 2130 μmol kg^{-1}.

(3) The Skagerrak water mass, which is formed by the outflowing water from the Baltic Sea and riverine water input from the southern Norwegian coast. It has lower salinities (30-34) and DIC concentrations between 1930 and 2030 μmol kg^{-1}.

Two linear trends can be obtained from the DIC-salinity scatter plot (Figure 3): one, with a negative slope encompassing the data from the Southern Bight and one with a positive slope which includes the samples from the Skagerrak and the southern Norwegian coast. Both regressions converge towards the Central North Sea water mass and represent the mixing of these three water masses.

Table 1: *Characteristics of the three main water masses influencing the surface water distribution of carbon dioxide during late summer. For each parameter, its concentration range in the surface layer is given for the 97 stations.*

	Southern Bight	Central North Sea	Skagerrak
Salinity	31.2-34.5	≈ 35	27.2-34.5
Temperature (ºC)	14.0-19.2	11.0-16.0	16.5-19.0
DIC (μmol kg^{-1})	2060-2130	2000-2070	1930-2030
pCO_2 (μatm)	290-490	220-350	190-300
$NO_{3/2}$ (μM)	0-4.70	0-0.20	0-0.20
PO_4^{3-}(μM)	0-1.00	0-0.05	0-0.04

The corresponding source water masses with DIC concentrations between 2090 and 2130 μmol kg^{-1} originate from the NW European, "lime-rich" continental landmass. The Baltic Sea water is characterized by low DIC concentrations relative to the two other

water masses. In the Baltic Proper, the low DIC surface water from the Scandinavian coast (originating from lime poor drainage areas) mixes with relatively high DIC surface water from the south-eastern Baltic Proper (originating from lime rich drainage areas) as reported by Thomas and Schneider (1999) and Thomas et al. (2003a). Characteristics of these three water masses are given in Table 1.

4.2. The CO_2 system in the northern North Sea

In order to explain the differences in pCO_2 and DIC concentrations between the northern and the southern North Sea, it is important to consider the influence of the bottom topography of the North Sea, which constitutes a major control for the biogeochemical cycling.

Profiles of DIC in the northern part of the North Sea showed a clear stratification of the water column, with low concentrations in the surface layer and higher concentrations in the deeper layer (Figure 4a, see also Figure 6b). The low DIC values in the surface layer were related to negative apparent oxygen utilization (AOU), i.e., oxygen production (Figure 4b and Figure 5), and depleted $NO_{3/2}$ and PO_4^{3-} conditions (Figures 4c and 4d). This indicates DIC, i.e. CO_2, NO_3^- and PO_4^{3-} consumption as well as oxygen release by primary production. In the northern North Sea, the biological production dominates the remineralization in the autotrophic upper layer of the water column and controls the CO_2 distribution. On the other hand, the increase in DIC concentrations within the deeper layer was caused by remineralization of organic matter, which had been exported to the deeper layer, as seen from the positive AOU and the increasing $NO_{3/2}$ and PO_4^{3-} concentrations in the deeper layer (see also Thomas et al., 1999; Osterroht and Thomas, 2000). This strong remineralization of particulate organic matter (POM) is predominant in the deeper layer of the northern North Sea, which makes this part of the water column heterotrophic. A direct consequence is that only a minor amount of carbon accumulates in the bottom sediments, which accounts for only less than 1% of the primary production in the North Sea (De Haas, 1997; De Haas et al., 2002).

In the Skagerrak area, at the transition to the Baltic Sea, the excess DIC value of approximately zero (Figure 2f) implies that the DIC concentrations found for the area are in the expected range when the less saline water from the Baltic sea mixes with Central North Sea water. The average value of 1900 μmol kg^{-1} found for DIC in this area is also in good agreement with values reported by Thomas and Schneider (1999). For the same range of salinity, between 30 and 31, these authors reported a similar value of 1900 μmol kg^{-1} in summer. This value is the result of biological production occurring in both the surface waters of the Baltic and the North Seas during spring and early summer, then mixed in the Skagerrak area.

Figure 2c and 2e show that along the northern Scottish coast and near the Shetland Islands, the DIC and pCO_2 are different from those in the more homogeneous central North Sea:

At the stations located at 58°N; 2.5°W and 58°N; 1.5°W, surface water DIC concentrations were around 1950 μmol kg^{-1} and pCO_2 was as low as 220 μatm. The strong oxygen super-saturation (AOU =-90 μmol kg^{-1}) and the low $NO_{3/2}$ and PO_4^{3-} concentrations in this area suggest that a phytoplankton bloom has developed there. This is confirmed by the higher chlorophyll concentrations of 4 to 5 μg L^{-1} present in this area compared to the remaining northern North Sea, where the average value was approximately 1 μg L^{-1}. The negative concentrations calculated for the excess DIC in this area also confirmed that strong biological production occurs in this area and reduces the DIC concentrations relative to the concentration expected with regard to the mixing line on Figure 3.

At the stations near the Orkney (59.5°N; 2.5°W) and Shetland Islands (60°N; 1.7°W), the concentrations of DIC, nitrate and phosphate were higher than in the northern North Sea, with values of 2070 μmol kg^{-1} (Figure 2e), 2.3 and 0.4 μmol L^{-1}, respectively. The water column at the station near the Orkney Islands was mixed down to the bottom (77 meters) by strong tidal currents in this area (Turrell et al., 1992). Therefore, no export of POM is possible from the surface layer and this POM is remineralized in the deeply mixed surface layer, which promoted relatively high DIC concentrations at this stations.

4.3. The CO_2 system in the shallow southern North Sea

In the North Sea, south of 54ºN, the surface distributions of pCO_2 and DIC (Figures 2c and 2e) revealed higher concentrations than in the northern North Sea. The pCO_2 data have been normalized to a temperature of 16.5°C representing the average surface water temperature during the cruise in order to eliminate the effects of different temperatures on the pCO_2 distribution (Figure 2d). The distributions of the normalized and the *in situ* data showed a similar pattern, providing evidence that the higher surface water temperature in the southern North Sea was not primarily responsible for the higher pCO_2 in this area. These higher concentrations in the southern North Sea can be explained by the mixing regime of the water column. In this part of the North Sea, the water column is entirely mixed even in late summer because of the shallow depths and the strong tidal currents as high as 1 m s^{-1} (Eisma, 1987). During our late summer cruise, vertical profiles of salinity and temperature (not shown) did not show any stratification in this area (compare Figure 4). The DIC profiles recorded at stations in the southern part of the North Sea, i.e. south of 54°N, showed a homogeneous concentration throughout the water column (Figure 4a). Positive values of AOU (Figures 4b and 5) associated with these higher concentrations of DIC suggest that remineralization of POM and/or inputs of brackish water, rich in organic matter occurred in the mixed water column, thus increasing the surface concentrations of DIC. This was confirmed by the moderate concentrations in $NO_{3/2}$ and PO_4^{3-} (Figures 4c and 4d) observed throughout the water column for most stations in the Southern Bight and by the positive values calculated for excess DIC (Figure 2f) in the surface layer of this area.

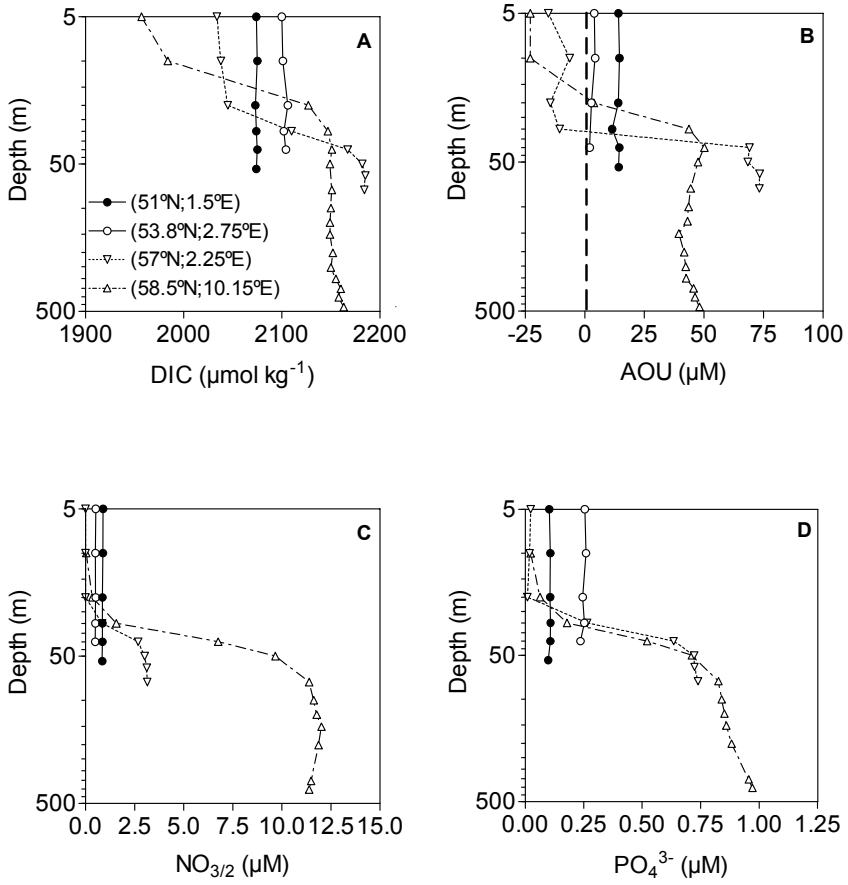

Figure 4: *Profiles of DIC (a), AOU (b), $NO_{3/2}$ (c) and PO_4^{3-} (d) in the southern and northern North Sea. Stations were situated at 51.00ºN; 1.50ºE (•), 53.80ºN; 2.75ºE (o), 57.00ºN; 2.25ºE (∇) and 58.50ºN; 10.15ºE (Δ). Depths are shown on a logarithmic scale.*

In the southern North Sea several stations, notably near the mouth of the Thames, Scheldt, Elbe and Humber estuaries, showed high DIC concentrations, where oxygen concentrations were slightly above the saturation level (Figure 5). This suggests that the terrestrial water inputs, enriched in dissolved inorganic carbon and nutrients, stimulated primary production within a narrow band of the coastal or estuarine waters. For example, the area situated in front of the Elbe estuary showed concentrations of DIC up to

2130 µmol kg^{-1} (Figure 2e) and negative values for the excess DIC calculated for this area (Figure 2f). This implies that the DIC concentrations found in this area are lower than expected with regard to the mixing line of brackish water from north European estuaries with Central North Sea water (Figure 3). At these stations the biological production dominates the remineralization of POM and induces an autotrophic state of the entirely mixed water column in a narrow band along the coast of the southern Bight.

To summarize, in most of the southern North Sea, the remineralization of POM dominates the biological production for the entire water column, which generates an overall heterotrophic state in late summer. Only at few stations along the coast influenced by riverine inputs from the main estuaries, the biological production dominates the remineralization of POM, which generates an autotrophic state of the water column.

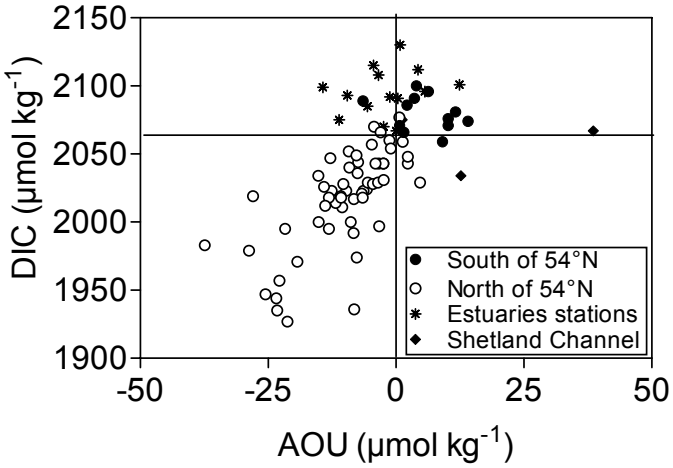

Figure 5: *DIC plotted versus AOU at 5 meters depth in the North Sea, south of 54°N (•), north of 54°N (o), influenced by freshwater inputs (*) and in the Shetland Channel (♦).*

4.4. The air-sea CO_2 fluxes during late summer

The flux (F) of CO_2 across the air-sea interface can be calculated using the formula:

$$F = k \times \alpha \times \Delta pCO_2 \qquad (1)$$

where k is the gas transfer velocity, α is the solubility coefficient of CO_2 calculated after Weiss (1974) and ΔpCO_2 (pCO_{2water}-pCO_{2air}) is the air-water gradient of pCO_2. This parameterization implies that fluxes at the air-sea interface into the surface water (sink) are

denoted with a negative sign, whereas fluxes into the atmosphere (source) are denoted by a positive sign. The gas transfer velocity is influenced by various factors such as air bubbles, surface films and air and water turbulence (Liss and Merlivat, 1986; Wanninkhof, 1992), but the wind speed has been recognised as the main force driving the gas exchange at the air-sea interface. Several algorithms have been proposed for the k-wind speed relationship. In our calculations we use the k-wind speed relationships proposed by Liss and Merlivat (1986), Wanninkhof (1992), Wanninkhof and McGillis (1999), Nightingale et al. (2000a), Nightingale et al. (2000b), hereafter referred to as L&M86, W92 (short term relationship), W&McG99 (short term relationship), N2000a and N2000b, respectively. In fact, it is difficult to choose one relationship because even the latest experiments using the most recent tracer techniques applied for N2000a and N2000b could not reliably distinguish, which was the more favourable relationship. We therefore chose to report the results computed with the different formulations. This is particularly important for the North Sea in late summer, where two different features (e.g. super-saturation in the southern North Sea, under-saturation in the northern North Sea) have opposing effects on the overall fluxes of CO_2 for the whole area.

We computed the CO_2 fluxes employing the above different parameterizations of the gas transfer velocity, using two different datasets for wind speeds:

The in-situ wind speeds recorded during the cruise were used to calculate instantaneous CO_2 fluxes. The wind speeds were corrected from 27 meters (height of the vessel's anemometer) to 10 meters using the relationship by Johnson (1999). The ΔpCO_2 values were calculated for the 22 000 surface water measurements, using an atmospheric partial pressure of CO_2 of 365 µatm, which was the average value of all the atmospheric measurements performed during the cruise. For each ΔpCO_2 observation, the CO_2 flux was calculated using the *in situ* wind speed and the different k parameterisations. The fluxes were interpolated onto a 0.05° by 0.05° grid in order to determine the flux for the two areas located between 51°N to 54°N and between 54°N to 60°N, as well as for the North Sea as a whole in late summer 2001 (Table 2).

We also used the 6-hourly wind speed data from the European Centre for Medium-Range Weather Forecast (ECMWF) 40-years reanalysis project (ECMWF, 2002): The wind speed data were recalculated for our cruise by ECMWF from observations made in the North Sea for this period. The North Sea was divided in 13 boxes (Thomas et al., 2004). For each box, the gas transfer velocity was calculated every six hours using ΔpCO_2 calculated from the measurements (Figure 2c) and the wind speed from ECMWF. The fluxes were calculated for each of the 13 boxes, using the 5 different formulations. These results were then used to obtain the fluxes in the two above areas as well as for the North Sea as a whole (Table 2). In the following discussion the first approach will refer to the calculations using the instantaneous wind speeds, whereas the second approach will refer to the calculations using the 6-hourly wind speed from the ECMWF project.

Table 2: *The CO_2 fluxes calculated using the two different approaches: using the instantaneous winds speeds recorded on board (1) and the wind speed data recalculated for our cruise by ECMWF from observations made in the North Sea for this period (2). Positive values denote fluxes into the atmosphere, whereas negative values denote fluxes into the surface water of the North Sea. L&M86 is the formulation from Liss and Merlivat (1996); W92 is the short term formulation given by Wanninkhof (1992); W&Mc99 is the short term formulation given by Wanninkhof and Mc Gillis (1999); N2000a corresponds to the formulation given by Nightingale et al. (2000a); and N2000b is the formulation given by Nightingale et al. (2000b).*

	51°N-54ºN	54 ºN-60°N	North Sea
Range of pCO_2 (µatm)	287-487	190-448	190-487
Average ΔpCO_2 (µatm)	+26	-43	-26
Average of instantaneous wind speed (m s^{-1})	10.5	8.5	8.9
Monthly average wind speed ECMWF (m s^{-1})	7.8	8.2	8.1
Fluxes of CO_2 (mmol m^{-2} day^{-1}) calculated using the algorithms by:			
L&M86 (1)	+3.7	-3.9	-2.1
(2)	+0.8	-2.4	-1.5
W92 (1)	+6.3	-6.3	-3.4
(2)	+1.7	-3.2	-1.6
W&Mc99 (1)	+8.3	-5.0	-1.8
(2)	+0.8	-2.9	-1.8
N2000a (1)	+4.8	-5.2	-2.8
(2)	+1.4	-3.8	-2.2
N2000b (1)	+4.6	-4.7	-2.5
(2)	+1.3	-3.4	-2.0

For the southern North Sea, the results obtained using the first approach is a factor of five to six higher than the results obtained with the second approach (Table 2). For this area, this large difference in the results are mainly due to the difference between the instantaneous wind speeds recorded on board and the actual wind speeds given by the ECMWF project for the time of observation. An event of strong winds (up to 25 m s^{-1}) occurred when sampling the southern area. Therefore the average of instantaneous wind speeds recorded along the cruise track in this area was 10.5 m s^{-1}, not typical for this period

of the year, when the 6-hourly ECWMF wind speed was on average 7.8 m s^{-1} for the whole month and the entire southern area. The CO_2 air-sea flux calculation using the instantaneous wind speed on a monthly basis is thus biased by the above storm event, which is extrapolated to the entire area. Associated with high surface pCO_2 these high wind speeds are responsible for the much higher fluxes calculated in this area using the first approach. This implies that the extrapolation of instantaneous wind speed is not reliable for budgeting the CO_2 fluxes.

The fluxes obtained with the instantaneous wind speeds range from +3.7 to +8.3 mmol m^{-2} day^{-1} using L&M86 and W&Mc99, respectively (Table 2). This large difference is due to the different formulations of the L&M86 and W&Mc99 relationships between gas exchange and wind speed. The L&M86 can be closely approximated by a quadratic relationship over a wind speed range of 0 to 15 m s^{-1} whereas the W&Mc99 relationship is a cubic relationship between the wind speed and the gas transfer velocity. For both relationships the gas transfer increases at an exponential rate as a function of the wind speed, which explains the large difference in the calculations. On the other hand, for the second approach, the value of +0.8 mmol m^{-2} day^{-1} found with W&Mc99 is in the same range of values obtained with the other formulations. The 6-hourly reanalysis wind speeds tend to average out the very extreme events through spatial and temporal gridding processes. As a consequence, the wind speeds from ECMWF are in a range of value where the L&M86 and W&Mc99 calculations give similar values for the gas transfer velocity.

For the northern North Sea, results from the two different approaches are in rather good agreement. Fluxes calculated using the instantaneous wind speeds range from -3.9 to -6.3 mmol m^{-2} day^{-1} for L&M86 and W92, respectively, whereas in the second approach fluxes range from -2.4 to -3.8 mmol m^{-2} day^{-1} for L&M86 and N2000a, respectively. The slightly higher fluxes calculated using the first approach are surely due to the slightly higher average instantaneous wind speed (8.5 m s^{-1}) compared to the ECMWF average wind speed (8.2 m s^{-1}). The comparison of the two approaches shows that fluxes calculated from instantaneous wind speeds should only be used when the wind speeds recorded are typical of the meteorological conditions usually encountered in the studied area. For *in situ* investigations, the application of the instantaneous fluxes is obvious, whereas for budgeting approaches these fluxes depend too much on the local and in situ weather situation. Therefore, for budgeting approaches it appears to be more reasonable to refer to CO_2 fluxes obtained using high resolution wind field data for the time of observation. For the following discussion, we will thus only focus on the fluxes calculated with our second approach using the ECMWF wind speed data.

For the southern North Sea, the average ΔpCO_2 was +26 µatm, with a maximum value of +122 µatm (Figure 2c). Therefore, the results from the five formulations show that the area situated between 51°N and 54°N releases CO_2 into the atmosphere at a rate between +0.8 and +1.7 mmol m^{-2} day^{-1} during late summer. On the other hand, the northern area showed an average ΔpCO_2 of –43 µatm, with areas strongly under-saturated like in the Skagerrak with ΔpCO_2 values of –176 µatm (Figure 2c). The results from the five formulations show that the area situated between 54°N and 60°N absorbs CO_2 at a rate ranging from -2.4 to -3.8 mmol m^{-2} day^{-1}. The North Sea as a whole acts as a sink of CO_2

for the atmosphere in late summer in the range of -1.5 to -2.2 mmol m^{-2} day^{-1}, despite the fact that at this time of the year, the southern part of the North Sea is a source of CO_2 for the atmosphere. This flux is lower than the values of -3.9 mmol m^{-2} day^{-1} and -16.4 mmol m^{-2} day^{-1} found in May-June by Kempe and Pegler (1991) and Frankignoulle and Borges (2001), respectively, both using the L&M86. In those two studies the surface waters of the southern bight of the North Sea were under-saturated in CO_2 compared to the atmosphere. Thus, this area was a sink of atmospheric CO_2 and enhanced the CO_2 uptake for the whole North Sea, which explains the higher fluxes reported by these authors. However, they confirmed that in the areas where the water column was entirely mixed (the Dogger Bank, for Kempe and Pegler, 1991), the surface water released CO_2 to the atmosphere. In our study in late summer, as explained in section 4.3, the water column in the Southern Bight was completely mixed and remineralization of POM was responsible for the higher source of CO_2 in the whole southern bight of the North Sea.

Thomas and Schneider (1999), using the W92 algorithms found that the surface waters of the Baltic Sea act as a strong sink of CO_2 of approximately -6.4 mmol m^{-2} day^{-1} in summer. Similarly, Tsunogai et al. (1997), Tsunogai et al. (1999) and Wang et al. (2000) found values between -1.8 and -4.7 mmol m^{-2} day^{-1} for the East China Sea using L&M86 and W92, respectively. Compared to the latter coastal seas and the results for the North Sea by Kempe and Pegler (1991) and Frankignoulle and Borges (2001) in early summer, our study shows that the North Sea acts as a weak sink of CO_2 for the atmosphere during late summer (mid August-September).

4.5. The North Sea: a Continental Shelf Pump

Once the CO_2 has been absorbed by the North Sea in summer, the fundamental issue concerning its eventual fate is related to the water circulation in the North Sea. The dominant feature in the North Sea is an anticlockwise circulation entering the North Sea west and east of the Shetland Channel. The current turns north-eastward in the central North Sea before finally leaving the North Sea along the Norwegian coast (Figure 6) (Thomas et al., 2003b). As a consequence of the circulation pattern, the most prevailing feature of the semi-enclosed North Sea is the short residence time of this water, which is less than one year (Lenhart and Pohlmann, 1997).

In the subsurface layer, the above strong remineralization of exported organic material increases the DIC concentrations and prevents carbon accumulation in the bottom sediments, which amounts to less than 1% of the primary production (De Haas, 1997; De Haas et al., 2002). Therefore, the inorganic carbon, which has been transported from the atmosphere into the subsurface layer, ultimately can be exported to the Atlantic Ocean. The transfer of atmospheric CO_2 from the atmosphere to the North Sea is evident from increasing specific DIC concentrations (water column inventory of DIC divided by the water column depth) along the pathway of the Atlantic Ocean water through the North Sea. Within the inflowing western branch, the specific DIC concentration increases in southward direction (Figure 6a), whereas within the outflowing eastern branch, the specific DIC concentration increases northward (Figure 6b). Comparing the idealised entrance and exit

of the Atlantic Ocean water at the Shetland Islands and the Norwegian coast, respectively, also here an increase of the specific DIC can be observed between inflowing and outflowing waters (from west to east, Figure 6c).

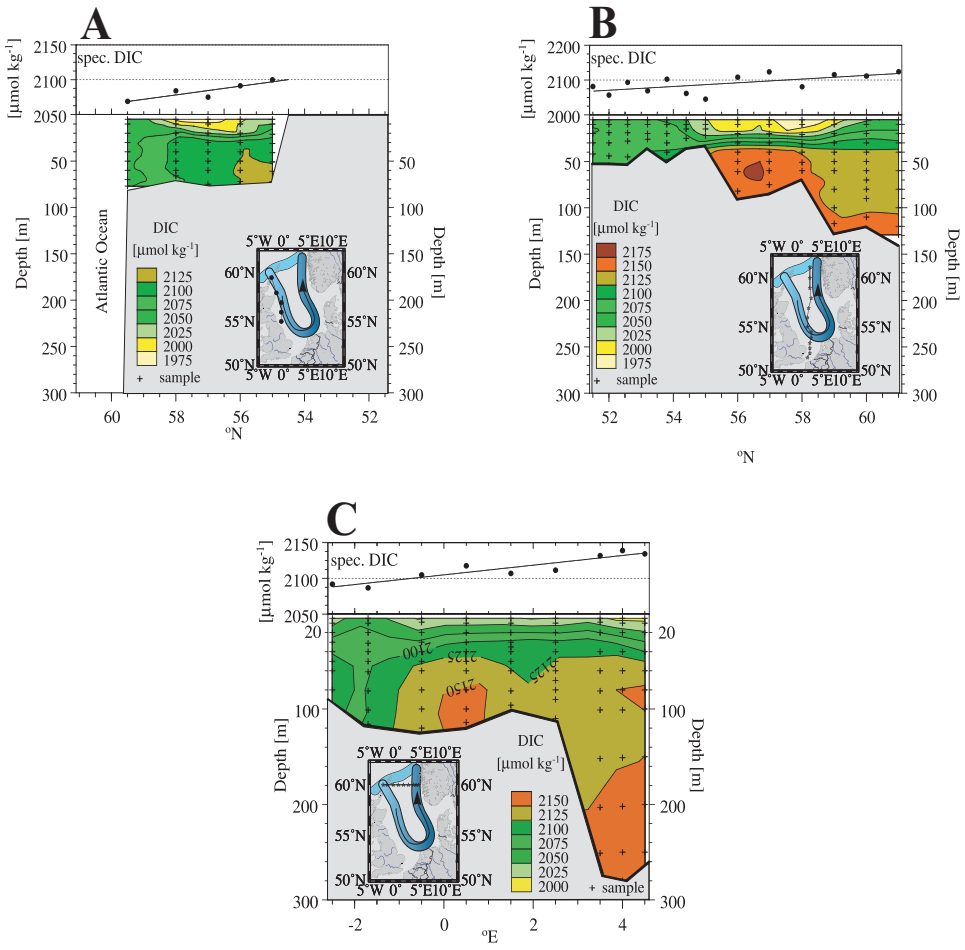

Figure 6: *Three sections of DIC (bottom panels) and specific DIC concentrations (top panels). Section on A covers the western, inflowing branch of the Atlantic Ocean circulation at approximately 0.5°W. The section on B covers the outflowing eastern branch at 2.5°E and the west-east section on C at 60°N shows the DIC concentrations at the entrance and at the exit, respectively. The underlying blue scheme indicates the general circulation and its darkening blue colour implies increasing DIC concentrations.*

The specific DIC concentration in the Atlantic Ocean water mass increases by 40 μmol kg^{-1} during the transport through the North Sea (Figure 6c). This DIC increase is generated both by the CO_2-uptake from the atmosphere and also by a net loss of dissolved organic carbon (DOC) in the northern North Sea as indicated by the higher DOC concentrations found in the inflowing compared to the outflowing waters (Thomas et al., 2004). Since the outflow of water along the Norwegian trench is 4725 km^3 $month^{-1}$ and this water is enriched with 40 μmol kg^{-1}, we estimate that 18.9×10^{10} mol C $month^{-1}$ is exported to the North Atlantic water during late summer when, at the same time, the North Sea absorbs 2.8×10^{10} mol C $month^{-1}$ from the atmosphere. Therefore, during late summer, the North Sea absorbs from the atmosphere a quantity of CO_2 equal to 15% of the carbon exported to the North Atlantic Ocean, implying that the North Sea acts as a continental shelf pump, further enhanced by heterotrophic activities.

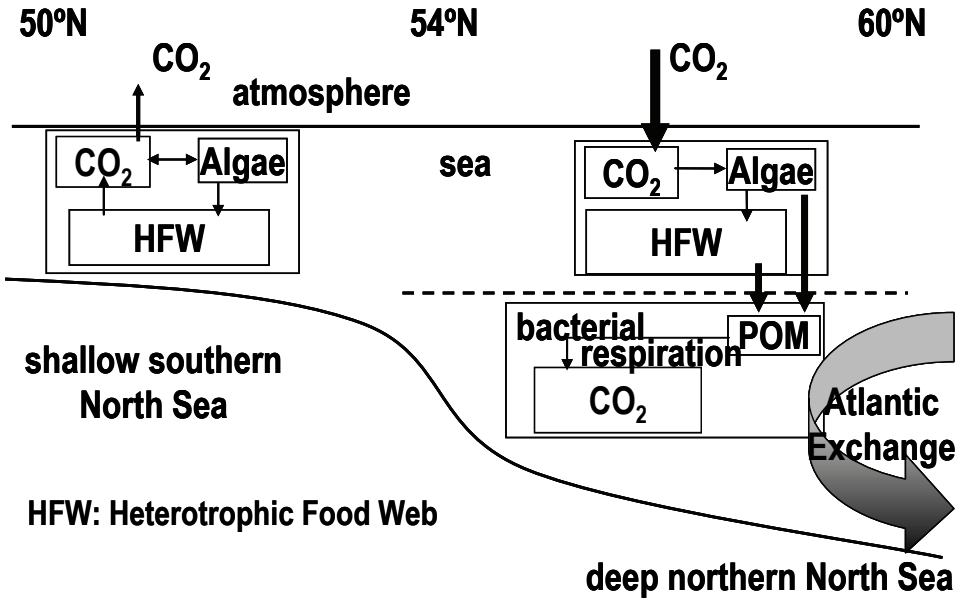

Figure 7: *Schematic representation of the mechanism of the continental shelf pump in the North Sea. Redrawn after Thomas et al. (2004).*

With regard to the hypothesis of the continental shelf pump to the North Sea, the two major hydrographical regimes exert a major control, on whether and on how much CO_2 is transferred from the atmosphere to the adjacent North Atlantic Ocean (Figure 7). For the shallower southern region the biological carbon cycling occurs in the mixed surface layer. This means that biological production by algae and respiration processes by heterotrophic

food web occur in the same compartment (Figure 7) avoiding or diminishing net effects of the carbon cycling on the DIC concentrations in the water column, since no export of POM into the subsurface layer is possible. The obvious consequence for this is the observed super-saturation of the surface waters in the southern region (Figure 2c). In contrast, in the northern region the stratification of the water column enables the export of POM from the surface layer to the deeper water column, thereby separating production from bacterial respiration processes. The POM is respired in the deeper layer and DIC is released. A net transport of carbon from the surface layer to the deeper layers occurs, which is ultimately replenished from the atmosphere. This is evident from the observed under-saturation of the surface waters in the northern region (Figure 2c) as well as from the increasing DIC concentrations in the subsurface layer (Figure 4a and Figure 6). The subsurface layer is then subjected to water mass transport to the North Atlantic Ocean (Figure 7), finally a net CO_2 transport from the atmosphere to the North Atlantic Ocean takes place.

5. Summary

The distributions of DIC and pCO_2 in the North Sea in late summer are mainly driven by the mixing regime of the water column influenced by the bottom topography of the North Sea. A clear boundary is evident in the distribution of DIC and pCO_2 as well as for related parameters such as AOU, $NO_{3/2}$ and PO_4 at 54°N. South of this border, the strong tidal currents mix the entirely shallow water column down to the bottom. By consequence the degradation of POM releases inorganic carbon into the surface water of this area. North of 54°N, the deeper water column is stratified, which results in a spatial separation of biological carbon uptake in the surface layer and degradation of POM in the bottom layer.

In the Southern Bight, inputs of less saline water from the major European estuaries with high inorganic carbon content increase the surface water concentration of DIC along the coast. In the northern part, inputs of less saline water from the Baltic Sea with a low DIC content dilute the dissolved inorganic carbon concentrations.

The southern North Sea acts as a source of CO_2 for the atmosphere in late summer with fluxes of +0.8 to +1.7 mmol m^{-2} day^{-1}, whereas the northern part acts as a sink of CO_2 for the atmosphere at a rate of -2.4 to -3.8 mmol m^{-2} day^{-1}. The North Sea as a whole constitutes a sink of atmospheric CO_2 ranging from -1.5 to -2.2 mmol m^{-2} day^{-1} or 0.4×10^{12} g C $month^{-1}$ despite the source in the southern part. This atmospheric CO_2 increases the DIC content of the deeper layer of the water column via the biological pump. In late summer, the North Sea exports 2.2×10^{12} g C $month^{-1}$ to the North Atlantic Ocean via the Norwegian trench. During the same period the North Sea takes up from the atmosphere a quantity of CO_2 equal to 15% of what is exported. The increase in DIC concentrations in the bottom layer is the result of CO_2 pumping occurring during the year and the remainder is generated by heterotrophic activities. During late summer the North Sea thus acts as a continental shelf pump exporting the CO_2 taken up from the atmosphere to the North Atlantic Ocean.

References

Bakker, D.C.E., de Baar, H.J.W., de Wilde, H.P.J., 1996. Dissolved carbon dioxide in Dutch coastal waters. Marine Chemistry, 55 (3-4): 247-263.

Borges, A.V. and Frankignoulle, M., 1999. Daily and seasonal variations of the partial pressure of CO_2 in surface seawater along Belgian and southern Dutch coastal areas. Journal of Marine Systems, 19: 251-266.

Borges, A.V. and Frankignoulle, M., 2002. Distribution and air-water exchange of carbon dioxide in the Scheldt plume off the Belgian coast. Biogeochemistry, 59: 41-67.

Brasse, S., Reimer, A., Seifert, R., Michaelis, W., 1999. The influence of intertidal mudflats on the dissolved inorganic carbon and total alkalinity distribution in the German Bight, southeastern North Sea. Journal of Sea Research, 42: 93-103.

Brasse, S., Nellen, M., Seifert, R., Michaelis, W., 2002. The carbon dioxide system in the Elbe estuary. Biogeochemistry, 59: 25-40.

De Haas, H., 1997. Transport, preservation and accumulation of organic carbon in the North Sea. Ph.D Thesis, Universiteit Utrecht, Utrecht, 149 pp.

De Haas, H., Van Weering, T.C.E., De Stigter, H., 2002. Organic carbon in shelf seas: sinks or sources, processes and products. Continental Shelf Research, 22: 691-717.

ECMWF, 2002. 40-year reanalysis of wind data ERA40. WWW Page, http://www.ecmwf.int.

Eisma, D., 1987. The North Sea: an overview. Phil. Trans. R. Soc. Lond., B316: 461-485.

Frankignoulle, M., Bourge, I., Canon, C., Dauby, P., 1996a. Distribution of surface seawater partial CO_2 pressure in the English Channel and in the Southern Bight of the North Sea. Continental Shelf Research, 16 (3): 381-395.

Frankignoulle, M., Bourge, I., Wollast, R., 1996b. Atmospheric CO_2 fluxes in a highly polluted estuary (the Scheldt). Limnology and Oceanography, 41 (2): 365-369.

Frankignoulle, M., Elskens, M., Biondo, R., Bourge, I., Canon, C., Desgain, S., Dauby, P., 1996c. Distribution of inorganic carbon and related parameters in surface seawater of the English Channel during spring 1994. Journal of Marine Systems, 7: 427-434.

Frankignoulle, M., Abril, G., Borges, A., Bourge, I., Canon, C., Delille, B., Libert, E., Théate, J.-M., 1998. Carbon dioxide emission from European estuaries. Science, 282: 434-436.

Frankignoulle, M. and Borges, A.V., 2001. European continental shelf as a significant sink for atmospheric carbon dioxide. Global Biogeochemical Cycles, 15 (3): 569-576.

Gattuso, J.-P., Frankignoulle, M., Wollast, R., 1998. Carbon and carbonate metabolism in coastal aquatic ecosystems. Annual Reviews of Ecological Systems, 29: 405-434.

Grasshoff, K., Ehrhardt, M., Kremling, K., 1983. Methods of seawater analysis. Verlag Chemie, 2nd edition, Weinheim.

Gruber, N. and Keeling, C.D., 2001. An improved estimate of the isotopic air-sea disequilibrium of CO_2: Implications for the oceanic uptake of anthropogenic CO_2. Geophysical Research Letters, 28 (3): 555-558.

Holm-Hansen, O., Lorenzen, C.J., Homes, R.W., Strickland, J.D.H., 1965. Fluorometric Determination of Chlorophyll. Journal de Conseil pour l'Exploration de la Mer, 30 (1): 3-15.

Hoppema, J.M.J., 1990. The distribution and seasonal variation of alkalinity in the Southern Bight of the North Sea and in the western Wadden Sea. Netherlands Journal of Sea Research, 26 (1): 11-23.

Hoppema, J.M.J., 1991. The seasonal behaviour of carbon dioxide and oxygen in the coastal North Sea along the Netherlands. Netherlands Journal of Sea Research, 28 (3): 167-179.

IPCC, 2001. The scientific basis. In: J.T. Houghton et al. (Editors), Contribution of Working Group I to the Third Assessment Report of the Intergovernmental Panel on Climate Change. Cambridge University Press, New York, USA.

Johnson, K.M., Wills, K.D., Butler, D.B., Johnson, W.K., Wong, C.S., 1993. Coulometric total carbon dioxide analysis for marine studies: maximizing the performance of an automated gas extraction system and coulometric detector. Marine Chemistry, 44: 167-187.

Johnson, H.K., 1999. Simple expressions for correcting wind speed data for elevation. Coastal engineering, 36: 263-269.

Kempe, S., Liebezeit, V., Dethlefsen, V., Harms, U., 1988. Biogeochemistry and Distribution of Suspended Matter in the North Sea and Implications to Fisheries Biology, Inst. Univ. Hamburg, Heft 65, 552 pp.

Kempe, S. and Pegler, K., 1991. Sinks and sources of CO_2 in coastal seas: the North Sea. Tellus, 43B: 224-235.

Kempe, S., 1995. Coastal seas: a net source or sink of atmospheric carbon dioxide? LOICZ/R&S/95-1, vi + 27 pp., LOICZ, Texel, The Netherlands.

Körtzinger, A., Thomas, H., Schneider, B., Gronau, N., Mintrop, L., Duinker, J.C., 1996. At-sea intercomparison of two newly designed underway pCO_2 systems — encouraging results. Marine Chemistry, 52: 133-145.

Lee, K., Wanninkhof, R.H., Takahashi, T., Doney, S., Feely, R.A., 1998. Low interannual variability in recent oceanic uptake of atmospheric carbon dioxide. Nature, 396: 155-159.

Lenhart, H. and Pohlmann, T., 1997. The ICES-boxes approach in relation to results of a North Sea circulation model. Tellus, 49A (1): 139-160.

Liss, P.S. and Merlivat, L., 1986. Air-sea gas exchange rates: Introduction and synthesis. In: P. Buat-Ménard (Editor), The Role of Air-Sea Exchange in Geochemical Cycling. D. Reidel Publishing Company, pp. 113-127.

Mackenzie, F.T., Lerman, A., Ver, L.M., 1998. Role of continental margin in the global carbon balance during the past three centuries. Geology, 26 (5): 423-426.

Nightingale, P.D., Liss, P.S., Schlosser, P., 2000a. Measurements of air-sea gas transfer during an open ocean algal bloom. Geophysical Research Letters, 27 (14): 2117-2120.

Nightingale, P.D., Malin, G., Law, C.S., Watson, A.J., Liss, P.S., Liddicoat, M.I., Boutin, J., Upstill-Goddard, R.C., 2000b. In situ evaluation of air-sea gas exchange

parameterizations using novel conservative and volatile tracers. Global Biogeochemical Cycles, 14 (1): 373-387.

Orr, J.C., Maier-Reimer, E., Mikolajewicz, U., Monfray, P., Sarmiento, J.L., Toggweiler, J.R., Taylor, N.K., Palmer, J., Gruber, N., Sabine, C.L., Le Quéré, C., Key, R.M., Boutin, J., 2001. Estimates of anthropogenic carbon uptake from four three-dimensional global ocean models. Global Biogeochemical Cycles, 15 (1): 43-60.

Osterroht, C. and Thomas, H., 2000. New production enhanced by nutrient supply from non-Redfield remineralisation of freshly produced organic material. Journal of Marine Systems, 25: 33-46.

Pegler, K. and Kempe, S., 1988. The carbonate system of the North Sea: determination of alkalinity and TCO_2 and calculation of PCO_2 and Sl_{cal} (spring 1986). Mitt. Geol.-Paläont. Inst. Univ. Hamburg, 65: 35-87.

Postma, H. and Rommets, J.W., 1984. Variations of particulate organic carbon in the Central North Sea. Netherlands Journal of Sea Research, 18: 31 pp.

Smith, S.V. and Hollibaugh, J.T., 1993. Coastal metabolism and the ocean organic carbon balance. Reviews of Geophysics, 31 (1): 75-89.

Stoll, M.H.C., 1994. Inorganic carbon behaviour in the North Atlantic Ocean. Ph.D Thesis, Rijksuniversiteit Groningen, Groningen, 193 pp.

Thomas, H., Ittekkot, V., Osterroht, C., Schneider, B., 1999. Preferential recycling of nutrients - the ocean's way to increase new production and to pass nutrient limitation? Limnology and Oceanography, 44 (8): 1999-2004.

Thomas, H. and Schneider, B., 1999. The seasonal cycle of carbon dioxide in the Baltic Sea surface waters. Journal of Marine Systems, 22: 53-67.

Thomas, H., England, M.H., Ittekkot, V., 2001. An off-line 3D model of anthropogenic CO_2 uptake by the oceans. Geophysical Research Letters, 28 (3): 547-550.

Thomas, H., Pempkowiak, J., Wulff, F., Nagel, K., 2003a. Autotrophy, nitrogen accumulation and nitrogen limitation in the Baltic Sea: a paradox or a buffer for eutrophication? Geophysical Research Letters, 30 (21): 2130-2133.

Thomas, H., Gattuso, J.-P., Smith, S.V., 2003b. Coastal Biogeochemistry at the EGS-AGU-EUG Joint Assembly, Nice, France, 6-11 April 2003. LOICZ newsletter 28, LOICZ, Texel, The Netherlands.

Thomas, H., Bozec, Y., Elkalay, K., De Baar, H., 2004. Enhanced open ocean storage of CO_2 from shelf sea pumping. Science, 304: 1005-1008.

Tsunogai, S., Watanabe, S., Nakamura, J., Ono, T., Sato, T., 1997. A preliminary study of carbon system in the East China Sea. Journal of Oceanography, 53: 9-17.

Tsunogai, S., Watanabe, S., Sato, T., 1999. Is there a "continental shelf pump" for the absorption of atmospheric CO_2? Tellus, 51B: 701-712.

Turrell, W.R., Henderson, E.W., Slesser, G., Payne, R., Adams, R.D., 1992. Seasonal changes in the circulation of the northern North Sea. Continental Shelf Research, 12 (2/3): 257-286.

Walsh, J.J., 1991. Importance of continental margins in the marine biogeochemical cycling of carbon and nitrogen. Nature, 350: 53-55.

Wang, S.-L., Chen, C.-T.A., Hong, G.-H., Chung, C.-S., 2000. Carbon dioxide and related parameters in the East China Sea. Continental Shelf Research, 20: 525-544.

Wanninkhof, R., 1992. Relationship between wind speed and gas exchange over the ocean. Journal of Geophysical Research, 97 (C5): 7373-7382.

Wanninkhof, R. and McGillis, W.R., 1999. A cubic relationship between air-sea CO_2 exchange and wind speed. Geophysical Research Letters, 26 (13): 1889-1892.

Weiss, R.F., 1970. The solubility of nitrogen, oxygen and argon in water and seawater. Deep-Sea Research, 17: 721-735.

Weiss, R.F., 1974. Carbon dioxide in water and seawater: the solubility of a non-ideal gas. Marine Chemistry, 2: 203-215.

Wollast, R., 1998. Evaluation and comparison of the global carbon cycle in the coastal zone and in the open ocean. In: K.H. Brink and A.R. Robinson (Editors), The Sea. John Wiley & Sons, Inc., New York, pp. 213-252.

Acknowledgements

The excellent co-operation of the captains and the crews of *RV Pelagia* as well as the scientific crew is gratefully acknowledged. We thank DKRZ, DWD and Dr. Johannes Pätsch for making available the ECMWF wind data. We are grateful to Prof. Leif Anderson and Dr. Rik Wanninkhof for their helpful comments on a previous version of our manuscript. This study has been encouraged by and contributes to the LOICZ core project of the IGBP. It has been supported by the Netherlands Organisation for Scientific Research (NWO), grants no. 810.33.004 and 014.27.001, and the Dutch-German bilateral co-operation NEBROC.

Chapter 3

Enhanced open ocean storage of CO_2 from shelf sea pumping

This chapter by Helmuth Thomas, Yann Bozec*, Khalid Elkalay and Hein J.W. de Baar has been published in Science, 304: 1005-1008. *Lead authors.*

Abstract

Seasonal field observations show that the North Sea, a northern European shelf sea, is highly efficient in pumping CO_2 from the atmosphere to the North Atlantic Ocean. The bottom topography controlled stratification separates production and respiration processes in the North Sea, causing a CO_2 increase in the subsurface layer, which is ultimately exported to the North Atlantic Ocean. Globally extrapolated, the net uptake of CO_2 by coastal and marginal seas is approximately 20% of the world ocean's uptake of anthropogenic CO_2 thus enhancing significantly the open ocean CO_2 storage.

1. Introduction

Coastal and marginal seas play a key role in the global carbon cycle by linking the terrestrial, oceanic and atmospheric carbon reservoirs. They host strong biological activity and buffer terrestrial and human impacts, before they reach the open ocean systems (*1*). The high biological activity, stimulated by both high inputs and efficient use of nutrients mediates CO_2 drawdown from the atmosphere and subsequent export to the subsurface layer via the biological pump. The ultimate outflow of these CO_2–enriched subsurface waters to the open ocean constitutes the continental shelf pump, a mechanism transferring atmospheric CO_2 into the open ocean, which is thought to significantly contribute to the global ocean's uptake of atmospheric CO_2 (*2*). However, only limited information is available hitherto about these CO_2 fluxes (*3-10*). In order to verify this mechanism for the North Sea, the CO_2 uptake was investigated by measuring the partial pressure difference of CO_2 (ΔpCO_2) between the North Sea surface water and the atmosphere. The measurements were carried out during four cruises four weeks each (*11*) for the first time ever in a marginal sea on a consecutive seasonal scale with high spatial resolution.

2. Results and Discussion

During the winter situation (Fig. 1a) the surface waters of almost the entire North Sea are in CO_2 equilibrium with the atmosphere. Only the northern eastern part reveals a weak undersaturation and some areas along the British and southeastern coasts are slightly supersaturated.

With the onset of the spring bloom the entire North Sea becomes strongly undersaturated (Fig. 1b), even in the southern non-stratified region. The remineralisation of organic matter exported to the subsurface layer increases the dissolved inorganic carbon (DIC) concentrations in this layer (Fig. 2), whereas the DIC in the surface water decreases.

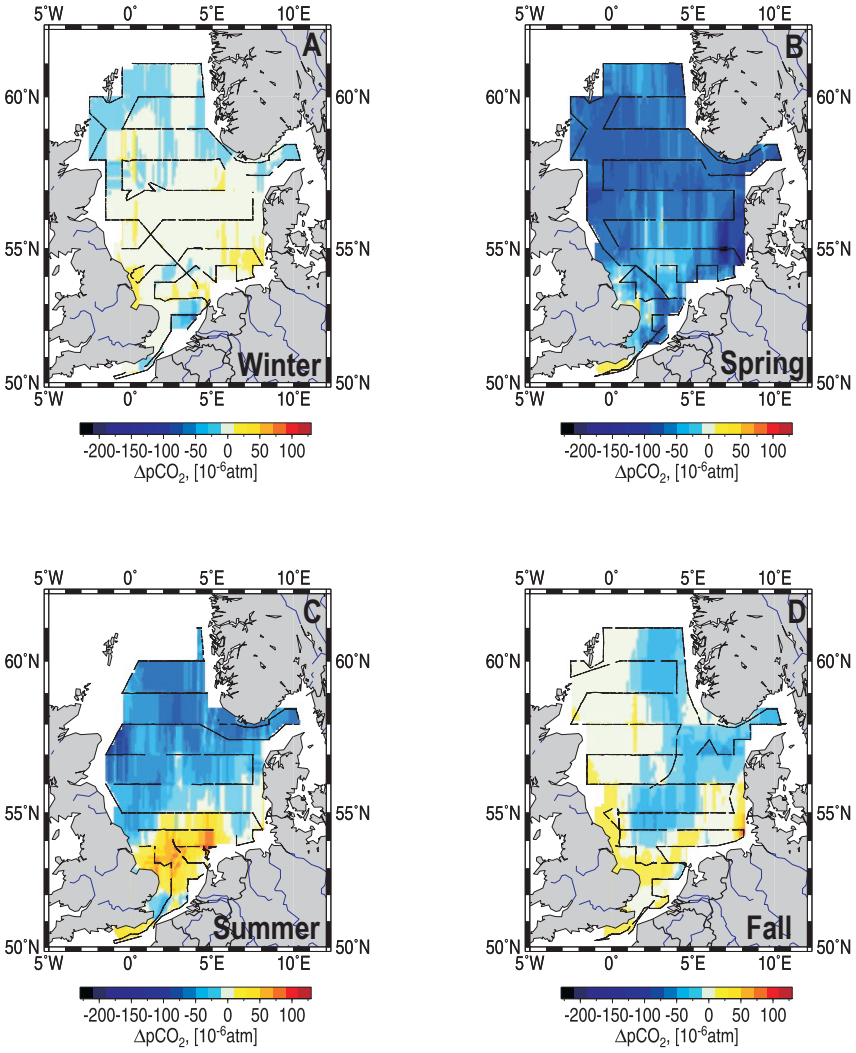

Figure 1: *Distribution of the CO_2 partial pressure difference (ΔpCO_2) during all 4 seasons. The surface water data were recorded in one minute intervals and the atmospheric data in hourly intervals using a continuous measurement system (23). Overall, approximately 90000 data points were collected. The data are shown relative to the atmospheric pCO_2 observed during each cruise. Negative values denote undersaturation of the surface waters. The cruises (11) took place in August/September 2001 (summer), November 2001 (fall), February/March 2002 (winter) and May 2002 (spring) on the research vessel RV Pelagia. The same colour scale has been applied to all plots.*

During summer the ΔpCO_2 distribution (Fig. 1c) shows clear differences between the two biogeochemical provinces of the North Sea: the shallower southern region with a non-stratified water column throughout the year and the deeper, stratified northern region (*12*). The northern region exhibits a strong CO_2 undersaturation up to –150 ppm ΔpCO_2, whereas the south is strongly supersaturated with ΔpCO_2 values up to approximately 100 ppm. Because of the slowdown of primary production in summer, respiratory processes dominate the carbon cycling in the southern region generating the observed supersaturation. In the stratified northern region this respiration further accumulates DIC in the subsurface layer thereby preventing the increase of the pCO_2 in the surface layer (Fig. 2). The transition in the southern region from strong undersaturation to strong supersaturation from spring to summer points to a decoupling of production and respiratory processes in time and space. This decoupling might allow lateral transport of the organic matter in the southern region (*13*).

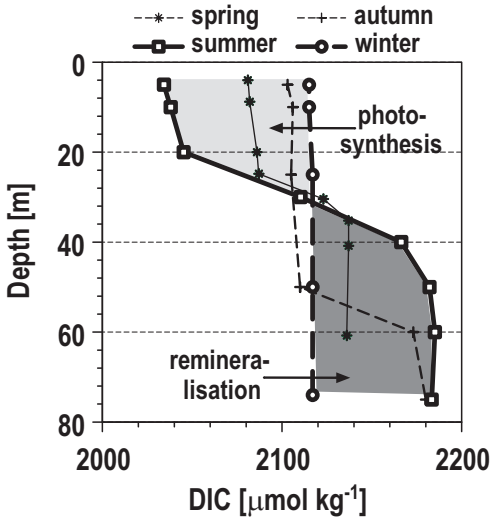

Figure 2: *Seasonal variations of dissolved inorganic carbon (DIC) observed at a representative station in the stratified northern North Sea (57°N/2.25°E). The light grey area indicates DIC loss in the surface water between winter and summer because of photosynthetic activity, whereas the darker gray area indicates the DIC increase in the subsurface waters during the same period because of organic matter remineralisation (see also (10) for comparison).*

In fall (Fig. 1d), biological activity decreases and the mixed layer is deepened in the northern region, allowing the ΔpCO_2 in both regions to begin to equilibrate. In the northern region the deepening of the mixed layer merges the DIC-enriched below thermocline waters (Fig. 2) into the surface layer and fall storms enhance CO_2 uptake from the atmosphere. In the southern region, decreasing temperatures and continuous CO_2 outgassing diminish the supersaturation.

In order to assess the annual CO_2 air-sea exchange in the North Sea the ΔpCO_2 data were assigned to 13 boxes (Fig. 3c). The data were averaged per season and per box and the ΔpCO_2 for the remaining months were linearly interpolated. The annual cycles of ΔpCO_2 show that only the most southern region is supersaturated during summer, whereas the remaining grid boxes remain undersaturated throughout the year, even in winter. The CO_2 air-sea fluxes (Fig. 3b), obtained using 6-hourly wind data for the time of observation (*14*), show in correspondence to the ΔpCO_2 features that the North Sea acts as a sink for CO_2 in wide areas throughout the year except for the summer months in the southern region.

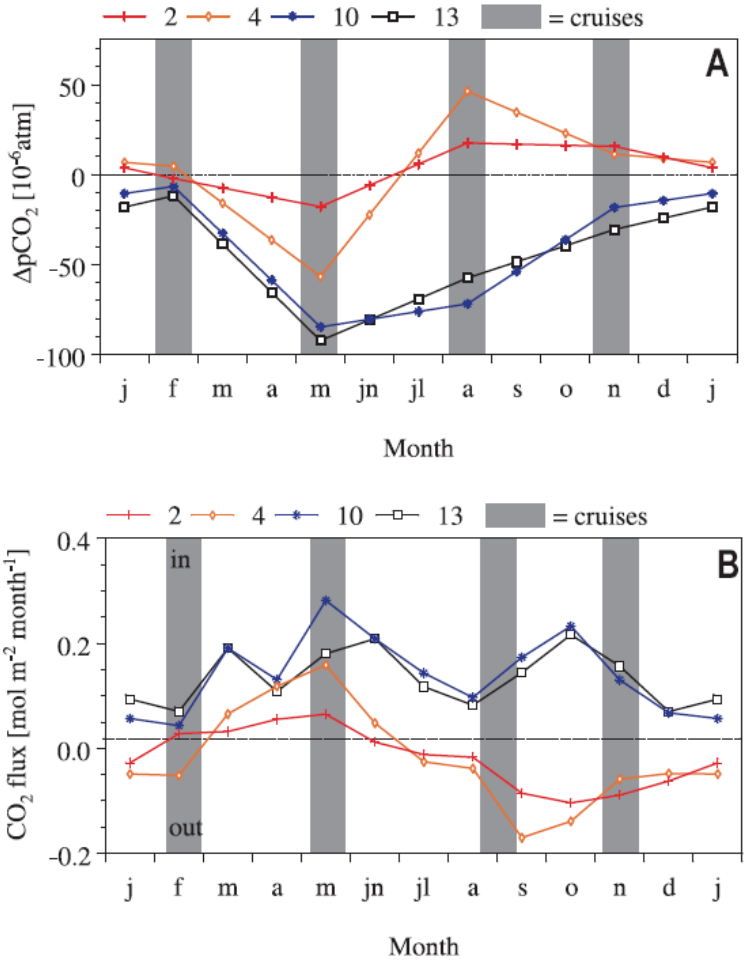

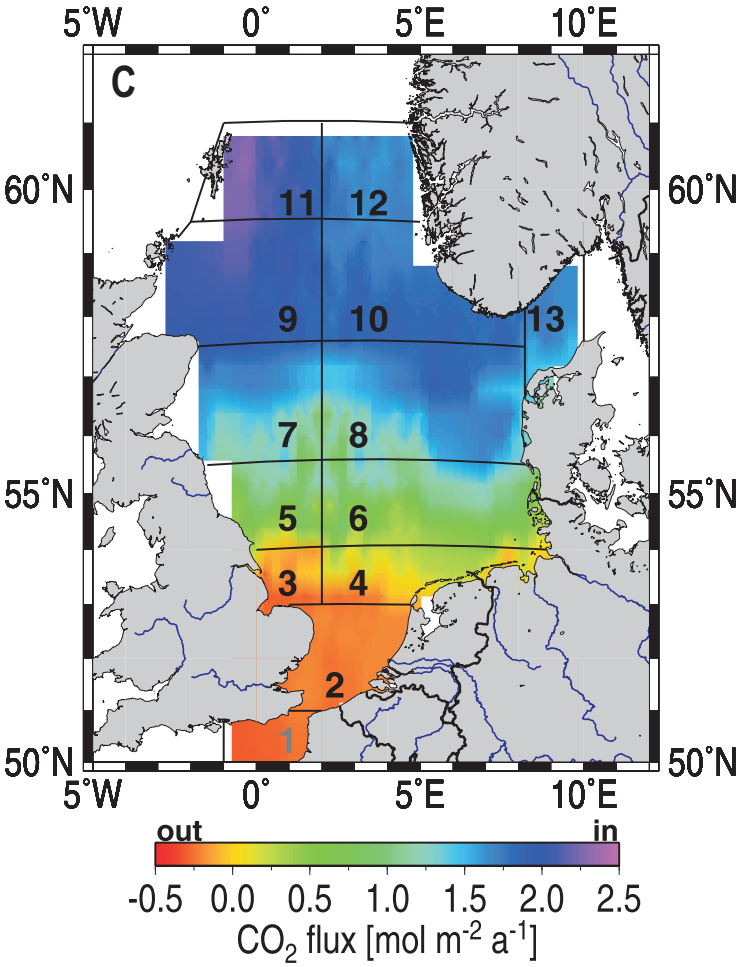

C

Figure 3: *Annual cycles of the ΔpCO_2 for selected areas in the North Sea. (a) The shaded areas indicate the time of observations. The fluxes (b) have been obtained according to Wanninkhof and McGillis (16). (c) shows the annual integration with an average CO_2 uptake of 1.38 mol C m^{-2} yr^{-1} for the boxes 2-13. Alternative parameterizations of the exchange coefficient provide the following fluxes: (24): 0.95 mol C m^{-2} yr^{-1}, (25): 1.68 mol C m^{-2} yr^{-1}, (26): 1.35 mol C m^{-2} yr^{-1}, (27): 1.28 mol C m^{-2} yr^{-1}. The average of all 5 parameterizations is 1.33 mol C m^{-2} yr^{-1}. There is good agreement among the three more recent parameterizations (16, 26, 27).*

Highest fluxes are obtained for the spring bloom situation in May because of the strong undersaturation, but also for October, when the fall storms force the CO_2 uptake, when the above equilibration process has just begun. Highest CO_2 release to the atmosphere was obtained for the late summer situation in the southern region because of the strong supersaturation of the surface waters. The annual integration (Fig. 3c) of the CO_2 air-sea fluxes shows that only the most southern region and the adjacent English Channel area act as weak sources for atmospheric CO_2, the latter in contrast to earlier findings (*15*). The remaining central and northern parts act as a strong sink approximately north of 54°N. Applying the CO_2 exchange coefficient by Wanninkhof and McGillis (*16*) highest annual uptake rates were obtained for the most northern regions up to 2.5 mol C m^{-2} yr^{-1}. The basin-wide CO_2 uptake by the North Sea is 1.38 mol C m^{-2} yr^{-1} or 8.5×10^{12} g C yr^{-1} (excluding the English Channel area). The North Sea thus acts as a rather strong sink for atmospheric CO_2, this also in comparison to other regions of the world ocean (*17*).

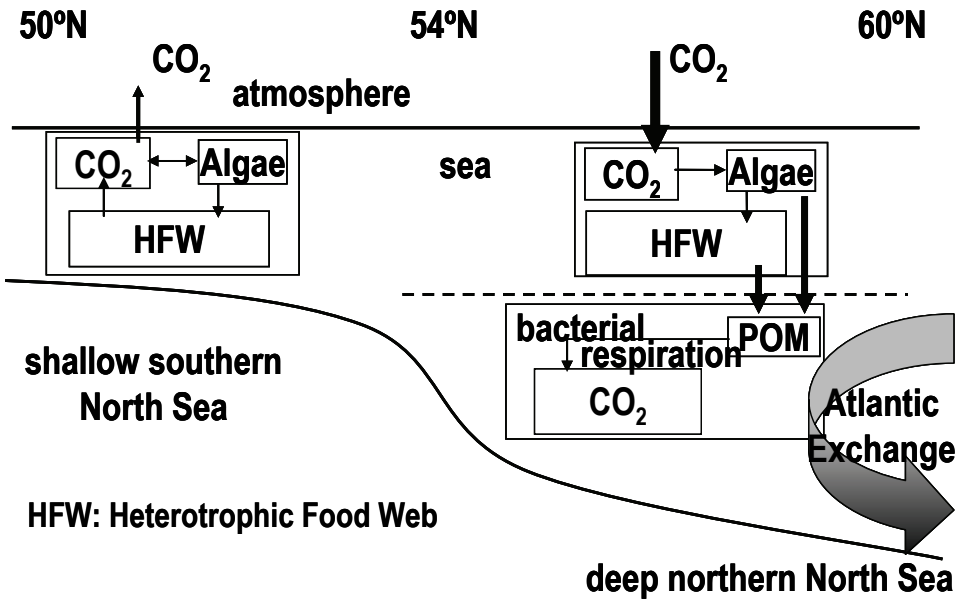

Figure 4: *Sketch of a south-north section through the North Sea. In the shallower southern part production and respiration processes occur in the mixed layer, whereas in the north the respiration processes mainly occur in the separated subsurface layer, which is subjected to the exchange circulation with the North Atlantic Ocean. The broken line indicates the thermocline and the darkening of the arrow implies the increase of DIC in the North Atlantic Ocean water circulated through the North Sea.*

Less than 1% of the annual primary production, ≈0.13 mol C m^{-2} yr^{-1}, is ultimately buried in the North Sea sediments (*18*). The largest part of the CO_2, taken up from the atmosphere and processed through the biological foodweb, is exported to the North Atlantic Ocean. The mechanism of this export (Fig. 4) is evident from the above observations described notably in Fig. 2 and also in Fig. 1 and 3. In the shallower continuously mixed southern area, the carbon metabolism (production and respiration) takes place within the same compartment thus preventing net CO_2 drawdown. As a consequence, the CO_2, taken up during the spring bloom is released back some time later causing the CO_2 supersaturation in summer. Over an annual scale the net CO_2 exchange with the atmosphere is low (Fig. 3). In contrast, the stratification in the northern part allows net CO_2 export from the surface layer to the subsurface layer (Fig. 2). Since this subsurface layer is subjected to major exchange circulation with the North Atlantic Ocean, the CO_2 released in the subsurface waters is largely exported and only partially mixed back into the surface layer during fall and winter convection. The northern North Sea remains undersaturated and this undersaturation is replenished by atmospheric CO_2 causing here the high net CO_2 uptake on an annual scale (Fig. 3). The overall North Sea thus acts as a highly efficient continental shelf pump exporting ≈93% of the CO_2 taken up from the atmosphere to the North Atlantic Ocean. Considering the North Atlantic Ocean water circulated through the North Sea (55900 km^3 yr^{-1} (*19*)) as the vehicle for this export, an increase of the DIC concentration within thes waters can be expected to be in the order of 13 μM.

The DIC and dissolved organic carbon (DOC) exchange fluxes between North Sea and North Atlantic Ocean have been investigated by sampling a section between the Orkney and the Shetland Islands and along 61°N towards Norway. The inflowing branch of North Atlantic Ocean water enters the North Sea along the western side of this section and the outflow along the Norwegian coast returns the water to the intermediate layers of the North Atlantic Ocean (*12*). A DIC increase of approximately 24μM has been observed between the waters entering the North Sea and the waters returning to the North Atlantic Ocean thus implying a further DIC source to complement the above "atmospheric" CO_2 input of 13μM. This DIC is generated by a net loss of DOC in the North Sea as indicated by the higher DOC concentrations found in the inflowing than in the outflowing waters (*19*). The DOC input from the Atlantic Ocean are respired to DIC by heterotrophic processes during the water mass transport through the North Sea generating the additional DIC source of approximately 11μM. These heterotrophic processes are also evident from the corresponding nutrient budgets (*19*) indicating a net loss of organic nutrients in the North Sea. The heterotrophic processes contribute to the DIC export into the intermediate layers of the North Atlantic Ocean, however they do not constitute a net carbon flux between the North Sea and the North Atlantic Ocean. Autotrophic processes, which are not evident from the nutrient budgets alone (*19, 20*) strongly dominate the North Sea carbon cycle as evident from the CO_2 uptake from the atmosphere, which supplies the net carbon export to the North Atlantic Ocean via the continental shelf pump.

3. Conclusion

Although coastal and marginal seas cover only 7% of the world ocean's surface (25.2×10^6 km^2) (*1*), their CO_2 uptake from the atmosphere plays a significant role in the global carbon budget. The seasonal amplitudes of the ΔpCO_2 can easily be in the order of 100 ppm with continuous undersaturation in the North Sea (Fig. 3) or even up to 400 ppm in the Baltic Sea (*6*). In contrast, in the open ocean regimes of similar latitudes, the seasonal amplitudes are only ≈40 ppm (*21*). These much higher ΔpCO_2 cycles cause significantly higher CO_2 uptake from the atmosphere by coastal and marginal seas (*17*), even though, for example, the southern part of the North Sea is a net source for atmospheric CO_2. Extrapolating the CO_2 uptake by the North Sea to the global scale, all coastal seas would have a net CO_2 uptake of 0.4 Pg C yr^{-1}, which is in the order of 20% of the global ocean's net annual uptake of anthropogenic CO_2 (1.9 ± 0.6 Pg C yr^{-1}) (*22*). Coastal and marginal seas thus contribute significantly more to the global carbon budget than expected from their surface area alone and enhance the open ocean storage of anthropogenic CO_2.

References and Notes

1. J.-P. Gattuso, M. Frankignoulle, R. Wollast, *Annual Reviews of Ecological Systems* 29, 405 (1998).
2. S. Tsunogai, S. Watanabe, T. Sato, *Tellus* 51B, 701 (1999).
3. K.-K. Liu, K. Iseki, S.-Y. Chao, in *The Changing Ocean Carbon Cycle: A midterm synthesis of the Joint Global Ocean Flux Study* R.B. Hanson, H.W. Ducklow, J. G. Field, Eds. (Cambridge University Press, Cambridge, 2000) pp. 187-239.
4. K.-K. Liu *et al.*, *EOS* 81, 641 (2000).
5. C.-T. A. Chen, Liu, K.-K., MacDonald, R., in *Ocean Biogeochemistry: A JGOFS synthesis* M. J. R. Fasham, Ed. (Springer, 2003) pp. 53-97.
6. H. Thomas, B. Schneider, *Journal of Marine Systems* 22, 53 (1999).
7. C.-T. A. Chen, S.-L. Wang, *Journal of Geophysical Research* 104, 20,675 (1999).
8. S. Kempe, K. Pegler, *Tellus* 43B, 224 (1991). The authors estimated an uptake of 1.4 mol CO_2 m^{-2} yr^{-1} from the atmosphere from pH and Alkalinity observations during May and June 1986.
9. C. Osterroht, H. Thomas, *Journal of Marine Systems* 25, 33 (2000).
10. H. Thomas, V. Ittekkot, C. Osterroht, B. Schneider, *Limnology and Oceanography* 44, 1999 (1999).
11. H. Thomas, "Shipboard report of the RV Pelagia cruises 64PE184. 64PE187, 64PE190 and 64PE195" (Royal Netherlands Institute for Sea Research, 2002).
12. L. Otto *et al.*, *Netherlands Journal of Sea Research* 26, 161 (1990).
13. A. V. Borges, M. Frankignoulle, *Journal of Marine Systems* 19, 251 (1999).
14. European Centre for Medium-Range Weather Forecasts, http://www.ecmwf.int/index.html (2002).
15. A. V. Borges, M. Frankignoulle, *Journal of Geophysical Research* 108, 1 (2003).
16. R. Wanninkhof, W. R. McGillis, *Geophysical Research Letters* 26, 1889 (1999).
17. For convenience, we give the area specific CO_2 uptake for selected areas. Positive values denote an uptake by the marine area. English Channel (grid box 1 in Fig 3c): -0.3 mol CO_2 m^{-2} yr^{-1} (area covered by this study: 15840 km^2); southern North Sea (grid boxes 2-4): -0.2 mol CO_2 m^{-2} yr^{-1} (72926 km^2), northern North Sea (grid boxes 5-13): 1.7 mol CO_2 m^{-2} yr^{-1} (438612 km^2); entire North Sea (grid boxes 2-13): 1.38 mol CO_2 m^{-2} yr^{-1} (511540 km^2); Baltic Proper: 0.9 mol CO_2 m^{-2} yr^{-1} (129000 km^2) (*6*); East China Sea 2 mol CO_2 m^{-2} yr^{-1} (0.9×10^6 km^2) (*7*); North Atlantic Ocean between 14°N and 50°N: 1.2 mol CO_2 m^{-2} yr^{-1} (27.1×10^6 km^2) (*21*); World Ocean 0.5-0.6 mol CO_2 m^{-2} yr^{-1} (360×10^6 km^2) (*21, 22*).
18. H. De Haas, T. C. E. Van Weering, H. De Stigter, *Continental Shelf Research* 22, 691 (2002).
19. H. Thomas *et al.*, in *Carbon and nutrient fluxes in global continental margins* L. Atkinson, K.-K. Liu, R. Quinones, L. Talaue-McManus, Eds. (Springer, New York, 2004).
20. H. Thomas, J. Pempkowiak, F. Wulff, K. Nagel, *Geophysical Research Letters* 30, 2130, DOI: 10.1029/2003GL017937 (2003).

21. T. Takahashi *et al.*, *Deep-Sea Research II* 49, 1601 (2002).
22. J. L. Sarmiento, N. Gruber, *Physics Today* 55, 30 (2002).
23. A. Körtzinger *et al.*, *Marine Chemistry* 52, 133 (1996).
24. P. S. Liss, L. Merlivat, in *The Role of Air-Sea Exchange in Geochemical Cycling* P. Buat-Ménard, Ed. (D. Reidel Publishing Company, 1986) pp. 113-127.
25. R. Wanninkhof, *Journal of Geophysical Research* 97, 7373 (1992).
26. P. D. Nightingale, P. S. Liss, P. Schlosser, *Geophysical Research Letters* 27, 2117 (2000).
27. P. D. Nightingale *et al.*, *Global Biogeochemical Cycles* 14, 373 (2000).

Acknowledgements

The excellent co-operation of the captains, the crews of *RV Pelagia* and the scientific staff is gratefully acknowledged. We thank DKRZ, DWD and J. Pätsch for making available the ECMWF wind data. This study has been encouraged by and contributes to the LOICZ core project of the IGBP. It was supported by the Research Council for Earth and Life Sciences (ALW) of the Netherlands Organization for Scientific Research (NWO) and the Dutch-German bilateral co-operation NEBROC. The comments by two anonymous reviewers, V. Ittekkot and G. Herndl greatly helped improve an earlier version of the manuscript.

Chapter 4

Assessment of the processes controlling the seasonal variations of dissolved inorganic carbon in the North Sea

This chapter by Yann Bozec, Helmuth Thomas, Laure-Sophie Schiettecatte, Alberto V. Borges, Khalid Elkalay and Hein J.W. de Baar is in revision for publication in Limnology and Oceanography.

Abstract

A seasonally resolving North Sea data set comprising dissolved inorganic carbon (DIC), partial pressure of CO_2 (pCO_2) and inorganic nutrients was exploited to assess the abiotic and biological processes governing the monthly variations of DIC. The North Sea's regional variability was accounted for by using the 15-box scheme as proposed by the International Council for the Exploration of the Seas (ICES). Between February and July, autotrophic processes control the seasonal variations of DIC and the CO_2 air-sea flux in the entire North Sea, while heterotrophic processes increase the DIC pool in the deeper layers. During this productive period, net community production (NCP) was high in the central and northern North Sea (<1.5 mol C m^{-2} $month^{-1}$) and revealed lower values in the coastal and southern areas (<1.2 mol C m^{-2} $month^{-1}$). The lower NCP in the south is caused by high remineralisation rates in this one-layered compartment, thus counteracting the higher gross primary production in this area. The North-Sea-wide carbon based NCP estimate yields an approximately three times higher NCP than previous estimates based on inorganic nutrients because of overconsumption of inorganic carbon in the northern North Sea. On an annual scale, the whole North Sea is closed to metabolism balance but acts as a strong sink of atmospheric CO_2.

Note: *In the present chapter, Bozec et al. (2005) refers to chapter 2, Thomas et al. (2004) refers to chapter 3 and Thomas et al. (2005) refers to chapter 5 of this PhD thesis.*

1. Introduction

Coastal and marginal seas play a key role in the global carbon cycle by linking the terrestrial, oceanic and atmospheric reservoirs (Walsh, 1991; Mackenzie et al., 2004). They occupy only 7% of the global ocean surface area but house 10-30% of the global marine primary production (Gattuso et al., 1998). Recent investigations have underlined the importance of coastal seas in the global carbon cycle and the necessity to introduce them in realistic models, notably to quantify the air-sea exchange of CO_2 (Chen, 2004; Thomas et al., 2004; Borges, 2005; Muller-Karger et al., 2005). However, even the latest global estimates of the oceanic uptake of atmospheric CO_2 (Sabine et al., 2004) do not include these coastal seas in the calculations, because of the small-scale variability observed within each marginal sea and between all marginal seas worldwide, and the difficulty in increasing the spatial resolution of global numerical models.

The coastal seas are heavily impacted by human activities, as nearly 40% of the global population lives within 100 km of the coastline. The increase of the human population, notably in the coastal zone, and improved agriculture, led to increasing loads of organic matter and nutrients transported via rivers and deposited in the coastal seas (Mackenzie, 2003). Moreover, since the onset of the industrial revolution, practices such as burning of fossil fuels and land-use changes have caused substantial increases in

atmospheric CO_2 concentration (Petit et al., 1999). Such changes could alter the biogeochemistry of coastal seas and considerably affect important processes such as CO_2 air-sea exchange. Changes in the coastal metabolism have already been observed: during the past 300 years, the coastal zone is thought to be net heterotrophic (Mackenzie et al., 1998; Mackenzie et al., 2004) and a net source of CO_2 to the atmosphere (Smith and Mackenzie, 1987; Mackenzie et al., 2004), whereas the present day individual coastal margin environment may show a net biological community production varying from net autotrophic to net heterotrophic (Smith and Hollibaugh, 1993; Gattuso et al., 1998; Mackenzie et al., 2004). This in turn has led to growing interest and debate on the role of all coastal seas in the global carbon cycle, notably with regards to the budget and fate of CO_2 (Thomas et al., 2004; Borges, 2005).

During the past decade, the air-sea exchange of CO_2 in the coastal margins was intensively investigated, notably in temperate marginal seas (Thomas and Schneider, 1999; Tsunogai et al., 1999; Frankignoulle and Borges, 2001; Algetsen et al., 2004; Kaltin and Anderson, 2005; Thomas et al., 2004; Bozec et al., 2005). The link between air-sea exchange of CO_2, biological processes and physical forcing have also been investigated in order to determine the Net Community Production (NCP) in coastal seas and open shelves, notably for the Baltic Sea and Bering Chukchi sea shelf (Thomas and Schneider, 1999; Osterroht and Thomas, 2000; Kaltin and Anderson, 2005). Similar investigations were made in adjacent areas of the North Sea such as the Norwegian Sea and the Nordic Seas (Falck and Gade, 1999; Falck and Anderson, 2005). Moreover, the link between the trophic state of the coastal seas and the air-sea exchange of CO_2 has recently been discussed. Heterotrophic systems do not necessarily release CO_2 to the atmosphere, and autotrophic systems do not necessarily act as sink of atmospheric CO_2 (Thomas et al., 2004; Borges, 2005).

The North Sea is amongst the best-studied coastal areas worldwide with respect to its physical, chemical and biological conditions, since it has been subject to detailed investigations for many decades. Earlier carbon cycle studies in the North Sea were confined to certain near-shore coastal areas such as the German Bight, the Wadden Sea or the Belgian coast (see for overview Bozec et al., 2005). An early basin-wide pioneering study relied on total alkalinity, dissolved inorganic carbon (DIC) and pH observations during late spring and provided first insights in the carbon cycle of the North Sea as a whole (Kempe and Pegler, 1991). Recently, an intense field study showed that the North Sea is a sink of CO_2 for the atmosphere and absorbs 1.4 mol C m^{-2} yr^{-1} (Thomas et al., 2004). Moreover, Bozec et al. (2005) underlined the importance of the late summer season on the annual air-sea fluxes of CO_2 and confirmed the importance of the regional variability in the carbon cycle in the North Sea.

In the present paper, we combined a comprehensive dataset of DIC and partial pressure of CO_2 (pCO_2) based on four consecutive cruises in the North Sea with data on physical processes, in order to quantify the effect of biological and physical processes on the DIC variations. Mass balance computations were carried out in different regions of the North Sea, in order to take into account the regional variability in these processes. Based on numerous investigations on the physical process in the North Sea (see for overview Otto et al., 1990), the European Regional Seas Ecosystem Model (ERSEM) provides robust water

fluxes (Lenhart et al., 1995; Lenhart and Pohlmann, 1997), taking into account the different regions of the North Sea (ICES, 1983). We firstly describe the seasonal variations in the horizontal and vertical distribution of the carbon dioxide system using the data from 4 consecutive cruises in 4 seasons. We adopted the ICES division of the North Sea into 15 boxes: these are 5 single boxes in the well-mixed shallow southern North Sea, and 5 sets of surface and deep boxes in the stratified deep northern North Sea. Secondly, we calculated the monthly impact on DIC variations of two major abiotic processes, air-sea CO_2 exchange and advection between the boxes. Based on the calculations of the monthly changes of DIC inventories due to physical and chemical processes, we obtain the monthly net biological term (either net autotrophic or net heterotrophic) for each of the 15 boxes of the North Sea. Finally, by vertical integration this yields the monthly DIC-based Net Community Production (NCP) that is compared to the NCP calculated from inorganic nutrients (nitrate and phosphate), from the same cruises, and from previous investigations.

2. Material and Methods

2.1. Sampling and analytical measurement

Data were obtained during four cruises in the North Sea (18 Aug. 2001-13 Sep. 2001; 06 Nov. 2001-29 Nov. 2001; 11 Feb. 2002-05 Mar. 2002 and 06 May 2002-26 May 2002), on board R.V Pelagia. The North Sea was covered during summer, fall, winter and spring by an adapted 1° by 1° grid with 97 stations (Figure 1). This grid was specifically designed to focus on the relevant regions for biogeochemical cycles such as the Shetland and English Channels (inflow of North Atlantic water), the Skagerrak area (inflow of Baltic Sea water) and the western Scandinavian coast (outflow to the North Atlantic). The stations were also denser in the Southern Bight (Figure 1) that receives the major freshwater inputs, whereas the stations distribution was sparser in the more homogenous central North Sea.

During each cruise, a total of 745 water samples were collected for DIC, dissolved oxygen (O_2), inorganic nutrients nitrate (NO_3^-), nitrite (NO_2^-) and phosphate (PO_4^{3-}), chlorophyll *a* (in surface waters in spring and summer), salinity and temperature. In the surface waters, salinity, temperature and pCO_2 were determined continuously from the ship's water supply yielding 22 000 surface measurements per cruise for these variables.

DIC samples from CTD casts were collected in 250 ml borosilicate bottles, which were kept cold in the dark until measurement (within 2 h of sampling). The DIC concentrations were determined by the coulometric method of Johnson et al. (1993), as previously described by Stoll (1994). A new coulometric cell was prepared approximately every 12 hours and calibrated versus Certified Reference Material (CRM) from Scripps Institution of Oceanography (batch #52). The accuracy and the precision of the system were controlled by the repeated measurements of CRM before and after each station. Three to four replicates were determined for each sample and CRM with a precision better than $\pm$ 2 μmol kg^{-1}.

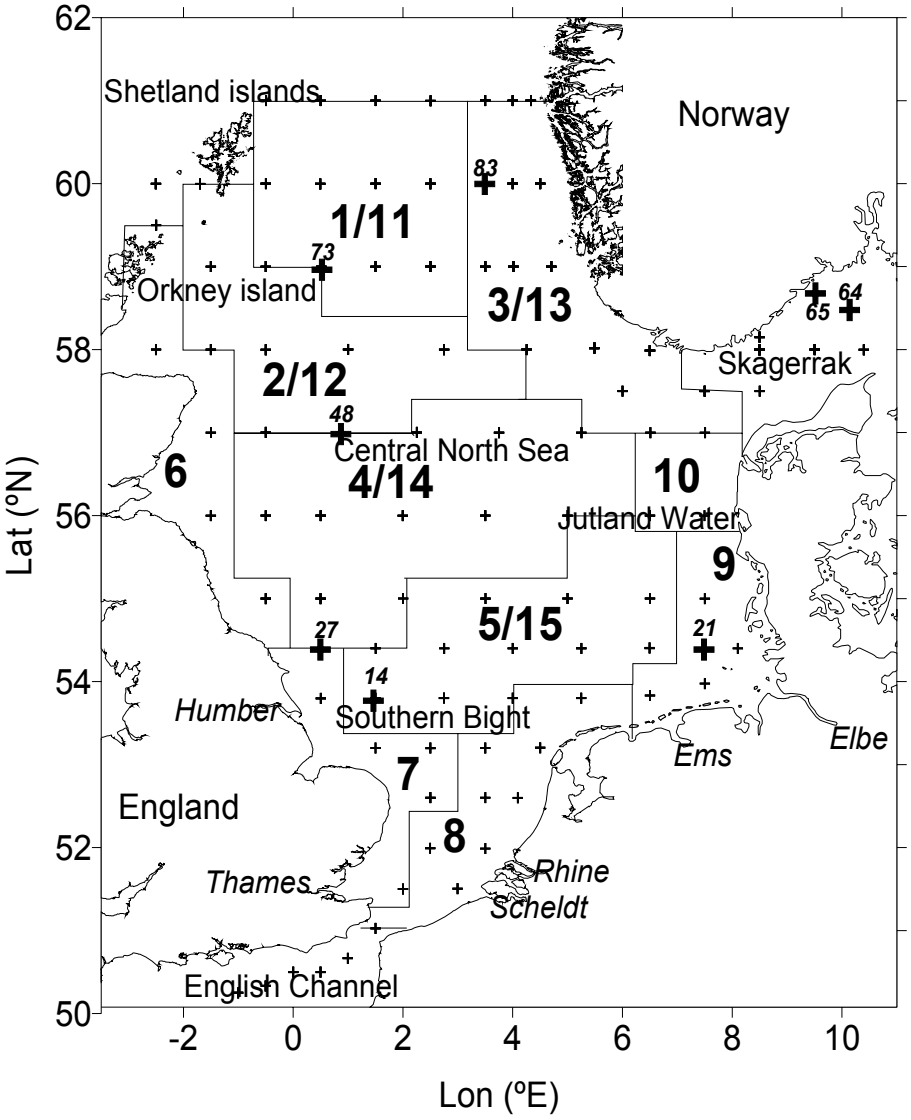

Figure 1: *Map of the study area and the International Commission for the Exploration of the Seas (ICES) boxes. Boxes 1, 2, 3, 4 and 5 represent the first 30 meters of the water column, whereas boxes 11, 12, 13, 14 and 15, represent the bottom layer of the water column. The other boxes are one-layer boxes and represent the whole water column. Crosses represent the stations sampled during the four cruises. Bold numbered crosses correspond to the stations for which the profiles are shown in Figure 4.*

The pCO_2 in surface waters was determined using an underway system with continuous flow equilibration. The water flow from the pump was about 60 L min^{-1}, which was reduced by a bypass just before the equilibrator to 2-3 L min^{-1}. The temperature difference between the equilibrator and the surface water was less than 0.5°C, and usually 0.1°C. The detection of pCO_2 was performed by a non-dispersive infrared spectrometer (Li-Cor 6262), calibrated against *National Oceanic and Atmospheric Administration* (NOAA) standards (molar fraction of 250.33, 374.40, and 453.65 ppm) every 6 h. The method for the Warnemünde underway system (IOW) is described in detail by Körtzinger et al. (1996) with an estimated error of approximately ± 1 µatm. The atmospheric pCO_2 was sampled at the antenna platform of the ship and determined every 2 hours.

NO_3^-, NO_2^- and PO_4^{3-} were analyzed within 10 h after sampling, using a technicon TRAACS 800 auto-analyzer according to Grasshoff et al. (1983). The standard deviation for the sum of NO_3^- and NO_2^- (NO_x) was ± 0.02 µmol L^{-1} and for PO_4^{3-} ± 0.01 µmol L^{-1}. The estimated accuracies were ± 1.5% and 3%, for NO_x and PO_4^{3-} respectively.

Sea-surface temperature and salinity were measured continuously with an AQUAFLOW thermo-salinograph with the water intake at a depth of about 3 m. Continuous temperature and salinity data were calibrated vs. the CTD measurements.
The concentration of chlorophyll *a* was determined from GF/F filtered samples by the fluorimetric method based on the method by Holm-Hansen et al. (1965) with a precision of ± 4%.

2.2. Calculation of the different parameters influencing the variability of DIC

The North Sea was divided into 5 sets of surface and deep boxes 1/11, 2/12, 3/13, 4/14, 5/15 in the stratified deep northern North Sea, and five single boxes 6, 7, 8, 9, 10 in the well-mixed shallow southern North Sea (ICES, 1983) (Figure 1). The boxes have different areas and depths, except for the surface boxes 1-5 all with a 30 m depth. The main factors controlling the distribution of DIC in the upper and lower layers of the North Sea are the horizontal and vertical advection between the boxes, the air-sea CO_2 exchange with the surface boxes (1-10), and the net biological term in each box. The freshwater DIC input into boxes 7, 8, 9 by rivers yields 3 additional DIC advection terms. The DIC input into box 3 from fjords is assessed by the monthly salinity changes within box 3. The net biological term, as derived from DIC inventory changes, is an overall term comprising the following processes: photosynthesis, respiration, biocalcification and calcium carbonate ($CaCO_3$) dissolution and exchanges of carbon with the surface sediments.

2.2.1. Advection term

Details on the North Sea circulation and water flows circulation have been largely reported (see overview by Otto et al., 1990). We used the mean net flows average over 10 years from the ERSEM model calculated by Lenhart et al. (1995) for the modified 15 International Council for the Exploration of the Seas (ICES) boxes (ICES, 1983), to

compute the monthly variations in DIC for each box due to the horizontal and vertical advection (ΔDIC_{adv}). For our calculation, we calculated the specific DIC (water column inventory of DIC divided by the water column depth) at every station for the upper layer (30 meters) and bottom layer (below 30 meters) of the water column for every cruise, and the average value of specific DIC for each box. Therefore, the DIC concentrations calculated in each box for every season rely on 12 to 60 measurements, depending on the number of stations per box and the vertical resolution of sampling in the water column. Since the mean flushing time for every box is of the order of 30 to 40 days (Lenhart et al., 1995) we assumed that the specific DIC calculated per box is representative of the whole month. The limit of 30 meters has been chosen in ERSEM because it is the average depth of the thermocline in the area where stratification occurs in the North Sea and is the boundary between boxes 1 and 11, 2 and 12, 3 and 13, 4 and 14 and 5 and 15 (Figure 1) (Lenhart et al., 1995).

2.2.2. Freshwater inputs

The advection term takes into account the lateral and vertical flows between all the boxes. However, for several boxes, which receive high freshwater inputs with different DIC content, it is necessary to quantify the impact of these inputs on the DIC variations.

The coastal boxes 6, 7, 8 and 9 receive high freshwater inputs from the Humber, Thames, Scheldt, Rhine, Ems, and Elbe estuaries. We introduced the annual integrated fluxes out of the estuaries calculated by Borges A.V (pers. comm.) in the relevant box, taking into account the seasonal variations of these fluxes. For these boxes, the advection term ΔDIC_{adv} represent the variations in DIC concentration due to the lateral and vertical advection and to the DIC fluxes from the estuaries.

For box 3, which receives high freshwater inputs with low DIC content from the Scandinavian coast, a term "monthly variations of DIC due to freshwater inflow" (ΔDIC_{sal}) has been introduced. We calculated the difference of DIC concentration (ΔDIC) between the summer and the fall cruises and the concomitant difference in salinity (ΔS) for the stations of box 3 influenced by these freshwater inputs. The plot of ΔDIC versus ΔS showed a linear relationship between these two parameters for the stations of box 3 situated along the Norwegian coast ($\Delta DIC_{sal} = 28.8\Delta S - 71.5$; $r^2 = 0.9$; $n = 10$). The slope of this linear regression is the changes in DIC due to the inputs of freshwater into the box 3 for the summer-fall period. Similar trend could be established for the fall-winter ($\Delta DIC_{sal} = 21.6\Delta S - 27.8$ $r^2 = 0.8$; $n = 12$), winter-spring ($\Delta DIC_{sal} = 16.7\Delta S - 31.5$ $r^2 = 0.9$; $n = 12$) and spring-summer ($\Delta DIC_{sal} = 18.5\Delta S - 104.1$ $r^2 = 0.7$; $n = 10$) periods. The monthly changes in DIC due to the freshwater inputs into box 3 were -10 mmol m^{-3} from summer to fall (salinity decreased by 0.40), +7 mmol m^{-3} from fall to winter (increase in salinity of 0.78), -6 mmol m^{-3} from winter to spring (decrease in salinity of 2.01) and +7 mmol m^{-3} from spring to summer (increase in salinity of 1.60).

2.2.3. The air-sea exchange term

The flux of CO_2 at the air-sea interface was recalculated from Thomas et al. (2004) for the ICES boxes using the pCO_2 measured during our cruises and the wind speed data provided by the European Centre for Medium-Range Weather Forecast (ECMWF). The flux (F) of CO_2 across the air-sea interface is calculated using:

$$F = k \times \alpha \times \Delta pCO_2 \quad (1)$$

where k is the gas transfer velocity, α is the solubility coefficient of CO_2 calculated according to Weiss (1974) and ΔpCO_2 (pCO_{2water}-pCO_{2air}) is the air-water gradient of pCO_2. In the following discussion, we present the results using the algorithms by Wanninkhof and McGillis (1999), here after referred to as W&McG99. We calculated an average value of these fluxes for each box every month. Once integrated over the upper part of the water column, these fluxes represent the monthly changes in DIC due to air-sea CO_2 exchange ($\Delta DIC_{air\text{-}sea}$). The effects of 3 different k-wind speed formulations (Wanninkhof, 1992; Nightingale et al., 2000a; Nightingale et al., 2000b) here after referred to as W92, N2000a and N2000b, respectively, on the calculation of the various DIC fluxes will be discussed in the last section of the article.

2.2.4. The diffusion term

The vertical diffusive fluxes of DIC (F_d) from the deeper layer into the upper layer of the water column through the halocline of the northern boxes (1/11 – 5/15) were calculated using Fick's law:

$$F_d = Kv.\ dc/dx \quad (2)$$

where K_v is the eddy diffusive coefficient and dc/dx represents the gradient of DIC at the boundary between the halocline and the bottom layer. The diffusion coefficient of Lenhart et al. (1995) given for each month were used. These coefficients varies from 50 to 600 $cm^2\ s^{-1}$ from summer to winter, respectively, and are in the same order of values than the value of 300 $cm^2\ s^{-1}$ in the Baltic Sea calculated by Osterroht and Thomas (2000). The diffusive fluxes were negligible for the whole year. This is due to the fact that the highest values of K_v in winter where associated with very small gradient of DIC, whereas when the strongest gradient of DIC were present in summer, the values of K_V were close to zero.

2.2.5. The biological term

We linearly interpolated the seasonal specific DIC variations between the observed values in each box (Figure 2) and calculated the observed DIC variation between two successive months (ΔDIC_{obs}) for the whole year. For all the boxes, equation (2) expressed ΔDIC_{obs} as a function of the relevant parameters for the DIC monthly variability:

$$\Delta DIC_{obs} = \Delta DIC_{bio} + \Delta DIC_{air\text{-}sea} + \Delta DIC_{adv} \quad (3)$$

Moreover, for box 3 the equation is extended

$$\Delta DIC_{obs} = \Delta DIC_{bio} + \Delta DIC_{air\text{-}sea} + \Delta DIC_{adv} + \Delta DIC_{sal} \quad (4)$$

by the freshwater effect for DIC input by fjords. The net impact of the overall biological processes on the monthly variations of DIC, can be calculated using the equation (5) (equation (6) for box 3):

$$\Delta DIC_{bio} = \Delta DIC_{obs} - (\Delta DIC_{air\text{-}sea} + \Delta DIC_{adv}) \quad (5)$$

$$\Delta DIC_{bio} = \Delta DIC_{obs} - (\Delta DIC_{air\text{-}sea} + \Delta DIC_{adv} + \Delta DIC_{sal}) \quad (6)$$

The obtained term ΔDIC_{bio} is an overall term inherently comprising photosynthesis, respiration, biocalcification and $CaCO_3$ dissolution and exchanges of carbon with the surface sediments. Within each box the net balance of photosynthesis and respiration yields monthly changes of the inventory of biogenic suspended particulate and dissolved organic carbon (POC and DOC). ΔDIC_{bio} in the deeper boxes comprises pelagic organic matter respiration, but also inherently considers carbon exchanges with the surface sediments. These carbon fluxes were caused by respiration of organic matter, which had settled temporarily onto the surface sediments. Long term, i.e., net carbon burial is not occurring in the North Sea, except for a trivial net burial in box 13, which accounts for less than 1% of all primary production of the whole North Sea (de Haas et al., 2002) and is deemed to be negligible on an annual scale for our purposes. In other words, neither box 13, nor other bottom boxes 6-12 and 14-15, have a burial loss term.

2.2.6. Production/dissolution of calcium carbonate

The ecosystem calcification has not been considered in a number of recent papers on carbon and nutrient cycles of the North Sea because it is not perceived as a significant component of the carbon cycle compared to the three main factors above. Blooms of the calcifying cocolithophores *Emilia Huxleyi* have only been reported in the northern part of the North Sea (Tyrell and Merico, 2004 and references therein), where the stratification of the water column is favorable for the occurrence of these blooms (Tyrell and Merico, 2004). Due to the high spatial variability in the occurrence of these blooms, it is difficult to quantify their impact on the monthly DIC variations. Since blooms of coccolithophores are likely to occur during the June-July period in the boxes 1, 2 and 3, the term ΔDIC_{bio} comprises the changes in DIC due to pelagic calcification and dissolution of $CaCO_3$. As far as the southern North Sea is concerned, to the best of our knowledge, blooms of calcifying pelagic species such as coccolithophores have only been reported in adjacent areas, for example in the English Channel (Tyrell and Merico, 2004), but not in the southern North Sea. The absence of stratification and the homogeneous shallow water column limit the incoming light, resulting in unfavorable conditions for the occurrence of these blooms

(Tyrell and Merico, 2004). It is therefore reasonable to assume that the pelagic calcification does not have a major impact on the monthly change in DIC in the southern area of the North Sea. Even if this process played a major role here, it was inherently considered in ΔDIC_{bio}.

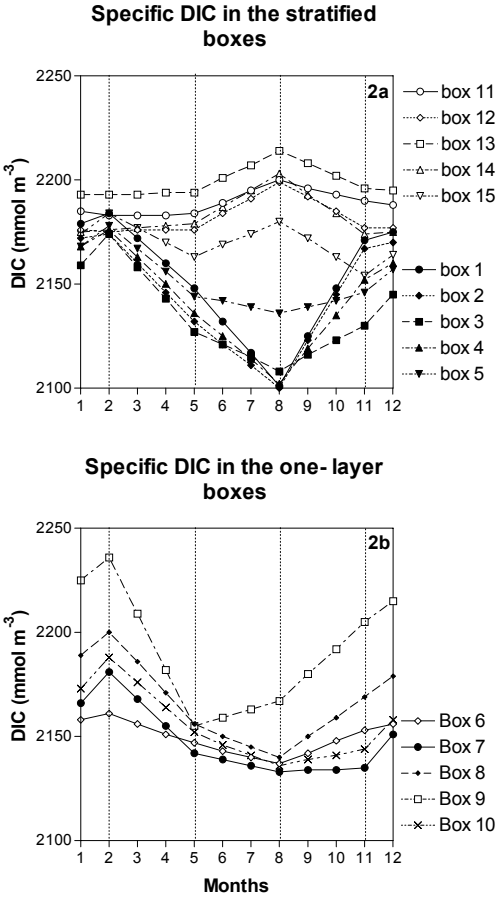

Figure 2: *Monthly variations of specific DIC in the stratified boxes (1/11, 2/12, 3/13, 4/14 and 5/15) (Figure 2a) and the one-layer boxes (6, 7, 8, 9 and 10) (Figure 2b) of the North Sea. The vertical doted lines correspond to the cruises.*

3. Observations

3.1. DIC distribution

During spring, the surface DIC had a rather homogeneous distribution in the central North Sea with an average value of 2085 μmol kg^{-1} (Figure 3a). However the inflow of North Atlantic water through the Shetland Channel in the north-western part of the North Sea had lower concentrations of 2070 μmol kg^{-1}. Lowest concentrations were found in the transition area between the North and Baltic Seas (Skagerrak) and along the south-western coast of Norway with concentrations as low as 1870 μmol kg^{-1}. The plume of the Scheldt River was marked by the highest concentrations of 2150 μmol kg^{-1}.

Bozec et al. (2005), investigated the surface distribution of DIC in late summer in detail. In short, the DIC distribution showed a clear boundary approximately at 54°N with higher concentrations in the southern area with values ranging from 2090 to 2130 μmol kg^{-1} compared to the central North Sea (values between 1980 and 2070 μmol kg^{-1}) (Figure 3b). The Skagerrak area had the lowest values between 1870 and 2030 μmol kg^{-1}.

In fall, increased wind speed induced mixing between the upper and bottom layers of the water column as well as a lateral mixing, which increased the surface concentrations of DIC almost in the whole North Sea (Figure 3c). Concentrations in the Skagerrak and along the south-western coast of Norway were 2070 μmol kg^{-1}, whereas along the Danish, German, Dutch and Belgium coasts DIC concentrations were close to 2110 μmol kg^{-1}. Values in the rest of the North Sea ranged between 2090 and 2110 μmol kg^{-1}.

In winter, the surface water of the whole North Sea had a homogeneous DIC concentration of 2120 μmol kg^{-1} (Figure 3d), mainly due to vertical and horizontal mixing of water masses. Only at the stations in the front of the Elbe and Scheldt estuaries in the southern area, DIC concentrations were higher than in the rest of the North Sea with values as high as 2150 μmol kg^{-1}. Again, in the Skagerrak area and along the south-western coast of Norway, concentrations of DIC were lower with values of 2090 μmol kg^{-1}.

It is difficult to compare the DIC concentrations in the deeper layer of the North Sea since bottom depths range approximately from 20 to 700 m. We therefore discuss the maps of DIC concentrations in the bottom of the North Sea and present several profiles representative of the different water column properties encountered in the North Sea. Figure 3 shows that surface and bottom DIC concentrations of the southern area (approximately south of 54ºN), where depth range from 20 to 60 meters, were very similar during the whole year. This is a direct consequence of the fact that for most of the year, the water column in this area was mixed down to the bottom (Figures 4a and 4b). However, in spring, at the deepest stations (40-60 meters) as well as in the German Bight, the water column was stratified (Figures 4c) and DIC concentrations were lower in the upper layer (2080 μmol kg^{-1}) than in the bottom layer (2110 μmol kg^{-1}) (Compare Figures 3a and 3e).

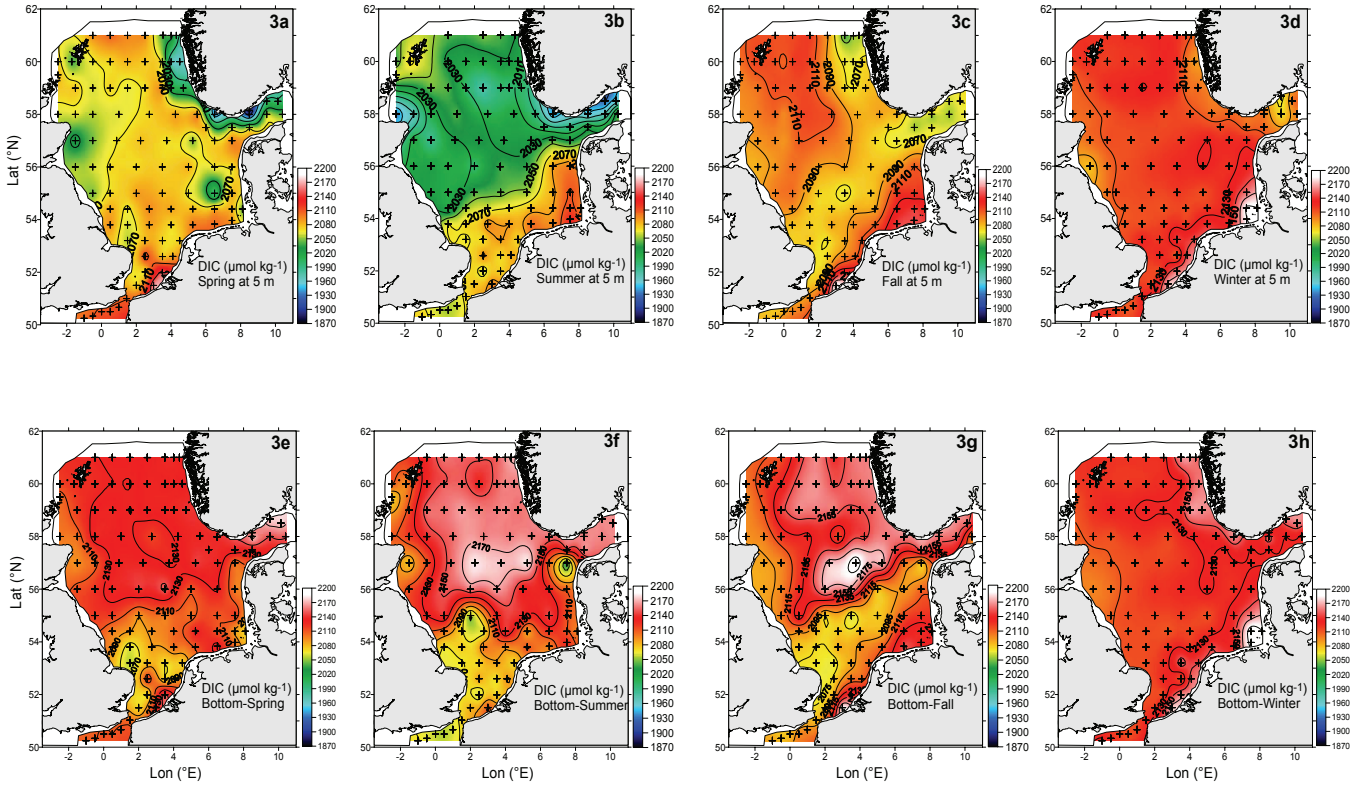

Figure 3: *Maps of DIC concentrations for the spring (Figure 3a), summer (Figure 3b), fall (Figure 3c) and winter (Figure 3d) in surface waters (5 m depth). Maps of DIC concentrations for the spring (Figure 3e), summer (Figure 3f), fall (Figure 3g) and winter (Figure 3h) in bottom waters.*

In the deeper layers of the northern North Sea, from spring to summer and from summer to fall, we observed increasing DIC concentrations from 2135 µmol kg^{-1} (spring) to 2155 µmol kg^{-1} (summer) and a maximum of 2175 µmol kg^{-1} (during fall) (Figures 3e, 3f, 3g). This is also evident from profiles recorded in the central and northern North Sea at several stations: for example at stations 48, 73 and 83 (Figures 4d, 4e and 4f) a clear increase was observed below the thermocline from spring to summer and from summer to fall.

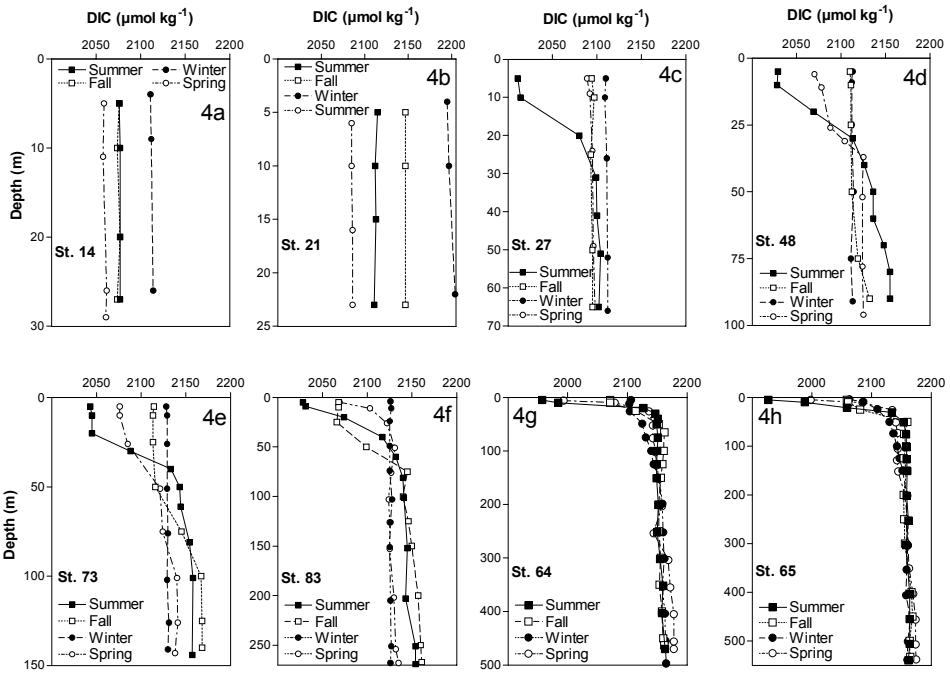

Figure 4: *Profiles of the vertical seasonal variations of DIC concentrations from the CTD data for 8 stations situated in the specific regions of the North Sea: Stations 14 (Figure 4a), 21 (Figure 4b), 27 (Figure 4c), 48 (Figure 4d), 73 (Figure 4e), 83 (Figure 4f), 64 (Figure 4g) and 65 (Figure 4h) The positions of the stations are indicated on Figure 1.*

At the very deep stations situated in the Skagerrak area, the bottom DIC concentrations were very similar throughout the year. For the stations 64 and 65 (Figures 4g and 4h), the DIC concentrations from 300 to 500 m were constant with values of approximately 2150 µmol kg^{-1} as also seen on the bottom map of DIC in the Skagerrak area (Figure 3). However, at these stations between 50 and 200 m, (similarly to the shallower stations of the central North Sea) DIC concentrations were much higher during summer and

fall (2165 µmol kg^{-1}) than during winter or spring (2120 µmol kg^{-1}). This suggests that the respiration of organic matter occurred just below the thermocline and increased the DIC concentrations, whereas in the deeper part of the water column the effect of respiration is not evident from the DIC measurements.

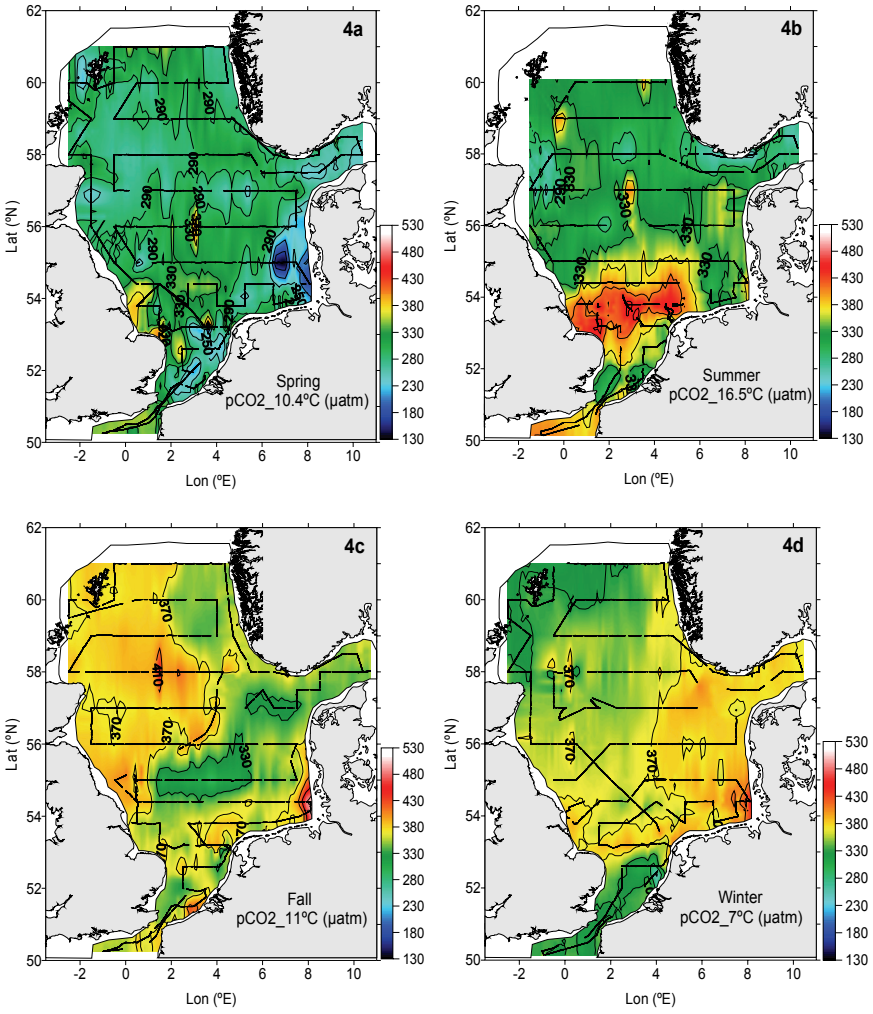

Figure 5: *Map of the normalized pCO_2 from continuous measurements (1 minute interval, 3 m depth) represented by the dotted black line. For each cruise, pCO_2 was normalized using the relationship of (Takahashi et al., 1993) to the average temperature of 10.4ºC, 16.5ºC, 11.0ºC and 7.0ºC for the spring (Figure 5a), summer (Figure 5b), fall (Figure 5c) and winter (Figure 5d) cruises, respectively.*

3.2. Surface pCO_2 distribution

Here we briefly describe the pCO_2 variations in the surface waters of the North Sea related to those of DIC since ΔpCO_2 data have been discussed by Thomas et al. (2004). In order to compare the pCO_2 distributions with those of DIC, pCO_2 was normalized to the average temperature of the surface water of the North Sea at each season using the relationship of Takahashi et al. (1993). For the four seasons, the surface distribution of the normalized pCO_2 presents a similar pattern than the one of pCO_2 at *in-situ* temperature, revealing that temperature was not the main factor controlling the pCO_2 distribution in the surface waters of the North Sea from a given cruise. During spring, most of the North Sea was undersaturated relative to the atmosphere (atmospheric pCO_2 was 361 µatm) (Figure 5a) with surface water pCO_2 ranging between 180 and 300 µatm. Only in the southern area and notably in front of the Humber and Thames estuaries the surface waters of the North Sea were in equilibrium or slightly supersaturated relative to the atmosphere. In summer, pCO_2 showed a similar distribution to the one of DIC with a supersaturation in the southern area and strong undersaturation in the northern North Sea (Figure 5b). During fall, the surface waters of the North Sea began to equilibrate with the atmosphere and revealed a more homogeneous distribution similar to the one of DIC (Figure 5c). The northern area was still slightly undersaturated but the deepening of the mixed layer together with the uptake of CO_2 from the atmosphere were responsible for an average value of 350 µatm, close to equilibrium measured in this area (365 µatm). In the southern area, outgassing and decreasing temperatures diminished the supersaturation observed in summer, with values ranging from 360 to 370 µatm. In winter, the pCO_2 was homogeneous and most of the North Sea was in equilibrium with the atmosphere (Figure 5d). Only the northern eastern part (where the lowest DIC concentrations were measured) revealed a weak undersaturation (pCO_2 of 355 µatm) and some areas along the British and southeastern coasts were slightly supersaturated with pCO_2 values of 375 µatm (atmospheric pCO_2 of 363 µatm).

3.3. Main properties of the ICES boxes

It is important to note that the separation of the North Sea into the ICES boxes was made, taking into account the different properties of the water column (stratification and maximum depth), as well as the spatial variability that may be encountered for the different parameters studied. This distinction into 15 boxes is necessary because each box has its quite unique month-by-month changes over the year, i.e., each box on its own is not representative of the North Sea as a whole, but together they are. Our dataset allowed an accurate estimate of the pCO_2, DIC and nutrient concentrations in each box. By using these boxes we focus on smaller and homogeneous areas, within which each parameter influencing the CO_2 and nutrient distributions can be taken into account. This increases the precision of the calculation of the different factors governing the variations of DIC and nutrients in every box, and allows an accurate computation for the whole North Sea, which takes into account the spatial variability of the ecosystem. Tables 1a and 1b summarize the surface water characteristics during the four cruises for the CO_2 system as well as for

related parameters. Data were gathered in the 10 one layer and upper-layer ICES boxes used for the calculation (Figure 1).

During summer and spring, boxes 1 and 2 had similar properties: the low pCO_2 and DIC values were observed in waters depleted in NO_x and PO_4^{3-}, whereas higher values of chlorophyll *a* were observed in these two boxes in spring compared to summer. In fall and winter, concentrations of NO_x increased to the average values of 6 and 9 µmol L^{-1}, and PO_4^{3-} of 0.45 and 0.65 µmol L^{-1}. The lower minimum of salinity observed in box 1 corresponds to an inflow of freshwater from the Scandinavian coast observed at the station between boxes 1 and 3.

Box 3 receives most of the freshwater inflow from the Scandinavian coast and the Baltic Sea, which originates from erosion of siliceous and calcareous soils, and have low DIC concentrations. In spring and summer, NO_x and PO_4^{3-} were depleted, whereas concentrations as high as 18 µmol L^{-1} were observed during winter for NO_x.

The boxes 4 and 5 are characteristic of the central North Sea. One station situated in box 5 received freshwater inputs form the German Bight but for the other stations, salinity was homogeneous with values ranging from 34.80 to 35.00 during the whole year. Chlorophyll *a* concentrations during spring and summer were lower compared to the other regions of the North Sea with an average concentration of 0.5 µg L^{-1} in summer and 1.5 µg L^{-1} in spring. The NO_x and PO_4^{3-} concentrations were depleted in spring and summer when DIC concentrations and pCO_2 values were lowest. The NO_x concentrations increased during fall and winter, however showed the lowest average concentrations of the North Sea at that time of the year with values ranging from 3.43 to 7.11 µmol L^{-1} for box 4 and ranging from 2.55 to 5.85 µmol L^{-1} for box 5.

The 5 other boxes are situated along the coast or in the southern region of the North Sea. Boxes 6 and 7 are characteristic of the Scottish and English coastal waters. Freshwater inputs were limited at our stations with minimum salinity of only 33.92 in box 7 during winter. The chlorophyll *a* concentrations observed in box 7 during winter were the lowest for the whole North Sea, whereas, during spring, high Chlorophyll *a* concentrations up to 7.2 µg L^{-1} were measured at the station situated in front of the Thames estuary. Box 7 was characterized by detectable NO_x concentrations in summer with concentrations up to 2.18 µmol L^{-1} in front of the Humber estuary. Boxes 8 and 9 were characterized by high freshwater inputs from the estuaries (Scheldt, Rhine, Ems and Elbe) that carry high DIC concentrations, compared to the freshwater inputs from the Scandinavian coast. These high DIC inputs in box 9 (German Bight) were concomitant with extremely high inorganic nutrient inputs during most of the year with maximum values of NO_x in winter as high as 61.90 µmol L^{-1}. The highest chlorophyll *a* values observed in the North Sea were measured in spring and summer in these boxes with average values of 5.0 and 4.5 µg L^{-1}, respectively. Box 10 is influenced by the inputs of Jutland waters, which carry rather high DIC concentrations during the whole year. Waters in this box were depleted in NO_x only during summer, whereas in spring this area received inorganic nutrient inputs from the coast. Chlorophyll *a* concentrations were similar in spring and summer with an average value of 1.0 µg L^{-1}.

Table 1a: *Range of values observed for the main parameters measured during the four cruises in the upper layer of the stratified ICES boxes. For DIC, NO_x, PO_4^{3-}, and Chl a, values were taken from the stations data, whereas for the temperature, salinity and pCO_2, values were taken from the continuous measurement made in each boxes.*

	Season	Salinity	Temp. (°C)	DIC (µmol kg^{-1})	pCO_2 (µatm)	NO_x (µmol L^{-1})	PO_4^{3-} (µmol L^{-1})	Chl *a* (µg L^{-1})
BOX1	Summer	34.20-35.25	12.80-17.70	1979-2059	260-300	0.00-0.35	0.00-0.11	0.23-3.31
	Fall	33.38-35.28	8.90-10.40	2088-2120	301-356	4.86-8.69	0.33-0.59	-
	Winter	35.15-35.35	7.35-9.26	2117-2131	340-365	8.47-10.87	0.59-0.73	-
	Spring	33.94-35.38	8.76-9.54	2063-2107	254-338	0.10-6.87	0.07-0.52	0.67-4.01
BOX2	Summer	34.67-35.02	12.70-15.70	1968-2043	220-340	0.00-1.84	0.01-0.31	0.22-2.85
	Fall	34.83-35.08	9.30-10.80	2098-2119	337-357	4.19-7.36	0.35-0.53	-
	Winter	34.76-35.11	7.12-8.03	2105-2118	339-354	7.11-8.62	0.55-0.62	-
	Spring	34.59-35.12	8.56-9.42	2047-2081	260-298	0.03-1.73	0.07-0.22	0.21-4.96
BOX3	Summer	30.46-34.75	13.70-17.80	1935-2031	240-310	0.01-0.20	0.00-0.04	0.27-0.92
	Fall	31.80-33.75	9.20-11.60	2039-2089	302-358	2.38-4.14	0.20-0.38	-
	Winter	32.38-35.30	5.12-8.61	2089-2126	339-368	7.26-18.01	0.52-1.13	-
	Spring	22.73-35.09	7.69-10.02	1927-2100	256-340	0.03-4.99	0.04-0.79	0.59-3.06
BOX4	Summer	34.58-35.02	15.40-16.50	1995-2040	220-380	0.00-0.17	0.01-0.03	0.26-1.05
	Fall	34.36-34.92	9.00-11.00	2072-2105	298-373	1.75-4.79	0.18-0.44	-
	Winter	34.60-35.00	5.90-7.71	2104-2131	339-366	6.04-8.00	0.55-0.68	-
	Spring	34.62-34.95	9.00-10.12	2045-2081	242-306	0.06-0.18	0.07-0.15	0.21-2.46
BOX5	Summer	33.11-34.79	14.50-18.40	2044-2100	340-460	0.00-0.52	0.01-0.26	0.22-1.72
	Fall	33.30-34.79	10.10-12.90	2061-2133	304-360	0.12-7.84	0.17-0.52	-
	Winter	34.07-34.84	5.98-6.89	2111-2133	332-375	3.96-13.24	0.40-0.68	-
	Spring	33.51-34.76	9.76-12.01	2059-2095	190-351	0.00-3.63	0.02-0.12	0.13-1.76

Table 1b: *Range of values observed for the main parameters measured during the four cruises for the one-layer ICES boxes. For DIC, NO_x, PO_4^{3-}, and Chl a, values were taken from the stations data, whereas for the temperature, salinity and pCO_2, values were taken from the continuous measurement made for each box.*

	Season	Salinity	Temp. (°C)	DIC (µmol kg^{-1})	pCO_2 (µatm)	NO_x (µmol L^{-1})	PO_4^{3-} (µmol L^{-1})	Chl *a* (µg L^{-1})
BOX6	Summer	34.26-34.79	11.70-15.40	2018-2067	220-280	0.00-0.34	0.03-0.22	0.40-5.31
	Fall	34.35-34.95	10.00-11.00	2084-2101	348-370	3.77-6.46	0.45-0.50	-
	Winter	34.09-34.76	6.63-8.18	2079-2107	346-356	6.08-9.49	0.58-0.68	-
	Spring	34.31-34.99	8.69-9.11	2020-2084	238-307	0.05-1.21	0.06-0.20	1.85-1.98
BOX7	Summer	33.95-34.36	13.80-18.20	2066-2096	300-460	1.15-2.18	0.17-0.25	0.45-1.51
	Fall	34.32-34.57	11.20-12.80	2068-2085	345-375	2.40-6.55	0.25-0.51	-
	Winter	33.92-34.92	6.21-8.93	2111-2131	352-369	7.62-14.48	0.43-0.81	-
	Spring	34.01-35.01	9.58-12.47	2054-2122	290-390	0.03-13.42	0.02-0.46	0.79-7.15
BOX8	Summer	32.88-34.36	17.40-19.00	2059-2099	340-430	0.07-2.10	0.02-0.45	0.54-5.55
	Fall	32.40-34.50	10.70-12.70	2082-2190	311-385	3.45-20.67	0.16-0.86	-
	Winter	33.36-34.91	6.59-8.90	2103-2177	302-371	7.28-23.31	0.18-0.72	-
	Spring	31.69-35.18	11.26-13.36	2067-2171	262-372	0.15-13.22	0.01-0.27	1.02-6.52
BOX9	Summer	30.04-32.20	17.90-19.20	2093-2130	370-450	0.14-4.72	0.06-1.00	2.01-3.80
	Fall	28.49-32.98	8.08-11.20	2119-2162	338-425	5.91-37.89	0.53-1.39	-
	Winter	25.58-33.82	4.59-6.68	2132-2195	350-371	14.28-61.9	0.44-1.14	-
	Spring	28.88-32.78	10.60-12.75	2040-2091	206-335	9.10-25.10	0.01-0.07	2.11-3.58
BOX10	Summer	32.26-33.45	17.10-17.30	2091-2101	290-380	0.04-0.37	0.02-0.13	1.05-1.50
	Fall	32.49-34.32	11.00-12.50	2090-2111	353-365	3.30-6.75	0.53-0.73	-
	Winter	33.58-34.36	5.55-6.19	2122-2137	348-366	8.49-13.74	0.53-0.60	-
	Spring	30.80-33.93	9.99-11.21	2071-2072	257-292	1.08-21.98	0.01-0.02	0.53-1.33

4. Results

4.1. ΔDIC_{bio}, ΔDIC_{adv} and $\Delta DIC_{air\text{-}sea}$ in the stratified boxes

The results of the DIC mass balance computations for the stratified boxes are shown in Figure 6 for the northern North Sea (boxes 1/11, 2/12, 3/13) and Figure 7 (boxes 4/14 and 5/15) for the central North Sea. For surface boxes 1, 2, 3, 4 and 5, the biological processes were the main factors controlling the DIC concentrations from February to August and decreased the DIC concentrations (revealing that gross primary production dominates community respiration) with maximum values for ΔDIC_{bio} of -49, -38, -50, -26 and -21 mmol m^{-3}, respectively, observed in April in box 5 and in May for other boxes. This strong uptake of DIC was accompanied by an uptake of CO_2 from the atmosphere to the surface layer, which was responsible for an increase of DIC concentrations of approximately 10 mmol m^{-3} during the whole period. Values of ΔDIC_{adv} were positive since the advection was mostly due to vertical influx of deeper water with higher DIC content. The impact of the advection was higher in the deeper areas (boxes 1, 2 and 3) because of the stronger gradient of DIC in the water column (compare Figure 4c and 4e) and was about 10 mmol m^{-3} in spring and 15 mmol m^{-3} in summer when the DIC gradient was more pronounced. During spring, in boxes 4 and 5, ΔDIC_{adv} was close to zero since in this shallow area, the water column was mixed down to the bottom. ΔDIC_{adv} increased slightly in summer, notably in the deeper areas, with the occurrence of thermal stratification.

For the period from August to November, ΔDIC_{adv} was the main factor increasing the surface DIC concentrations in boxes 1 and 2 with values of 10 mmol m^{-3}. During this period the surface waters of boxes 1, 2 and 3 were still undersaturated in CO_2 compared to the atmosphere, which, associated to higher wind speeds, caused an influx of CO_2 responsible for an increase of DIC concentrations in the surface waters of 5 to 10 mmol m^{-3}. In box 4, both air-sea CO_2 exchange and community respiration exceeding gross primary production, increased the surface waters DIC concentrations by 8 and 5 mmol m^{-3}, respectively. In box 5, the air-sea CO_2 exchange was close to zero, and the main factor increasing the surface DIC concentrations was the community respiration in excess of gross primary production with a ΔDIC_{bio} of +5 mmol m^{-3}. The positive ΔDIC_{bio} values for boxes 1 and 2 were of the same order of magnitude than the error on the results.

From November to January, no significant variations in the DIC surface concentrations were observed in boxes 1, and 2. At this time of the year, the water column was mixed down to 150 m (Figures 4e and 4f) and the surface distribution of DIC was homogeneous (Figure 3d) because of high wind speeds. ΔDIC_{adv} was therefore zero during winter. Results from box 3 revealed a very high advection term during the September-January period. ERSEM overestimates the Baltic Sea water inflow due to inadequate parameterization of the surface water level for the Baltic Sea (Thomas et al., 2005). We corrected this valued using the net Baltic Sea carbon input given by Thomas et al. (2005), which induces an overall error of 4% on ΔDIC_{adv} in this box. This error might be responsible for the biological signal calculated for the September-January period in this box.

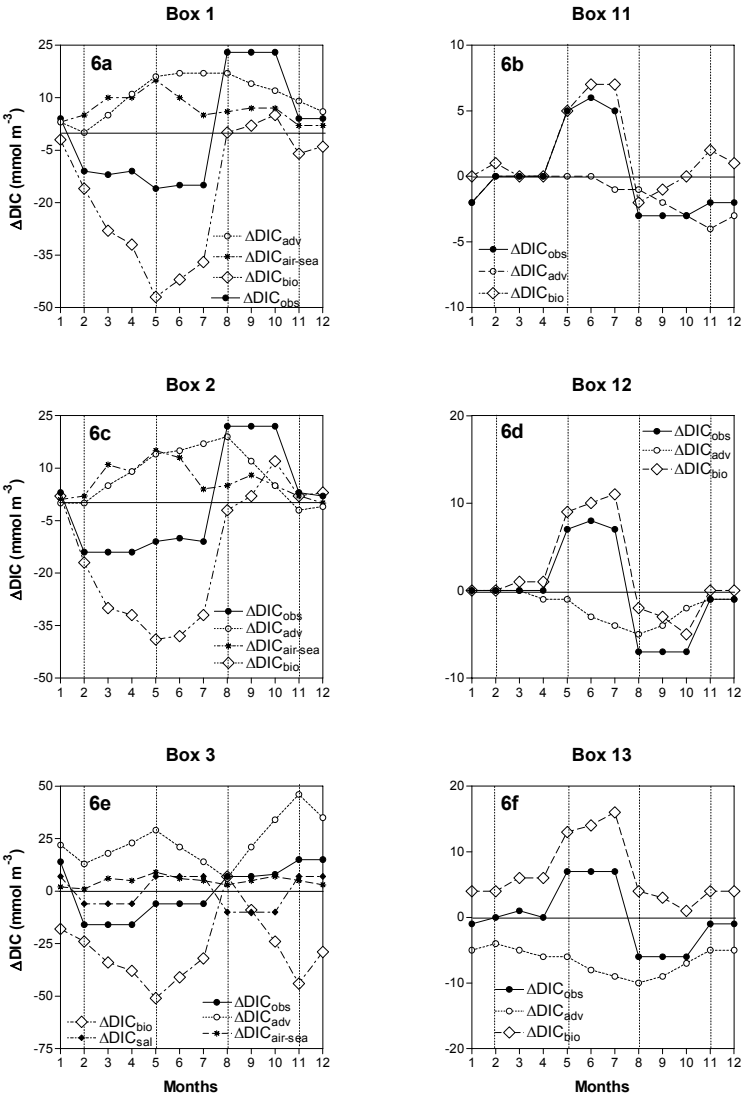

Figure 6: *Monthly effects of advection (ΔDIC_{adv}), air-sea CO_2 exchange ($\Delta DIC_{air\text{-}sea}$) and biological processes (ΔDIC_{bio}) on the variations of DIC (ΔDIC_{obs}) in northern North Sea for the stratified boxes 1 (Figure 6a), 11 (Figure 6b), 2 (Figure 6c), 12 (Figure 6d) and 13 (Figure 6f). For box 3 (Figure 6e) the term ΔDIC_{sal} is included in the plot. The dotted vertical lines correspond to the cruises.*

For this period, the positive values of ΔDIC_{bio} in box 5 (to a minor extend in box 4) showed that community respiration in excess of gross primary production increased DIC concentrations by 5 to 8 mmol m^{-3}. Boxes 5 and 15 represent a shallower area of the North Sea. The average depth in these two boxes is 36 m (maximum of 67 m), which implies that during most of the year the water column is mixed down to the bottom (Lenhart et al., 1995). The positive values of ΔDIC_{bio} calculated in winter might therefore be due to remineralisation of re-suspended sediment material together with respiration of organic material produced from February to August in the upper layer of the water column.

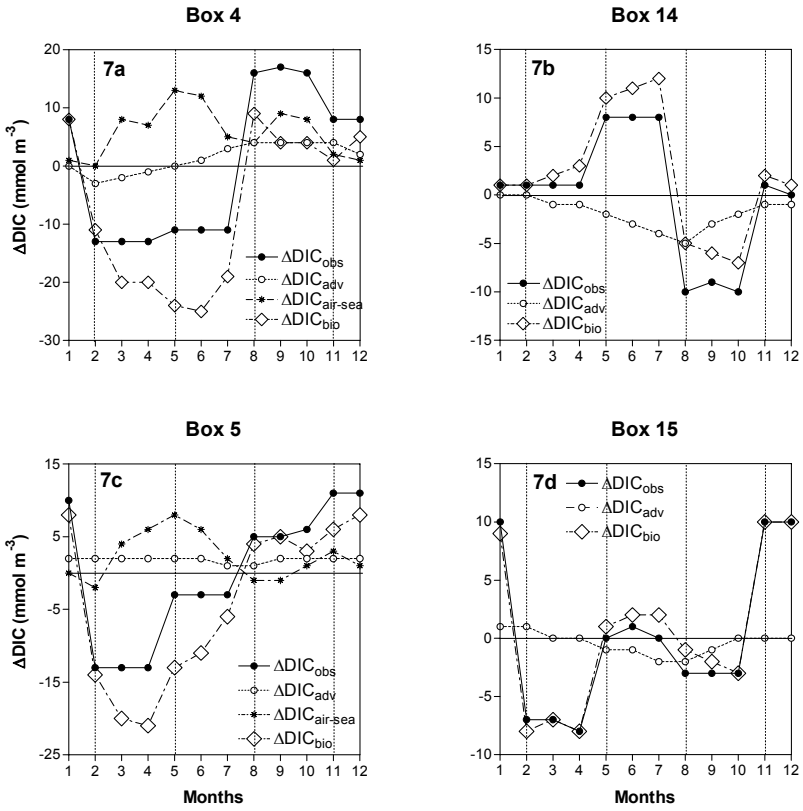

Figure 7: *Monthly effects of advection (ΔDIC_{adv}), air-sea CO_2 exchange ($\Delta DIC_{air\text{-}sea}$) and biological processes (ΔDIC_{bio}) on the variations of DIC (ΔDIC_{obs}) in the central North Sea boxes 4 (Figure 7a), 14 (Figure 7b), 5 (Figure 7c) and 15 (Figure 7d). The dotted vertical lines correspond to the cruises.*

For boxes 11, 12 and 14 there were no significant variations in DIC concentrations from November to May, whereas community respiration dominated gross primary production and increased the DIC concentrations by 5 mmol m^{-3} in the deeper box 13. Only for box 15, gross primary production in excess of community respiration decreased the DIC concentration by 8-9 mmol m^{-3} from February to May. Phytoplankton growth starts in February (Joint and Pomroy, 1993; Moll, 1997) and the fully mixed nature of boxes 5 and 15 at this period of the year allows DIC uptake in the whole water column.

For the period from April to August, positive values of ΔDIC_{bio} ranging from 5 to 10 mmol m^{-3} showed that community respiration in excess of gross primary production governs the DIC variation in the deeper part of the northern and central North Sea (boxes 11, 12, 13, 14 and 15 on Figures 6 and 7). The comparison of ΔDIC_{bio} in the upper and deeper layers of the stratified boxes (Figure 8a) shows that degradation of organic matter occurred in the bottom layer, between 2 to 3 months after the productive period started in the upper layer. This important results confirms that, part of the organic material produced during spring and early summer in the upper layers is respired in the bottom layer as also suggested by Bozec et al. (2005).

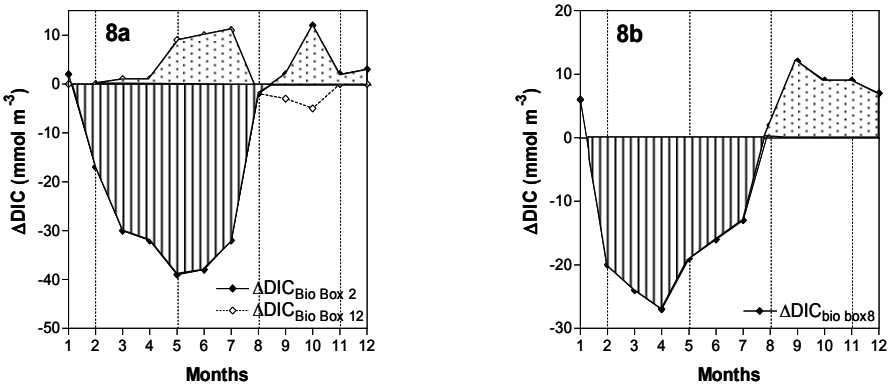

Figure 8: *Impact of the biology term (ΔDIC_{bio}) on the DIC variations in the stratified boxes 2 and 12 (Figure 8a), and in the one layer box 8 (Figure 8b). The negative integration area represents period when gross primary production exceeds community respiration and governs the DIC variations in box 2 and 8, i.e., positive NCP causes a decrease in DIC. The positive integration area represents the period when community respiration exceeds gross primary production and governs the DIC variations in boxes 12 and 8, i.e., negative NCP causes an increase in DIC.*

4.2. ΔDIC_{bio}, ΔDIC_{adv} and $\Delta DIC_{air\text{-}sea}$ in the one layer boxes

Figure 9 shows the relative importance of biology, advection and air-sea CO_2 exchange on the monthly DIC variations for the five one-layer boxes. From February to August, ΔDIC_{bio} values of -5 mmol m^{-3} to -27 mmol m^{-3} show that gross primary production in excess of community respiration governed the DIC pool in the area covered by these boxes. In box 6, with the highest ΔDIC_{bio} values, $\Delta DIC_{air\text{-}sea}$ corresponded to an increase in the DIC concentration of 10 to 12 mmol m^{-3}, whereas ΔDIC_{adv} was close to zero. In the three other boxes, positive values for $\Delta DIC_{air\text{-}sea}$ were also found, however with a much lower impact on the DIC concentrations since ΔpCO_2 values were small, approximately 10 µatm (Figure 5).

For the August-November period, the input of CO_2 from the atmosphere was the main factor governing the DIC variations in box 6. During this period of the year, surface waters in box 6 were still undersaturated in CO_2 with respect to the atmosphere and the higher wind speeds enhanced the air-sea CO_2 exchange, with $\Delta DIC_{air\text{-}sea}$ ranging between 5 and 9 mmol m^{-3}. Box 6 is the deeper one layer box, with an average depth of 70 m, therefore stratification of the water column can occur from mid-May to late September (Lenhart and Pohlmann, 1997) as observed during our summer cruise at three stations. The higher DIC concentrations observed in the deeper layer at these stations for this period of the year suggest that degradation of organic matter occurred in the deeper layer, whereas gross primary production in excess of community respiration drives the DIC variations in the upper layer. From August to November, ΔDIC_{bio} appears to be close to zero and with no effect on the DIC concentrations since gross primary production and community respiration cancelled each other out in the whole water column over that period.

On the other hand, in the very shallow boxes 8 and 9, community respiration in excess of gross primary production processes governed the DIC variations from August to February with ΔDIC_{bio} ranging between 5 to 15 mmol m^{-3}, concomitant with a release of CO_2 to the atmosphere, which decreased the DIC concentrations in the surface layer by 5 mmol m^{-3} in box 8. Similarly, in box 7, degradation of organic matter started governing the DIC variations in mid-October until February and increased the DIC concentration by 10 to 15 mmol m^{-3}, which gave a $\Delta DIC_{air\text{-}sea}$ of -2 to -3 mmol m^{-3}.

Box 10 is exceptional, because it has the smallest volume (404 km^3), and acts as a transition box for the water flow from the southern circulation system into the Norwegian trench, and therefore shows the shortest flushing time between 2 and 29 days (Lenhart and Pohlmann, 1997). During the February-August period, the results showed a similar pattern to the one in the three other one-layer boxes with gross primary production in excess of community respiration governing the DIC variations with ΔDIC_{bio} values ranging from -10 to -20 mmol m^{-3}. This was concomitant with an atmospheric CO_2 uptake causing an increase in the DIC concentrations of 5 to 10 mmol m^{-3} during the whole period. These results are consistent and correspond to the period when the flushing time of the box is the longest (20-30 d) and the mixing minimum (Lenhart and Pohlmann, 1997). However, for the following period (August to February), the very high ΔDIC_{adv} values induced a very strong biological uptake of DIC. This seems unlikely and is probably due to the short

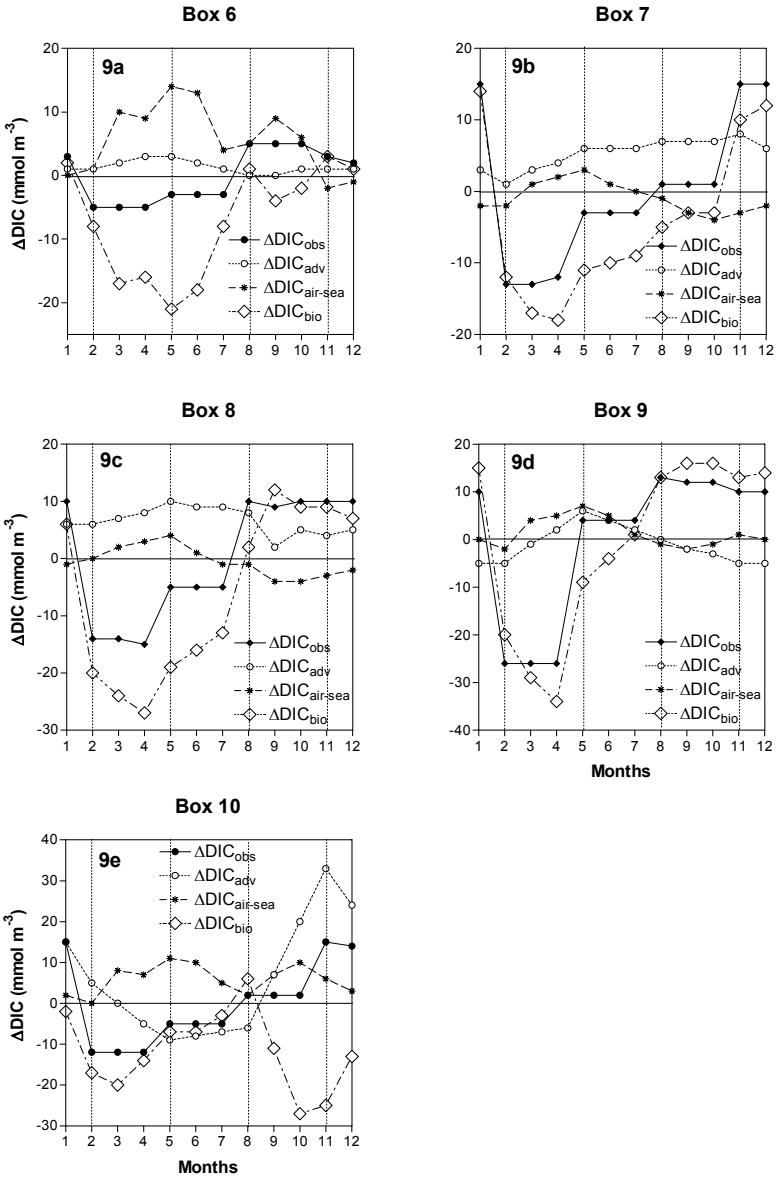

Figure 9: *Monthly effects of advection (ΔDIC_{adv}), air-sea CO_2 exchange ($\Delta DIC_{air\text{-}sea}$) and biological processes (ΔDIC_{bio}) on the variations of DIC (ΔDIC_{obs}) in the one-layer boxes 6 (Figure 9a), 7 (Figure 9b), 8 (Figure 9c), 9 (Figure 9d) and 10 (Figure 9e).*

flushing time of 2 to 5 days for this box at that time of the year, which is not compatible with the temporal scale applied to our calculation. This period of the year for box 10 was not taken into account for the calculation of the NCP in the next section.

In the stratified boxes, gross primary production in excess of community respiration was observed in the upper layer, whereas predominant degradation of organic matter was observed in the bottom boxes with a delay of 2 to 3 months. In the one-layer boxes, the degradation of organic matter largely predominates from August to January (Figure 8b). This predominant degradation of organic matter is responsible for the higher DIC and pCO_2 values during late summer in the southern area, leading to a source of CO_2 to the atmosphere of 0.8 to 1.4 mmol m^{-2} day^{-1} for this area (Bozec et al., 2005). This degassing of CO_2 driven by heterotrophic processes during the July-January period has a strong impact on the annual budget of air-sea exchange of CO_2, with the result that the southern area is an annual source of CO_2 of 0.2 mol C m^{-2} yr^{-1} (Thomas et al., 2004).

5. Discussion

5.1 Net Community Production of Carbon

We calculated the net community production (NCP_C) for each ICES box, based on the ΔDIC_{bio} values and the 30 meters depth of the upper boxes and the maximum depth of each one-layer box. In the following section, we will compare the NCP_C values calculated, firstly between the different regions of the North Sea; secondly with data from the literature; and finally with calculations based on the same mass balance approach using our inorganic nutrients dataset.

NCP is defined as the difference between gross primary production (GPP) and community respiration (R). In autotrophic systems, production of organic matter is larger than its consumption (GPP > R) and there is storage and/or export of excess organic matter. In heterotrophic systems, decomposition of organic matter predominates (R > GPP), and such systems must therefore be supported by external inputs of organic matter (Odum, 1956).

From February to July, the upper layer of the central and northern North Sea was clearly autotrophic with positive values of NCP_C ranging between 0.3 mol C m^{-2} $month^{-1}$ to a maximum of 1.4 mol C m^{-2} $month^{-1}$ in May (Figure 10a). For the rest of the year, NCP_C values were close to zero in all these boxes, because primary production and degradation processes cancelled each other out. Note that, although the upper layers of boxes 1 and 2 were not net autotrophic from August to November, they were still absorbing CO_2 from the atmosphere because of the pre-existing strong undersaturation observed in late summer. Only box 3, showed positive NCP_C values, which suggest that high gross primary production occurred in this area at that time of the year. The larger uncertainty on the ΔDIC_{adv} in this box might be responsible for the ΔDIC_{bio} signal calculated for the September-January period since no phytoplankton activity was observed at that time of the year. It is more likely that the NCP_C in this area is about the same value than for the

adjacent boxes 1 and 2. Taking into account this assumption, the upper layer of the northern North Sea is clearly autotrophic with a calculated NCP_C of 4.6 mol C m^{-2} (Table 2) during the productive period (February to July) and a NCP_C of 4.9 mol C m^{-2} yr^{-1} for the whole year (Table 2).

Table 2: *Net community production for the February-July period and the whole year calculated for: each surface ICES box; the upper layer of the North Sea; the area covered by the one-layer boxes; the area covered by all the deeper boxes; the area between 51ºN-57ºN previously investigated by Smith et al. (1997); the upper layer of the North Sea; and the whole North Sea. NCP_C values are based on the DIC, whereas NCP_N values are based on NO_x data and converted in C units using the Redfield C:N ratio of 6.6. NCP_P is the Net Community production for the area between 51ºN and 57ºN based on the phosphate data measured during our cruises converted in C units using the C:P ratio of 106:1. NCP_P^* is the value found by Smith et al. (1997) for this area. For the upper layer boxes, the DIC, NO_x and PO_4^{3-} uptakes have been integrated over the first 30 meters of the water column, whereas for the one layer boxes, they have been integrated on the whole water column using the maximum depth of each box.*

Boxes	February-July		Annual	
	NCP_C (mol C m^{-2})	NCP_N (mol C m^{-2})	NCP_C (mol C m^{-2} yr^{-1})	NCP_N (mol C m^{-2} yr^{-1})
1	6.0	3.3	6.2	3.1
2	5.7	3.3	5.1	2.5
3	6.5	1.3	10.3	1.6
4	3.5	1.7	2.6	1.3
5	2.2	2.1	1.3	1.9
6	6.1	3.9	6.0	2.5
7	5.0	4.7	3.0	2.2
8	6.0	5.2	3.7	2.2
9	3.8	4.7	0.3	0.1
10	2.7	4.0	5.4	4.0
Upper boxes	4.6	2.2	4.9	2.0
One layer boxes	4.5	4.7	3.1	0.8
Deeper boxes	-5.7	-	-6.6	-
51°N -57°N	-	-	2.1	0.6
Smith et al., 1997	-	-	-	(NCP_P = 0.5) (NCP_P^* = 0.4)
N. Sea upper layer	4.6	3.1	4.3	1.6
N. Sea all	0.8	-	-0.1	-

The deeper boxes of the central and northern area were clearly heterotrophic with NCP_C values ranging between -0.2 mol C m^{-2} $month^{-1}$ to -5.4 mol C m^{-2} $month^{-1}$ with a minimum observed from April to July in the boxes 11, 12 and 13 (Figure 10b). During the whole year, NCP_C for the deeper layers of the northern North Sea covered by theses boxes was -6.6 mol C m^{-2} yr^{-1} (Table 2).

The one-layer boxes of the southern area, for the February-July period, were autotrophic with NCP_C values ranging from 0.1 mol C m^{-2} $month^{-1}$ to 1.2 mol C m^{-2} $month^{-1}$ (Figure 10c). In the deepest box 6, the NCP_C values were in the same range than in the north with a maximum in May of 1.5 mol C m^{-2} $month^{-1}$. For the August-January period, the southern boxes were heterotrophic characterized by NCP_C values ranging between -0.2 to -1.0 mol C m^{-2} $month^{-1}$. The NCP_C calculated for the whole area covered by the one-layer boxes for the productive period (February to July) was very similar than in the northern area with a value of 4.5 mol C m^{-2} for the whole period (Table 2). However, since GPP is much higher in this area than in the northern area (Joint and Pomroy, 1993; Moll, 1997), these results show that high community respiration occurs during the productive period in the one-layer boxes of the Southern Bight. Integrated over the year, NCP_C is lower than in the northern area with a value of 3.1 mol C m^{-2} yr^{-1} (Table 2).

NCP is commonly computed from nitrate or phosphate uptake and converted in carbon units using the Redfield ratios C:N:P = 106:16:1 (Redfield et al., 1963). In the North Sea, previous investigations of NCP were based on such computations (Kempe and Pegler, 1991; Helder et al., 1996; Smith et al., 1997). However, the Redfield ratio is not always appropriate to infer the NCP from nitrate or phosphate fluxes, particularly in regions where NCP has been observed during periods with depleted nitrate and phosphate in surface waters (Thomas et al., 1999; Osterroht and Thomas, 2000; Bégovic and Copin Montégut, 2002; Falck and Anderson, 2005; Kaltin and Anderson, 2005).

Smith et al. (1997) calculated, from a dissolved inorganic phosphate (DIP) mass balance approach, the NCP in the areas between 51ºN-54 ºN and 54ºN-57°N. For the area between 51ºN-54ºN, the monthly variations observed by Smith et al. (1997) follow the same trend than our results with positive values of NCP from February to August and negative values from September to January. For this area, these authors report NCP values for the February-July period, ranging from 0.5 mol C m^{-2} $month^{-1}$ (in February) to 0.2 mol C m^{-2} $month^{-1}$ (in August) with a maximum of 1.2 mol C m^{-2} $month^{-1}$ in April-May. These results are in good agreement with our monthly NCP_C values in the coastal boxes between 51ºN-54ºN (Figure 10c). The good agreement between these two calculations, one based on DIC, the other on DIP shows that in the coastal areas of the southern North Sea, phosphorus (and nitrogen) are available during the whole productive period (Brockmann et al., 1990), which imply that the NCP is equivalent to new primary production as defined by Dugdale and Goering (1967). However, for the northern part of the North Sea, between 54ºN-57°N, our monthly NCP_C were systematically higher than values calculated by Smith et al. (1997) from April to August suggesting an overconsumption of carbon relative to inorganic nutrients.

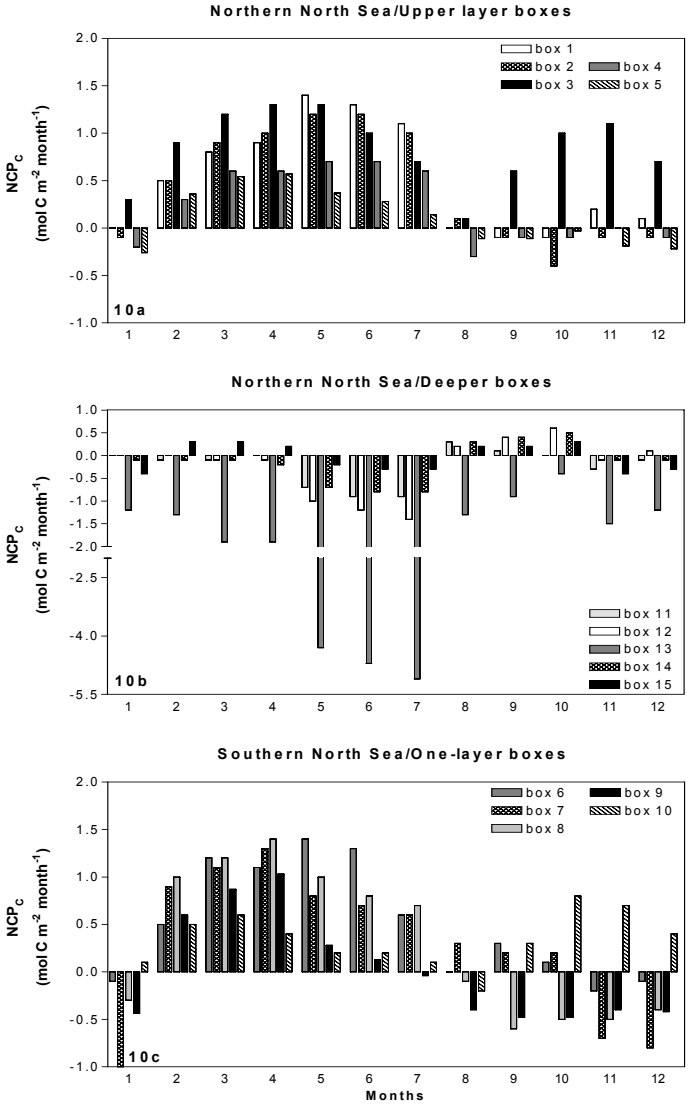

Figure 10: *Monthly net community production calculated from DIC data (NCP_C) in the upper layer boxes (1, 2, 3, 4, 5) (Figure 10a), deeper boxes (11, 12, 13, 14, 15) (Figure 10b) and one layer boxes (6, 7, 8, 9, 10) (Figure 10c). For the upper boxes, the NCP_C was calculated for the top 30 m of the water column. For the bottom boxes, the NCP_C was calculated from 30 m to the seafloor. For the one-layer boxes, the NCP_C was calculated from the maximum depth.*

We applied the mass balance approach of DIC to NO_x measured during our four cruises in the North Sea. The air-sea exchange term was replaced in equation (3) by the atmospheric deposition term from De Leeuw et al. (2001). For each box, the monthly atmospheric deposition increased NO_x concentrations in the mixed layer by 0.20 µmol L^{-1} to 0.60 µmol L^{-1}. This variability is due to the fact that atmospheric deposition decreases rapidly with increasing distance from the coast (De Leeuw et al., 2001). Moreover, air masses arriving over the North Sea having passed over intensively farmed and industrial regions of the southern United Kingdom or continental Europe, will typically exhibit greater concentrations of anthropogenic nitrogen than air masses arriving from the north. We computed the net nitrogen consumption and converted it to NCP in carbon units (NCP_N) using the Redfield ratio of 6.6 (Figure 11).

For the northern North Sea surface boxes, the monthly NCP_C and NCP_N values were similar from February to April (Figure 11a and 11b). This corresponds to the period when the upper layers were not depleted in nitrate (Table 1b) (Brockmann et al., 1990). NCP_C values were still very high in the May-July period but NCP_N values were 1.4 to 2.6 fold lower and corresponded to a period of depleted NO_x surface concentrations. Table 2 shows that NCP_C of 4.6 mol C m^{-2} calculated for the February-July period correspond to an overconsumption of carbon in the upper layer of the northern North Sea of 2.4 mol C m^{-2}. Similarly, Bégovic and Copin Montégut (2002) found an overconsumption of carbon of 1.5 to 3 mol C m^{-2} (with NCP_C values ranging between 4.3 mol C m^{-2} in 1998 and 7.8 mol C m^{-2} in 1999) during the productive period in the central western Mediterranean Sea. In the Baltic Sea, Thomas et al. (1999) and Osterroht and Thomas (2000) showed that the NCP based on DIC exceeds NCP based on NO_3^- by a factor of 1 to 2.5. Recently, Falck and Anderson (2005) found in the surface waters of the Norwegian Sea an export production of 5.2 mol C m^{-2} yr^{-1} based on DIC mass balance budget, which corresponds to an over consumption of carbon of 3.7 mol C m^{-2} yr^{-1}, compared to the calculation based on nitrogen. Our NCP_C estimates for the surface waters of the northern North Sea, are within the range of values in these temperate seas (some adjacent to the North Sea). Similarly to these studies, inorganic carbon consumption continues after nitrate is depleted in the surface waters. Thus, primary production based on regenerated nitrogen and phosphate consumes "new" DIC. This suggests that, as reported in the Baltic Sea (Thomas et al., 1999; Osterroht and Thomas, 2000), preferential recycling of nutrients occurs to sustain carbon consumption in the northern North Sea, where atmospheric inputs are minor and therefore insufficient to sustain the new production. Since nitrate and phosphate show a similar trend, it is likely that the overconsumption of DIC is based on dissolved organic nitrogen (DON) and phosphate (DOP) utilisation, as observed in the Norwegian Sea (Falck and Anderson, 2005), rather than on ammonia or nitrogen fixation. In the surface waters of the northern North Sea, the NCP based on nitrate includes only the new production, which occurs until April, and is therefore underestimated compared to the NCP based on carbon. This also explains our higher NCP_C values compared to those from Smith et al. (1997) for the area between 54ºN-57ºN, where nitrate and phosphate are both depleted in April.

For the one-layer boxes in the southern North Sea, the monthly calculated NCP_C and NCP_N followed a similar trend with similar values within a ratio of 0.8 to 1.1 (Figure 11c and 11d). As mentioned above, during spring and summer, nitrate concentrations in the mixed layer of the North Sea were below analytical detection limit except in coastal areas such as the German bight, Jutland waters and along the southwestern United Kingdom coast. In these areas, NO_x concentrations were never exhausted mainly due to the inputs from rivers and higher atmospheric inputs than in the central North Sea, due to the proximity of the coast. These NO_x inputs sustain net carbon production during the productive period (February to July). The NCP_N is then equivalent to the new production and in the southern North Sea, NCP_C and NCP_N values for the productive period were close, with values of 4.5 mol C m^{-2} and 4.7 mol C m^{-2}, respectively (Table 2).

For the whole surface North Sea, we computed an annual NCP_C of 4.3 mol C m^{-2} yr^{-1} and a NCP_N of 1.6 mol C m^{-2} yr^{-1} (Table 2). As explained above, the NCP_C is a factor 2 to 3 higher than NCP_N because it represents new primary production minus heterotrophic respiration, whereas only part of the new primary production is represented by the NCP_N term for most of the North Sea.

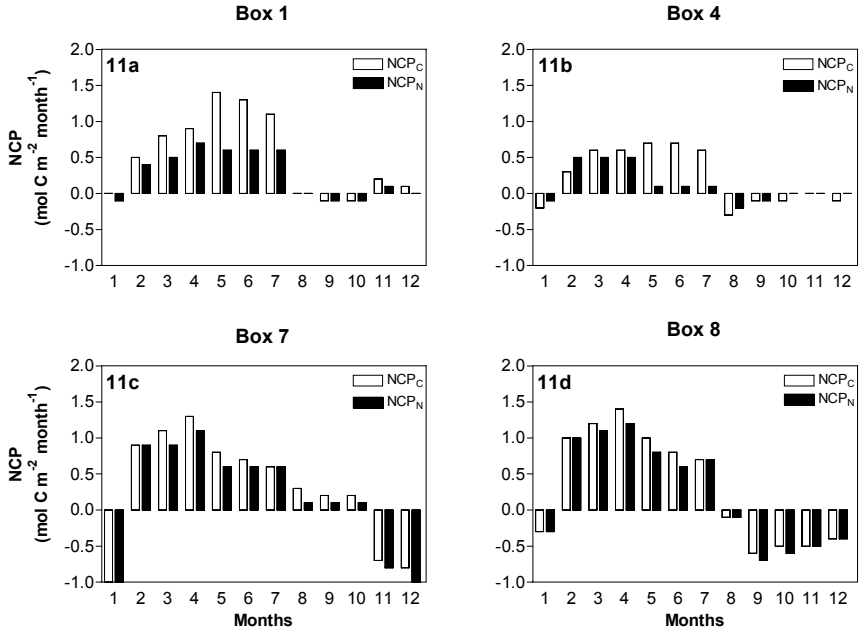

Figure 11: *Monthly net community production calculated from DIC (NCP_C) and NO_x (NCP_N) converted in C units using the Redfield ratio of 6.6 for two northern (Figure 11a) and central (Figure 11b) boxes as well as for two southern boxes (Figure 11c and 11d) of the North Sea.*

In order to provide a consistent comparison with the budget of Smith et al. (1997), we computed NCP_C, NCP_N and NCP_P (NCP based on DIP) for the same area situated between 51°N and 57°N. We found a NCP_C value of 2.1 mol C m^{-2} yr^{-1}, 5 fold higher than the NCP_P of 0.4 mol C m^{-2} yr^{-1} calculated by Smith et al. (1997), because the NCP_P between 54°N and 57°N is underestimated in their calculation. However, our NCP_P of 0.5 mol C m^{-2} yr^{-1} is similar to their NCP_P value of 0.4 mol C m^{-2} yr^{-1} for the same area. Moreover, our estimates of NCP_N and NCP_P of 0.6 and 0.5 mol C m^{-2} yr^{-1}, respectively (Table 2), are very close and show that the regenerated production is mainly based on DON and DOP. This shows that previous investigations of NCP based on mass balance approaches of phosphate and nitrate provide underestimates for the North Sea.

Finally, in the whole North Sea at annual scale, production and consumption of organic matter balance each other with a NCP_C of -0.1 mol C m^{-2} yr^{-1}. This estimate is within the range of values derived from previous computations based on organic carbon by Radach and Lenhart (1995) of -0.05 mol C m^{-2} yr^{-1}, for the same area of 513,000 km^2. Recent budgets of carbon based on DOC for the North Sea by Thomas et al. (2005) concluded that this system is net heterotrophic with NCP of -0.5 ± 0.2 mol C m^{-2} yr^{-1}, for an area of 575,300 km^2. This area includes the Skagerrak (Figure 1), where the water column is the deepest in the North Sea, in average 600 m. The community respiration largely dominates the gross primary production in the deep-water column and is responsible for the higher estimates of NCP for this area of 575,300 km^2.

It is usually assumed that NCP accounts for 0.5 to 2% of the GPP in the North Sea (Helder et al., 1996; Smith et al., 1997), although highly variable. For the southern area, values range between 79 g C m^{-2} yr^{-1} in box 7 to 261 g C m^{-2} yr^{-1} in box 9 (Joint and Pomroy, 1993; Moll, 1997), whereas in the surface waters of the central North Sea they are close to 250 g C m^{-2} yr^{-1} and in the surface waters of the northern North Sea to 200 g C m^{-2} yr^{-1} (Joint and Pomroy, 1993; Moll, 1997). For the surface waters of the northern area we calculated a NCP_C of 58.8 g C m^{-2} yr^{-1} so that it might account for 20 to 30% of GPP. For the southern area, we calculated a NCP_C of approximately 37.2 g C m^{-2} yr^{-1}, which represent 15% of GPP of this area of the North Sea, an estimate higher than previous investigations. Our DIC and pCO_2 dataset makes it possible to estimate the NCP directly from changes in the DIC pool rather than inferring it from changes in inorganic nutrient, thus reducing the uncertainty on the NCP estimates.

5.2. Robustness of the NCP calculations

For the NCP_c computations, we relied on numerous stations with a high vertical resolution for each cruise (each season). The DIC values attributed to each box were representative of the area studied at the time of the cruise since the flushing times of the boxes are in the order of 30 days.

The estimate of the air-sea exchange of CO_2 depends on the parameterization of the gas transfer velocity. The results above were calculated using W&McG99 parameterization. The air-sea CO_2 exchanges computed from the three parameterizations W&McG99, N2000a and N2000b were very similar and did not significantly change the NCP_C estimates. Using the W92 parameterization would decrease the annual NCP_C for the whole North Sea by 3% and the NCP_C calculated for the productive period (February-July) by 10% compared to the results using the W&McG99 parameterization. Moreover, the monthly variations of NCP_C showed similar trends based on the air-sea CO_2 exchange computed using the parameterizations of W92 and W&McG99. Therefore, the calculation of the NCP_C is relatively insensitive to the choice of the gas transfer velocity parameterization as also shown in other coastal ecosystems characterized by relatively low air-sea CO_2 fluxes (Gazeau et al. 2005). However, in ecosystems characterized by very large air-water CO_2 fluxes such as estuaries, this term can be very significant in the NCP computations (Gazeau, F., pers. comm.).

We have used the average values of the advection term calculated for the years 1982-1992 given by Lenhart et al. (1995). Lenhart and Pohlmann (1997) showed that the inter-annual variations for these flows are minor. Since the meteorological conditions observed for the years 2001-2002 were similar to the common climatological conditions in the North Sea, we can assume a similarity of the water flow estimates. Moreover, reducing the mixing term in one box by 50% would only affect our value for the annual NCP_C by 2% and the NCP_C for the productive period by 5%. A larger uncertainty concerns the calculation made in box 3, for which the modeled water flows overestimate the inflow from the Baltic Sea and induce erratic variations in the DIC changes due to biological process in fall and winter. We assumed in the annual calculation of the NCP_C that in box 3, at this period of the year, the NCP_C is of the same order of magnitude than for the adjacent boxes 1 and 2.

Therefore, our NCP_C values calculated for the whole year and for the productive period in the North Sea, are given with a range of uncertainty of ± 10% and ± 20%, respectively. Since our estimate of the annual NCP_C for the whole North Sea is -0.1 mol C m^{-2} yr^{-1} we cannot conclude unambiguously on the trophic status of this system that is probably close to metabolic balance. Nevertheless, the seasonal variations and the spatial differences of NCP_C both vertically and horizontally described above are significant.

6. Summary and conclusions

Based on a robust dataset of DIC, pCO_2 and related parameters covering every season during one year, combined with hydrodynamic data in the North Sea, we calculated the monthly variations of DIC due to abiotic and biological processes in the 15 ICES boxes. In the surface layer of the northern and central North Sea, autotrophy governs DIC changes from February to July and most of the organic carbon produced during this period is then respired in the bottom layer, mainly from April to July. During the remainder of the year, lateral and vertical advection and air-sea exchange of CO_2 govern the monthly DIC changes. On the other hand, in the shallow southern North Sea, the biological processes

govern the DIC variation during the whole year, with predominant autotrophy from February to July and predominant heterotrophy from August to January.

In the surface layer, we calculated an annual NCP based on DIC of 4.3 ± 0.4 mol C m^{-2} yr^{-1} whereas, NCP based on nitrate was 1.6 ± 0.2 mol C m^{-2} yr^{-1}. The large difference between the two computations is due to the fact that nitrate is recycled in the surface layer of the northern North Sea, which leads to an underestimation of the NCP as also observed in other ecosystems such as the Nordic, Norwegian and Mediterranean seas. This shows that carbon overconsumption occurs in open oceanic and coastal waters and in both oligotrophic and eutrophic systems.

Autotrophic surface waters were usually associated with an uptake of atmospheric CO_2, whereas heterotrophic surface waters were usually associated with degassing of CO_2 from the surface water into the atmosphere. However, in the northwestern North Sea, the surface waters were still absorbing CO_2 form the atmosphere from August to November although they were not net autotrophic. This was due to the pre-existing strong CO_2 undersaturation in late summer. Moreover, for the whole North Sea (513,000 km^2), the annual NCP_C is -0.10 ± 0.02 mol C m^{-2} yr^{-1}, which shows that this system is close to metabolic balance although it is a strong sink for atmospheric CO_2 of 1.4 mol C m^{-2} yr^{-1}.

References

Algetsen, G., J. Wikner, S. Sobek, L. J. Tranvik, and M. Jansson. 2004. Seasonal variation of CO_2 saturation in the Gulf of Bothnia: Indications of marine net heterotrophy. Global Biogeochemical Cycles 18. [doi: 10.1029/2004GB002232].

Bégovic, M., and C. Copin Montégut. 2002. Processes controlling annual variations in the partial pressure of CO_2 in surface waters of the central northwestern Mediterranean Sea (Dyfamed site). Deep-Sea Research II 49: 2031-2047.

Borges, A. V. 2005. Do we have enough pieces of the jigsaw to integrate CO_2 fluxes in the Coastal Ocean? Estuaries, 28(1): 3-27.

Bozec, Y., H. Thomas, K. Elkalay, and H. De Baar. 2005. The continental shelf pump in the North Sea - evidence from summer observations. Marine Chemistry 83: 131-147.

Brockmann, U. H., R. W. P. M. Laane, and H. Postma. 1990. Cycling of nutrient elements in the North Sea. Netherlands Journal of Sea Research 26: 239-264.

Chen, C.-T. A. 2004. Exchange of Carbon in the Coastal Seas, p. 341-351. *In* C. B. Field [ed.], The global carbon cycle: integrating human, climate and the natural world. SCOPE, ISSN.

De Haas, H., T. C. E. Van Weering, and H. De Stigter. 2002. Organic carbon in shelf seas: sinks or sources, processes and products. Continental Shelf Research 22: 691-717.

De Leeuw, G., L. Cohen, L. M. Frohn, G. Geernaert, O. Hertel, B. Jensen, T. Jickells, L. Klein, G. J. Kunz, S. Lund, M. Moerman, F. Müller, B. Pedersen, K. von Salzen, K. H. Schlünzen, M. Schulz, C. A. Skjoth, L.-L. Sorensen, L. Spokes, S. Tamm, and E. Vignati. 2001. Atmospheric input of nitrogen into the North Sea: ANICE project overview. Continental Shelf Research 21: 2073-2094.

Dugdale, R. C., and J. J. Goering. 1967. Uptake of new and regenerated forms of nitrogen in primary productivity. Limnology and Oceanography 12: 196-206.

Falck, E., and L. G. Anderson. 2005. The dynamics of the carbon cycle in the surface water of the Norwegian Sea. Marine Chemistry, 94(1-4): 43-53.

Falck, E., and H. G. Gade. 1999. Net community production and oxygen fluxes in the Nordic Seas based on O_2 budget calculations. Global Biogeochemical Cycles 13: 1117-1126.

Frankignoulle, M., and A. V. Borges. 2001. European continental shelf as a significant sink for atmospheric carbon dioxide. Global Biogeochemical Cycles 15: 569-576.

Gattuso, J.-P., M. Frankignoulle, and R. Wollast. 1998. Carbon and carbonate metabolism in coastal aquatic ecosystems. Annual Reviews of Ecological Systems 29: 405-434.

Gazeau, F., C. M. Duarte, J.-P. Gattuso, C. Barrón, N. Navarro, S. Ruíz, Y. T. Prairie, M. Calleja, B. Delille, M. Frankignoulle, and A. V. Borges. 2005. Whole system metabolism and CO_2 fluxes in a Mediterranean Bay dominated by seagrass beds (Palma Bay, NW Mediterranean). Biogeosciences 2: 43-60.

Grasshoff, K., M. Ehrhardt, and K. Kremling. 1983. Methods of seawater analysis. 2nd Edition.

Helder, W., C. Schrum, and G. Shimmield. 1996. North Sea Budget, p. 13-20. *In* J. Hall, S. V. Smith and P. R. Boudreau [eds.], Report on the International Workshop on Continental Shelf Fluxes of Carbon, Nitrogen and Phosphorus. LOICZ/R&S/96-9.

Holm-Hansen, O., C. J. Lorenzen, R. W. Homes, and J. D. H. Strickland. 1965. Fluorometric Determination of Chlorophyll. Journal de Conseil pour l'Exploration de la Mer, 30: 3-15.

ICES, 1983. Flushing times of the North Sea. ICES Cooperative Research Report 123, pp.125.

Johnson, K. M., K. D. Wills, D. B. Butler, W. K. Johnson, and C. S. Wong. 1993. Coulometric total carbon dioxide analysis for marine studies: maximizing the performance of an automated gas extraction system and coulometric detector. Marine Chemistry 44: 167-187.

Joint, I., and A. Pomroy. 1993. Phytoplankton biomass and production in the southern North Sea. Marine Ecology Progress Series 99: 169-182.

Kaltin, S., and L. G. Anderson. 2005. Uptake of atmospheric carbon dioxide in the Arctic seas: evaluation of the relative importance of processes that influence pCO_2 in water transported over the Bering-Chukchi Sea shelf. Marine Chemistry, 94(1-4): 67-79.

Kempe, S., and K. Pegler. 1991. Sinks and sources of CO_2 in coastal seas: the North Sea. Tellus 43B: 224-235.

Körtzinger, A., H. Thomas, B. Schneider, N. Gronau, L. Mintrop, and J. C. Duinker. 1996. At-sea intercomparison of two newly designed underway pCO_2 systems — encouraging results. Marine Chemistry 52: 133-145.

Lenhart, H., and T. Pohlmann. 1997. The ICES-boxes approach in relation to results of a North Sea circulation model. Tellus 49A: 139-160.

Lenhart, H. J., G. Radach, J. O. Backhaus, and T. Pohlmann. 1995. Simulations of the North Sea circulation, its variability, and its implementation as hydrodynamical forcing in ERSEM. Netherlands Journal of Sea Research 33: 271-299.

Mackenzie, F. T. 2003. Our changing planet, 3rd Edition, NJ: Pearson Education.

Mackenzie, F. T., A. Lerman, and A. J. Andersson. 2004. Past and present of sediment and carbon biogeochemical cycling models. Biogeosciences 1: 11-32.

Mackenzie, F. T., A. Lerman, and L. M. Ver. 1998. Role of continental margin in the global carbon balance during the past three centuries. Geology 26: 423-426.

Moll, A. 1997. Modelling Primary Production in the North Sea. Oceanography 10: 24-26.

Muller-Karger, F. E., R. Varela, R. Thunell, R. Luerssen, H. Chuanmin, and J. J. Walsh. 2005. The importance of continental margins in the global carbon cycle. Geophysical Research Letters 32. [doi:01610.01029/02004GL021346].

Nightingale, P. D., P. S. Liss, and P. Schlosser. 2000a. Measurements of air-sea gas transfer during an open ocean algal bloom. Geophysical Research Letters 27: 2117-2120.

Nightingale, P. D., G. MAlin, C. S. Law, A. J. Watson, P. S. Liss, M. I. Liddicoat, J. Boutin, and R. C. Upstill-Goddard. 2000b. In situ evaluation of air-sea gas exchange parameterizations using novel conservative and volatile tracers. Global Biogeochemical Cycles 14: 373-387.

Odum, H. T. 1956. Primary production in flowing waters. Limnology and Oceanography 1: 102-117.

Osterroht, C., and H. Thomas. 2000. New production enhanced by nutrient supply from non-Redfield remineralisation of freshly produced organic material. Journal of Marine Systems 25: 33-46.

Otto, L., J. T. F. Zimmerman, G. K. Furnes, M. Mork, R. Saetre, and G. Becker. 1990. Review of the physical oceanography of the North Sea. Netherlands Journal of Sea Research 26: 161-238.

Petit, J. R., J. Jouzel, D. Raynaud, N. I. Barkov, J.-M. Barnola, I. Basile, M. Bender, J. Chappelaz, M. Davis, M. Delaygue, V. M. Kotlyakov, M. Legrand, V. Y. Lipenkov, C. Lorius, L. Pépin, C. Ritz, E. Saltzman, and M. Stievenard. 1999. Climate and atmospheric history of the past 420,000 years from the Vostock ice core, Antarctica. Nature 399: 429-436.

Radach, G., and H. J. Lenhart. 1995. Nutrient dynamics in the North Sea: fluxes and budgets in the water column derived from ERSEM. Netherlands Journal of Sea Research 33: 301-335.

Redfield, A. C., B. H. Ketchum, and F. A. Richards. 1963. The influence of organisms on the composition of sea-water, p. 26-77. *In* M. N. Hill [ed.], The Sea. Interscience publisher.

Sabine, C. L., R. A. Feely, N. Gruber, R. M. Key, K. Lee, J. L. Bullister, R. Wanninkhof, C. S. Wong, D. W. R. Wallace, B. Tilbrook, F. J. Millero, T.-H., Peng, A. Kozyr, T. Ono and A. F. Ríos. 2004. The Oceanic Sink for Anthropogenic CO_2. Science 305: 367-371.

Smith, S. V., P. R. Boudreau and P. Ruardij. 1997. N and P Budget for the Southern North Sea. http://data.ecology.su.se/mnode/Europe/NorthSea/NORTHSEA.HTM.

Smith, S. V., and J. T. Hollibaugh. 1993. Coastal metabolism and the ocean organic carbon balance. Reviews of Geophysics 31: 75-89.

Smith, S. V., and F. T. Mackenzie. 1987. The ocean as a net heterotrophic system: implications from the carbon biogeochemical cycle. Global Biogeochemical Cycles 1: 187-198.

Stoll, M. H. C. 1994. Inorganic carbon behaviour in the North Atlantic Ocean, Ph.D Thesis, p. 193. Rijksuniversiteit Groningen.

Takahashi, T., J. Olafsson, J. G. Goddard, D. W. Chipman, and N. Sutherland. 1993. Seasonal variation of CO_2 and nutrients in the high-latitude surface oceans: A comparative study. Global Biogeochemical Cycles 7: 843-878.

Thomas, H., Y. Bozec, H. J. W. De Baar, K. Elkalay, M. Frankignoulle, L.-S. Schiettecatte, G. Kattner, and A. V. Borges. 2005. The Carbon budget of the North Sea. Biogeosciences 2: 87-96.

Thomas, H., Y. Bozec, K. Elkalay, and H.J.W. De Baar. 2004. Enhanced open ocean storage of CO_2 from shelf sea pumping. Science 304: 1005-1008.

Thomas, H., V. Ittekkot, C. Osterroht, and B. Schneider. 1999. Preferential recycling of nutrients - the ocean's way to increase new production and to pass nutrient limitation? Limnology and Oceanography 44: 1999-2004.

Thomas, H., and B. Schneider. 1999. The seasonal cycle of carbon dioxide in the Baltic Sea surface waters. Journal of Marine Systems 22: 53-67.

Tsunogai, S., S. Watanabe, and T. Sato. 1999. Is there a "continental shelf pump" for the absorption of atmospheric CO_2? Tellus 51B: 701-712.

Tyrell, T., and A. Merico. 2004. *Emiliana huxleyi*: bloom observations and the conditions that induce them, p. 75-97. *In* H. R. Thierstein and J. R. Young [eds.], Coccolithophores. From Molecular Processes to Global Impact. Springer.

Walsh, J. J. 1991. Importance of continental margins in the marine biogeochemical cycling of carbon and nitrogen. Nature 350: 53-55.

Wanninkhof, R. 1992. Relationship between wind speed and gas exchange over the ocean. Journal of Geophysical Research 97: 7373-7382.

Wanninkhof, R., and W. R. McGillis. 1999. A cubic relationship between air-sea CO_2 exchange and wind speed. Geophysical Research Letters 26: 1889-1892.

Weiss, R. F. 1974. Carbon dioxide in water and seawater: the solubility of a non-ideal gas. Marine Chemistry 2: 203-215.

Acknowledgements

We thank captains and crews of *RV Pelagia* for excellent co-operation during the cruises. This study has been supported by the Netherlands Organisation for Scientific Research (NWO), grants no. 810.33.004 and 014.27.001, the Dutch-German bilateral co-operation NEBROC, the Belgium Federal Office for Scientific, Technical and Cultural Affairs (CANOPY project, EV/03/20). This study has been encouraged by and contributes to the LOICZ core project of the IGBP and to CARBO-OCEAN, an integrated project of the European Union (contract no. 511176-2).

Chapter 5

The Carbon budget of the North Sea

This chapter is based on the article by Helmuth Thomas, Yann Bozec, Hein J.W. de Baar, Khalid Elkalay, Michel Frankignoulle, Laure-Sophie Schiettecatte, Gerhard Kattner and Alberto Vieira Borges, published in Biogeosciences, 2: 87-96.

Abstract

A carbon budget has been established for the North Sea, a shelf sea of the NW European continental shelf. The carbon exchange fluxes with the North Atlantic Ocean dominate the gross carbon budget. The net carbon budget - more relevant to the issue of the contribution of the coastal ocean to the marine carbon cycle - is dominated by the carbon inputs from rivers, the Baltic Sea and the atmosphere. The North Sea acts as a sink for organic carbon and thus can be characterised as a heterotrophic system. The dominant carbon sink is the final export to the North Atlantic Ocean. More than 90% of the CO_2 taken up from the atmosphere is exported to the North Atlantic Ocean making the North Sea a highly efficient continental shelf pump for carbon.

Note: *In the present chapter, Bozec et al. (2005a) refers to Chapter 2, Thomas et al. (2004) refers to Chapter 3 and Bozec et al. (2005b), refers to chapter 4 of this thesis.*

1. Introduction

During the last decade many efforts have been made to investigate, understand and quantify the global carbon cycle, since the greenhouse gas carbon dioxide (CO_2) plays a key role in controlling climate on Earth. It has also been realised that the CO_2 released by human activities is in part responsible for global warming by affecting the heat balance on Earth (IPCC, 2001). Large international projects such as the World Ocean Circulation Experiment (WOCE) or the Joint Global Ocean Flux Study (JGOFS) as well as many national programs have been devoted to understand and assess the ocean's role in the global carbon cycle. Evidence has been provided that the atmosphere and the ocean absorb major amounts of the anthropogenic CO_2, whereas the role of the terrestrial biosphere, which is commonly assessed as a closing term of the global carbon balance, still remains unclear. This in part is caused by the uncertainty in the assessment of the oceanic uptake of anthropogenic CO_2 (Sarmiento et al., 2000; Gruber and Keeling, 2001; IPCC, 2001; Orr et al., 2001; Thomas et al., 2001; Takahashi et al., 2002; Sabine et al., 2004). One of the reasons for this uncertainty is the lack of reliable information on the coastal oceans, which hitherto have only barely been considered in the oceanic and global carbon budgets.

Coastal and marginal seas reveal strong biological activity, in part triggered by terrestrial and human impacts, and play an important role in the global carbon cycle by linking the terrestrial, oceanic and atmospheric carbon reservoirs (Gattuso et al., 1998). The high biological activity causes high CO_2 fluxes between the coastal and marginal seas and the atmosphere and the adjacent open oceans, respectively. Considering the surface area, coastal seas thus might have a contribution disproportionately high to the open ocean storage of CO_2 (Thomas et al., 2004) via a mechanism called the "continental shelf pump" (Tsunogai et al., 1999). High biological activity enables CO_2 drawdown from the

atmosphere and subsequent export to the subsurface layer. The outflow of these CO_2–enriched subsurface waters ultimately transfers the atmospheric CO_2 into the intermediate layers of the open ocean. During the last years detailed field studies have been initiated in a few areas such as the East China Sea, the NW European shelf, the Baltic Sea and the North Sea (Chen and Wang, 1999; Thomas et al., 1999; Thomas and Schneider, 1999; Frankignoulle and Borges, 2001; Borges and Frankignoulle, 2002; Borges and Frankignoulle, 2003; Thomas et al., 2003b; Bozec et al., 2005a; Thomas et al., 2004). However, there is only limited information available on a global scale about these CO_2 fluxes (Liu et al., 2000b; Liu et al., 2000a; Chen et al., 2003).

The North Sea is amongst the best-studied coastal areas world-wide with respect to its physical, chemical and biological conditions, since it has been subject to detailed investigations for many decades. Earlier carbon cycle studies in the North Sea were confined to certain near-shore coastal areas such as the German Bight, the Wadden Sea or the Belgian coast (Hoppema, 1991; Frankignoulle et al., 1996; Borges and Frankignoulle, 1999; Brasse et al., 1999; Borges and Frankignoulle, 2002). An early basin-wide pioneer study relied on total alkalinity, dissolved inorganic carbon (DIC) and pH observations during late spring and provided first insights in the North Sea carbon cycle (Pegler and Kempe, 1988; Kempe and Pegler, 1991). Recently, an intense field study has been carried out covering all seasons with high spatial resolution in order to comprehensively investigate the carbon cycle and its controlling processes in the North Sea (Thomas, 2002; Bozec et al., 2005a; Thomas et al., 2004). Here we establish for the first time a full carbon budget for the North Sea including the CO_2 air-sea exchange (Thomas et al., 2004). We rely our study on data from the above program, data from the European Union projects EUROTROPH and BIOGEST, as well as further complementary data.

2. Site description and methods

2.1. Hydrography

The North Sea (Fig. 1) is located on the north-western European continental shelf with an open northern boundary to the North Atlantic Ocean. In the west and south the North Sea is enclosed by the British Islands, and the European continent (France, Belgium, Netherlands, Germany and Denmark) and the Norwegian West Coast constitute the south-eastern and eastern boundary. The Baltic Sea waters enter the North Sea via the Skagerrak between Denmark and Norway. In the south the English Channel constitutes a further connection to the North Atlantic Ocean. The continuous water exchange across the northern boundary dominates the water budget (OSPARCOM, 2000). Only a minor fraction of this North Atlantic inflow reaches the region south of the Dogger Bank (approx. 55Nº 3ºE; Fig.1), which is controlled by the inputs via the English Channel. As a consequence, the most prevailing feature of the semi-enclosed North Sea is an anticlockwise "u-shaped" circulation of North Atlantic Ocean water entering at the north-western boundaries via the Shetland Channel and the Faire Island Channel and leaving along the Norwegian Trench at

the eastern boundary (Fig. 1) with residence times of about one year (Lenhart and Pohlmann, 1997; Thomas et al., 2003a). For details refer to (OSPARCOM, 2000).

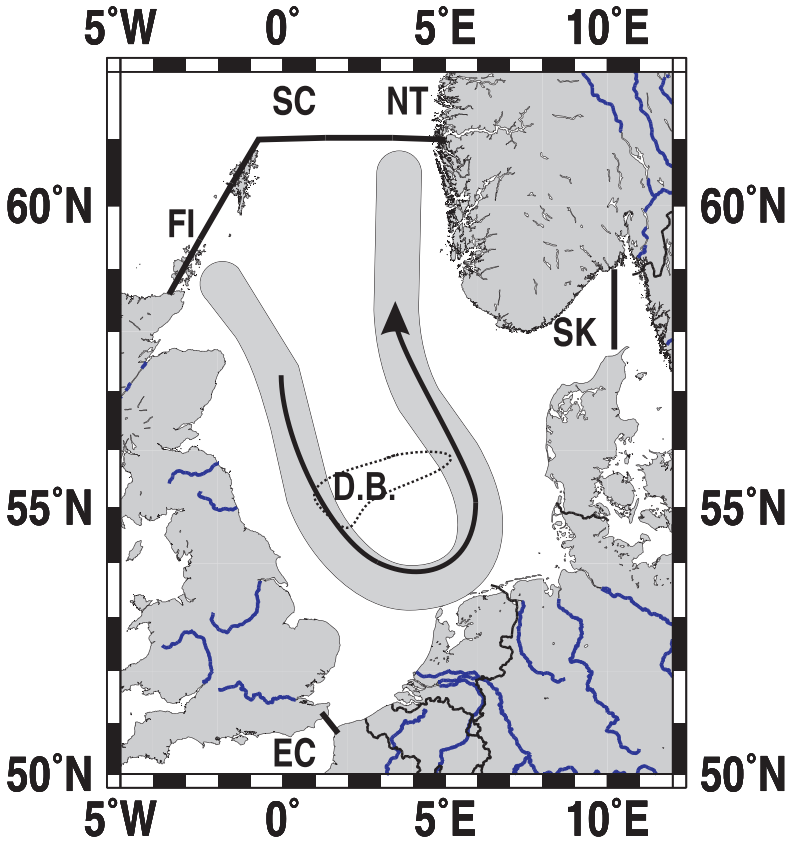

Figure 1: *The Budgeting area for the North Sea. The boundaries of the budgeting area are: English Channel (EC), Skagerrak (SK), Faire Island Channel (FI), Shetland Channel (SC), Norwegian Trench (NT). The arrow indicates the dominant anticlockwise circulation of North Atlantic Ocean water through the North Sea. The location of the Dogger Bank (D.B.) is indicated.*

2.2. Bottom topography and carbon cycling

The bottom topography constitutes a major control of the hydrodynamical conditions as well as for biogeochemical cycling in the North Sea (Frankignoulle and Borges, 2001; Bozec et al., 2005a; Thomas et al., 2004). The deeper northern part reveals

depths down to approximately 150 m on the shelf, down to 400 m in the Norwegian Channel and 700 m in the Skagerrak. This seasonally stratified part of the North Sea is a rather oceanic system, dominated by the influence of North Atlantic Ocean water. Terrestrial influences play a minor role, riverine inputs from the Scandinavian peninsula and the Baltic Sea inputs "dilute" the North Atlantic Ocean water only in a narrow band along the Norwegian coast. In the northern North Sea stratification enables net export of carbon and nutrient to the deeper layers via sinking of particulate organic matter (POM). In contrast, the water depths south of the Dogger Bank are less than 50 m deep, and even less than 20 m deep near the coast. This much smaller, shallow and continuously mixed southern region receives the vast majority of the riverine fresh water supplied to the North Sea. Together with the inputs from the Wadden Sea (Brasse et al., 1999), these inputs exert a significant control of the biogeochemical cycles. The southern region is strongly affected by terrestrial and anthropogenic nutrient inputs (organic and inorganic) and the permanently mixed water column does not enable export of POM to any deeper layers. The POM is mineralised in the whole water column, causing high turnover of the carbon and nutrients and preventing final burial of POM.

Final burial of POM can be observed only in the deeper basins of the Skagerrak and the Norwegian Channel, whereas in the remaining parts of the North Sea almost no POM burial occurs. The overall POM burial can be considered as insignificant on an annual time scale and amounts to less than 1% of the annual primary production (Radach and Lenhart, 1995; De Haas et al., 2002). The lack of ultimate POM burial in both regions of the North Sea has different consequences for the carbon cycling: 1) In the southern part, most of the carbon, fixed as POM by photosynthetic activity, is recycled within the mixed water column or within the sediment surface. On an annual time scale the net CO_2 exchange with the atmosphere is small, since the net removal of DIC by photosynthetic activity is negligible except for the period of the spring bloom. 2) In the northern part the stratification enables net removal of CO_2 by the export of POM to the sub-surface layer and finally DIC export to the North Atlantic Ocean (Thomas et al., 2004; Bozec et al., 2005a).

2.3. The water budget

One of the most critical terms in establishing a carbon budget of entire coastal seas or marine areas in general is the water budget, since the gross and net carbon fluxes related to water mass transport usually dominate the budget. Information available on the various components of the water budget of the North Sea (ICES, 1983; Eisma and Kalf, 1987; Otto et al., 1990; Lenhart et al., 1995; Smith et al., 1996; Lenhart and Pohlmann, 1997) adequately describes the main features of the hydrodynamical circulation. Nevertheless, the exchange flows between the North Atlantic Ocean and the North Sea through the English Channel and across the northern boundary from the different simulations exhibit some discrepancies and are difficult to compare, since they rely on different model structures or forcing conditions. Most critical for our purposes appear to be reliable estimates of the river runoff and the Baltic Sea inflow. The latter one has been reported to be in the range between 1800 km^3 yr^{-1} and 3800 km^3 yr^{-1} [and one assessment of 300 km^3 yr^{-1}] (Lenhart et

al., 1995; Lenhart and Pohlmann, 1997; Smith et al., 1997). However, the (net-) inflow has been reported rather consistently to be on the order of 500 km^3 yr^{-1} from various Baltic Sea studies (Stigebrandt, 2001; Thomas et al., 2003b; Thomas et al., 2005). In order to overcome this problem, our carbon budget calculations rely on the water budget of Eisma and Kalf (1987), which describes reliably the influx from the Baltic Sea (Stigebrandt, 2001; Thomas et al., 2003b) as well as the magnitude of the riverine inputs (OSPARCOM, 2000). There is notable evidence that the water transport across the northern boundaries can be subdivided into transports in the upper and lower parts of the water column (Lenhart et al., 1995; Pätsch and Radach, 1997). The relative information has been used (Tab. 1), since it enables us to consider the high resolution DIC and dissolved organic carbon (DOC) data recently obtained.

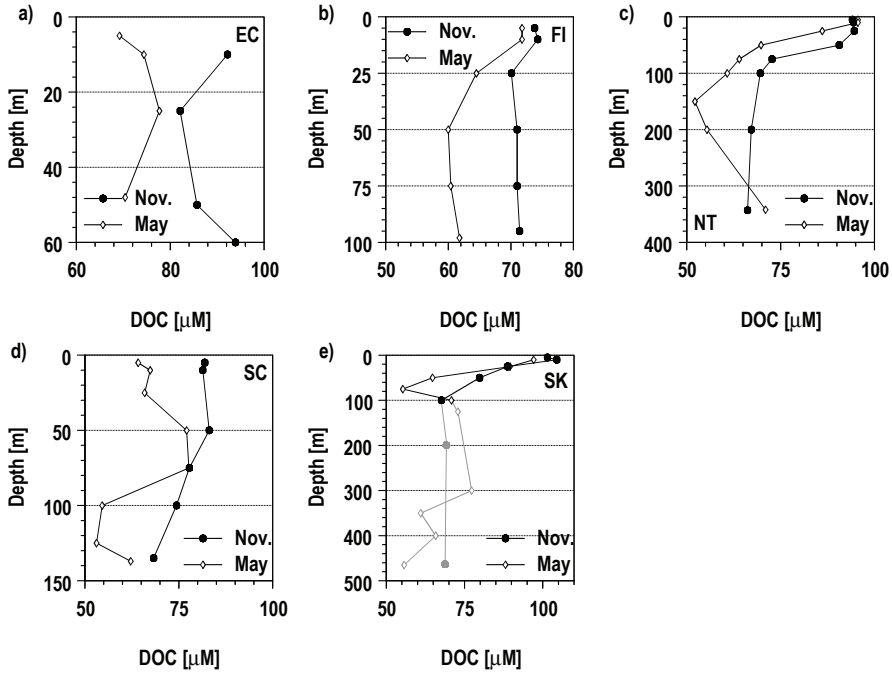

Figure 2: *Dissolved organic carbon (DOC) profiles relied on for establishing the DOC fluxes into and out of the North Sea (Table 1). The profiles are shown for the English Channel (EC) (a, 51°N 1.5°W); for the Faire Island Channel (FI) (b, 60°N 2.5°W); for the Norwegian Trench (NT) (c, 61°N 4°E); for the Shetland Channel (SC) (d, 61°N 0.5°E) and for the Skagerrak (SK) (e, 58°N 10.24°E). For the SK station only the upper 100m of the profile (black colour) have been considered, whereas the deeper samples (grey colour) have been ignored due to the shallower sill depth in the Skagerrak..*

2.4. The carbon budget for the North Sea

In order to establish a carbon budget for the North Sea, one box was defined with the following boundaries: the Strait of Dover in the South, the Faire Island Channel in the Northwest, the Shetland Channel and the Norwegian Trench in the North along 61ºN and the Skagerrak in the east (Fig. 1). The carbon fluxes across these boundaries have been computed using the water transports and the corresponding DIC and DOC concentrations. Although POM plays a key role in the carbon metabolism, it only plays a negligible role in importing or exporting carbon across the North Sea boundaries (De Haas et al., 2002; Thomas et al., 2005). The fluxes of POM thus have been neglected in the present budget except for the final burial of POM in the North Sea. Riverine inputs and carbon burial have been considered as further sinks or sources to the North Sea box. We assume the system to be in a steady state, i.e., the fluxes into and out of the box balance each other (eq. 1). Accordingly, the following components of the North Sea carbon fluxes were considered (eq. 2): inflow with river run-off (F_R), inflow from the Baltic (F_B), inflow from the Atlantic Ocean via the Shetland Channel (F_S), via the Faire Island Channel (F_F) and via the English Channel (F_E), sedimentation (F_S), outflow to the Atlantic Ocean (F_O), net exchange with the atmosphere (F_A). Carbon flows into the box are denoted by a positive sign increasing the carbon content within the box. Carbon flows out of the box are denoted by a negative sign decreasing the carbon content within the box:

$$\Sigma(F_{into\ the\ box}) = \Sigma(F_{out\ of\ the\ box}) \quad (1)$$

or

$$F_R + F_B + F_S + F_F + F_E + F_S + F_O + F_A = 0 \quad (2)$$

The required DIC and DOC data (Tab. 1) have been obtained during the recent North Sea carbon cycle study (Thomas, 2002). The DIC data have been discussed in detail by Bozec et al. (2005a) and Bozec et al. (2005b). DOC data for the relevant stations at the North Sea boundaries are shown in Fig 2. The uncertainty of the DOC data is less than 1μM. For each station the average of the observations has been used as an annual average for the budget calculation. Riverine freshwater inputs to the North Sea amount to 300 km^3 per year (OSPARCOM, 2000). The riverine DIC and DOC data were compiled from various sources, notably the EU BIOGEST program (Borges et al., in preparation). The final inputs were compiled applying the "apparent zero end member" method (Kaul and Froelich, 1984) and upscaled using the "rate curve estimation" method (Cooper and Watts, 2002). The inorganic carbon inputs from the Baltic Sea have been taken from Thomas et al. (2003b). The sedimentation of organic carbon has been estimated according to De Haas et al. (2002) considering only the sedimentation of marine material.

Table 1: *One-box carbon budget of the North Sea. The budgetting area is 575300 km^2, and the water volume 42294 km^3. The water budget is according to Eisma and Kalf (1987). The Baltic Sea inputs are taken from Thomas et al. (2003b). The inflow and outflows were separated into upper and lower water column and the corresponding contributions to the entire flux have been given in paranthesis ([ ]) (Pätsch and Radach, 1997). The overall flux across these boundaries has been calculated accordingly. Sedimentation of organic carbon is according to De Haas et al. (2002). DIC and DOC data are taken from Thomas (2002), riverine inputs from Borges et al. (in preparation). Positive flows indicate inputs into the North Sea and negative ones flows out of the North Sea. The CO_2 air-sea exchange is adopted from Thomas et al. (2004). The uncertainty of the DIC and DOC concentrations is approximately ±1µM (0.05%) and ±1µM (1.25%), respectively. A 10% error of both the air-sea flux and the sedimentation estimates has been assumed. The errors given in the last three columns are due to the analytical errors in the DIC and DOC measurements as well as due to the assumed errors in the estimates of the air-sea fluxes and of sedimentation. The unbalanced term is within the range of uncertainty. The heterotrophy increases the DIC pool at the expense of the DOC pool. It does not constitute a net carbon flux across the North Sea boundaries.*

	Water input/output [km^3 yr^{-1}]	Carbon				
		Input/Output concentration		Input/Output fluxes		
		DIC [µmol l^{-1}]	DOC/POC [µmol l^{-1}]	DIC [10^{12} mol yr^{-1}]	DOC/POC [10^{12} mol yr^{-1}]	Total C [10^{12} mol yr^{-1}]
Baltic Sea	500	2118	78	1.059 (±0.05%)	0.039 (±1.5%)	1.098 (±0.08%)
Atlantic Ocean:						
Via English Channel	4900	2100	80.5	10.290 (±0.05%)	0.395 (±1.5%)	10.685 (±0.08%)
Via Faire Island and Pentland Firth	9000	Upper: 2094 [58%] Lower: 2108 [42%]	Upper: 71.2 [58%] Lower: 66.0 [42%]	18.898 (±0.05%)	0.621 (±1.5%)	19.520 (±0.07%)
Via Shetland Channel	42000	Upper: 2102 [53%] Lower: 2126 [47%]	Upper: 73.9 [53%] Lower: 71.6 [47%]	88.758 (±0.05%)	3.058 (±1.5%)	91.812 (±0.07%)
Rivers	300			0.778 (±0.05%)	0.088 (±1.5%)	0.866 (±0.16%)
Outflow to the North Atlantic Ocean via Norwegian Trench	-56700	Upper: 2075 [14%] Lower: 2142 [86%]	Upper: 93.4 [14%] Lower: 63.4 [86%]	-120.92 (±0.05%)	-3.831 (±1.5%)	-124.751 (±0.07%)
Atmosphere		1.38 mol C m^{-2} yr^{-1}		0.794 (±10%)		0.794 (±10%)
Sedimentation (marine part. Organic Carbon)			-0.13mol C m^{-2} yr^{-1}		Shelf: 0.007 Deep basins: 0.067	-0.073 (±10%)
Subtotals:						
Input:				120.577 (±0.08%)	4.201 (±1.13%)	124.779 (±0.09%)
Output:				-120.92 (±0.05%)	-3.904 (±1.5%)	-124.824 (±0.07%)
Heterotrophy signal		0.59 (±32%)mol C m^{-2}	-0.52 (±26%)mol C m^{-2}	0.34 (±32%)	-0.30 (±26%)	
Unbalanced: (0.04% of total input)						0.045 (±236%)

The uncertainty of the calculations has been estimated with regard to the analytical uncertainty of the DIC and DOC concentration values as well as with regard to an assumed 10% uncertainty of each the air-sea flux and sedimentation estimates (Tab. 1). The errors have been propagated using the formula:

$$X = (\sum_i x_i^2)^{0.5} \quad (3)$$

where X denotes the combined error and x the partial errors. The unbalanced term of the budget (0.04% of the total inputs) is within the range of uncertainty (0.09% of the total inputs) and the budget thus can be considered as a closed budget.

3. Results

3.1. Carbon fluxes in the North Sea

The carbon budget of the North Sea is clearly dominated by the carbon exchange across the northern North Sea boundaries (Fig. 3a, Tab. 1). The Atlantic Ocean supplies more than 98% of the carbon: 74% via the Shetland Channel, 16% via the Faire Island Channel and 9% via the English Channel. Moreover, the Baltic Sea supplies approximately 1% of the carbon. Finally, rivers provide 0.7% and the atmosphere 0.6% of the overall carbon import. The dominant role of the North Atlantic Ocean is even more pronounced in exporting carbon from the North Sea. More than 99% of all carbon is exported to the North Atlantic Ocean via the Norwegian Trench, which constitutes the only notable carbon sink of the North Sea over an annual scale. Only less than 1% of primary production is exported to sediment for burial, which still might play a relevant role over geological time scales.

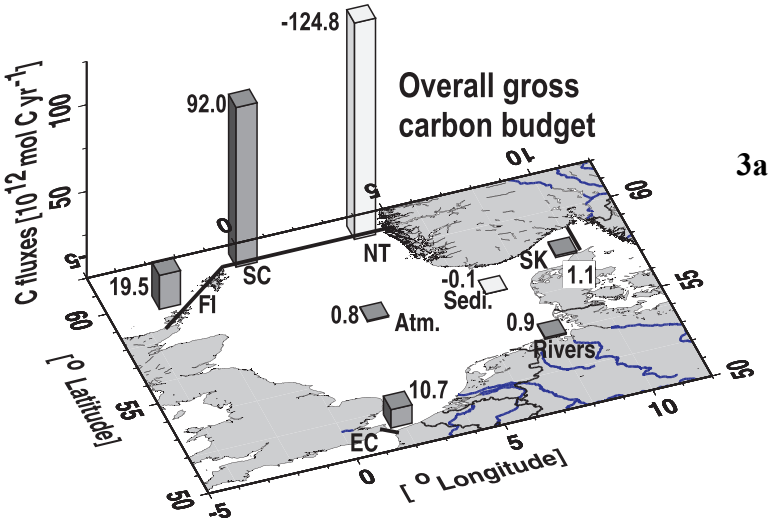

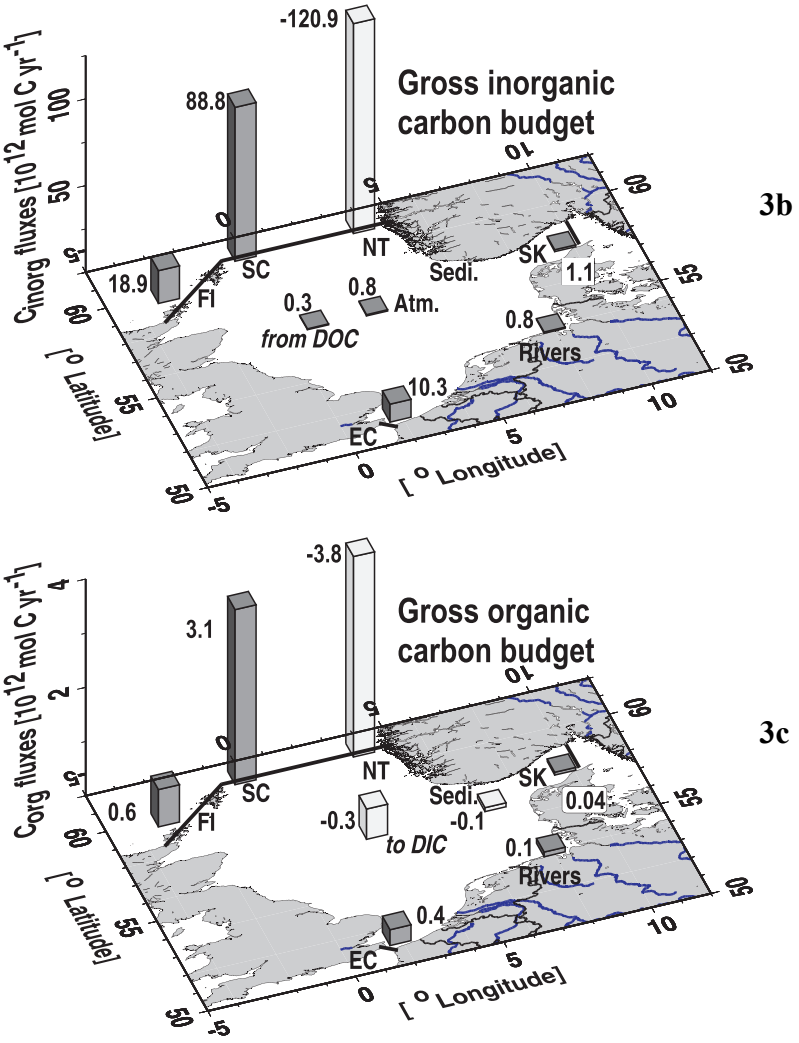

Figure 3: *Gross carbon budgets of the North Sea. The gross carbon fluxes across the boundaries (see Fig.1) as well as the fluxes across the air-sea and sediment water interfaces are shown. (a) shows the total (inorganic and organic) gross carbon fluxes and (b) and (c) the gross inorganic and organic carbon fluxes, respectively. The lighter columns denote carbon sinks (negative values) and the darker columns carbon sources (positive values), respectively. Note the different scales of the plots.*

The separation of the gross carbon fluxes into its inorganic (Fig. 3b) and organic (Fig. 3c) fractions shows that inorganic species (including DIC and atmospheric CO_2) are the major vehicles for the carbon transport. Inorganic species account for 97% of the inputs and for 97% of the exports. About 3% of the carbon is imported to the North Sea as organic carbon and 3% of the carbon exports leaves the North Sea as DOC and less than 1% is exported to the sediments. Moreover, the North Sea acts as a sink for organic carbon, i.e., in the view of the budget a part of the organic carbon imported to the North Sea is converted to DIC and thus leave the North Sea as inorganic carbon.

The main features relevant for carbon budgets for coastal areas are more evident when considering the net carbon fluxes, in our case when ignoring the gross fluxes of carbon because of the exchange with the North Atlantic Ocean. For this purpose, the carbon fluxes entering the North Sea via the Faire Island Channel, the Shetland Channel and the English Channel have been subtracted from the carbon outflow via the Norwegian Trench. The riverine inputs, the uptake of atmospheric CO_2 and the carbon import from the Baltic Sea can now be identified as the major carbon sources controlling the carbon cycling (Fig. 4a). All are of the similar order of magnitude (Tab. 1). It is evident that the carbon content of the North Atlantic Ocean is enriched, while it circulates through the North Sea, by the three suppliers (the atmosphere, the Baltic Sea and the rivers). The overall enrichment of the carbon content of the Atlantic Ocean water amounts to 2.73 10^{12} mol C yr^{-1}, which is approximately 2% of the initial carbon content or – related to the North Sea surface - 4.8 mol C m^{-2} yr^{-1}. The atmosphere represents 29% of this enrichment, the Baltic Sea 40% and the riverine input 31%.

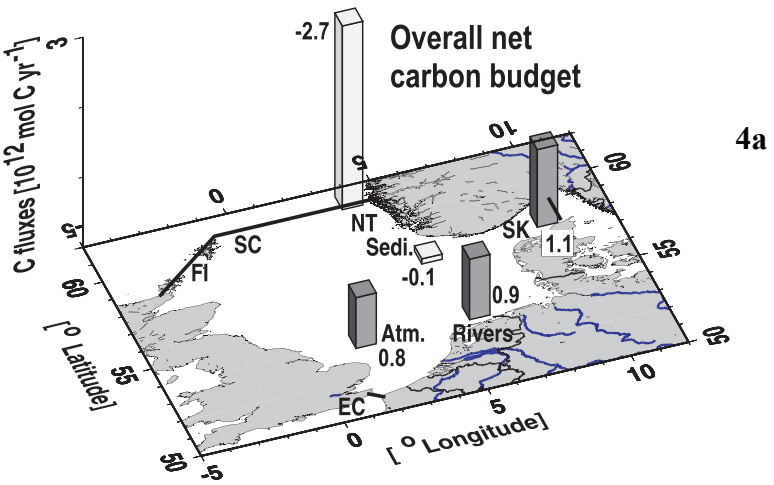

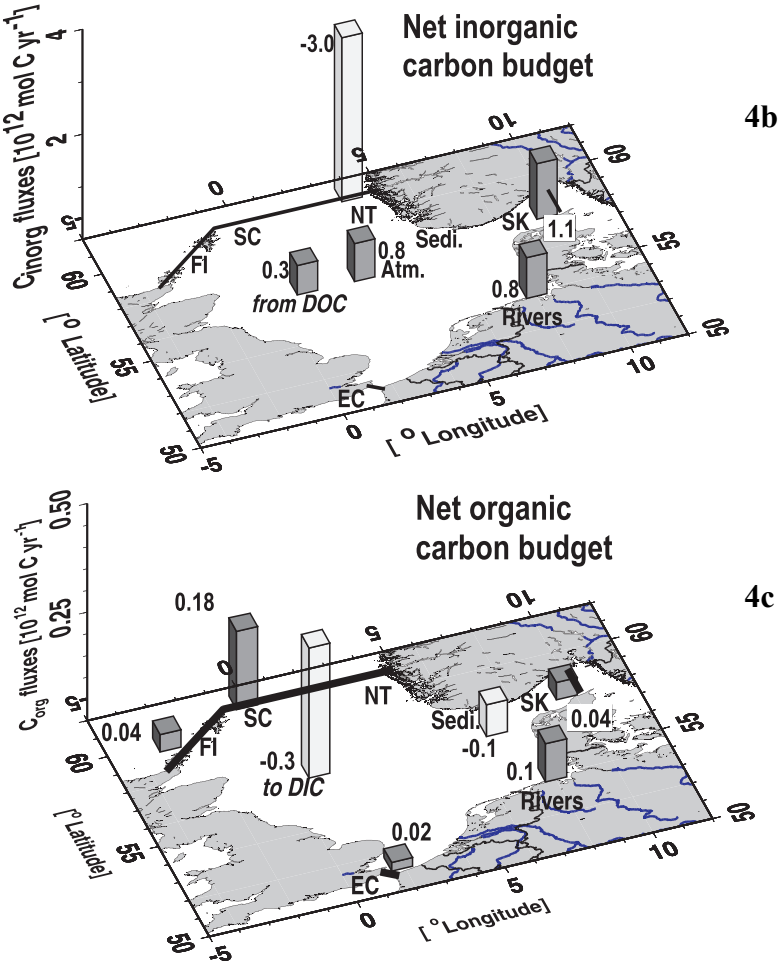

Figure 4: *Net carbon budgets of the North Sea. The net fluxes are calculated from the gross fluxes minus the carbon imports via Faire Island Channel, Shetland Channel and English Channel representing the circulation of Atlantic Ocean water through the North Sea. The net (residual) carbon fluxes across the boundaries as well as the fluxes across the air-sea and sediment water interfaces are shown. A: overall net carbon budget; B: the net budget of inorganic carbon; C: net budget of organic carbon. The lighter columns denote carbon sinks (negative values) and the darker columns carbon sources (positive values), respectively. Note the different scales of the plots.*

A closer look to the net fluxes of the inorganic and organic species shows that the inorganic carbon pool is increased not only by the atmosphere, the Baltic Sea and the rivers, but also from the North Sea DOC pool (Fig. 4b). Considering the observed increase of DIC between the inflowing and outflowing waters, it has been shown that the uptake of atmospheric CO_2 and the "internal" conversion of DOC to DIC contribute with similar order of magnitude to the DIC increase. Approximately 9% of the entire DOC inputs are transferred to the inorganic pool, which is equivalent to 4 times the riverine organic carbon inputs. The major difference between both DIC sources is that the conversion of DOC to DIC does not constitute a net carbon flux, whereas the uptake of atmospheric CO_2 constitutes a net import of carbon. About 10% of the latter are transferred to the sediments and 90% to the North Atlantic Ocean by the continental shelf pump (Thomas et al., 2004; Bozec et al., 2005a; Table 1). The North Sea thus acts as a highly efficient continental shelf pump. For the organic carbon pool (Fig. 4c) the situation is different. The Atlantic Ocean acts as the major source of DOC in the North Sea, while rivers and the Baltic Sea play a rather modest role in the organic carbon budget of the North Sea. Still, these inputs are biogeochemically significant, especially in the southern part, which receives the largest part of the river runoff. Final POM burial acts as a minor sink of organic carbon and the loss of DOC to the DIC pool constitutes the major sink for DOC.

3.2. The trophic state of the North Sea

The trophic status of marine areas can be defined with regard to the production or consumption of organic matter (Odum, 1956; Smith and Hollibaugh, 1993; Gattuso et al., 1998): autotrophic systems are net-producers of organic matter at the expense of inorganic nutrients and carbon: i.e., gross primary production (GPP) is larger than respiration (R).

These systems can export all or part of the excess organic carbon. In contrast, in heterotrophic systems *R* dominates *GPP*, i.e., these systems are net-consumers of organic matter and release inorganic nutrients and carbon. In the "ideal" situation of a real 1-box marine ecosystem, the atmosphere fuels the carbon demand of an autotrophic system unless there is a further inorganic carbon source such as rivers available. Depending on the initial conditions of the water, these systems reveal enhanced uptake of atmospheric CO_2 or in the case of supersaturated waters, any CO_2 release to the atmosphere will be diminished. Similarly, heterotrophic 1-box systems require an organic carbon source and produce inorganic carbon. Accordingly, these systems reveal enhanced CO_2 release to the atmosphere or in case of undersaturated waters, any CO_2 uptake from the atmosphere will be diminished. As examples for such 1-box systems might serve the permanently well-mixed systems like the English Channel (Borges and Frankignoulle, 2003) and the Southern Bight of the North Sea (Thomas et al., 2004; Bozec et al., 2005a) or the south-western Baltic Proper (Thomas and Schneider, 1999), all weak sources of atmospheric CO_2. Also, near-shore coastal regions influenced by anthropogenic and/or terrestrial organic and inorganic carbon inputs such as estuaries and estuarine plumes are sources of CO_2 (Frankignoulle et al., 1998; Borges and Frankignoulle, 2002; Borges et al., 2003).

Complications arise from the transfer of these definitions, originally introduced with regard to individual species, onto marine ecosystems with more than one compartment, since production and respiration processes may be separated in space. In stratified systems, autotrophic processes generally dominate in the surface layer causing the CO_2 uptake and heterotrophic processes dominate the subsurface layer (Thomas et al., 2004; Bozec et al., 2005a) causing in the case of the North Sea the net DIC export to the North Atlantic Ocean. Full carbon (this study) and organic carbon and nutrient (Lenhart et al., 2004) budgets indicate the entire North Sea (575,300 km^2) as a heterotrophic system, which still acts as a sink for atmospheric CO_2. As further examples for such systems might serve seasonally stratified regions such as the Gulf of Biscay (Frankignoulle and Borges, 2001), or permanently stratified regions such as the Baltic Sea (Thomas and Schneider, 1999). The opposite situation is often found in upwelling systems, which commonly are strong producers and exporters of organic matter, however the autotrophic activity is masked by DIC-rich upwelled waters causing a CO_2 release to the atmosphere as for example in the Arabian Sea (Lendt et al., 2003).

These complications are also evident when comparing the findings of the carbon budget presented here with the findings by Smith et al. (1997), who report an autotrophic state of the North Sea, this in contrast to the findings of Borges and Frankignoulle (2003), Thomas et al. (2004), Bozec et al. (2005b) and of the present study. The major differences between their (Smith et al., 1997) and our present assessment are firstly the area covered and secondly the data referred to. Smith et al.'s (1997) budget exclude the northern areas of the North Sea, of which deeper layers apparently host a significant part of the heterotrophic activity (Bozec et al., 2005b). This line of argument is supported by Lenhart et al. (2004), who assessed the trophic state employing an ecosystem model in order to establish an organic carbon balance. They report a general heterotrophic state of the North Sea, which is of the same order of magnitude than the one reported here for the same area of 575,300 km^2. Moreover, Bozec et al. (2005b) were able to provide detailed figures for the northern and southern North Sea, showing the dominating heterotrophy in the northern North Sea and autotrophy in the southern part, the latter confirming the results by Smith et al. (1997).

The aim of this study is to make a statement on the entire North Sea system, while no details can be given for the southern part solely, since we apply a one-box budget. As shown by Bozec et al. (2005b), the different findings for the southern North Sea by Smith et al. (1997) on the one side and the findings of Borges and Frankignoulle (2003), Thomas et al. (2004) on the other side might also be caused by the application of different data (PO_4 vs. inorganic and organic carbon data, respectively). Our budget shows that the heterotrophy of the entire North Sea is to a large extent related to the degradation of DOC imported from the North Atlantic Ocean. This feature obviously could not be captured in the Smith et al.'s (1997) budget based on inorganic phosphorous mass balance approach. Problems with applying nutrient data for the assessment of the trophic state have for example been reported by Thomas et al. (2003b) and Bozec et al. (2005b).

It has been shown that the speciation of the inputs into these systems from rivers or adjacent basins – for example the North Atlantic Ocean (see above) - plays an important role in determining the trophic state. Primarily inorganic inputs support autotrophic activity, whereas primarily organic inputs support heterotrophic activity (Thomas et al., 2003b;

Vichi et al., 2004; Lenhart et al., 2004). While the riverine inputs are of higher relevance for estuaries, near-shore areas and narrow shelves (Frankignoulle et al., 1998; Borges and Frankignoulle, 2002; Borges et al., 2003), these inputs become less relevant, the more oceanic systems become.

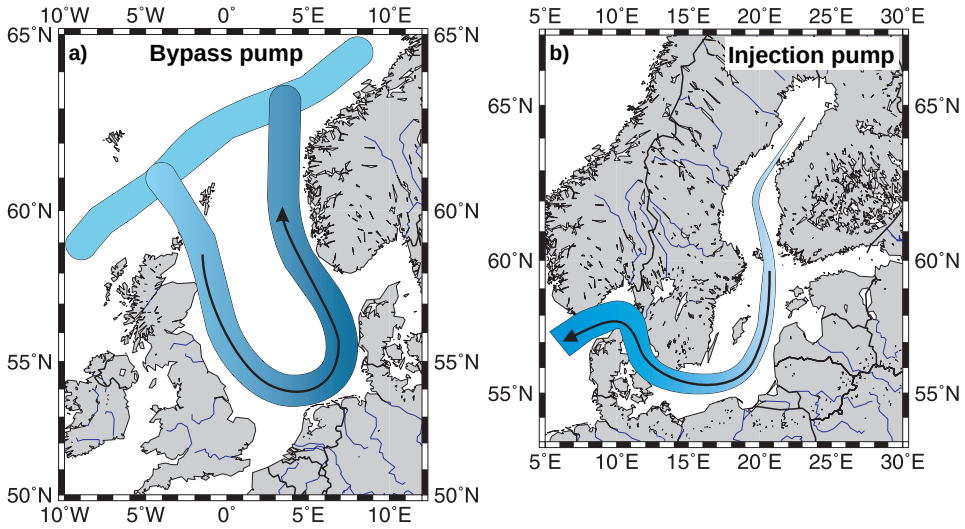

Figure 5: *Different operational modes of the continental shelf pump: the bypass pump in the North Sea (a) and the injection pump in the Baltic Sea (b).*

3.3. Discussion of the budget

The error estimate given in Table 1 is based on the analytical uncertainty of DIC and DOC as well as on the assumed errors of the sedimentation and air-sea flux estimates. This error term does not take into account any uncertainty related to the water budget. Moreover, a seasonal data coverage could not be achieved for all stations and parameters. The error estimate (Tab. 1) thus reflects the lower bound of the uncertainty. As indicated in section two, the carbon budget is closely related to the water budget of the North Sea. Despite the fact that the water exchange with the North Atlantic Ocean dominates both the carbon and the water budget, the carbon budget is highly sensitive to the net water fluxes from the land and the Baltic Sea. While the water import from the Baltic Sea is well established (e.g. Stigebrandt, 2001), available information on the riverine inputs must be carefully evaluated. For example the runoff of the major rivers amounts to approximately 130 km^3 yr^{-1}, whereas the total river runoff to the North Sea amounts to 300 km^3 yr^{-1}

(OSPARCOM, 2000). Given the comparable magnitude of the net players of the carbon budget (Fig. 3), a reliable knowledge on these fluxes is essential. This also holds true for the inflow from the Baltic Sea, which has been overestimated in all modelling studies (see section 2.2). In order to derive the net carbon fluxes, a reliable knowledge of the gross fluxes, i.e., on the carbon exchange between North Sea and North Atlantic Ocean is required. The assessment of the gross flows benefited from the high resolution carbon cycle data set (Thomas, 2002) and allowed to unravel the net flows from the much larger gross flows.

4. The continental shelf pump: operational modes in the North Sea and the adjacent Baltic Sea

The carbon budget describes the North Sea as an overall heterotrophic semi-enclosed sea. The main feature is the circulation of Atlantic Ocean water through the North Sea, of which carbon content is increased during this transport. Major sources increasing the carbon contents of the Atlantic Ocean water are the Baltic Sea, the rivers and the atmosphere. The uptake of atmospheric CO_2 by the North Sea amounts to 1.38 mol C m^{-2} yr^{-1}, of which more than 90% are transferred to the Atlantic Ocean. The continental shelf pump is thus more effective than in the Baltic Sea, which exports approximately 43% of the CO_2 air-sea flux to the North Sea and the remaining 57% to the sediments (Thomas et al., 2003b). This can be explained by different bottom topographic and hydrographic conditions, which cause different operational modes for the continental shelf pump. The brackish Baltic Sea rather serves as a collecting basin for fresh water, which finally is transported following a “one-way road” via the Skagerrak to the North Sea. The permanent halocline and the deeper basins enable effective export of organic matter from the surface layer, which is equivalent to CO_2 draw-down from the atmosphere. Once this carbon escapes the surface layer it can hardly be exported to the North Sea and only the remaining part in the surface layers is available to the continental shelf pump. In contrast, the North Sea reveals almost no carbon preservation in sediments, which ultimately implies that the entire CO_2 draw-down caused by biological activity is available for export to the Atlantic Ocean. The relatively short flushing time of the North Sea and its bottom topography play a major role in preventing sedimentation and accumulation of POM (De Haas et al., 2002). Once the CO_2 has been taken up by the North Sea, it is rapidly exported to the Atlantic Ocean. The North Sea thus can be seen as a bypass pump (Fig. 5a), which increases the carbon content of Atlantic Ocean water while it is circulated through the North Sea. In contrast, the Baltic Sea rather acts as an injection pump (Fig. 5b), which injects “new” water and corresponding carbon loads to the adjacent aquatic system, which is in this case the North Sea.

References

Borges, A.V., and M. Frankignoulle: Daily and seasonal variations of the partial pressure of CO_2 in surface seawater along Belgian and southern Dutch coastal areas. Journal of Marine Systems, 19, 251-266, 1999.

Borges, A.V., and M. Frankignoulle: Distribution and air-water exchange of carbon dioxide in the Scheldt plume off the Belgian coast. Biogeochemistry, 59, 41-67, 2002.

Borges, A.V., and M. Frankignoulle: Distribution of surface carbon dioxide and air-sea exchange in the English Channel and adjacent areas. Journal of Geophysical Research, 108, 1-14, 2003.

Borges, A.V., S. Djenidi, G. Lacroix, J. Théate, B. DeLille, and M. Frankignoulle: Atmospheric CO_2 flux from mangrove surrounding waters. Geophysical Research Letters, 30, 12-11/12-14, 2003.

Bozec, Y., H. Thomas, K. Elkalay, and H. De Baar: The continental shelf pump in the North Sea - evidence from summer observations. Marine Chemistry, 93, 131-147, 2005a.

Bozec, Y., H. Thomas, L.-S. Schiettecatte, A.V. Borges, K. Elkalay and H.J.W. de Baar. Assessment of the processes controlling the seasonal variations of dissolved inorganic carbon in the North Sea. *In revision for Limnology and Oceanography,* 2005b.

Brasse, S., A. Reimer, R. Seifert, and W. Michaelis: The influence of intertidal mudflats on the dissolved inorganic carbon and total alkalinity distribution in the German Bight, southeastern North Sea. Journal of Sea Research, 42, 93-103, 1999.

Chen, C.-T.A., and S.-L. Wang: Carbon, alkalinity and nutrient budgets on the East China Sea continental shelf. Journal of Geophysical Research, 104, 20,675-20,686, 1999.

Chen, C.-T.A., K.-K. Liu, and R. MacDonald, Continental margin exchanges, in *Ocean Biogeochemistry: A JGOFS synthesis*, edited by M.J.R. Fasham, pp. 53-97, Springer, 2003.

Cooper, D.M., and C.D. Watts: A comparison of river load estimation techniques: application to dissolved organic carbon. Environmetrics, 13, 733-750, 2002.

De Haas, H., T.C.E. Van Weering, and H. De Stigter: Organic carbon in shelf seas: sinks or sources, processes and products. Continental Shelf Research, 22, 691-717, 2002.

Eisma, D., and J. Kalf: Dispersal, concentration and deposition of suspended matter in the North Sea. J Geological Society of London, 161-178, 1987.

Frankignoulle, M., and A.V. Borges: European continental shelf as a significant sink for atmospheric carbon dioxide. Global Biogeochemical Cycles, 15, 569-576, 2001.

Frankignoulle, M., I. Bourge, C. Canon, and P. Dauby: Distribution of surface seawater partial CO_2 pressure in the English Channel and in the Southern Bight of the North Sea. Continental Shelf Research, 16, 381-395, 1996.

Frankignoulle, M., G. Abril, A. Borges, I. Bourge, C. Canon, B. DeLille, E. Libert, and J.-M. Théate: Carbon dioxide emission from European estuaries. Science, 282, 434-436, 1998.

Gattuso, J.-P., M. Frankignoulle, and R. Wollast: Carbon and carbonate metabolism in coastal aquatic ecosystems. Annual Reviews of Ecological Systems, 29, 405-434, 1998.

Gruber, N., and C.D. Keeling: An improved estimate of the isotopic air-sea disequilibrium of CO_2: Implications for the oceanic uptake of anthropogenic CO_2. Geophysical Research Letters, 28, 555-558, 2001.

Hoppema, J.M.J.: The seasonal behaviour of carbon dioxide and oxygen in the coastal North Sea along the Netherlands. Netherlands Journal of Sea Research, 28, 167-179, 1991.

ICES, Flushing times of the North Sea. ICES Cooperative Research Report, pp. 125, 1983.

IPCC, 2001. The scientific basis. In: J.T. Houghton et al. (Editors), Contribution of Working Group I to the Third Assessment Report of the Intergovernmental Panel on Climate Change. Cambridge University Press, New York, USA, pp. 881.

Kaul, L., and P. Froelich: Modelling estuarine nutrient biogeochemistry in a simple system. Geochimica et Cosmochimica Acta, 48, 1417-1433, 1984.

Kempe, S., and K. Pegler: Sinks and sources of CO_2 in coastal seas: the North Sea. Tellus, 43B, 224-235, 1991.

Lendt, R., H. Thomas, A. Hupe, and V. Ittekkot: Response of the near-surface carbonate system of the northwestern Arabian Sea to the southwest monsoon and related biological forcing. Journal of Geophysical Research, 108, 15-11/15-14, 2003.

Lenhart, H., and T. Pohlmann: The ICES-boxes approach in relation to results of a North Sea circulation model. Tellus, 49A, 139-160, 1997.

Lenhart, H.J., G. Radach, J.O. Backhaus, and T. Pohlmann: Simulations of the North Sea circulation, its variability, and its implementation as hydrodynamical forcing in ERSEM. Netherlands Journal of Sea Research, 33, 271-299, 1995.

Lenhart, H.J., J. Pätsch, W. Kühn, A. Moll, T. Pohlmann: Investigation on the trophic state of the North Sea for three years (1994-1996) simulated with the ecosystem model ERSEM - the role of a sharp NAOI decline. Biogeosciences Discussion 1, 725-754, 2004.

Liu, K.-K., K. Iseki, and S.-Y. Chao, Continental margin carbon fluxes, in *The Changing Ocean Carbon Cycle: A midterm synthesis of the Joint Global Ocean Flux Study*, edited by J.G. Field, pp. 187-239, Cambridge University Press, Cambridge, 2000a.

Liu, K.-K., L. Atkinson, C.T.A. Chen, S. Gao, J. Hall, R. MacDonald, L. Talaue McManus, and R. Quinones: Exploring continental margin carbon fluxes on a global scale. EOS, 81, 641-644, 2000b.

Odum, H. T. Primary production in flowing waters. Limnology and Oceanography 1: 102-117. 1956.

Orr, J.C., E. Maier-Reimer, U. Mikolajewicz, P. Monfray, J.L. Sarmiento, J.R. Toggweiler, N.K. Taylor, J. Palmer, N. Gruber, C.L. Sabine, C. Le Quéré, R.M. Key, and J. Boutin: Estimates of anthropogenic carbon uptake from four three-dimensional global ocean models. Global Biogeochemical Cycles, 15, 43-60, 2001.

OSPARCOM, Quality Status Report 2000 - Region II Greater North Sea, pp. 136, OSPAR Commission, London, 2000.

Otto, L., J.T.F. Zimmerman, G.K. Furnes, M. Mork, R. Saetre, and G. Becker: Review of the physical oceanography of the North Sea. Netherlands Journal of Sea Research, 26, 161-238, 1990.

Pätsch, J., and G. Radach: Long-term simulation of the eutrophication of the North Sea: Temporal development of nutrients, chlorophyll and primary production in comparison to observations. Journal of Sea Research, 275-310, 1997.

Pegler, K., and S. Kempe: The carbonate system of the North Sea: determination of alkalinity and TCO_2 and calculation of PCO_2 and Sl_{cal} (spring 1986). Mitt. Geol.-Paläont. Inst. Univ. Hamburg, 65, 35-87, 1988.

Radach, G., and H.J. Lenhart: Nutrient dynamics in the North Sea: fluxes and budgets in the water column derived from ERSEM. Netherlands Journal of Sea Research, 33, 301-335, 1995.

Sabine, C.L., R.A. Feely, N. Gruber, R.M. Key, K. Lee, J.L. Bullister, R. Wanninkhof, C.S. Wong, D.W.R. Wallace, B. Tilbrook, F.J. Millero, T.-H. Peng, A. Kozyr, T. Ono, and A.F. Rios: The Oceanic Sink for Anthropogenic CO_2. Science, 305, 367-371, 2004.

Sarmiento, J.L., P. Monfray, E. Maier-Reimer, O. Aumont, R.J. Murnane, and J.C. Orr: Sea-air CO_2 fluxes and carbon transport: A comparison of three ocean general circulation models. Global Biogeochemical Cycles, 14, 1267-1281, 2000.

Smith, J.A., P.E. Damm, M.D. Skogen, R.A. Flather, and J. Pätsch: An investigation into the variability of circulation and transport on the north-west European shelf using three hydrodynamic models. Deutsche Hydrographische Zeitschrift, 48, 325-348, 1996.

Smith, S.V., and J.T. Hollibaugh: Coastal metabolism and the ocean organic carbon balance. Reviews of Geophysics, 31, 75-89, 1993.

Smith, S.V., P.R. Boudreau, and P. Ruardij: NP Budget for the Southern North Sea. http://data.ecology.su.se/mnode/Europe/NorthSea/NORTHSEA.HTM, 1997.

Stigebrandt, A., Physical Oceanography of the Baltic Sea, in *A System Analysis of the Baltic Sea*, edited by P. Larsson, pp. 19-74, Springer, Berlin Heidelberg, 2001.

Takahashi, T., S.C. Sutherland, C. Sweeney, A. Poisson, N. Metzl, B. Tilbrook, N.R. Bates, R. Wanninkhof, R.A. Feely, C.L. Sabine, J. Olafsson, and Y. Nojiri: Global sea –air CO_2 flux based on climatological surface ocean pCO_2, and seasonal biological and temperature effects. Deep-Sea Research II, 49, 1601-1622, 2002.

Thomas, H., *Shipboard report of the RV Pelagia cruises 64PE184. 64PE187, 64PE190 and 64PE195*, 63 pp., Royal Netherlands Institute for Sea Research, Texel, NL, 2002.

Thomas, H., and B. Schneider: The seasonal cycle of carbon dioxide in the Baltic Sea surface waters. Journal of Marine Systems, 22, 53-67, 1999.

Thomas, H., M.H. England, and V. Ittekkot: An off-line 3D model of anthropogenic CO_2 uptake by the oceans. Geophysical Research Letters, 28, 547-550, 2001.

Thomas, H., J.-P. Gattuso, and S.V. Smith: Coastal Biogeochemistry at the EGS-AGU-EUG Joint Assembly, Nice, France, 6-11 April 2003. LOICZ newsletter, 28, 2003a.

Thomas, H., V. Ittekkot, C. Osterroht, and B. Schneider: Preferential recycling of nutrients - the ocean's way to increase new production and to pass nutrient limitation? Limnology and Oceanography, 44, 1999-2004, 1999.

Thomas, H., J. Pempkowiak, F. Wulff, and K. Nagel: Autotrophy, nitrogen accumulation and nitrogen limitation in the Baltic Sea: a paradox or a buffer for eutrophication? Geophysical Research Letters, 30, 2130, DOI: 2110.1029/2003GL017937, 2003b.

Thomas, H., Y. Bozec, K. Elkalay, and H. De Baar: Enhanced open ocean storage of CO_2 from shelf sea pumping. Science, 304, 1005-1008, 2004.

Thomas, H., J. Pempkowiak, F. Wulff, and K. Nagel, Carbon and nutrient budgets of the Baltic Sea, in *Carbon and nutrient fluxes in global continental margins*, edited by L. Talaue-McManus, Springer, New York, 2005.

Tsunogai, S., S. Watanabe, and T. Sato: Is there a "continental shelf pump" for the absorption of atmospheric CO_2? Tellus, 51B, 701-712, 1999.

Vichi, M., P. Ruardij, and J.W. Baretta: Link or sink: a modelling interpretation of the open Baltic biogeochemistry. Biogeosciences, 1, 79-100, 2004.

Acknowledgements

The excellent co-operation of the captains and the crews of *RV Pelagia* is gratefully acknowledged. This study has been encouraged by and contributes to the LOICZ core project of the IGBP and to CARBO-OCEAN, an integrated project of the European Union (contract no. 511176-2). It has been supported by the Netherlands Organisation for Scientific Research (NWO), grants no. 810.33.004 and 014.27.001, the Dutch-German bilateral co-operation NEBROC, the Belgium Federal Office for Scientific, Technical and Cultural Affairs (CANOPY project, EV/03/20) and EU EUROTROPH project (EVK3-CT-2000-00040) AVB and MF are, respectively a post-doctoral researcher and a senior research associate at the FNRS. An earlier version of this paper greatly benefited from two anonymous reviewers' and the editor's comments.

Chapter 6

The CO_2 system in a Redfield context during an iron enrichment experiment in the Southern Ocean

This chapter by Yann Bozec, Dorothee C.E. Bakker, Carmen Hartmann, Helmuth Thomas, Richard G.J. Bellerby, Phil D. Nightingale, Ulf Riebesell, Andrew J. Watson and Hein J.W. de Baar has been published in Marine Chemistry, 95(1-2): 89-105.

Abstract

In November 2000, a second iron enrichment experiment (EisenEx) was carried out in the Southern Ocean. Iron was added on the 8th of November in the centre of an eddy at 21°E, 48°S. During the cruise, the carbonate parameters dissolved inorganic carbon (DIC), fugacity of CO_2 (fCO_2) and pH on the hydrogen ion scale (pH_T) were determined from water samples from both inside and outside the iron fertilized patch. Before the start of the experiment, the surface properties of the eddy were quite uniform with respect to the carbonate system and representative of the High Nutrient Low Chlorophyll (HNLC) regions in the Southern Ocean. The response of the carbon dioxide system to the initial ≈ 4 nM iron (Fe) infusion and to two subsequent reinfusions at 15 m depth was measured every day during the study. The changes in the carbon dioxide system and major nutrients were strongly influenced by the meteorological conditions with a rapid succession of calm, often sunny spells and storm force winds during the 21 days of experiment. Twenty days after the first Fe-infusion, the maximum changes of the carbonate parameters in surface waters of the patch relative to outside patch were -15 μmol kg^{-1} in DIC, -23 μatm in fCO_2, +0.033 units in pH_T, -1.61 μM in nitrate, -0.16 μM in phosphate in a mixed layer of 80 meter depth. In addition to the daily measurements, several transects were made across the patch that showed a response of the carbonate system to the influence of iron, concomitant with a response in nutrients and chlorophyll. The relative changes in dissolved inorganic carbon to nutrient concentrations inside the patch during the experiment give N/P = 12, C/P = 82, C/N = 5.9, C/Si = 2.9 and N/Si = 0.5. The effect of the influx of atmospheric CO_2 on the DIC inventory was small with values between 0.05 and 0.10 μmol kg^{-1} d^{-1}, and did not significantly affect these ratios. Although the observed change in DIC in the Fe-enriched surface waters was lower than in the previous Fe-enrichment experiments, the equivalent biological C-uptake of 1.08×10^9 mol C across the patch after 20 days was significant due to the large horizontal dispersion of the patch. The ratio of biological carbon uptake to Fe added ($C_{biological\ uptake}/Fe_{added}$) was 2.5×10^4 mol mol^{-1}.

1. Introduction

In three vast oceanic regions (the Southern Ocean, the North Pacific and the Equatorial Pacific), large stocks of major nutrients such as nitrate, phosphate and silicate are available but phytoplankton growth and therefore the biological pump of CO_2 are generally sub-optimal. This is the well known paradox of the HNLC (High Nutrients Low Chlorophyll) regions. Martin and Fitzwater (1988) suggested that the lack of iron in these areas could limit the phytoplankton growth. Then Martin (1990) hypothesized that large-scale iron fertilization of the HNLC regions would remove CO_2 from the atmosphere and would sequester it into the deep ocean. This would in turn reduce the greenhouse effect. The “iron hypothesis” was indeed confirmed by *in vitro* enrichment experiments using incubation bottles (Martin and Fitzwater, 1988; de Baar et al., 1990). However, these experiments were widely discussed (Banse, 1990; Broecker, 1990; Miller et al., 1991; Kurz

and Maier-Reimer, 1993), because they did not mimic the open ocean conditions and excluded parameters such as grazing by zooplankton, sinking of particles to the aphotic layer and advection. However, natural iron (Fe)-fertilization (Martin et al., 1994; de Baar et al., 1995; de Baar et al., 1997; Blain et al., 2000) as well as mesoscale *in situ* experiments (Martin et al., 1994; Coale et al., 1996; Boyd et al., 2000; Tsuda et al., 2003) revealed unambiguously that phytoplankton growth was stimulated by iron enrichment.

In parallel, it has also been shown that the amount of available iron affects the ratio of algal uptake of silicic acid to that of nitrate and phosphate (de Baar et al., 1997; Boyle, 1998; Hutchins and Bruland, 1998; Takeda, 1998). Moreover, variation from the global mean "Redfield" ratio of N:P of about 15:1 (Fanning, 1992), as have been observed in Southern Ocean waters, may be directly related to Fe supply (de Baar et al., 1997).

During the IronEx I experiment the effects of algal growth on CO_2 uptake remained low compared to the potential for uptake of CO_2 in the nutrient replete surface waters of the Equatorial Pacific Ocean, since iron fertilized waters were subducted within 4-5 days (Martin et al., 1994; Watson et al., 1994). The IronEx II experiment provided substantial CO_2 uptake (Coale et al., 1996; Cooper et al., 1996; Millero et al., 1998; Steinberg et al., 1998) and it was suggested that, if the Southern Ocean could be similarly influenced, large-scale increases in the iron supply could lower the atmospheric CO_2 concentration by 6-21% based on models of enhanced nutrient utilization (Cooper et al., 1996). The SOIREE experiment demonstrated the occurrence of iron limitation of algal growth in the Southern Ocean (Boyd et al., 2000). After 13 days, approximately 1.1×10^8 moles of carbon had been incorporated into organic matter across the patch (Watson et al., 2000; Bakker et al., 2001). However the fate of SOIREE bloom could not be ascertained during the 13 days-experiment. Knowledge of this fate is crucial for the CO_2 budget. If biomass is respired again in the surface layer by zooplankton and bacteria, no net removal of CO_2 from the atmosphere occurs. However, if the organic matter leaves the surface layer, the equivalent CO_2 amount is removed from the atmosphere for thousands of years.

A large part of the Southern Ocean consists of a broad eastward flowing ring of water, the Antarctic Circumpolar Current (ACC). One of the fronts in the ACC, the Antarctic Polar Front (APF), separates the Polar Frontal Zone (PFZ) to the north from the Antarctic Zone. The purpose of the EisenEx experiment was to determine if phytoplankton of the ACC is iron-limited in spring, to compare the reaction and the evolution of the pelagic ecosystem after fertilization to that in SOIREE in austral autumn and to follow the evolution of the bloom over time under stormy spring conditions (Smetacek, 2001).

During the 21 days of experiment we measured vertical profiles of dissolved inorganic carbon (DIC) concentration and the fugacity of carbon dioxide (fCO_2) inside and outside the iron enriched waters (inside and outside "the patch") in order to study the changes in the carbon system due to iron fertilization. We also continuously measured DIC, fCO_2 and pH_T (pH on the hydrogen ion scale) during the different surface water mappings of the patch in order to study the spatial changes for these parameters.

In the present paper we firstly detail the patch deployment, as well as the data acquisition and data analysis for the carbonate parameters. Secondly, we focus on the

reaction and evolution of the carbonate system under contrasting meteorological conditions during the 21 days of the experiment. In section 3.4, the changes in DIC are compared to the changes in major nutrients such as nitrate, phosphate and silicate in order to study the Redfield ratios. In section 3.5, the impact of CO_2 air-sea exchange on these ratios is evaluated and discussed. Finally, we established the biological carbon uptake within the patch and related it to the Fe input.

2. Materials and Methods

2.1 Patch deployment

The experiment was performed in the Atlantic sector of the Southern Ocean at 21° E, 48° S in austral spring (6-29 November 2000) during cruise Ant XVIII/2 of R.V. *Polarstern*. The core of an eddy originating from the Southern Polar Front (Strass et al., 2001) was selected after a 750 km surveying transect along the 20°E meridian between the Subantarctic front at 45°S and the Antarctic zone at 52°S. This eddy provided a stable water mass with favourable chemical, biological and physical conditions for the experiment (Smetacek, 2001). In the centre of the eddy marked with a drifting buoy, an area of about 50 km^2 was enriched with iron (Fe(II) from dissolution of $FeSO_4$ in acidified seawater). This iron sulphate solution, containing a constant ratio of the inert tracer sulphur hexafluoride (SF_6), was released during 15 hours in the mixed layer, at a depth of 16 ± 2 meters in the wake of the ship's propeller in order to avoid the escape of volatile SF_6 into the atmosphere and to ensure that the tracer and iron were rapidly mixed throughout the mixed layer. The first iron fertilization resulted in an ambient surface water concentration of dissolved iron of 4.5 ± 3 nM (Croot and Laan, 2001). The first Fe-infusion of the EisenEx experiment was initiated at 17:20 GMT on the 7th of November 2000 and ended at 6:45 GMT on the 8th of November. All times in this paper are relative to 0:00 GMT on 8 November 2000, which was taken as the start of the experiment (t=0). Two re-infusions of iron were made on days 7 and 16 of the experiment to maintain the elevated iron concentrations within the Fe-enriched water body ("the patch"). Here day 7 indicates the seventh day after the first iron addition (t = 7 to t = 8).

2.2 Ship's surface water supply

The ship's water supply provided large volumes of water from 11 meters depth for continuous sampling of SF_6, DIC, fCO_2, and pH_T. The temperature difference between the ship's inlet and the laboratory outlet, warming by an average of 0.2ºC (standard deviation of 0.1ºC for 8362 points), was monitored and corrected for with the relationship of Takahashi et al. (1993).

2.3 Sampling stations

Sampling was performed inside and outside the Fe-enriched patch throughout the experiment. The positions of the sampling stations were based from surveys of the surface water SF_6 concentration (Watson et al., 2001). "In-stations" were situated in areas of high SF_6 concentration, whereas "out-stations" were within waters of the eddy that had a background SF_6 concentration. Vertical profiles were obtained from a 24 bottles (12 L) rosette coupled to a conductivity-temperature-depth (CTD) profiler (Sea-Birds Electronics SBE 911plus), and equipped with a Haardt fluorometer calibrated with Chlorophyll *a* discrete samples (precision of ± 4%). Usually samples were taken at about 12 different depths between 5 and 200 meters. Samples for DIC, fCO_2 and nutrients were taken from the same cast at the same depths in order to obtain a coherent dataset.

2.4 Determination of DIC

The concentration of dissolved inorganic carbon was analysed on samples from regular CTD-casts inside and outside the patch, as well as on water from the ship's surface water supply every 7-8 minutes during the mappings of the patch. Samples from CTD casts were collected in 1 L glass bottles, which were kept cold before measurement. DIC was determined by the coulometric method of Johnson et al. (1993), as described by Stoll (1994). A new coulometric cell was prepared on the discrete and online systems approximately every 12 hours. Every coulometric cell was calibrated by Certified Reference Material (CRM) (batch #49). The accuracy and the precision of the system were evaluated by the measurement of two standards on each coulometric cell. Three to four replicate measurements for each sample and standard indicated a precision better than 1 μmol kg^{-1}. The repeated measurement of the standard every 20 samples allowed us to correct for possible drift in the measurement. In the present paper we only present data obtained with the cells with the optimal accuracy. The dissolved inorganic carbon data discussed below have an overall accuracy of ± 2 μmol kg^{-1}.

2.5 Determination of fCO_2

Analysis of the fugacity of CO_2 was made from regular CTD-casts inside and outside the patch, as well as on water from the ship's surface water supply. The atmospheric CO_2 content was analysed in parallel in order to determine the CO_2 air-sea gradient. Marine air was collected through tubing from the crow's nest. Seawater was introduced at a rate of 3 L min^{-1} into a fast response equilibrator with a showerhead (adapted after Robertson et al., 1993; Bakker et al., 1997). Every four minutes an infrared LICOR 6262 analyser determined the molar fraction of CO_2 of a sample from the equilibrator headspace or from marine air. Samples from the equilibrator headspace and marine air were dried before analysis. The calibrated value for the mixing ratio of CO_2 in a dry sample (xCO_2dry) was corrected to the mixing ratio of CO_2 in a wet sample for the

equilibrator temperature and sea surface salinity, while using the infrared CO_2 analyser's (LI-COR 6262) reading for pressure. The formula for the water vapour pressure of seawater from the LI-COR 6262 handbook was used (LI-COR., 1996). The partial pressure of CO_2 (pCO_2) in the equilibrator was calculated from the mixing ratio in a wet sample and atmospheric pressure. The atmospheric pressure was determined using the atmosphere sensor of the ship's PODAS system, corrected to sea level, with a frequency of one minute, an accuracy of 0.1 mbar and averaged to 10 minutes. A Pt-100 thermometer monitored the temperature of the water in the equilibrator. The pCO_2 in seawater was calculated by correction for warming of the water with the relationship by Takahashi et al. (1993). The fCO_2 was calculated, while using the equations by Weiss (1974). Standards of 295.1 and 406.1 µmol CO_2 mol^{-1} (σ of 0.6 and 0.1 µmol mol^{-1}, respectively), which had been calibrated against certified NOAA standards, were analysed every 45 minutes. The time delay between sampling and analysis was taken as 4 minutes for fCO_2 in air and surface water. The accuracy and precision of online surface water fCO_2 data were estimated as 1.0 µatm and 0.6 µatm, respectively, as determined in a previous cruise (Bakker et al., 2001).

2.6 Determination of pH_T

Underway pH_T was determined using an automated marine pH sensor (AMpS), as previously described by Bellerby et al. (2002). In brief, the pH of seawater was measured from samples automatically drawn from the ship's continuous laboratory supply through a flow injection manifold coupled to a fibre optic array. The method of determination was dual spectrophotometric analysis of the seawater after the addition of a sulfonephtalein indicator. The background absorption spectrum of natural seawater was taken and an aliquot of thymol blue was injected into seawater enclosed in a flow cell. After the solution was fully mixed, spectral scans were taken along with solution temperature. The pH_T was estimated from the change in absorption between blanks and sample runs. The frequency of determination was 25 samples per hour. The method has an on-line precision of better than 0.001 pH units and an estimated accuracy of better than 0.004 pH units (Bellerby et al., 2002).

2.7 Determination of nutrients and oxygen

Dissolved nutrients silicate, nitrate+nitrite ($NO_{3/2}$) and phosphate (PO_4^{3-}) were measured in all samples within 10 hours after sampling, using a Technicon Autoanalyzer II system (Hartmann et al., 1997). All nutrient samples were analysed in duplicate, which gives a precision of ± 0.05 µM for nitrate+nitrite and silicate in the concentration range from zero to 20 µM, and ± 0.1 µM for the higher concentrations. For phosphate the precision was ± 0.01 µM. For calibration, 3 standards were run at the beginning and 2 standards at the end of each run, which give an accuracy of ± 0.1 µM for $NO_{3/2}$ and silicate and ± 0.01 µM for phosphate. In the results and discussion below, we discuss the sum of nitrate and nitrite in order to consider the complete pool, which is the relevant entity when

deriving uptake by plankton versus uptake of phosphate and silicate. Note that nitrite concentrations were always below 0.2 µM.

Dissolved oxygen was determined (de Baar, 2001) with the method of Pai et al. (1993) with an estimated accuracy of ± 1 µmol kg^{-1}.

Table 1: *The physical, chemical and biological properties of the surface waters before iron addition during the four Fe-enrichment experiments and their standard deviations on the means (±). From Martin et al., 1994, Watson et al., 1994, Coale et al., 1996, Cooper et al., 1996, Steinberg et al., 1998, Boyd et al., 2001, Bakker et al., 2001 and this study.*
[#]pH has been normalized to a temperature of 4°C.

Parameters	IronEx I	IronEx II	SOIREE	EisenEx
Temperature (°C)	22.9 ± 0.2	25.2 ± 0.5	2.0 ± 0.5	3.5 ± 0.2
Salinity	35.36 ± 0.01	35.07 ± 0.03	-	33.80 ± 0.01
Chlorophyll *a* (µg L^{-1})	0.24 ± 0.02	0.3 ± 0.02	0.25 ± 0.03	0.48 ± 0.03
DIC (µmol kg^{-1})	2044 ± 3	2051 ± 5	2136.6 ± 2.7	2131 ± 2
fCO_2 (µatm)	471 ± 7	538 ± 12	350 ± 2	360 ± 2
pH[#]	8.253 ± 0.008	8.275 ± 0.016	-	8.076 ± 0.001
NO_3^- (µM)	10.8 ± 0.4	10.4 ± 0.3	25.4 ± 0.3	23.5 ± 0.1
PO_4^{3-} (µM)	0.92 ± 0.02	0.80 ± 0.03	1.42 ± 0.02	1.60 ± 0.01
SiO_2 (µM)	3.9 ± 0.1	5.0 ± 0.2	9.5 ± 0.4	14.2 ± 0.1
O_2 (µM)	230 ± 1	220 ± 1	-	350 ± 1
Fe (nM)	~ 0.06	~ 0.02	~ 0.08	~ 0.08

3. Results and Discussion

3.1 Experimental site study

The physical, biological and chemical properties of the eddy were determined in a fine-scale hydrographical survey before the iron addition. The purpose of this survey was to measure the "natural" conditions of the eddy relative to which any subsequent change would occur. The results of the surface survey are given in table 1 along with the results from three other iron enrichment experiments. The carbonate system in surface waters of the eddy had quite uniform properties. Surface water properties were representative of the HNLC regions in the Southern Ocean and were rather similar to the properties encountered in the SOIREE experiment (61° S, 140°E), a previous iron enrichment experiment in a different sector of the Southern Ocean (Boyd et al., 2000). The DIC, fCO_2 and pH_T in the eddy's surface waters were DIC = 2131 ± 2 µmol kg^{-1}, fCO_2 = 360 ± 2 µatm and pH_T = 8.076 ± 0.001 (table 1). These data provide baseline values for the carbonate system, relative to which the changes due to the iron addition were determined.

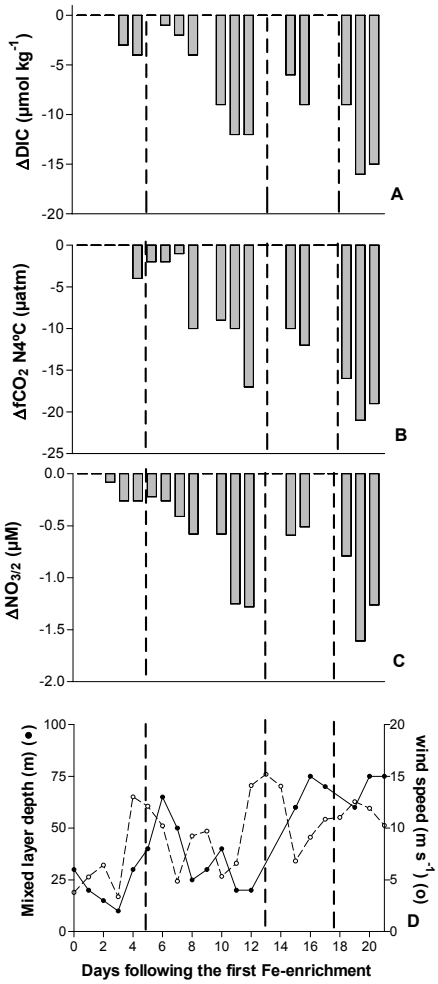

Figure 1: *Daily changes (Δ) in surface DIC (a), fCO_2 (normalized at a temperature of 4°C) (b) and nitrate (c) between inside the patch and outside the patch as well as changes in the mixed layer depth (—) and daily average wind speed (---) (d) during the experiment. For each day, the Δ for DIC and nitrate correspond to the difference between the CTD data at the in station and the CTD data at the corresponding out station. For fCO_2, the Δ were computed from surface measurement at the in station and surface measurement at the corresponding out station. For the wind speed, the height of the anemometer was 38 meters and wind speeds have been corrected to 10 meters height using the relationship by Johnson (1999). The dashed lines indicate the two severe storms on days 4-5 and days 12-13 as well as the strong gale on days 17-18.*

3.2 Meteorological and hydrographical forcing

During EisenEx, the development of the algal bloom and thus the algal carbon uptake were strongly influenced by physical processes. The average wind speed of 8.0 m s^{-1} encountered in the first week of the experiment was distinctly lower than average values in this region (Dentler, 2001). The wind and mixing conditions of the second and third week of the experiment were typical for the region of the Antarctic Circumpolar Current (ACC) (Mitchell et al., 1991) with alternating periods of medium and strong storms. The average wind speeds were 10.4 m s^{-1} and 12.1 m s^{-1}, respectively. Due to horizontal dispersion, the patch, marked by the inert tracer SF_6, increased from initially 50 km^2 to about 950 km^2 at the time of our last mapping on day 17-18 of the experiment (Watson et al., 2001). Very likely, the succession of high winds promoting deep mixing, and sunny and calm days (with an average wind speed around 5 m s^{-1}) allowing development of a strong stratification, were an important factor in the development of the phytoplankton in the centre of the patch (Gervais et al., 2002) and thus in the algal uptake of inorganic carbon and nutrients.

3.3 Inorganic carbon uptake during EisenEx

The response of the carbonate system to the iron enrichment within the patch was measured for 21 days following the first addition. The changes in DIC, fCO_2 and pH_T were determined relative to measurements in the eddy before the experiment and to measurements outside of the patch during the experiment.

Algal response to the iron addition was characterized by an increase in chlorophyll *a* from 0.50 µg L^{-1} on day 0 to 0.75 g L^{-1} on day 3. On day 4 after the iron enrichment, a difference of surface water DIC between outside and inside the patch (ΔDIC) of 4 µmol kg^{-1} was observed in EisenEx (figure 1a), which is similar to that in SOIREE (Bakker et al., 2001), but is 2 to 3 times lower than that during IronEx II, two days after iron release (Cooper et al., 1996; Steinberg et al., 1998). The response was slower and initial changes in the carbonate system occurred later during both EisenEx and SOIREE than during the IronEx II experiment. Algal carbon uptake was observed within two days of the first iron infusion in IronEx I and II (Watson et al. 1994; Cooper et al., 1996; Millero et al., 1998; Steinberg et al., 1998), whereas it was only observed after 4-5 days during EisenEx and SOIREE. The low temperature of the Southern Ocean waters was deemed to be responsible for this slow response in SOIREE (Boyd et al., 2000) and this might also be the case for EisenEx (table 1).

A severe storm (maximum wind speed of 25.2 m s^{-1}), after 5-6 days decreased ΔDIC in the patch center from 5 to 2 µmol kg^{-1} by mixing up of water with higher DIC concentrations from below (as mixed layer depths increased from around 25 m to about 60 m) and by horizontal dispersion of the patch. On days 10 and 12, rapid carbon uptake was observed, ΔDIC was 9 and 12 µmol kg^{-1} (figure 1a), respectively, in a mixed layer of 20 meters (figures 1d and 2a). On day 12, this ΔDIC was related with an equivalent

increase in oxygen concentrations of 10 µM (figure 2b) and a decrease in $NO_{3/2}$ of 1.3 µM (figure 1c). The iron was initially injected at 16 ± 2 meters depth in the initially shallow surface mixed layer of 30 meters. Thus, the storm after 5-6 days may have improved the iron availability for algae below the shallow surface layer. The twofold increase in chlorophyll *a* concentration after 12 days (Riebesell, personal communication) showed that an algal bloom had developed in the calm and sunny conditions and was responsible for the DIC and $NO_{3/2}$ decrease (figure 1a and 1c) and the increase in oxygen concentrations (figure 2b).

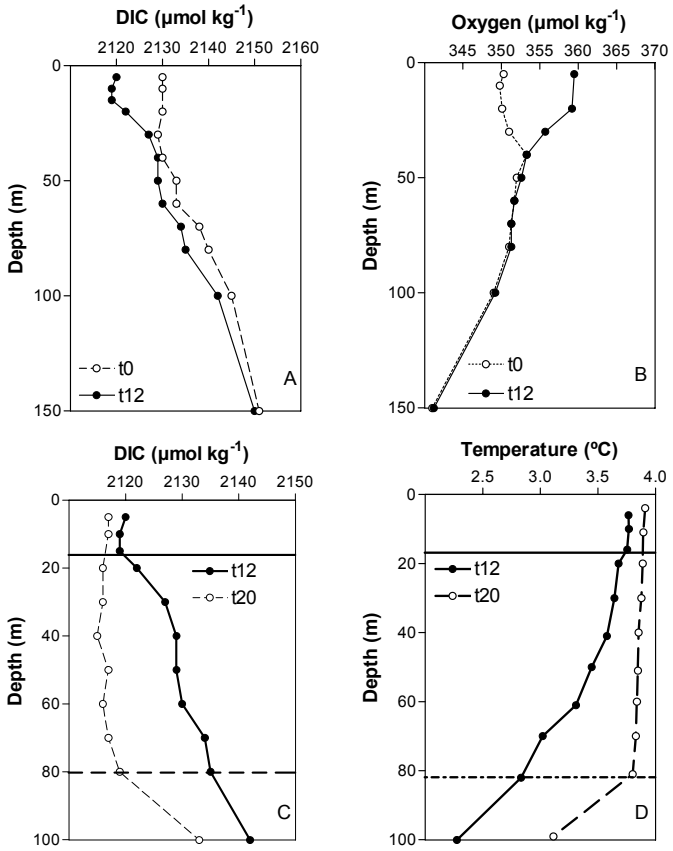

Figure 2: *Upper panel: DIC (a) and O_2 (b) profiles on day 0 and day 12. Bottom panel: Changes in the mixed layer depth evident from DIC (c) and temperature (d) profiles on day 12 and 20.*

The ΔDIC decrease to 6 μmol kg^{-1} on day 15 is related to the second severe storm (maximum wind speed of 26.9 m s^{-1}), that occurred on day 13 (figure 1d). Twenty days after the first Fe-infusion a maximum ΔDIC = 15 μmol kg^{-1} was observed in an 80 m deep mixed layer (figure 2c and 2d) with a concomitant maximum fCO_2 decrease of 23 μatm (figure 1b) and an increase in pH_T of 0.025 units compared to the outside patch. The concentrations of DIC below the euphotic zone both inside and outside the patch remained constant during the experiment with values at 150 and 200 m of 2150 μmol kg^{-1} and 2160 μmol kg^{-1}, respectively (figure 3).

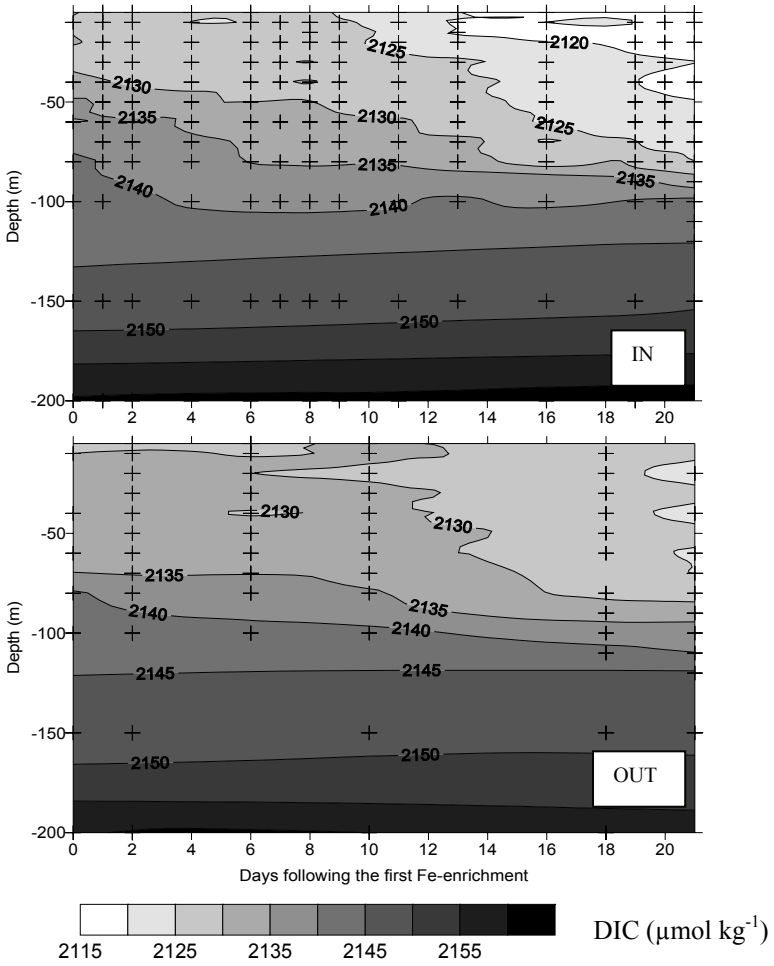

Figure 3: *Contour plots for DIC evolution inside and outside the patch in the first 200 meters of the water column. Crosses represent the sampling frequency in time and depth.*

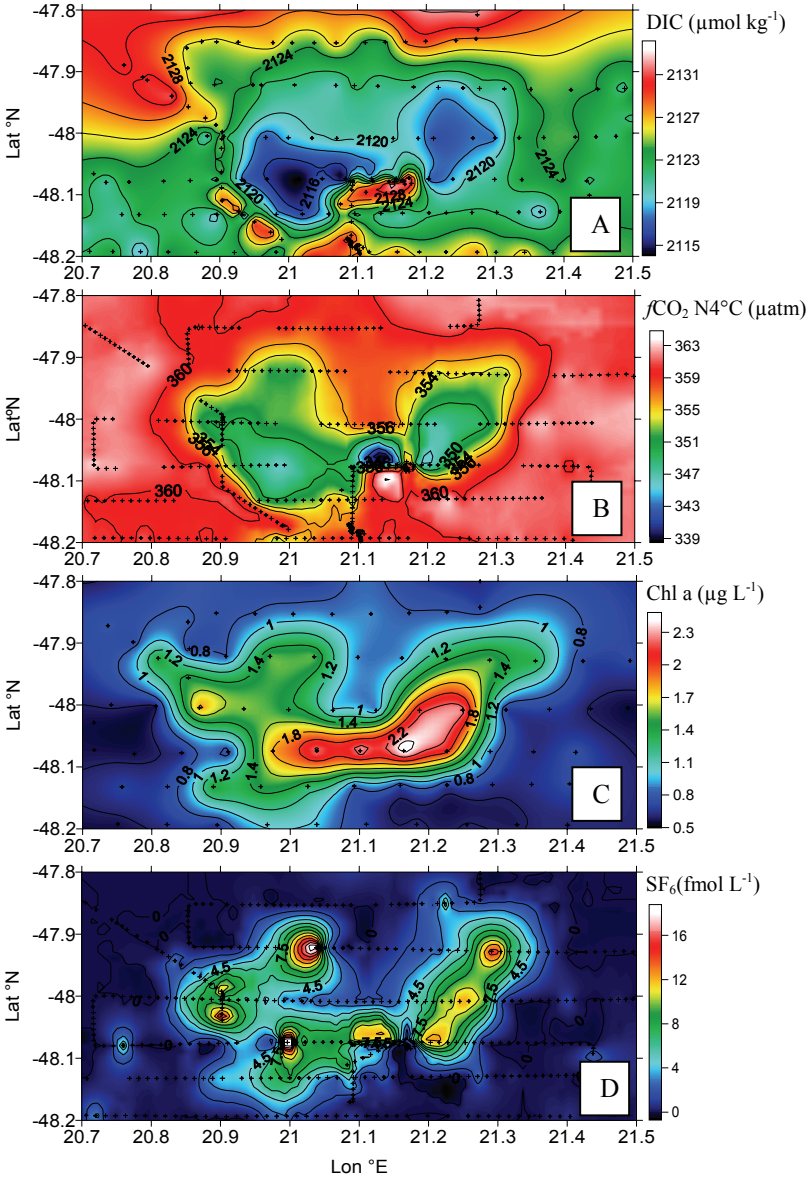

Figure 4: *Shape and location of the patch on day 18 from surface DIC (a), fCO_2 (normalized at a temperature of 4°C) (b) and SF_6 (d) data measured continuously, and from chlorophyll a (c) measured on CTD samples. The surface water measurements for each parameter were interpolated at a 0.5° latitude by 0.5° longitude grid by kriging. Crosses are the locations of the surface samples for each parameter.*

Although changes in DIC and fCO_2 did not occur linearly throughout the experiment, they were well correlated during the 21 days of experiment (figure 1) (the linear regression of surface water changes in fCO_2 relative to average DIC in the mixed layer for each day gives r^2=0.87, n=15). The variable DIC and fCO_2 uptake in this dynamic environment differ from the almost linear DIC and fCO_2 uptake during IronEx II (Cooper et al., 1996; Steinberg et al.; 1998) and SOIREE (Bakker et al., 2001). The maximum DIC and fCO_2 uptake during IronEx II were 27 μmol kg^{-1} and 70-90 μatm, respectively, after 6-9 days of significant carbon uptake over the 25 m deep mixed layer (table 2) (Cooper et al., 1996; Steinberg et al., 1998). These changes were 2-3 times those of 15-18 μmol kg^{-1} and 32-38 μatm after 13 days of SOIREE, which corresponded to 8-9 days of significant carbon uptake over the upper 50 meters (Bakker et al., 2001).

In addition to the daily measurements taken inside and outside the patch, seven surface water mappings were completed during the 21 days of the experiment, in order to study the spatial distribution of the biogeochemical response to the Fe-enrichment. On days 17 and 18, a final grid study was conducted for 34 hours in the fertilized waters, clearly visible from DIC, fCO_2, chlorophyll *a* and SF_6 in surface water (figure 4). During this surface survey, DIC (figure 4a) and SF_6 (figure 4d) were inversely related. The crossings of the patch with the highest SF_6 concentrations corresponded to low DIC, whereas the background SF_6 concentrations were related to outside patch DIC concentrations. The lowest values in DIC were concomitant with fCO_2 minima (figure 4b). The maximum uptake of DIC and fCO_2 during this grid study were 8-9 μmol kg^{-1} and 17-20 μatm, respectively. These values are in good agreement with DIC and fCO_2 at the inside station on day 19 and the outside station on day 20 (figures 1a and 1c). The changes in the carbonate system directly correspond to the growth of phytoplankton as indicated by the corresponding chlorophyll *a* increases in figure 4c.

3.4 Relationship of changes in CO_2 to nutrients

During EisenEx, the iron addition promoted an increase in chlorophyll *a* (figure 4c) and a decrease in DIC, nitrate (figure 1c) and phosphate (table 2), indicating that iron limits algal growth and nutrient utilisation. While a significant increase in diatom abundance was observed in the patch by the end of the experiment, a decrease of silicate occurred both inside and outside the patch (figure 5) (Assmy et al., 2001). The decrease in silicate concentrations in the surface waters was slightly higher outside patch than inside patch. While the weakly silicified *Pseudonitzschia* became the dominant diatom during EisenEx, the highly silicified *Fragiliaropsis kerguelenis* dominated the SOIREE bloom. As a consequence, the silicate uptake of 2.5 μmol L^{-1} measured during SOIREE (Boyd et al., 2000) was much larger than during our experiment. Takeda et al. (1998) observed similar uptake of silicate in incubations bottles for both, iron limited and iron enriched cultures of *Pseudonitzschia* diatoms and concluded that the iron nutritional status of the diatoms appears to affect silicate utilization physiologically. Hutchins and Bruland (1998) found ratios of Si/diatoms per cell, which were 2.9 times higher for diatoms growing under Fe-

limited conditions than in Fe-replete conditions. Recent results from Brzezinski et al. (2003) point to the operation of an efficient silicate pump. This "pump" for diatoms growing under low Fe-concentrations in the Southern Ocean, enriches particles in silica relative to organic matter prior to their export into deeper waters. This could explain the relatively large uptake of silicate observed outside the EisenEx patch and would lead to more silicified, faster sinking diatoms under iron limitation than in iron enriched waters (Hutchins and Bruland, 1998; De La Rocha et al., 2000). Indeed, Waite and Nodder (2001) reported sinking rates of diatoms significantly lower inside the patch than outside the patch during the SOIREE experiment. These authors also reported that the primary bloom species reduced their sinking rates most markedly within the patch, showing a decrease of 87% of initial sinking rates after 13 days. On one hand the addition of iron enhanced diatoms growth and therefore the CO_2 uptake from the atmosphere, whereas on the other hand, the production of less silicified diatoms decreased their sinking rates and therefore diminished the CO_2 export to the deeper layers. Thus, during *in-situ* Fe-enrichment experiments, the iron addition caused opposing effects on the uptake and export of CO_2 to the deeper layers.

Table 2: *Maximum changes in the chemical parameters during IronEx I (3 days after first Fe-addition in a mixed layer of 35 m depth), IronEx II (8 days after the first iron addition in a mixed layer of 50 m depth), SOIREE (13 days after the first Fe-addition in upper 50 m depth) and EisenEx (on t18 in a mixed layer of 60 m depth; except for O_2 on t12 in 20 m depth) as well as the iron level reached after the first fertilisation. Signs "±" are followed by the standard deviations on the means for each parameter. From Martin et al., 1994, Watson et al., 1994, Coale et al., 1996, Cooper et al., 1996, Steinberg et al., 1998, Boyd et al., 2000, Bakker et al., 2001 and this study.*

Parameters	IronEx I	IronEx II	SOIREE	EisenEx
Chlorophyll ($\mu g\ L^{-1}$)	+ 0.41 ± 0.02	+ 3.90 ± 0.02	+ 3.11 ± 0.02	+ 2.32 ± 0.03
DIC($\mu mol\ kg^{-1}$)	- 6 ± 2	- 27 ± 2	-18 ± 3	- 15 ± 2
fCO_2 (µatm)	- 13 ± 6	- 73 ± 6	-38 ± 2	- 23 ± 2
pH	-	-	-	+ 0.025 ± 0.001
O_2 (µM)	+ 2.8 ± 1	+ 32 ± 1	-	10 ± 1
NO_3^- (µM)	- 0.7 ± 0.2	-4.0 ± 0.2	- 3.0 ± 0.3	- 1.6 ± 0.1
PO_4^{3-} (µM)	- 0.02 ± 0.02	- 0.25 ± 0.02	- 0.20 ± 0.02	- 0.16 ± 0.01
SiO_2 (µM)	- 0.02 ± 0.02	- 4.0 ± 0.2	- 2.5 ± 0.4	≈ 0
Fe (nM)	≈ 4	≈ 2	≈ 3.8	4.5 ± 3.0

The relationship between changes in the inorganic carbonate system and nutrients during photosynthesis is frequently examined using the Redfield equation (Redfield et al., 1963).

$$106\ CO_2 + 122\ H_2O + 16\ NO_3^- + H_2PO_4^- + 3H^+ \leftrightarrow [(CH_2O)_{106}(NH_3)_{16}H_3PO_4]_{organic} + 138\ O_2 \qquad (1)$$

Large deviations from the Redfield proportions have been observed for Antarctic diatoms growing under suboptimal conditions of Fe supply (de Baar et al., 1997). During EisenEx, the least squares fits of the data inside the Fe-enriched patch give N/P = 12, C/P= 82, C/N = 5.9, C/Si = 2.9 and N/Si = 0.5 (figure 6). The N/P, C/P and C/N ratios are lower than the average oceanic values of 16, 106 and 6.6, but comparable to the ratios found in IronEx II (Steinberg et al., 1998) and during spring 1992 at 50°S ; 6°W (de Baar et al., 1997) (Table 3). Takahashi et al. (1985) pointed out that equation (1) assumes that the organic carbon is in the form of carbohydrate, while many organisms, such as diatoms, produce a large quantity of lipid material. Similarly, based on investigations of organic matter containing a large quantity of lipid material, Hedges et al. (2002) reported C/N ratios of approximately 6.0 in the Southern Ocean. Therefore, formation of lipids will lower the carbon to nutrient and the carbon to oxygen ratio. The C/P, C/N, and N/P ratios reported in this study, as well as studies by de Baar et al. (1997) and Steinberg et al. (1998), are lower than Redfield ratios, presumably because diatoms are responsible for a large part of the algal growth. Stoll et al. (2002) reported a similar value of 0.5 for N/Si (table 3) in a diatom bloom in the Polar front zone. These findings support strong diatom growth as a possible cause of the lower values determined in some oceans for C/P, C/N and N/P ratios (Takahashi et al., 1985; de Baar et al., 1997; Steinberg et al., 1998). Moreover, lower C/N and C/P ratios are also commonly observed in an early stage of a bloom, as a consequence of luxury consumption of nitrate and phosphate (Droop, 1973; Thomas et al., 1999). Relatively small changes in DIC, $NO_{3/2}$ and PO_4^{3-} outside of the patch, together with the low abundance of diatoms (Assmy et al., 2001) suggest that no bloom started there. Thus, the lower ratios obtained during this study inside the patch could be a combination of high production of diatoms together with luxury consumption in the early stage of a phytoplankton bloom induced by iron-enrichment. Outside the patch some diatom growth under iron limited conditions could be responsible for the Si-uptake, which was slightly higher than inside the patch.

Table 3: *Slopes of linear regressions of nutrients observed during IronEx II (Steinberg et al., 1998), a diatom bloom in the Antarctic Circumpolar Current at 50ºS ; 6ºW (de Baar et al., 1997) and during EisenEx, compared to the Redfield ratios (Redfield, 1963). It was not possible to derive a similar trend for O_2 versus DIC consumption, because of a lack of consistent O_2 data for the whole course of the EisenEx experiment.*

In Patch	EisenEx	IronEx II	Spring 1992 (50ºS ; 6ºW)	Redfield Ratio
ΔC/ΔP	82 ± 5	90 ± 5	86	106
ΔC/ΔN	5.9 ± 0.2	6.2 ± 0.2	4.7 - 6.1	6.6
ΔN/ΔP	12.0 ± 0.2	14.3 ± 0.2	14.2	16
ΔC/ΔSi	2.9 ± 0.3	5.1 ± 0.3	-	-
ΔN/ΔSi	0.5 ± 0.1	-	0.11-0.15	-

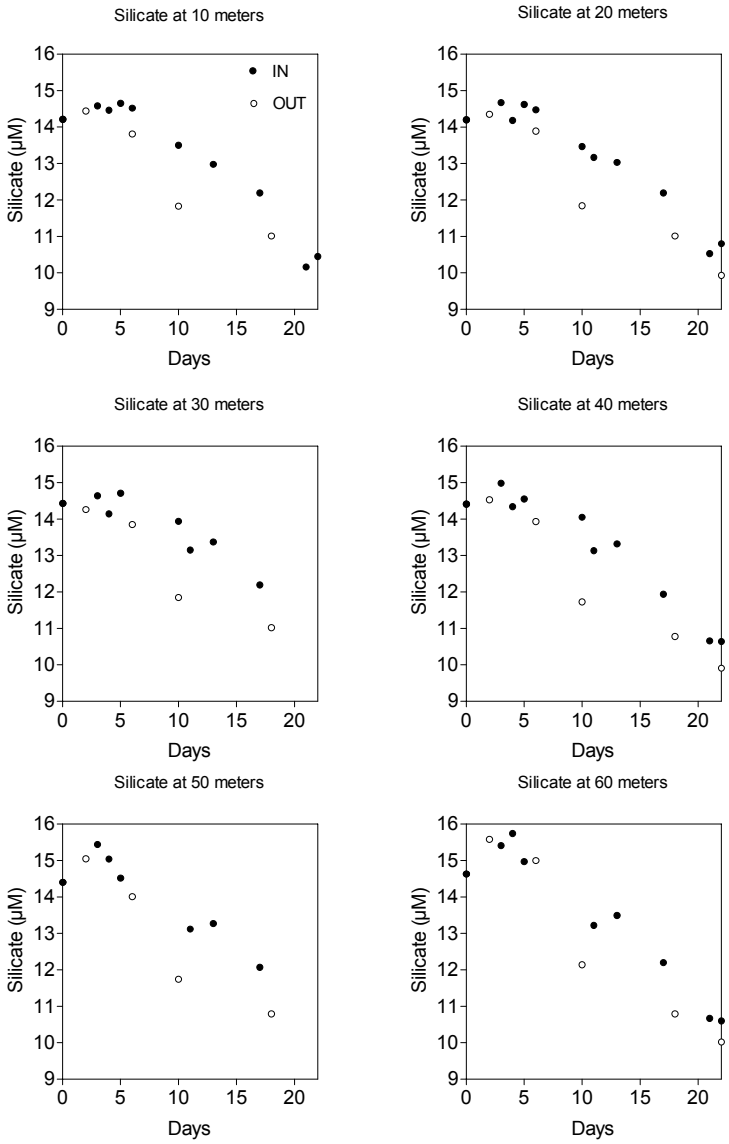

Figure 5: *Evolution of silicate inside (●) and outside (○) the Fe-enriched patch at 10, 20, 30, 40, 50 and 60 meters depth.*

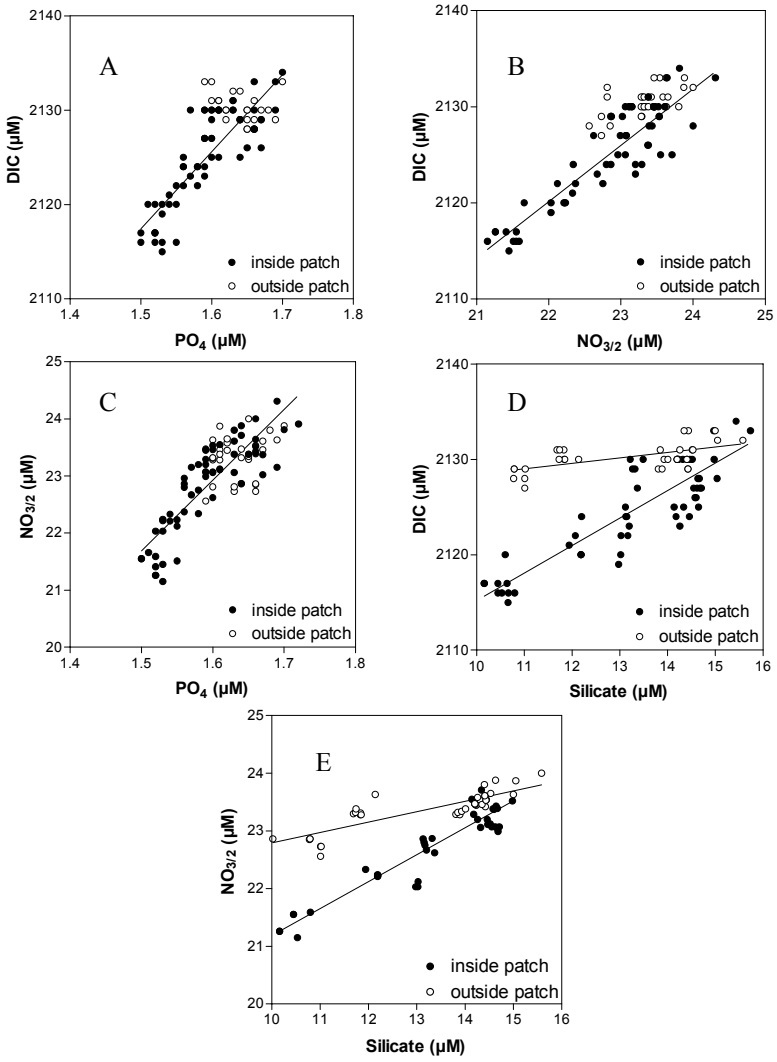

Figure 6: *The changes in DIC, $NO_{3/2}$, PO_4^{3-} and silicate for individual CTD samples in the upper 60 meters inside (•) and outside (o) the iron enriched patch during the experiment. Fits inside the patch are: a) DIC = 81.5 PO_4^{3-} + 1995.4, r^2 = 0.72, n = 57; b) DIC = 5.9 $NO_{3/2}$ + 1990.3, r^2 = 0.81, n = 57; c) $NO_{3/2}$ = 12.0 PO_4^{3-} + 3.65, r^2 = 0.73, n = 61; d) DIC = 2.935 Si + 2085.6 5, r^2 = 0.76, n = 57 and e) $NO_{3/2}$ = 0.476 Si + 16.394, r^2 = 0.88, n = 43.*

3.5 Effect of air-sea fluxes on Redfield ratios

As mentioned above, several severe storms with high wind speed occurred during our experiment and have influenced the CO_2 air-sea exchange. It is important to study the impact of this exchange on the observed DIC changes and the carbon to nutrient ratios. The flux (F) of CO_2 across the air-sea interface can be calculated from the relation:

$$F = k.s.(fCO_{2water} - fCO_{2air}),$$

in which k is the gas transfer velocity, s the solubility of CO_2 calculated after Weiss (1974), fCO_{2water} the fugacity of CO_2 in the surface water and fCO_{2air} the fugacity of CO_2 in air. The main factor influencing k is turbulence at the air-sea interface that is mainly generated by wind stress; thus, k is usually parameterised as a function of wind speed. Several algorithms have been proposed for the k-wind speed relationship. We applied two commonly used algorithms (Liss and Merlivat, 1986; Wanninkhof, 1992) and two recently proposed ones (Wanninkhof and Mc Gillis, 1999; Nightingale et al., 2000), here after referred to as L&M86, W92, W&Mc99 and N2000, respectively. We decided to use the four relationships because even the latest experiments using the most recent tracer techniques (Wanninkhof and Mc Gillis, 1999; Nightingale et al., 2000) could not reliably distinguish, which was the optimal relationship. Moreover, the W&Mc99 relationship is constrained by k measurements up to wind speeds of 15 m s^{-1} and could achieve a better calibration span for the wind speed measured during our experiments. It will be interesting to compare the results from W&Mc99 to L&M86 for EisenEx.

Outside the patch the fCO_2 in surface water and air approximately stayed in equilibrium during the experiment with an average value of 362 µatm. Inside the patch we calculated F using the four formulations and the wind speed corrected to 10 m height. For each day a flux was calculated using an average daily wind speed, an average fCO_2 in the surface water and the concomitant average value for fCO_{2air}. The values calculated using the four different formulations range between -0.09 mmol m^{-2} d^{-1} and –9.93 mmol m^{-2} d^{-1}. Once integrated across the mixed layer and corrected for density, values range from -0.02 µmol $kg^{-1}d^{-1}$ -0.33 µmol $kg^{-1}d^{-1}$, using L&M86 and W&Mc99, respectively. The average fluxes of carbon from the atmosphere integrated across the mixed layer were –0.05, -0.08, -0.10 and –0.07 µmol $kg^{-1}d^{-1}$ for L&M86, W92, W&Mc99 and N2000, respectively. For the 21 days of experiment the total flux of carbon from the atmosphere into the mixed layer, where the DIC uptake occurred, ranged between 1.0 and 2.0 µmol kg^{-1} using L&M86 and W&Mc99, respectively. These values are of the same order of values as the accuracy of the DIC measurements. We corrected the ΔDIC measured at every station using the daily air-sea fluxes calculated inside the patch and integrated across the mixed layer at the corresponding day. Plots (not shown) similar to figure 6 using DIC corrected for the air sea exchange, changed the ratio in table 3 as follows: C/P from 81.6 to 82.0, C/N from 5.9 to 6.1 and C/Si from 2.9 to 3.0. These changes are smaller than the uncertainties on these

ratios and do not alter any of our conclusions. The air-sea exchange of CO_2 had a negligible impact on the carbon to nutrient ratios.

3.6 Overall biological uptake

The high wind velocity leading to the deepening of the wind mixed layer is deemed to be detrimental to the average light climate for the growth rate of the phytoplankton (de Baar and Boyd, 2000; Lancelot et al., 2000; Van Oijen et al., 2004). This, in combination with the severe dilution of the patch with ambient waters, is likely to be the major reason, why the overall removal of DIC and major nutrients was on the one hand significant, but on the other hand by no means utilizing the full growth potential of the available major nutrient stocks. By considering the area covered by the Fe-enriched surface waters, we assessed the total biological C uptake for the whole patch.

From the mapping on day 18 (figure 4), we assume that the area where the highest ΔDIC was observed covers approximately $1/4^{th}$ (or 250 km^2) of the patch. We considered that the ΔDIC of 15 μmol kg^{-1} observed on day 20 was only situated in these 250 km^2 of the patch centre. For the rest of the patch (approximately 750 km^2 on day 20) we assumed that the ΔDIC was closer to 10 μmol kg^{-1}, according to the results of the last mapping on day 18. These changes were observed in the mixed layer of 80 meters. Therefore, the total C uptake in the centre of the patch was 1232 mmol m^{-2} and for the rest of the patch 1026 mmol m^{-2} on day 20. These results are in good agreement with the cumulative ^{14}C primary production of approximately 1000 mmol m^{-2} integrated over the same depth at the same date, which exceeded primary production in non fertilized water by a factor three (Gervais et al., 2003). In total on day 20 the ΔDIC observed in the Fe-enriched waters was equivalent to a C uptake of 1.08×10^9 mol C, or 1.3×10^{10} g C. This can be compared to the amount of iron added during the experiment. In total 4.2×10^4 mol of Fe were added, which gives a ratio C-uptake versus Fe (C/Fe) of 2.5×10^4 mol mol^{-1}. During the SOIREE experiment, the C- uptake was 1.1×10^8 mol C after 13 days of experiment (Bakker et al., 2001), which is tenfold lower than during EisenEx after 20 days. Thus, although the ΔDIC observed during the EisenEx experiment was not that extensive compare to the previous iron enrichment experiments, the large dispersion of the patch caused a total C-uptake for the whole patch that was larger than during previous Fe fertilization experiments.

One major consequence of the stormy conditions is the increase of the mixed layer depth that might induce a light limitation. In the Southern Ocean, optimal light conditions prevail during austral summer (December-January), when incoming solar irradiance is most intense, day length is longest, and the wind mixed layer is the shallowest due to relatively low wind velocities. During the recent SEEDS experiment in the Subarctic Pacific Ocean, the very shallow and stable wind mixed layer of 10 meters depth allowed a complete removal of 20 μM of nitrate within two weeks, because of the optimum light availability. However the nitrate uptake remained confined to a small area (Tsuda et al., 2003). This illustrates the importance of weather conditions on the key factors, such as light conditions and iron availability, for phytoplankton growth and the concomitant CO_2 uptake during Fe-enrichment experiments.

4. Conclusion

The EisenEx experiment demonstrated that iron is a limiting nutrient for phytoplankton growth in the Southern Ocean. We observed an uptake of CO_2 within five days after the first Fe-addition. This uptake was strongly influenced by the changes in mixed layer depth due to the succession of storms and calm weather during the experiment. A maximum uptake of DIC of 15 μmol kg^{-1} in a mixed layer of 80 meters depth occurred 20 days after the first Fe-infusion, and was concomitant with a maximum uptake of fCO_2 of 23 μatm and an increase in pH of 0.025 units. The uptake of CO_2 and nutrients were well correlated suggesting that algal growth was responsible for the decrease in CO_2 in the surface waters of the patch compared to the outside patch. A similar uptake of silicate was observed inside and outside the patch. The presence of diatoms growing under Fe-depleted conditions outside the patch might be responsible for substantial silicate uptake outside the patch.

In the surface waters of the patch, we found values of 82, 5.9, 12, 2.9, and 0.5 for the ratios C/P, C/N, N/P, C/Si and N/Si, respectively. Those values are in agreement with values reported for diatom blooms in the Southern Ocean (Fanning, 1992; de Baar, 1995). The sudden availability of iron in surface waters rich in major nutrients might have created a state of luxury consumption, as suggested by Droop et al. (1973). This effect in combination with the strong growth of diatoms might explain the low ratios calculated. The effect of air-sea exchange of CO_2 on DIC uptake was small and did not significantly affect the values for these ratios.

Overall the observed changes in the water column in DIC due to Fe fertilization were relatively modest but once integrated for the whole patch, equivalent to a significant uptake of 1.1×10^9 mol C and a C/Fe ratio of 2.5×10^4 mol mol^{-1}. In that respect the EisenEx experiment has underlined the major impact of weather conditions on factors such as iron availability and light conditions, which are directly responsible for the overall CO_2 uptake during *in-situ* Fe-enrichment.

References

Assmy, P., Freier, U., Henjes, J., Klaas, C., Smetacek, V., 2001. Phytoplankton composition and species abundance during EisenEx. Berichte zur Polar- und Meeresforschung, 400: 171-178.

Bakker, D.C.E., de Baar, H.J.W., Bathmann, U.V., 1997. Changes of carbon dioxide in surface water during spring in the Southern Ocean. Deep Sea Research II, 44 (1-2): 91-128.

Bakker, D.C.E., Watson, A.J., Law, C.S., 2001. Southern Ocean iron enrichment promotes inorganic carbon drawdown. Deep Sea Research II, 48: 2483-2507.

Banse, K., 1990. Does iron really limit phytoplankton production in the offshore subarctic Pacific? Limnology and Oceanography, 35: 772-775.

Bellerby R.G.J., Olsen, A., Johannessen, T., Croot, P., 2002. The Automated Marine pH Sensor (AMpS): a high precision continuous spectrophotometric method for seawater pH measurements. Talanta 56: 61-69.

Blain, S., Tréguer, P., Belviso, S., Bucciarelli, E., Denis, M., Desabre, S., Fiala, M., Martin-Jézéquel, V., Le Fèvre, J., Mayzaud, P., Marty, J.C., Razouls, S., 2000. A biogeochemical study of the island mass effect in the context of the iron hypothesis: Kerguelen islands, Southern Ocean. Deep Sea Research II, 48: 163-187.

Boyd, P.W., Watson, A.J., Law, C.S., Abraham, E.R., Trull, T., Murdoch, R., Bakker, D.C. E., Bowie, A.R, Buesseler, K.O., Chang, H., Charette, M.A., Croot, P., Downing, K., Frew, R.D., Gall, M., Hadfield, M., Hall, J.A., Harvey, M., Jameson, G., La Roche, J., Liddicoat, M.I., Ling, R., Maldonado, M., McKay, R.M., Nodder, S.D., Pickmere, S., Pridmore, R., Rintoul, S., Safi, K., Sutton, P., Strzepek, R., Tanneberger, K., Turner, S.M., Waite, A., Zeldis, J., 2000. A mesoscale phytoplankton bloom in the polar Southern Ocean stimulated by iron fertilization. Nature, 407: 695-702.

Boyle, E.A., 1998. Pumping iron make thinner diatoms. Nature, 393: 733-734.

Broecker, W.S., 1990. Comment on "Iron deficiency limits phytoplankton growth in Antarctic waters" by John Martin et al. Global Biogeochemical Cycles 4: 3-4.

Brzezinski, M.A, Dickson, M-L., Nelson, D.M., Sambrotto, R., 2003. Ratios of Si, C and N uptake by microplankton in the Southern Ocean. Deep Sea Research II, 50: 619-633.

Coale, K.H., Johnson, K.S., Fitzwater, S.E., Gordon, R.M., Tanner, S., Chavez, F.P., Ferioli, L., Sakamoto, C., Rogers, P., Millero, F., Steinberg, P., Nightingale, P., Cooper, D., Cochlan, W.P., Landry, M.R., Constantinou, J., Rollwagen, G., Trasvina, A., Kudela, R., 1996. A massive phytoplankton bloom induced by an ecosystem-scale iron fertilization experiment in the equatorial Pacific Ocean. Nature, 383: 495-511.

Cooper, D.J., Watson, A.J., Nightingale, P.D., 1996. Large decrease in ocean-surface CO_2 fugacity in response to *in situ* iron fertilization. Nature, 383: 511-513.

Croot, P., Laan, P., 2001. Ferrous wheels in the ocean: The Southern Ocean fairground. Berichte zur Polar- und Meeresforschung, 400: 149-158.

De Baar, H.J.W., Buma, A.G.J., Nolting, R.F., Cadée, G.C., Jacques, G., Tréguer, P., 1990. On iron limitation of the Southern Ocean: experimental observations in the Weddell and Scotia Seas. Marine Ecology Progress Series, 65: 105-122.

De Baar, H.J.W., de Jong, J.T.M., Bakker, D.C.E., Löscher, B.M., Veth, C., Bathmann, U.V., Smetacek V., 1995. Importance of iron for plankton blooms and carbon dioxide drawdown in the Southern Ocean. Nature, 373: 412-415.

De Baar, H.J.W., van Leeuwe, M.A., Scharek, R., Goeyens, L., Bakker, K.M.J., Fritsche, P., 1997. Nutrient anomalies in *Fragilariopsis kerguelensis* blooms, iron deficiency and nitrate/phosphate ratio (A.C. Redfield) in the Antarctic Ocean. Deep-Sea Research II, 44 (1-2): 229-260.

De Baar, H.J.W., Boyd, P.W., 2000. The role of iron in Plankton Ecology and Carbon Dioxide Transfer of the Global Oceans. In: Hanson, R.B., Dicklow, H.W., Field, J.G. (Editors), The Dynamic Ocean Carbon Cycle: A Midterm Synthesis of the Joint Global Ocean Flux Study, International Geosphere Biosphere Programme Book Series, 5. Cambridge Univ. Press, pp. 61-140

De Baar, H.J.W., 2001. Dissolved oxygen. Berichte zur Polar- und Meeresforschung 400: 84-86.

De La Rocha, C., Hutchins, D.A., Brezinski, M.A., Zhang, Y., 2000. Effects of iron and zinc deficiency on elemental composition and silica productions by diatoms. Marine Ecology Progress Series, 195: 71-79.

Dentler, F.-U., 2001. Meteorologische Bedingungen. Berichte zur Polar- und Meeresforschung. 400: 67-72.

Droop, M.R., 1973. Some thoughts on nutrient limitation in algae. Journal of Phycology, 9: 264-272.

Fanning, K.A., 1992. Nutrient provinces in the sea: concentration ratios, reaction ratios and ideal covariation. Journal of Geophysical Research, 97: 5693-5712.

Gervais, F., Riebesell, U., Gorbunov, M.Y., 2002. Changes in the size-fractionated primary productivity and chlorophyll *a* in response to iron fertilization in the southern Polar Frontal Zone. Limnology and Oceanography, 47: 1324-1335.

Hartmann, C., Hollman, B., Kattner, G., Richter, K.-U., Terbuggen, A., 1997. Nutrients, dissolved and particulate matter. Berichte zur Polar- und Meeresforschung, 221: 44-52.

Hedges, J.I., Baldock, J.A., Gelinas, Y., Lee, C., Peterson, M.L., Wakeham, S.G., 2002. The biochemical and elemental compositions of marine plankton: A NMR perspective. Marine Chemistry, 78: 48-63.

Hutchins, D.A., Bruland, K.W., 1998. Iron limited diatom growth and Si:N uptake ratios in a coastal upwelling regime. Nature, 393: 561-564.

Johnson, K.M., Wills, K.D., Butler, D.B., Johnson, W.K., Wong, C.S., 1993. Coulometric total carbon dioxide analysis for marine studies: maximizing the performance of an automated gas extraction system and coulometric detector. Marine Chemistry, 44: 167-187.

Johnson, H.K., 1999. Simple expressions for correcting wind speed data for elevation. Coastal engineering, 36: 263-269.

Kurz, K.D., Maier-Reimer, E., 1993. Iron fertilization of the austral ocean-the Hambourg model assessment. Global Biogeochemical Cycles, 7: 229-244.

Lancelot, C., Hannon, E., Becquevort, S., Veth, C., de Baar, H.J.W., 2000. Modelling phytoplankton blooms and carbon export production in the Southern Ocean: Dominant controls by light and iron in the Atlantic sector in Austral spring 1992. Deep-Sea Research I, 47: 1621-1662.

LI-COR, 1996. LI-6262 CO_2/H_2O analyser. Operating and service manual. LI-COR inc. Lincoln, Nebraska, U.S.A.

Liss, S., Merlivat, L., 1986. Air-Sea gas exchange rate: introduction and synthesis. In: P. Buat-Menard (Editor), The Role of Air-Sea exchange in Geochemical Cycling. Reidel Publishing Company, pp.113-127.

Martin, J.M., Fitzwater, S.E., 1988. Iron deficiency limits phytoplankton growth in the northeast Pacific subarctic. Nature, 331: 341-343.

Martin, J.M., 1990. Glacial to interglacial CO_2 change: The iron hypothesis. Paleoceanography, 5: 1-13.

Martin, J.M., Coale, K.H., Johnson, K.S., Fitzwater, S.E., Gordon, R.M., Tanner, S.J., Hunter, C.N., Elrod, V.A., Nowicki, J.L., Coley, T.L., Barber, R.T., Lindley, S., Watson, A.J., Van Scoy, K., Law, C.S., Liddicoat, M.I., Ling, R., Stanton, T., Stockel, J., Collins, C., Anderson, A., Bidigare, R., Ondrusek, M., Lasata, M., Millero, F.J., Lee, K., Yao, W., Zhang, J.Z., Friederich, G., Sakamoto, C., Chavez, F., Buck, K., Kolber, Z., Greene, R., Falkowski, P., Chisholm, S.W., Hoge, F., Swift, R., Yungel, J., Turner, S., Nightingale, P., Hatton, A., Liss, P., Tindale, N.W., 1994. Testing the iron hypothesis in ecosystems of the equatorial Pacific Ocean. Nature, 371: 123-129.

Miller, C.B., Frost, B.W., Booth, B., Wheeler, A., Landry, M.R., Welschmeyer, N., 1991. Ecological processes in subarctic Pacific: iron limitation cannot be the whole story. Oceanography, 4: 71-78.

Millero, F.J., Yao, W., Lee, K., Zhang, J.-Z., Campbell, D.M., 1998. Carbonate system in waters near the Galapagos Islands. Deep-Sea Research II, 45: 1115-1134.

Mitchell, B.G., Brody, E.A., Holm-Hansen, O., McClain, C., Bishop, J., 1991. Light limitation of phytoplankton biomass and macronutrient utilization in the Southern Ocean. Limnology and Oceanography, 36 (8): 1662-1677.

Nightingale, P.D., Malin, G., Law, C.S., Watson, A.J., Liss, P.S., Liddicoat, M.I., Boutin, J., Upstill-Goddard, R.C., 2000. In situ evaluation of air-sea gas exchange parameterizations using novel conservative and volatile tracers. Global Biogeochemical Cycles, 14 (1): 373-387.

Pai, S.-C., Gong, G.-C., Liu, K.-K., 1993. Determination of dissolved oxygen in seawater by direct spectrophotometry of total iodine. Marine Chemistry, 41: 343-351.

Redfield, A.C., Ketchum, B.H., Richards, F.A., 1963. The influence of organisms on the composition of sea-water. In: Hill, M.N. (Editors), The Sea, 2. Interscience, New York, pp. 26-77.

Robertson, J.E., Watson, A.J., Langdon, C., Ling, R.D., Wood, J.W., 1993. Diurnal variation in surface pCO_2 and O_2 at 60°N, 20°W in the North Atlantic. Deep-Sea Research II, 40 (1-2): 409-422.

Smetacek, V., 2001. EisenEx: International team conducts iron experiment in the Southern Ocean. U.S. JGOFS Newsletter, 11 (1): 11-14.

Steinberg, P.A., Millero, F.J., Xiaorong, Z., 1998. Carbonate system response to iron enrichment. Marine Chemistry, 62: 31-43.

Stoll, M.H.C., 1994. Inorganic carbon behaviour in the North Atlantic Ocean. Ph.D. Thesis, Rijksuniversiteit Groningen, The Netherlands, 193 pp.

Stoll, M.H.C., Thomas, H., De Baar, H.J.W., Zondervan, I., De Jong, E., Bathmann, U.V., Fahrbach, E., 2002. Biological versus physical processes as drivers of large oscillations of the air-sea CO_2 flux in the Antarctic marginal ice zone during summer. Deep-Sea Research I, 49: 1651-1667.

Strass, V.H., Leach, H., Cisewski, B., Gonzalez, S., Post, J., da Sylva Duarte, V., Trumm, F., 2001. The physical setting of the Southern Ocean iron fertilisation experiment. Berichte zur Polar- und Meeresforschung, 400: 94-130.

Takahashi, T., Broecker, W.S., Langer, S., 1985. Redfield ratio based on chemical data from isopycnal surfaces. Journal of Geophysical Research, 90 (C4): 6907-6924.

Takahashi, T., Olafsson, J., Goddard, J.G., Chipman, D.W., Sutherland, S.C., 1993. Seasonal variation of CO_2 and nutrients in the high-latitude surface oceans: a comparative study. Global Biogeochemical Cycles 7 (4): 843-878.

Takeda, S., 1998. Influence of iron availability on nutrient consumption ratio of diatoms in oceanic waters. Nature, 393: 774-777.

Thomas, H., Ittekkot, V., Osterroht, C., Schneider, B., 1999. Preferential recycling of nutrients - the ocean's way to increase new production and to pass nutrient limitation? Limnology and Oceanography, 44 (8): 1999-2004.

Tsuda, A., Takeda, S., Saito, H., Nishioka, J., Nojiri, Y., Kudo, I., Kiyosawa, H., Shiomoto, A., Imai, K., Ono, T., Shimamoto, A., Tsumune, D., Yoshimura, T., Aono, T., Hinuma, A., Kinugasa, M., Suzuki, K., Sohrin, Y., Noiri, Y., Tani, H., Deguchi, Y., Tsurushima., N., Ogawa, H., Fukami, K., Kuma, K., Saino, T., 2003. A Mesoscale Iron Enrichment in the Western Subarctic Pacific induces a Large Centric Diatom Bloom. Science, 300 (5621): 958-961.

Van Oijen, T., van Leeuwe, M.A., Granum, E., Weissing, F.J., Bellerby, R., Gieskes, W.W.C., de Baar, H.J.W., 2004. Light rather than iron controls photosynthate production and allocation in Southern Ocean phytoplankton populations during austral autumn. Journal of Plankton Research, 26: 885-900.

Waite, A.M., Nodder, C.S., 2001 The effect of in situ iron addition on the sinking rates and export flux of the Southern Ocean diatoms. Deep-Sea Research II, 48: 2635-2654.

Wanninkhof, R., 1992. Relationship between wind speed and gas exchange over the Ocean. Journal of Geophysical Research 97 (C5): 7373-7382.

Wanninkhof, R., Mc Gillis, W.R., 1999. A cubic relationship between air-sea CO_2 exchange and wind speed. Geophysical Research Letters, 26 (13): 1889-1892.

Watson, A.J., Law, C.S., Van Scoy, K.A., Millero, F.J., Yao, W., Friederich, G.E., Liddicoat, M.I., Wanninkhof, R.H., Barber, R.T., Coale, K.H., 1994. Minimal effect of iron fertilization on sea surface carbon dioxide concentrations. Nature, 371: 143-145.

Watson, A.J., Bakker, D.C.E., Ridgwell, A.J., Boyd, P.W., Law, C.S., 2000. Effect of iron supply on Southern Ocean CO_2 uptake and implications for glacial CO_2. Nature, 407: 730-733.

Watson, A.J., Messias, M.-J., Goldson, L., Skjelvan, I., Nightingale, P., Liddicoat, M., 2001. Berichte zur Polar- und Meeresforschung, 400: 76-80.

Weiss, R.F., 1974. Carbon dioxide in water and seawater: the solubility of a non-ideal gas. Marine Chemistry, 2: 203-215.

Acknowledgements:

We thank Captain J. Keil and the crew of R.V. *Polarstern* for their great support. We express our gratitude to Victor Smetacek (AWI), the chief scientist. Nutrients analyses were performed by K-U. Richter and C. Harms (AWI). The pH measurements were performed by Solveig Kringstad (University of Bergen). Malcolm Liddicoat and Laura Goldson are thanked for their help with the SF_6 release and with underway SF_6 measurements. We thank two anonymous reviewers for their excellent comments on a previous version of the manuscript. This work was supported by an EU CARUSO grant (ENV4-CT97-0472).

Chapter 7

Iron and mixing affect biological carbon uptake in SOIREE and EisenEx, two Southern Ocean iron fertilisation experiments

This chapter by Dorothee C.E. Bakker, Yann Bozec, Philip D. Nightingale, Laura Goldson, Marie-José Messias, Hein J.W. de Baar, Malcolm Liddicoat, Ingunn Skjelvan, Volker Strass, and Andrew J. Watson has been published in Deep Sea Research I, 52: 1001-1019.

Abstract

This study explores the changes in the surface water fugacity of carbon dioxide (fCO_2) and biological carbon uptake in two Southern Ocean iron fertilisation experiments with different hydrographic regimes. the Southern Ocean Iron Release Experiment (SOIREE) was carried out south of the Antarctic Polar Front (APF) at 61°S, 141°E in February 1999 in a stable hydrographic setting. The EisenEx experiment was conducted in a cyclonic eddy north of the APF at 48°S, 21°E in November 2000 and was characterised by a rapid succession of low to storm-force wind speeds and dynamic hydrographic conditions. The iron additions promoted an algal bloom in both studies. They alleviated algal iron limitation during the 13-day SOIREE experiment and probably during the first 12 days of EisenEx. The fCO_2 in surface water decreased at a constant rate of 3.8 µatm day^{-1} from 4-5 days onwards in SOIREE. The fCO_2 reduction was 35 µatm after 13 days. The evolution of surface water fCO_2 in the iron enriched waters (or 'patch') displayed a saw tooth pattern in EisenEx, in response to algal carbon uptake in calm conditions and deep mixing and horizontal dispersion during storms. The maximum fCO_2 reduction was 18-20 µatm after 12 and 21 days with lower values in between. The iron enriched waters in EisenEx absorbed four times more atmospheric CO_2 than in SOIREE between 5 and 12 days, as a result of stronger winds. The total biological uptake of inorganic carbon across the patch was 1389 ton C (±10%) in SOIREE and 1433 ton C (±27%) in EisenEx after 12 days (1 ton = 10^6 g). This similarity probably reflects the comparable size of the iron additions, as well as algal growth at a similar near-maximum growth rate in these regions. The findings imply that the different mixing regimes had less effect on the overall biological carbon uptake across the iron-enriched waters than suggested by the evolution of fCO_2 in surface water.

Note: *In the present chapter, Bozec et al. (2005) refers to chapter 6 of this thesis.*

1. Introduction

The availability of light, nutrients, and trace elements, as well as grazing pressure, influence phytoplankton growth and carbon cycling in the oceans. High Nutrients Low Chlorophyll (HNLC) regions have low chlorophyll concentrations, despite high concentrations of nitrate, silicate, and phosphate. Recent experiments have demonstrated that iron is an important, but not the only, limiting factor for algal growth in HNLC regions (De Baar and Boyd, 2000; and references therein). Four Lagrangian, *in situ* iron fertilisation experiments have been carried out in the Southern Ocean to date: the Southern Ocean Iron Release Experiment (SOIREE), EisenEx and the SOFeX north and south experiments. Iron addition promoted development of an algal bloom, build-up of biomass, and uptake of inorganic carbon (Boyd et al., 2000; Watson et al., 2000; Smetacek, 2001; Gervais et al.,

2002; Coale et al., 2004; Bozec et al., 2005). Carbon export increased in the two SOFeX experiments (Buesseler et al., 2004).

An increase in carbon export upon iron addition corresponds to the equivalent storage of the greenhouse gas carbon dioxide (CO_2) on time scales of a few months to thousands of years. Therefore iron fertilisation has been suggested as a tool to reduce the atmospheric CO_2 concentration (Martin, 1990). However, iron fertilisation of the oceans for mitigating global warming is controversial. The magnitude and duration of carbon storage remain uncertain and direct verification of the carbon storage is virtually impossible (Gnanadesikan et al., 2003). Iron fertilisation experiments demonstrate that carbon storage is less efficient than assumed in geo-engineering proposals (Boyd et al., 2004). A modelling study suggest that remineralisation of exported organic carbon in the water column, and long-term effects of nutrient depletion on export production may drastically reduce the potential for carbon storage (Gnanadesikan et al., 2003). In addition, iron fertilisation is likely to have negative side effects, such as the marine production of the greenhouse gases nitrous oxide (N_2O), and methane (CH_4) (Fuhrman and Capone, 1991; Law and Ling, 2001; Jin and Gruber, 2003), and of dimethyl sulphide, alkyl nitrates, and halocarbons (Turner et al., 1996, 2004; Chuck, 2002; Chuck et al., 2002). Large-scale iron fertilisation would promote major changes in marine ecology, and marine biogeochemical cycles (Chisholm et al., 2001).

Here, we will present the evolution of surface water fugacity of CO_2 (fCO_2) in the EisenEx experiment. This study complements the description of changes in dissolved inorganic carbon (DIC) in Bozec et al. (2005) (Chapter 6 of this thesis). We will quantify the biological uptake of DIC in the mixed layer across the iron enriched waters ('patch') and in the centre of the patch. This article will compare changes in inorganic carbon chemistry in EisenEx with those in SOIREE (Watson et al., 2000; Bakker et al., 2001). The study will explore how the meteorological and hydrographic conditions affected biological carbon uptake upon iron fertilisation (Table 1).

2. Methods

2.1. The SOIREE experiment

The SOIREE experiment was carried out for 13 days in austral summer (9-22 February 1999) (Figure 1; Table 1). After an initial site survey the R.V. *Tangaroa* sailed along a spiralling track, while releasing iron and an inert tracer, SF_6 (sulphur hexafluoride). An iron enriched patch of ~50 km^2 was created at 61°S, 141°E, south of the Antarctic Polar Front (APF) (Boyd et al., 2000). Iron was added a further three times (Figure 2). The total addition of iron was 1745 kg (Bowie et al., 2001). The iron additions theoretically increased the surface water iron concentration to 3.8, 2.7, 2.6, and 2.5 nM in the successive iron releases (Bowie et al., 2001). These concentrations were approximately 10-fold higher than the concentrations of dissolved iron (0.1 nM) and total iron (0.4 nM) in non-fertilised waters.

Table 1: *Main features of the SOIREE and EisenEx iron experiments. Abbreviations are SAF: Subantarctic Front, APF: Antarctic Polar Front. Numbers refer to: [1] Boyd et al., 2000; [2] Smetacek, 2001; [3] Strass et al., 2001; [4] Cisewski et al., 2005; [5] Abraham et al., 2000; [6] Bowie et al., 2001; [7] De Baar, 2001; [8] Law et al., 2003; [9] Goldson, 2004; [10] Watson et al., 2001; [11] Bakker et al., 2001; [12] This study; [13] Bozec et al., 2005.*

Feature	SOIREE	EisenEx
Location	61°S, 141°E; Indian sector; south of the APF [1].	48°S, 21°E; Atlantic sector; between the SAF and the APF; in a cyclonic eddy shed by the APF [2, 3, 4].
Timing	Summer; 09-22/02/1999; 13 days; 42 days in SeaWiFS [5].	Spring; 07-29/11/2000; 22 days.
Iron addition	0, 3, 5, 7 days; 1745 kg Fe (768, 312, 312, 353 kg) [6].	0, 8, 16 days; 2340 kg Fe (3 x 780 kg) [7].
Meteorology	Storms after 1 and 4 days; overcast.	Succession of storms (5, 13 days) and low wind events; overcast periods and sunny spells.
Mixed layer	60-80 m deep [8]	14-100 m deep [4, 9]; occasional diurnal stratification.
Patch	Low shear; horizontal advection 7% day^{-1}, stretching [5].	Strong horizontal dispersion; initial doubling of size in 4-5 days; distortion; rotation [10].
Surface water fCO_2 decrease	From 4 to 5 days onwards at a rate of 3.8 µatm day^{-1}; 32-38 µatm in 13 days; top hat effect for 13 days [11].	From 4 to 7 days onwards; irregular saw tooth: 18-20 µatm after 12 and 21 days with lower values in between; possible top hat effect for 12 days [12].
DIC reduction	15-18 µmol kg^{-1} in 13 days; across the upper 50 m [11].	12-15 µmol kg^{-1} in 22 days; occasional DIC gradients in the mixed layer [12, 13].

2.2. The EisenEx experiment

The EisenEx experiment (cruise ANT 18-2 of R.V. *Polarstern)* took place for 22 days in austral spring (8-30 November 2000) (Figure 1; Table 1). An iron enriched patch tagged with SF_6 was created in a cyclonic eddy at 48°S, 21°E, north of the APF (Smetacek, 2001; Strass et al., 2001; Cisewski et al., 2005). The characteristics of the eddy water denoted an APF origin. In total 2340 kg of iron was released in three additions (Figure 3) (De Baar, 2001).

2.3. Studying the iron enriched waters in SOIREE and EisenEx

In both experiments, SF_6 was used to distinguish the waters inside and outside the iron enriched patch, while taking SF_6 as a proxy for the added iron. Mapping of the surface water expression of the patch was carried out repeatedly for several parameters, notably for SF_6, dissolved iron, and fCO_2. The ship's continuous surface water supply was at 5 m (SOIREE) and 11 m depth (EisenEx). Water temperature and salinity were registered near the water intake. Regular CTD casts were taken inside and outside the patch. Samples for biological and chemical parameters were taken from the Niskin bottles on the CTD rosette. The ship's GPS position was corrected for Lagrangian drift. In SOIREE, the correction was based on ADCP measurements (courtesy of Ed Abraham, NIWA). For EisenEx a drift correction for the main mapping periods was based on drifting buoys with a drogue at

20-30 m depth and ADCP measurements (courtesy of Boris Cisewski, AWI). Times (in days) were adjusted relative to the midpoint of the first iron addition: 9 February 1999 12:00 UTC in SOIREE and 8 November 2000 00:00 UTC in EisenEx.

Sensors on the ships routinely measured meteorological parameters, such as air temperature, wind speed, and wind direction. Atmospheric pressure was corrected to sealevel. Wind speed was measured at 15 m (SOIREE) and 38 m height (EisenEx) above the sea surface and was corrected to 10 m height, while assuming neutral boundary conditions. For SOIREE a factor of 0.96 was used. A factor of 0.87-0.90 was calculated for 10 minute wind speed with formulae by Large and Pond (1981) for EisenEx.

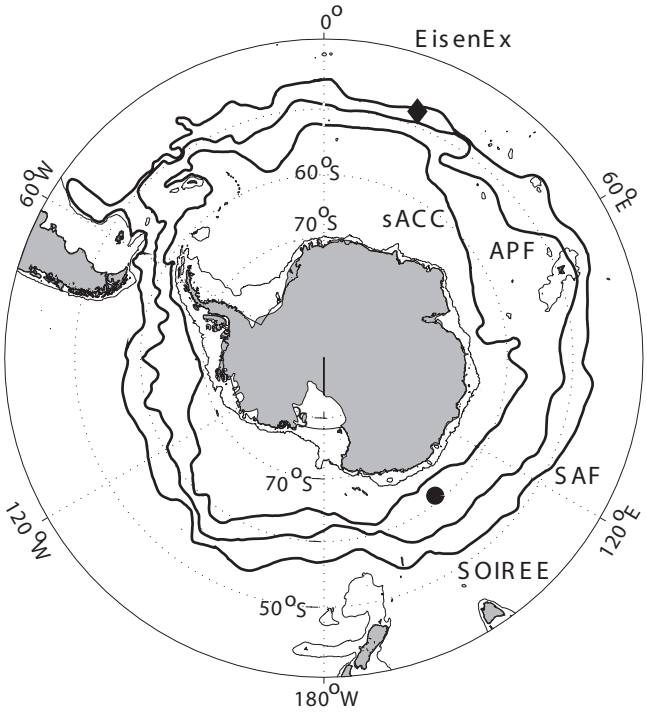

Figure 1: *The location of the SOIREE (circle) and EisenEx (diamond) experiments in the Southern Ocean. The approximate position of the circumpolar Subantarctic Front, the Antarctic Polar Front (APF), and the Southern ACC Front has been indicated (thick lines) (after Orsi et al., 1995), as well as land (grey) and the 1000 m depth contour (thin line) (from ETOPO 5, 1988).*

2.4. Sulphur hexafluoride analysis

Semi-continuous analysis of the surface water concentration of SF_6 was carried out. Water from the ship's surface water supply was pumped directly into the continuous SF_6 mapping system (Watson et al., 2001; Law et al., 2003). Dissolved SF_6 was stripped from the water, trapped cryogenically, separated from oxygen and quantified by a gas chromatograph with an Electron Capture Detector. Every 195 seconds a measurement was made and time stamped by GPS. The time delay between sampling and analysis was 5-8 minutes.

2.5. The fCO_2 in surface water and marine air

Online measurements of fCO_2 in surface water and marine air were made throughout SOIREE (Watson et al., 2000; Bakker et al., 2001) and EisenEx with similar techniques. Marine air was collected through tubing from the crow's nest. Seawater from the ship's surface water supply was introduced into a fast response equilibrator with a showerhead. A Pt-100 sensor accurately monitored the temperature of the water in the equilibrator. Every four minutes an infrared LI-COR 6262 analyser determined the mixing ratios of CO_2 and moisture in a sample from the equilibrator headspace or from marine air. Samples were dried before analysis in EisenEx, but not in SOIREE. Two secondary CO_2 standards, which had been calibrated against three certified NOAA standards (~250, 350, 450 µmol mol^{-1}), were analysed every 45 minutes. The secondary standards had CO_2 mixing ratios of 206.5, 512.5 (SOIREE), 295.1, and 406.1 µmol mol^{-1} (EisenEx) with an accuracy better than 0.6 µmol mol^{-1}. The relationship between the LI-COR readings (in µmol mol^{-1}) and the mixing ratios of the NOAA standards was linear with an accuracy of 0.2 µmol mol^{-1}. The zero and span of the instrument were not changed during the cruises. Average warming of the water between the seawater inlet and the equilibrator was 0.5°C in SOIREE and 0.2°C (standard deviation $\sigma = 0.1$°C for 8362 values) in EisenEx. The equation by Takahashi et al. (1993) was used to correct for the warming. The fCO_2 measurements were time stamped by a GPS sensor. The time delay between sampling and analysis was 4 minutes for fCO_2 in air and surface water.

The precision and accuracy of surface water fCO_2 and the mixing ratio of atmospheric CO_2 in SOIREE were estimated as 0.6 µatm, 1.0 µatm (1 µatm = 0.101325 Pa), 0.6, and 1.0 µmol mol^{-1}, respectively (Bakker et al., 2001). We assume that these values for surface water fCO_2 also apply in EisenEx. A comparison of atmospheric CO_2 mixing ratios during EisenEx with independent data suggests a precision and an accuracy better than 0.6 µmol mol^{-1} (section 3).

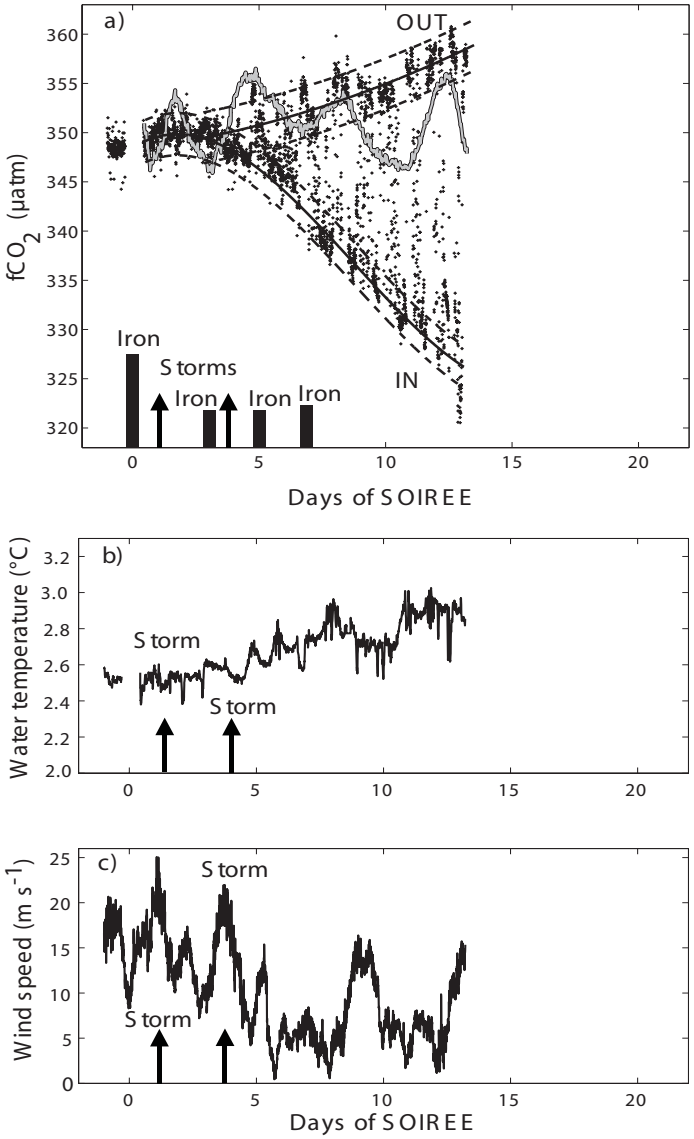

Figure 2: (a) The evolution of fCO_2 in surface water (+, individual measurements) and air (grey line) in SOIREE. The lines indicate fits of fCO_2 at the 10% lowest (upper line) and highest (lower line) SF_6 concentrations for each day (Watson et al., 2000; Bakker et al., 2001). The dashed lines correspond to 84% and 74% of the root mean square error of the fits, respectively. Black bars indicate the timing and the relative size of the iron additions. The arrows point to the occurrence of storms. (b) Water temperature at 5 m depth, and (c) wind speed.

2.6. Dissolved inorganic carbon

The concentration of DIC was determined on samples from regular CTD casts inside and outside the patch (Bakker et al., 2001; Bozec et al., 2005). In SOIREE samples were also taken from the ship's surface water supply. Samples were collected in 250 ml (SOIREE) and 1000 ml (EisenEx) glass bottles. The samples were kept cold before measurement in water from the continuous seawater supply. The DIC concentration was determined by the coulometric method of Johnson et al. (1993). Three replicate analyses were made on each sample. A DIC seawater standard (DOE, 1994) was measured for each coulometric cell. Precision and accuracy were estimated as better than 2.7 μmol kg^{-1} in SOIREE (Bakker et al., 2001) and as 2.0 μmol kg^{-1} in EisenEx (Bozec et al., 2005).

2.7. Spatial interpolation of surface water fCO_2

Surface water fCO_2 was interpolated for mapping periods on a 0.5 km × 0.5 km grid by Ordinary Kriging for SOIREE (Bakker et al., 2001) and EisenEx (Figure 4). This interpolation method for irregularly spaced data expresses the spatial correlation between the data in a semi-variogram (Journel and Huijbregts, 1977; Bailey and Gatrell, 1995). Ordinary Kriging provides the best linear unbiased estimate. The interpolation was performed with the program Easy_Krig versions 1.0 (SOIREE) and 2.1 (EisenEx) (courtesy of Dezhang Chu, Woods Hole Oceanographic Institution). An exponential cosine function type 1 was fitted to the semi-variogram. Interpolated fCO_2 was used if the standard deviation of the fitting error did not exceed the standard deviation of the data. Surface water fCO_2 had been drift corrected prior to the interpolation. No Lagrangian drift correction was available for 17.8-18.8 days in EisenEx. Sea surface temperature varied little during the mapping periods ($\sigma \leq 0.1$°C in EisenEx).

Fits were made between surface water fCO_2 and the 5% (EisenEx) or 10% (SOIREE) highest or lowest SF_6 values for successive periods. The fits indicate which waters had been enriched in iron and SF_6 (Figures 2 and 3; Table 2). Bakker et al. (2001) provide details of the fits for SOIREE. Use of a 5% or 10% criterion for EisenEx did not greatly affect estimates of the net DIC change (section 2.8) across the patch (+2%) and reduced the net DIC change in the patch centre after 18 days by 14%. The 5% setting gave a slightly more accurate fit than 10%. For EisenEx, fits with fCO_2 corrected to 3.6°C rather than fCO_2 had low accuracy. Table 3 lists the criteria used for defining which grid points on the fCO_2 maps were inside the patch and in the patch centre (Bakker et al., 2001). "Background fCO_2" was calculated from the fit of fCO_2 to the 10% (SOIREE) and 5% (EisenEx) lowest SF_6 values.

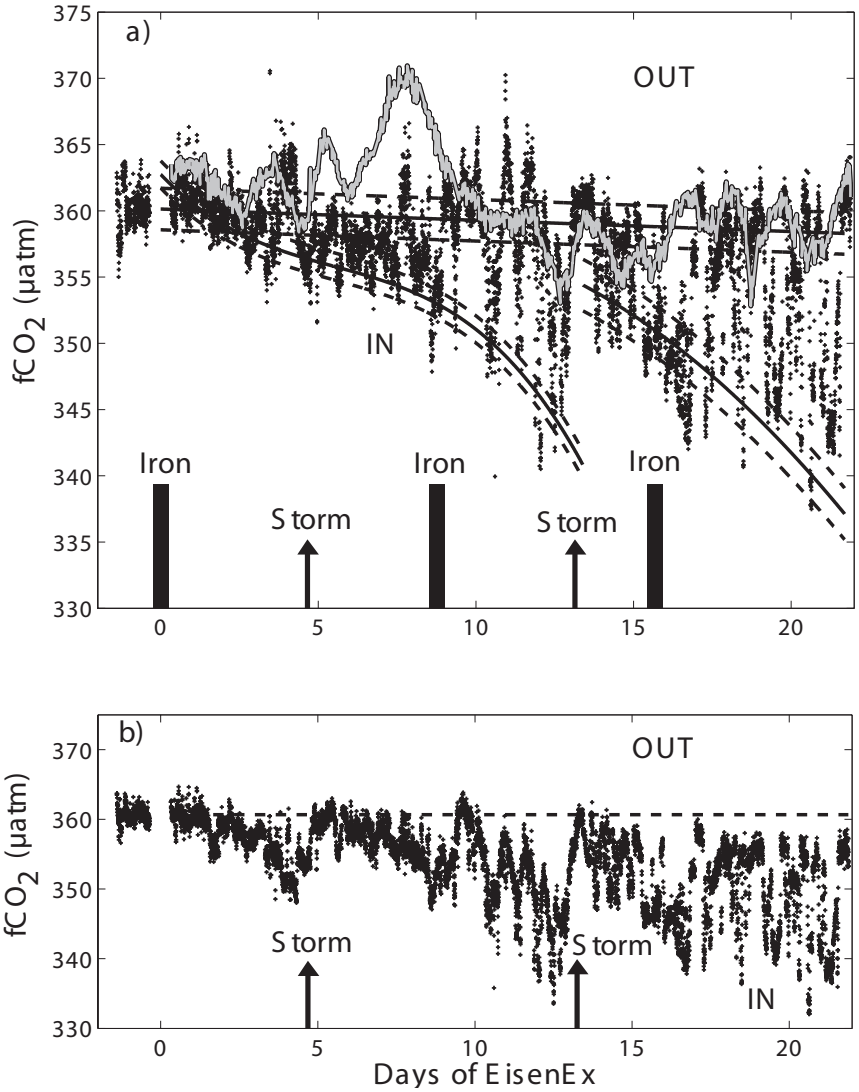

Figure 3: *(a) The evolution of fCO_2 in surface water (+) and air (grey line) in EisenEx with fits of fCO_2 at the 5% lowest (upper line) and highest (lower line) SF_6 concentrations for successive periods. The dashed lines correspond to 84% and 74% of the root mean square error of the fits, respectively. Black bars indicate the timing and the relative size of the iron additions. Arrows indicate the occurrence of storms. (b) Surface water fCO_2 corrected to 3.6°C (+), average atmospheric fCO_2 (dashed line), (c) water temperature at 11 m depth, (d) wind speed, and (e) the mixed layer depth for a density change of 0.02 kg m^{-3} at CTD stations inside the patch (Goldson, 2004).*

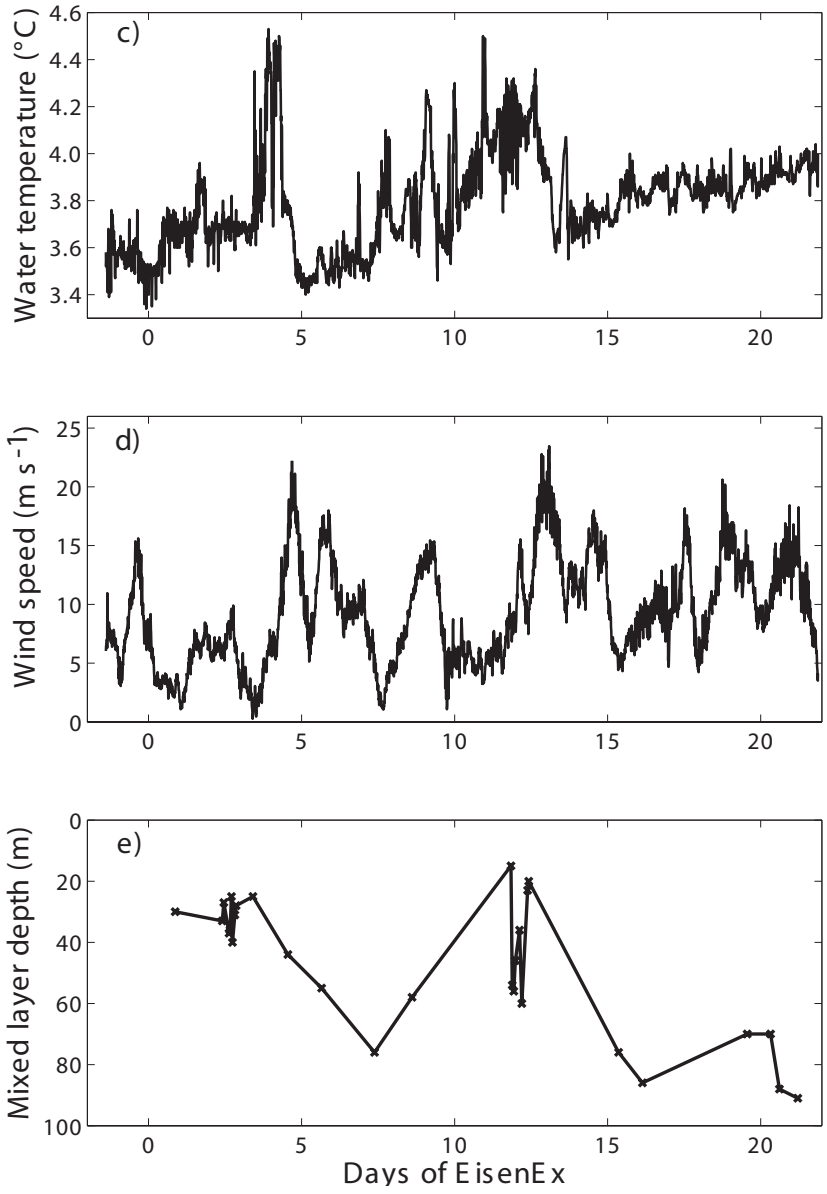

Figure 3 (Continued.)

Table 2: *Fits for surface water fCO_2 in EisenEx at the 5% lowest and highest SF_6 as a function of time with the equation $fCO_2 = a_3t^3 + a_2t^2 + a_1t + a_0$, correlation coefficient r and root mean square error (RMS). Fits (1) and (2) at the 5% highest SF_6 correspond to the periods before and after the second storm (Figure 3).*

	Lowest 5%	Highest 5% (1)	Highest 5% (2)
a_3	0	-0.0200	0
a_2	0	0.331	-0.098
a_1	-0.085	-2.475	1.344
a_0 (µatm)	360.1	362.7	353.9
r	-0.24	-0.89	-0.76
RMS (µatm)	1.9	1.4	2.6
Number	184	124	78
Period (days)	0.0-18.8	0.0-11.5	13.7-18.8

2.8. Integration of DIC changes

2.8.1. Net changes in DIC

Net changes in DIC (ΔDIC_{fCO2}) were calculated for the mixed layer of the patch and the patch centre by using the fCO_2 maps (Figure 4; Table 3) (Bakker et al., 2001). A fit between surface water fCO_2 and DIC in the upper 20 m was made for SOIREE. Details of the fit are in Table 3 and Bakker et al. (2001). Warming of the water during EisenEx (Figure 3) was taken into account by using surface water fCO_2 corrected to 3.6°C, rather than fCO_2, in the fit (Tables 3 and 4). The DIC change at a grid point was taken as the difference between DIC corresponding to fCO_2 at that grid point and DIC at background fCO_2 in SOIREE, while both fCO_2 values had been corrected to 3.6°C in EisenEx (Table 3). The vertically integrated change in DIC at the grid points was obtained by multiplication of the surface water DIC change with a 50 m depth interval for SOIREE, as changes in DIC uniformly occurred in the upper 50 m, but not below 50 m depth (Bakker et al., 2001). The net DIC change across the mixed layer was calculated for EisenEx by multiplying the surface water DIC change with the mixed layer depth and a factor 0.8, as DIC changes in the lower part of the mixed layer were often lower than in surface water (Figure 5) (Bozec et al., 2005). The mixed layer depth was calculated from a 0.02 kg m^{-3} change in potential density from the sea surface in EisenEx (Goldson, 2004). This criterion gave mixed layer depths, which corresponded to the maximum depth with DIC uptake (Figure 5). The addition of the vertically integrated DIC change at the grid points provided the total net DIC change (ΔDIC_{fCO2}) across the patch. The average DIC change across the mixed layer was calculated for the patch centre.

The accuracy of the net DIC reduction (ΔDIC_{fCO2}) was obtained by repeating the above procedure for different assumptions. Bakker et al. (2001) describe this procedure for SOIREE. The accuracy of ΔDIC_{fCO2} in EisenEx was calculated by using six additional scenarios with different criteria for the interpolation of surface water fCO_2 (linear interpolation), for the fit of fCO_2 at 3.6°C against DIC (fCO_2 rather than fCO_2 at 3.6°C), for the intensity of the DIC change in the mixed layer (factors of 0.6 and 1.0), and for the

characterisation of the patch and the patch centre (fCO_2 at 10% highest SF_6 and 100% of RMS). These scenarios changed the net DIC reduction across the patch after 18 days by -4%, +10%, -25%, +25%, +2%, and -3%, respectively. The uncertainty due to the mapping scenario was defined as the standard deviation of the net DIC change in the seven scenarios.

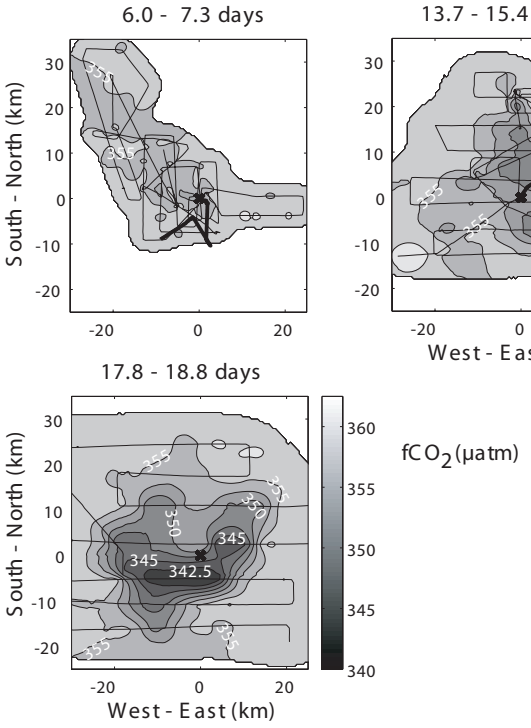

Figure 4: *The spatial distribution of surface water fCO_2 for mapping periods (in days) in EisenEx. Surface water fCO_2 measurements along the ship's track (thin line) were interpolated to an 0.5 km by 0.5 km grid by Kriging. The contour lines are at 2.5 µatm intervals from 342.5 to 362.5 µatm. The thick line shows the trajectory of the Lagrangian buoy with a cross for its departure point, except in the final map, for which no trajectory is available.*

2.8.2. Air-sea exchange of CO_2

The effect of CO_2 air-sea transfer on DIC (ΔDIC_{AirSea}) was calculated for the patch and the patch centre. Equation (1) was used to estimate the air-sea flux (F_{AirSea}) from fCO_2 at grid points, and averages of wind speed, atmospheric fCO_2, water temperature, and salinity for each mapping period:

$$F_{AirSea} = k.K_0 \, (fCO_{2water} - fCO_{2air}) \qquad (1)$$

with transfer velocity (k) and solubility (K_0). The skin temperature was taken equal to the bulk water temperature. The quadratic relationship for short term, shipboard wind speed by Wanninkhof (1992) was used for the calculation of the gas transfer velocity from average wind speed. Addition and averaging of the fluxes at the grid points provided the air-sea flux for the patch and the patch centre, respectively. The effect of air-sea exchange on DIC over time was calculated by interpolation of the flux between successive mapping periods. The error in ΔDIC_{AirSea} has been taken as 55%, reflecting uncertainty in the gas transfer velocity (50%) (Liss and Merlivat, 1986; Wanninkhof and McGillis, 1999; Nightingale et al., 2000) and from the mapping scenarios (5%).

Table 3: *Calculation of DIC changes for the mixed layer of the patch and the patch centre in SOIREE (Bakker et al., 2001) and EisenEx. Fits of surface water fCO_2 to the 5 or 10% lowest (L) or highest (H) SF_6 concentrations for successive periods (Figures 2 and 3) help distinguish where fCO_2 grid points are relative to the patch. RMS is the root mean square error of such a fit. Details of the fits are in Tables 2 and 4 (EisenEx) and in Bakker et al. (2001) (SOIREE). Numbers refer to: [1] Law et al., 2003; [2] Goldson, 2004.*

	SOIREE	EisenEx
Surface water fCO_2	Drift correction; Kriging 0.5 km x 0.5 km.	Drift correction, except 17.8-18.8 days; Kriging 0.5 km x 0.5 km.
Background fCO_2	Fit of fCO_2 at 10% lowest SF_6	Fit of fCO_2 at 5% lowest SF_6
In the patch	$fCO_2 \leq fCO_{2L} - 84\%\ RMS_L$	$fCO_2 \leq fCO_{2L} - 84\%\ RMS_L$
Patch centre	$fCO_2 \leq fCO_{2H} + 74\%\ RMS_H$	$fCO_2 \leq fCO_{2H} + 74\%\ RMS_H$
Warming	No correction	Correction of fCO_2 maps to 3.6°C
Surface ΔDIC	$\Delta DIC = 0.43\ \Delta fCO_2 + 1984.1$	$\Delta DIC = 0.50\ \Delta fCO_{2\_3.6°C} + 1948.8$
ΔDIC over depth	Surface ΔDIC across 50 m depth.	Surface ΔDIC for the mixed layer depth and a factor 0.8.
Vertical Diffusion	$K_z = 0.11 \pm 0.2\ cm^2\ s^{-1}$ [1]; Δz = 50-90 m.	$K_z = 0.54 \pm 0.77\ cm^2\ s^{-1}$ [2]; Δz from 80% of the mixed layer depth to 120 m.

2.8.3. Vertical diffusion

Vertical diffusion (F_{VDif}) of DIC across the pycnocline was calculated from the change in DIC (ΔDIC) over depth (Δz) and the vertical diffusivity K_z with the equation:

$$F_{VDif} = - K_z\ \Delta DIC / \Delta z \qquad (2)$$

The vertical diffusivity was 0.11 $cm^2\ s^{-1}$ (±0.2 $cm^2\ s^{-1}$) in SOIREE (Law et al., 2003) and 0.54 $cm^2\ s^{-1}$ (±0.77 $cm^2\ s^{-1}$) in EisenEx (Goldson, 2004). For SOIREE the vertical diffusive flux of DIC (ΔDIC_{VDif}) into the upper 50 m was estimated from the DIC gradient between 50 and 90 m depth (Bakker et al., 2001). In EisenEx the flux was calculated from the DIC gradient between 80% of the mixed layer depth and 120 m depth. The diffusive flux into the patch and the patch centre was calculated as the sum and the average of the flux at the individual grid points, respectively. The DIC change by vertical

diffusion over time was calculated by interpolation of the flux between successive mapping periods. The error in ΔDIC_{VDif} was taken as the sum of the uncertainties in Kz and from the mapping scenario.

2.8.4. Horizontal dispersion

Horizontal dispersion increased the size of the patch at a rate of 0.07 day^{-1} (±0.03 day^{-1}) in SOIREE (Abraham et al., 2000). The rate of horizontal dispersion in EisenEx was calculated from the evolution of the patch size, as seen in surface water SF_6 (method courtesy of Anthony Kettle – UEA). A linear fit to the surface area of six SF_6 patches (A, in km^2) over time (t, in days) has the equation:

$$A = 48.9\ t + 63.7 \quad (3)$$

($r^2 = 0.98$, $\sigma = 65.5$ km, n = 6). This fit allows estimation of the daily rate of horizontal dispersion of the patch (fraction day^{-1}) as:

$$(1/A)(dA/dt) = 48.9 / (48.9\ t + 63.7) \quad (4)$$

Horizontal dispersion did not affect the DIC budget for the patch as a whole, at least if the patch was fully constrained in the fCO_2 maps. The effect of horizontal dispersion on DIC (ΔDIC_{HDis}) in the patch centre was calculated for SOIREE and EisenEx by correcting ΔDIC_{fCO2} for vertical diffusion and air-sea exchange. A fit to the corrected DIC change as a function of time was multiplied with the horizontal dispersion rate. Integration of this product provided ΔDIC_{HDis}. The error in ΔDIC_{HDis} was calculated as sum of the errors in the coefficients in the integral. An additional error was added for the uncertainty in the mapping scenarios.

Table 4: *Fits for surface water fCO_2 at 3.6°C (A) and surface water fCO_2 (B) to DIC in the upper 20 m depth in EisenEx with the equations $DIC = a_1\ fCO_{2\_3.6°C} + a_0$, $DIC = a_1\ fCO_2 + a_0$, correlation coefficient r and the root mean square error (RMS). Fit A was used in the standard scenario, while B was used for determining the robustness of the estimates.*

	A for fCO_2_3.6°C	B for fCO_2
a_1	0.50	0.54
a_0	1948.8	1931.6
r	0.91	0.82
RMS (µmol kg^{-1})	2.0	2.8
Number	24	24
Period (days)	4.5-22.0	4.5-22.0

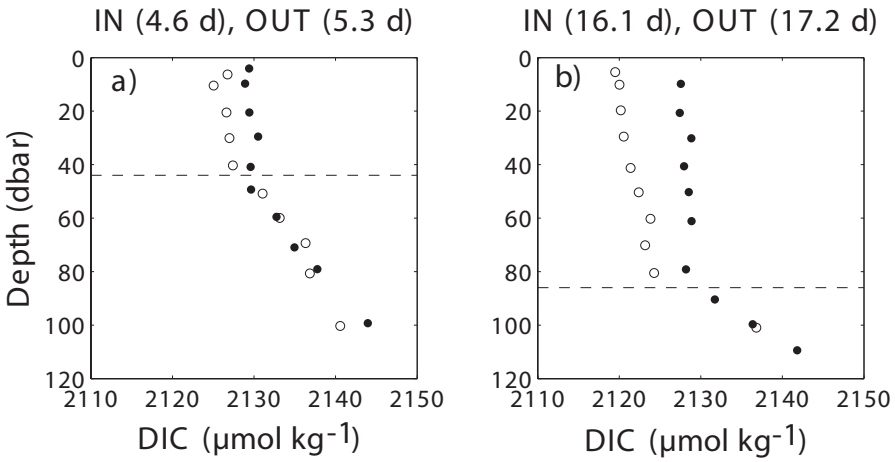

Figure 5: *The vertical distribution of DIC at CTD stations in the patch centre ('IN', open circles) and outside the patch ('OUT', closed circles). The dashed line indicates the mixed layer depth at the IN stations from the 0.02 kg m^{-3} density criterion (Goldson, 2004). The timing of the casts is in days (d).*

3. Results

3.1. Hydrographic setting and carbonate chemistry in SOIREE

Stable hydrographic conditions provided an ideal setting for the SOIREE experiment. Storms after days 1 and 4 mixed the added iron across the mixed layer, which had a depth of approximately 60 m to 75 m (Law et al., 2003) (Figure 2; Table 1). The waters had homogeneous physical, chemical, and biological characteristics prior to the iron fertilisation (Boyd et al., 2000; Bakker et al., 2001).

The iron additions in SOIREE promoted a phytoplankton bloom (Boyd et al., 2000). Algal carbon uptake reduced surface water fCO_2 and DIC from 4-5 days onwards. Surface water fCO_2 decreased at a rate of 3.8 µatm day^{-1} and the iron enriched waters became a sink for atmospheric CO_2 (Figure 2) (Watson et al., 2000; Bakker et al., 2001). The reduction of DIC occurred evenly over the upper 50 m depth. No change in DIC was apparent below 50 m depth. After 13 days surface water fCO_2 and DIC had decreased by 32-38 µatm and 15-18 µmol kg^{-1}, respectively, relative to ambient waters (Table 1) (Bakker et al., 2001).

Maps of surface water fCO_2 highlight the evolution of a gradually stretching patch (Figure 6) (Bakker et al., 2001). Comparison of surface water fCO_2 and SF_6 indicated a uniform fCO_2 reduction across the patch centre, a 'top hat effect' (Bakker et al., 2001).

A top hat effect was also seen in the photosynthetic competency (Fv/Fm) (Boyd and Abraham, 2001). The constant rate of the fCO_2 decrease, the increase in Fv/Fm from 0.3 to 0.4, and the top hat effect in fCO_2 and Fv/Fm suggest that sufficient iron had been added to overcome iron limitation in the centre of the SOIREE patch (Bakker et al., 2001; Boyd and Abraham, 2001). The algae were growing at a maximum rate for the specific environmental conditions (Bakker et al., 2001). The concentrations of nitrate, phosphate, and silicate did not become limiting during the experiment, even as silicate concentrations decreased to 7 μM after 13 days (Boyd et al., 2000). Light limitation did not affect algal growth in the upper 65 m (Boyd et al., 2000). Ocean colour observations indicated a 150 km long, 4 km wide SOIREE bloom, 42 days after the first iron addition (Abraham et al., 2000).

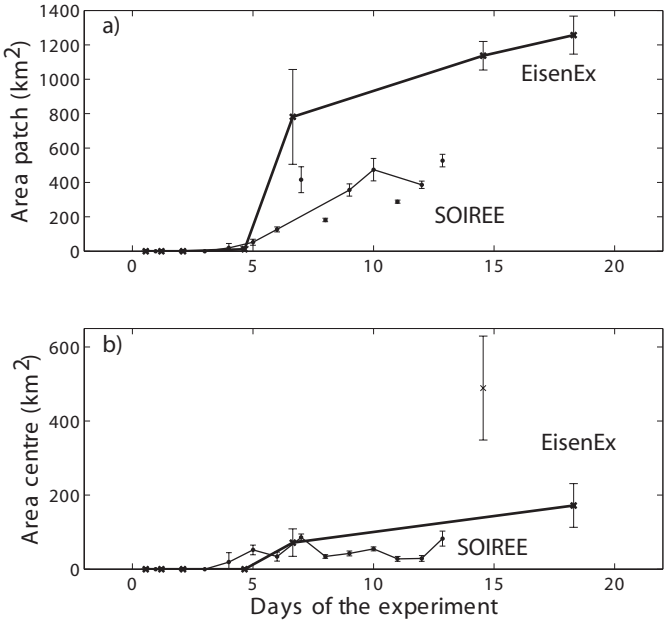

Figure 6: *(a) The size of the patch and (b) the patch centre in SOIREE (points) and EisenEx (crosses), as seen in the fCO_2 maps. Error bars indicate the uncertainty in the data, which was determined from the different mapping scenarios for SOIREE (Bakker et al., 2001) and EisenEx (section 2).*

3.2. A dynamic setting and surface water fCO_2 changes in EisenEx

A succession of calm, sunny spells and strong winds dominated the EisenEx experiment with severe storms after 5 and 13 days (Figure 3; Table 1). Deep mixing occurred during storms, while shallow stratification and surface warming took place during

calm spells (Figure 3) (Cisewski et al., 2005). Initially high horizontal dispersion of 43% day^{-1} decreased to 14% day^{-1} after 6 days, and to 5% day^{-1} after 18 days (equation 4). The major nutrients, nitrate, phosphate, and silicate, were not limiting during the experiment (Bozec et al., 2005). Severe light limitation of algal growth due to heavy cloud cover was present on a few days (Gervais et al., 2002).

A small reduction of surface water fCO_2 may have occurred in the EisenEx patch within 5 days (Figure 3). Then two days with gale to storm force winds doubled the mixed layer depth from 44 m after 5 days to 76 m after 7 days and reduced sea surface temperature by an average 0.6°C (Figure 3). The storm strongly enlarged the patch, as seen in SF_6 (Watson et al., 2001). Any extra algal biomass and fCO_2 reduction in the iron-enriched waters would have been diluted with ambient water by deep mixing and horizontal dispersion.

Surface water fCO_2 remained relatively constant for several days after the storm (Figure 3). A small fCO_2 decrease in the iron enriched waters is apparent after 7 days (Figure 4). The patch is irregular in shape, both in fCO_2 and SF_6. Between 8 and 12 days surface water fCO_2 decreased at a fairly uniform rate in the patch (Figure 3). Surface water warming and shallowing of the mixed layer to 15-60 m depth occurred in this period of low to moderate wind speed (Figure 3). After 12 days surface water fCO_2 in the patch was about 18 µatm below the ambient value. A top hat effect may have occurred in the patch centre between 4 and 12 days, but disappeared after that (Figure 7). A top hat effect in the first 12 days lends support to the hypothesis of algal growth at a rate close to the maximum rate in the centre of the EisenEx patch.

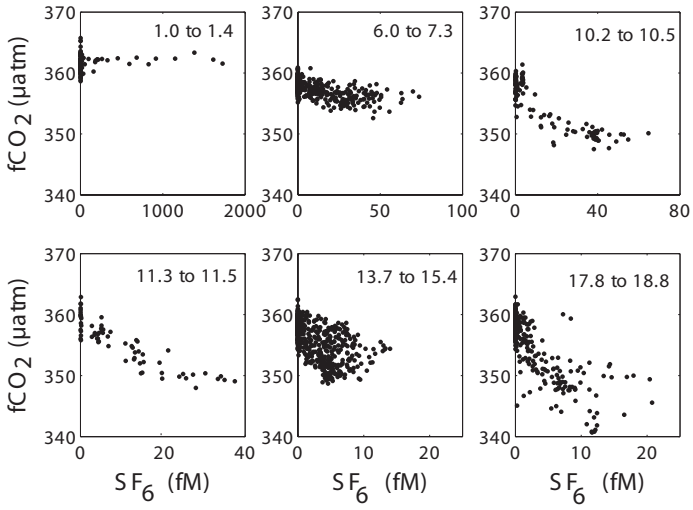

Figure 7: *Surface water fCO_2 as a function of SF_6 for different periods in EisenEx. The timing of the data is in each graph (in days).*

On day 13, another storm doubled the mixed layer depth from 40 to 90 m. Mixed layer deepening and horizontal dispersion reduced the fCO_2 anomaly in the iron enriched waters from 18 to 10 µatm (Figure 3). After this second storm the mixed layer depth varied between 80 and 100 m. Surface water fCO_2 in the patch gradually decreased. The fCO_2 reduction reached 20 µatm after 21 days (Figure 3). Surface water fCO_2 maps for this period show a patch, irregular in shape, expanding in size, and rotating clockwise in the eddy (Figures 4 and 6). As algal biomass and the mixed layer depth increased, light limitation may have developed occasionally (Gervais et al., 2002).

3.3. Atmospheric fCO_2 and CO_2 air-sea transfer in EisenEx

The mixing ratio of CO_2 in dry air (xCO_2) was relatively constant at 368.0 µmol mol^{-1} (σ = 0.6 µmol mol^{-1}) during EisenEx. Atmospheric mixing ratios of 367.6 to 367.8 µmol mol^{-1} were observed at Cape Point (34°21'S, 18°29'E), Crozet (46°27'S, 51°51'E), Syowa station (69°00'S, 39°35'E), and Halley Bay (75°35'S, 26°30'W) in November 2000 (WDCGG, 2003; data courtesy of C. Labuschagne, E.G. Brunke, G. Coetzee (South African Weather Service, Stellenbosch), T.J. Conway, and P.P. Tans (National Oceanographic and Atmospheric Administration - Climate Monitoring and Diagnostics Laboratory, Boulder, Colorado, USA)). The good correspondence between the EisenEx and the WDCGG data demonstrates the almost constant atmospheric CO_2 mixing ratio over large distances in subantarctic and Antarctic air.

Air-sea transfer of CO_2 in EisenEx reflects the variation in wind speed, atmospheric pressure, and surface water fCO_2. The effect of changes in atmospheric pressure between 985.6 and 1030.1 mbar (1 mbar = 10^2 Pa) on the fCO_2 air-sea gradient (17 µatm) was of a similar magnitude as the reduction in surface water fCO_2 upon iron fertilisation (20 µatm) (Figure 3). Ambient waters had surface water fCO_2 close to the atmospheric value and had little overall CO_2 air-sea transfer. The iron enriched waters became a sink for atmospheric CO_2. Oceanic CO_2 uptake in the patch occasionally exceeded 10 mmol m^{-2} d^{-1} from 5 days onwards, when gale to storm force winds coincided with air-sea fCO_2 gradients of 8-20 µatm.

3.4. Processes acting on DIC in EisenEx

Correction of the net DIC change (ΔDIC_{fCO2}) in the iron enriched waters, for DIC changes by horizontal dispersion (ΔDIC_{HDis}), vertical diffusion (ΔDIC_{VDif}) and CO_2 air-sea exchange (ΔDIC_{AirSea}) allows calculation of the DIC change by biological activity or net community production (ΔDIC_{NCP}) with equations 5 and 6:

$$\Delta DIC_{NCP} = \Delta DIC_{fCO2} - \Delta DIC_{VDif} - \Delta DIC_{AirSea} \quad \text{(patch)} \quad (5)$$

$$\Delta DIC_{NCP} = \Delta DIC_{fCO2} - \Delta DIC_{VDif} - \Delta DIC_{AirSea} - \Delta DIC_{HDis} \quad \text{(patch centre)} \quad (6)$$

(after Bakker et al., 2001). The terms in the right hand side of the equations have been calculated for the mixed layer of the patch and the patch centre from the surface water fCO_2 maps, as described in section 2. Unfortunately, few surface water fCO_2 maps are available for the EisenEx patch (Figure 4). The uncertainty in ΔDIC_{NCP} in the patch and the patch centre has been calculated as the sum of the uncertainty of the terms in equations 5 and 6, respectively.

The net DIC reduction (ΔDIC_{fCO2}) across the mixed layer of the patch increased fivefold from 519 ton C (1 ton = 10^6 g) after 7 days to 2840 ton C after 18 days, while the patch increased in size from 781 km^2 to 1257 km^2 (Figure 6; Table 5). Both the DIC reduction and the size of the EisenEx patch may well have continued to increase after 18 days. Vertical diffusion and air-sea exchange added similar, relatively small amounts of DIC to the mixed layer of the iron enriched waters (6% each of ΔDIC_{NCP}). From the above we calculated a biological carbon uptake of 3217 ton C after 18 days (Figure 9; Table 5).

The net DIC reduction (ΔDIC_{fCO2}) in the patch centre increased from 94 mmol m^{-2} after 7 days to 402 mmol m^{-2} after 18 days, while the patch centre expanded in size from 72 km^2 to 172 km^2 (Figures 6 and 8; Table 6). The large surface area of and the low DIC change in the patch centre after 15 days were probably artefacts of a partial mismatch between SF_6 and fCO_2 (Turner et al., 2005). These data for 15 days were excluded from the calculation of DIC changes by horizontal dispersion and biological activity in the patch centre. The method allows calculation of the biological DIC uptake in the patch centre, if the rate of algal carbon uptake exceeded the horizontal dispersion rate. As a result, the method probably underestimates algal carbon uptake in the initial stages of EisenEx, which had high horizontal dispersion (equation 4). Horizontal dispersion had diluted the biological DIC change in the patch centre (702 mmol m^{-2}) by 36% after 18 days.

Table 5: *Changes in DIC across the patch in SOIREE (Bakker et al., 2001) and EisenEx (this study). The DIC uptake by net community production (ΔDIC_{NCP}) was calculated by correction of the net DIC reduction (ΔDIC_{fCO2}) for changes by vertical diffusion (ΔDIC_{VDif}) and CO_2 air-sea exchange (ΔDIC_{AirSea}) (equation 3). The EisenEx values for 12.0 days were obtained by linear interpolation.*

		SOIREE 12.0 days	EisenEx 12.0 days	EisenEx 18.3 days
Area	km^2	387 ± 6%	1022 ± 7%	1257 ± 6%
ΔDIC_{fCO2}	10^6 g C	-1353 ± 6%	-1236 ± 15%	-2840 ± 15%
ΔDIC_{VDif}	10^6 g C	16 (-100% to 103%)	87 (-100% to 157%)	196 (-100% to +158%)
ΔDIC_{AirSea}	10^6 g C	20 ± 52%	111 ± 58%	180 ± 56%
ΔDIC_{NCP}	10^6 g C	-1389 ± 10%	-1433 ± 27%	-3217 ± 26%
$\Delta DIC_{NCP}/\Delta Fe$	mol mol^{-1}	-3.7×10^3	-4.3×10^3	-6.4×10^3

4. Discussion

4.1. Changes in DIC for SOIREE and EisenEx

The evolution of biological DIC uptake and CO_2 air-sea exchange in the patch and the patch centre will be compared for both experiments with the objective to assess how they were affected by the contrasting mixing regimes. For EisenEx, the available data were linearly interpolated to 12 days, as indicated by a hash ($^{\#}$) in the following discussion. This interpolation does not reflect reality, as it neglects the impact of the second storm.
The patch expanded in size from 4 to 5 days onwards in the experiments (Figure 6). After 12 days, the EisenEx patch (1022 $km^{2\#}$) was more than twice the size of the SOIREE patch (387 km^2) (Table 5). The patch continued to grow in size for at least another 6 days in EisenEx and for 30 days in SOIREE (Abraham et al., 2000). The patch centre did not increase much in size after its first appearance in the experiments (Figure 6), which suggests that a balance was soon reached between horizontal dispersion and algal carbon uptake. The patch centre in EisenEx (118 $km^{2\#}$) was 4 times larger than that in SOIREE (29 km^2) after 12 days (Table 6). The large dimensions of the patch and the patch centre in EisenEx reflect the initially strong horizontal dispersion.

Table 6: *Average changes in DIC in the patch centre for SOIREE and EisenEx. The DIC change by net community production (ΔDIC_{NCP}) was calculated by correction of the net DIC change (ΔDIC_{fCO2}) for changes by vertical diffusion (ΔDIC_{VDif}), CO_2 air-sea exchange (ΔDIC_{AirSea}) and horizontal dispersion (ΔDIC_{HDis}) (equation 4). The terms in equation 4 do not quite add up to the value of ΔDIC_{NCP}, as a result of the fitting procedure for ΔDIC_{HDis} (section 2). Some EisenEx values for 12 days were calculated by linear interpolation ($^{\#}$). References are: [1] Bakker et al. (2001); [2] Bozec et al. (2005).*

		SOIREE 12.0 days	EisenEx 12.0 days	EisenEx 18.3 days
ΔfCO_2	µatm	-32 to –38 [1]	-13 to -18	-13 to -18
ΔDIC 0-20 m	µmol kg^{-1}	-15 to –18 [1]	-12 [2]	-9 [2]
Area	km^2	29 ± 27%	118$^{\#}$ ± 37%	172 ± 33%
ΔDIC_{fCO2}	mmol m^2	-624 ± 4%	-235$^{\#}$ ± 16%	-402 ± 16%
ΔDIC_{VDif}	mmol m^2	7 (-100% to 103%)	9$^{\#}$ (-100% to 157%)	18 (-100% to 157%)
ΔDIC_{AirSea}	mmol m^2	17 ± 52%	20$^{\#}$ ± 55%	38 ± 54%
ΔDIC_{HDis}	mmol m^2	189 ± 74%	115$^{\#}$ ± 83%	251 ± 60%
ΔDIC_{NCP}	mmol m^2	-837 ± 21%	-377$^{\#}$ ± 42%	-702 ± 37%

After 12 days vertical diffusion and air-sea exchange had added 4-5 times more DIC to the mixed layer of the patch in EisenEx than in SOIREE (Table 5), as a result of the higher vertical diffusivity (Table 3) and stronger winds after 5 days in EisenEx (Figures 2 and 3). The evolution of biological DIC uptake (ΔDIC_{NCP}) in both experimental patches was strikingly similar with initial DIC uptake after 4-5 days (Figure 9; Table 5). The total biological DIC reduction after 12 days was comparable in SOIREE (1389 ton C ± 10%) and EisenEx (1433 ton C$^{\#}$ ± 27%), despite differences in surface water fCO_2, the size of the

patch, and the mixed layer depth. The ratio of biological DIC uptake to iron added was 3.7×10^3 mol mol^{-1} in SOIREE and 4.3×10^3 mol mol^{-1} in EisenEx (Table 5).

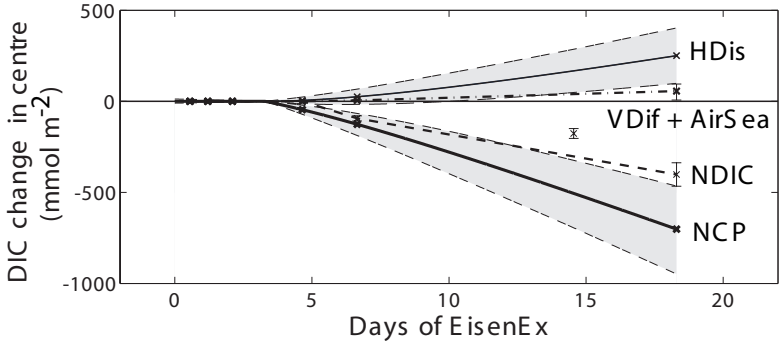

Figure 8: *Average changes in DIC for the mixed layer of the patch centre during EisenEx. The crosses mark data points, which were based on the fCO_2 maps. The dashed line indicates the net DIC change (ΔDIC_{fCO2}, here NDIC). The dashed-dotted line corresponds to the joint supply of DIC by vertical diffusion (ΔDIC_{VDif}) and CO_2 air-sea exchange (ΔDIC_{AirSea}). The thin line indicates the supply of DIC to the patch centre by horizontal dispersion (ΔDIC_{HDis}). These terms allow calculation of DIC uptake by net community production (ΔDIC_{NCP}) (thick line) with equation 6. Error bars and grey shaded areas indicate the uncertainty in the estimates, which results from the uncertainty in the mapping scenario, the gas transfer velocity, the vertical diffusivity, and the rate of horizontal dispersion (section 2).*

The average net DIC reduction in the patch centre in SOIREE (624 mmol m^{-2}) strongly exceeded that in EisenEx (235 mmol m$^{-2\#}$) after 12 days (Table 6). Vertical diffusion and air-sea exchange had added small amounts of DIC to the mixed layer. Horizontal diffusion had lowered the biological DIC change by 23% in SOIREE and by 31% in EisenEx. Biological DIC uptake in the patch centre in SOIREE (837 mmol m^{-2}) was twice that in EisenEx (377 mmol m^{-2}) (Figure 9).

Biological DIC uptake can be compared to the rate of carbon-14 uptake, which is often taken as an indicator for net primary productivity. These ^{14}C uptake rates have not been corrected for horizontal dispersion. In SOIREE, ^{14}C uptake in the upper 65 m of the patch centre increased from 26 to 92 mmol C m^{-2} d^{-1} over 13 days (from Gall et al. (2001) upon correction with a factor 12/14). In EisenEx, ^{14}C uptake changed from 17 mmol m^{-2} d^{-1} to 58 mmol m^{-2} d^{-1} after 12 days (Gervais et al., 2002). Both ^{14}C uptake and biological DIC reduction in the patch centre differed by a factor 2 between the experiments after 12 days. The high initial horizontal dispersion in EisenEx was a major factor in the reduction of ^{14}C uptake and biological DIC uptake in the centre of the EisenEx patch relative to SOIREE.

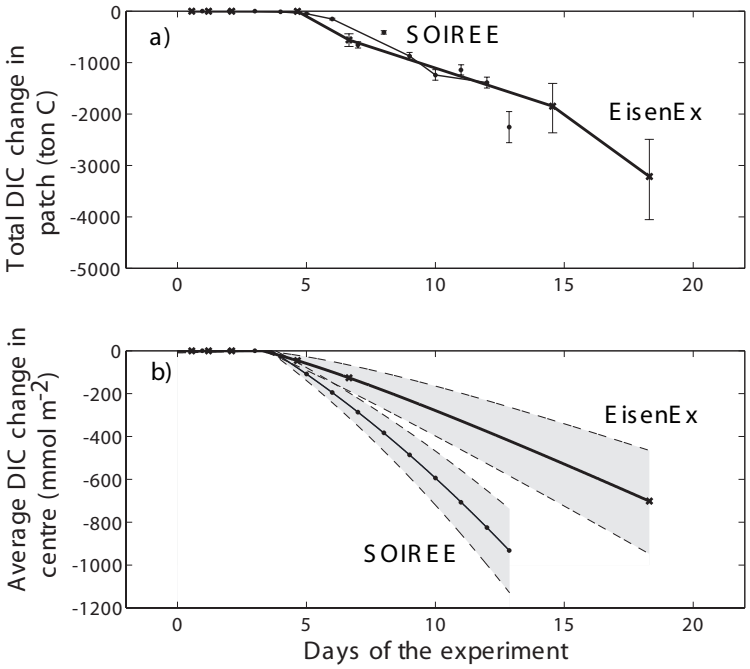

Figure 9: *The DIC reduction by net community production (ΔDIC_{NCP}) in (a) the patch and (b) the patch centre during SOIREE (points) and EisenEx (crosses). Grey shaded areas show the uncertainty in the estimates, which results from the uncertainty in the mapping scenario, the gas transfer velocity, the vertical diffusivity, and the rate of horizontal dispersion (section 2).*

4.2. Different estimates for the net DIC reduction in EisenEx

Bozec et al., (2005) obtain 1232 mmol m^{-2} for the net DIC reduction in the centre of the EisenEx patch after 20 days, three fold higher than the value of 402 mmol m^2 (± 16%) after 18 days in this study (Table 6). Here we compare the values. The estimates differ by two days in a period, when surface water DIC in the patch centre decreased by 1-3 µmol kg^{-1} day^{-1} (Bozec et al., 2005). Furthermore, Bozec et al. report the maximum DIC reduction, while this study presents the average reduction in the patch centre, at a time when the DIC reduction was no longer uniform across the centre (Figure 7). Finally, Bozec et al. assume uniform DIC uptake across the mixed layer, while a factor 0.8 is used here.
Bozec et al., (2005) calculate a net DIC reduction of 13×10^3 ton C across the EisenEx patch after 20 days, four times more than our estimate of 2840 ton (± 15%) for 18 days (Table 5). The discrepancy results from the aforementioned assumptions for the patch

centre, as well as from a high DIC reduction of 10 µmol kg^{-1} and a 100 m deep mixed layer across the edge of the patch (750 km^2) in Bozec et al., (2005).

5. Conclusion

Two iron enrichment experiments in the Southern Ocean had a different evolution of surface water fCO_2, largely as a result of contrasting mixing regimes (Figures 2 and 3; Table 1). Surface water fCO_2 decreased at a regular rate in SOIREE, while its evolution resembled a saw tooth in EisenEx. The SOIREE experiment was a textbook example of algal response and biogeochemical changes upon alleviation of iron limitation.

The hydrographic and meteorological settings of the experiments were characteristic for the regions and seasons, in which the experiments were carried out (Boyd et al. (2000) – on SOIREE). Moderate to high wind speeds and homogenous water properties were encountered south of the APF in late summer during SOIREE. The rapid passage of weather systems and presence of eddies, which dominated EisenEx, are typical for the area between the Subantarctic Front and the APF, south of Africa.

Biological activity had taken up comparable amounts of DIC across the experimental patches after 12 days. It seems possible that the similar amount of iron added (Table 1), as well as algal growth at a comparable near-maximum growth rate, determined the size of the biological DIC uptake across the patches, despite differences in algal composition, water temperature, insolation, mixed layer depth, and grazing pressure. Horizontal dispersion strongly affected the vertically integrated biological DIC uptake in the patch centres, but would have had little effect on the overall biological carbon uptake across the patches. The different mixing regimes had less effect on the overall biological DIC uptake across the patches than suggested by the evolution of surface water fCO_2.
By analogy, some natural algal blooms may differ less in their overall biological carbon uptake than a comparison of algal densities and surface water fCO_2 changes suggests. This only holds true, if algal carbon uptake rates are similar, algal carbon uptake dominates DIC changes, and algal density does not influence the evolution of the algal bloom, e.g. by coagulation of particles or by attracting grazers.

The iron additions made the fertilised waters sinks for atmospheric CO_2. Replenishment of CO_2 by air-sea exchange was small in comparison to algal carbon uptake. The EisenEx bloom was four times more 'efficient' than the SOIREE bloom in drawing down atmospheric CO_2 (Table 5), as a result of a higher proportion of strong winds in EisenEx from five days onwards. Algal growth and biological carbon uptake continued, as the ships left the SOIREE and EisenEx sites after 12 and 22 days, respectively. No change in carbon export was observed in SOIREE (Charette and Buesseler, 2000; Nodder and Waite, 2001). An increase in carbon export may have occurred in EisenEx (Riebesell, personal communication). It is impossible to determine the fate of both blooms and how much carbon eventually left the surface ocean, thus creating a non-permanent oceanic sink for atmospheric CO_2.

In addition to more efficient uptake of atmospheric CO_2, the waters of the EisenEx area had a shorter north-south travel distance to subduction sites north of the Subantarctic

Front than the SOIREE site. As surface water at these sites sinks and mixes with deeper water to become Subantarctic Mode Water (SAMW) and Antarctic Intermediate Water (AAIW) (Sloyan and Rintoul, 2001), the EisenEx area has a better potential for storing atmospheric CO_2 and transporting carbon away from the sea surface than at the SOIREE site.

The factor four difference between the estimates of the net DIC uptake based on the same data set (this study; Bozec et al., 2005) demonstrates how difficult it is to quantify the short-term biological carbon uptake upon iron fertilisation during an intensive field campaign. The uncertainty in the values becomes even larger if proxies such as chlorophyll are used for estimating carbon uptake (e.g. Abraham et al., 2000; Boyd et al., 2000). Accurate quantification of carbon export is even more demanding. The difficulty in determining carbon storage upon iron fertilisation (Gnanadesikan et al., 2003) and the low efficiency of carbon export are fundamental obstacles for the application of the method with the purpose of carbon storage.

References

Abraham, E.R., Law, C.S., Boyd, P.W., Lavender, S.J., Maldonado, M.T., Bowie, A.R., 2000. Importance of stirring in the development of an iron fertilized phytoplankton bloom. Nature 407, 727-730.

Bailey, T.C., Gatrell, A.C., 1995. Interactive spatial data analysis. Addison Wesley Longman Limited, Harlow, U.K., 413 pp.

Bakker, D.C.E., Watson, A.J., Law, C.S., 2001. Southern Ocean iron enrichment promotes inorganic carbon drawdown. Deep-Sea Research Part II 48, 2483-2507.

Bowie A.R., Maldonado, M.T., Frew, R.D., Croot, P.L., Achterberg, E.P., Mantoura, R.F.C., Worsfold, P.J., Law, C.S., Boyd, P.W., 2001. The fate of added iron during a mesoscale fertilisation experiment in the Southern Ocean. Deep-Sea Research Part II 48, 2703-2743.

Boyd, P.W., Watson, A.J., Law, C.S., Abraham, E.R., Trull, T., Murdoch, R., Bakker, D.C.E., Bowie, A.R., Buesseler, K.O., Chang, H., Charette, M.A., Croot, P., Downing, K., Frew, R.D., Gall, M., Hadfield, M., Hall, J.A., Harvey, M., Jameson, G., LaRoche, J., Liddicoat, M.I., Ling, R., Maldonado, M., McKay, R.M., Nodder, S.D., Pickmere, S., Pridmore, R., Rintoul, S., Safi, K., Sutton, P., Strzepek, R., Tanneberger, K., Turner, S.M., Waite, A., Zeldis, J., 2000. A mesoscale phytoplankton bloom in the polar Southern Ocean stimulated by iron fertilization. Nature 407, 695-702.

Boyd, P.W., Abraham, E.R., 2001. Iron mediated changes in phytoplankton photosynthetic competence during SOIREE. Deep-Sea Research Part II 48, 2529-2550.

Boyd, P.W., Law, C.S., Wong, C.S., Nojiri, Y., Tsuda, A., Levasseur, M., Takeda, S., Rivkin, R., Harrison, P.J., Strzepek, R., Gower, J., McKay, R.M., Abraham, E., Arychuk, M., Barwell-Clarke, J., Crawford, W., Crawford, D., Hale, M., Harada, K., Johnson, K., Kiyosawa, H., Kudo, I., Marchetti, A., Miller, W., Needoba, J., Nishioka, J., Ogawa, H., Page, J., Robert, M., Saito, H., Sastri, A., Sherry, N., Soutar, T., Sutherland, N., Taira, Y., Whitney, F., Wong, S.K.E., Yoshimura, T., 2004. The decline and fate of an iron-induced subarctic phytoplankton bloom. Nature 428, 549-553.

Bozec, Y., Bakker, D.C.E., Hartmann, C., Thomas, H., Bellerby, R.G.J., Nightingale, P.D., Riebesell, U., Watson, A.J., Baar, H.J.W. de, 2005. The CO_2 system in a Redfield context during an iron enrichment experiment in the Southern Ocean. Marine Chemistry, 89(1-2): 89-105.

Buesseler, K.O., Andrew, J., Pike, S., Charette, M.A., 2004. The effects of iron fertilization on carbon sequestration in the Southern Ocean. Science 304, 414-417.

Charette, M.A., Buesseler, K.O., 2000. Does iron fertilization lead to rapid carbon export in the Southern Ocean? Geochemistry, Geophysics, Geosystems 1, 2000GC000069.

Chisholm, S.W., Falkowski, P.G., Cullen, J.J., 2001. Discrediting ocean fertilization. Science 294, 309-310.

Chuck, A.L., 2002. Biogenic halocarbons and light alkyl nitrates in the marine environment. Ph.D. thesis. University of East Anglia, Norwich, 200 pp.

Chuck, A.L., Turner, S.M., Liss, P.S., 2002. Direct evidence for a marine source of C_1 and C_2 alkyl nitrates. Science 297, 1151-1154.

Cisewski, B., Strass, V.H., Prandke, H., 2005. Upper ocean vertical mixing in the Antarctic Polar Front Zone. Deep-Sea Research II, accepted.

Coale, K.H., Johnson, K.S., Chavez, F.P., Buesseler, K.O., Barber, R.T., Brzezinski, M.A., Cochlan, W.P., Millero, F.J., Falkowski, P.G., Bauer, J.E., Wanninkhof, R.H., Kudela, R.M., Altabet, M.A., Hales, B.E., Takahashi, T., Landry, M.R., Bidigare, R.R., Wang, X., Chase, Z., Strutton, P.G., Friederich, G.E., Gorbunov, M.Y., Lance, V.P., Hilting, A.K., Hiscock, M.R., Demarest, M., Hiscock, W.T., Sullivan, K.F., Tanner, S.J., Gordon, R.M., Hunter, C.N., Elrod, V.A., Fitzwater, S.E., Jones, J.L., Tozzi, S., Koblizek, M., Roberts, A.E., Herndon, J., Brewster, J., Ladizinsky, N., Smith, G., Cooper, D., Timothy, D., Brown, S.L., Selph, K.E., Sheridan, C.C., Twining, B.S., Johnson, Z.I., 2004. Southern Ocean iron enrichment experiment: carbon cycling in high- and low-Si waters. Science 304, 408-414.

De Baar, H.J.W., Boyd, P.W., 2000. The role of iron in plankton ecology and carbon dioxide transfer of the global oceans. In: Hanson, R.B., Ducklow, H.W., Field, J.G. (Eds.), The changing ocean carbon cycle. A midterm synthesis of the Joint Global Ocean Flux Study. International Geosphere - Biosphere Programme Book Series. Cambridge University Press. Cambridge etc. pp. 61-140.

De Baar, H.J.W., 2001. Production of iron fertilizer batches in seawater. Berichte zur Polar- und Meeresforschung 400, 145-148.

DOE, 1994. Handbook of methods for the analysis of the various parameters of the carbon system in sea water; version 2. Dickson, A.G., Goyet, C. (Eds.). ORNL/CDIAC 74.

ETOPO 5, 1988. Digital relief of the surface of the earth. Data Announcement 88-MGG-02. National Oceanographic and Atmospheric Administration, National Geophysical Data Center, Boulder, Colorado, USA.

Fuhrman, J.A., Capone, D.G., 1991. Possible biogeochemical consequences of ocean fertilization. Limnology and Oceanography 36, 1951-1959.

Gall, M.P., Strzepek, R., Maldonado, M., Boyd, P.W., 2001. Phytoplankton processes. Part 2: Rates of primary production and factors controlling algal growth during the Southern Ocean Iron RElease Experiment (SOIREE). Deep-Sea Research Part II 48, 2571-2590.

Gervais, F., Riebesell, U., Gorbunov, M.Y., 2002. Changes in the size-fractionated primary productivity and chlorophyll a in response to iron fertilization in the southern Polar Frontal Zone. Limnology and Oceanography 47, 1324-1335.

Gnanadesikan, A., Sarmiento, J.L., Slater, R.D., 2003. Effects of patchy ocean fertilization on atmospheric carbon dioxide and biological production. Global Biogeochemical Cycles 17, 1050, doi: 10.1029/2002GB001940.

Goldson, L., 2004. Vertical mixing across the seasonal pycnocline of the Southern Ocean: Studies using sulphur hexafluoride tracer. Ph.D. thesis. University of East Anglia, Norwich, U.K. 219 pp.

Jin, X., Gruber, N., 2003. Offsetting the radiative benefit of ocean iron fertilization by enhancing ocean N_2O emissions. Geophysical Research Letters 30 (24), 2249, doi: 10.1029/2003GL018458.

Johnson, K.M., Wills, K.D., Butler, D.B., Johnson, W.K., Wong, C.S., 1993. The performance of an automated continuous gas extractor and coulometric detector. Marine Chemistry 44, 167-188.

Journel, A.G., Huijbregts, Ch.J., 1977. Mining Geostatistics. 7th ed. Academic Press, London etc. 600 pp.

Large, W.G., Pond, S., 1981. Open ocean momentum flux measurements in moderate to strong winds. Journal of Physical Oceanography 11, 324-336.

Law, C.S., Ling, R., 2001. Nitrous oxide flux and response to increased iron availability in the Antarctic Circumpolar Current. Deep-Sea Research Part II 48, 2509-2527.

Law, C.S., Abraham, E.R., Watson, A.J., Liddicoat, M.I., 2003. Vertical diffusion and nutrient supply to the surface mixed layer in the Antarctic Circumpolar Current. Journal of Geophysical Research 108, 3272, doi: 10.1029/2002JC001606.

Liss, P.S., Merlivat, L., 1986. Air-sea exchange rates: introduction and synthesis. In: Buat-Ménard, P. (Eds.), The role of air-sea exchange in geochemical cycling. D. Reidel Publishing Company, Dordrecht, The Netherlands, etc. pp. 113-127.

Martin, J.M., 1990. Glacial to interglacial CO_2 change: The iron hypothesis. Paleoceanography 5, 1-13.

Nightingale, P.D., Malin, G., Law, C.S., Watson, A.J., Liss, P.S., Liddicoat, M.I., Boutin, J., Upstill-Goddard, R.C., 2000. *In-situ* evaluation of air-sea gas exchange parameterisations using novel conservative and volatile tracers. Global Biogeochemical Cycles 14 (1), 373-387.

Nodder, S.D., Waite, A.M., 2001. Is Southern Ocean organic carbon and biogenic silica export enhanced by iron stimulated increases in biological production? Sediment trap results from SOIREE. Deep-Sea Research Part II 48, 2681-2701.

Orsi, A.H., Whitworth III, T., Nowling Jr., W.D., 1995. On the meridional extent and fronts of the Antarctic Circumpolar Current. Deep-Sea Research Part I 42, 641-673.

Sloyan, B.M., Rintoul, S.R., 2001. Circulation, renewal and modification of Antarctic Mode and Intermediate Water. Journal of Physical Oceanography 31, 1005-1030.

Smetacek, V., 2001. EisenEx: International team conducts iron experiment in Southern Ocean. US JGOFS News January, 11, 14.

Strass, V.H., Leach, H., Cisewski, B., Gonzalez, S., Post, J., da Silva Duarte, V., Trumm, F., 2001. The physical setting of the Southern Ocean iron fertilization experiment. Berichte zur Polar- und Meeresforschung 400, 94-130.

Takahashi, T., Olafsson, J., Goddard, J.G., Chipman, D.W., Sutherland, S.C., 1993. Seasonal variation of CO_2 and nutrients in the high-latitude surface oceans: a comparative study. Global Biogeochemical Cycles 7, 843-878.

Turner, S.M., Nightingale, P.D., Spokes, L.J., Liddicoat, M.I., Liss, P.S., 1996. Increased dimethyl sulphide concentrations in seawater from *in situ* iron enrichment. Nature 383, 513-517.

Turner, S.M., Harvey, M.J., Law, C.S., Nightingale, P.D., Liss, P.S., 2004. Iron induced changes in oceanic sulfur biogeochemistry. Geophysical Research Letters 31, L14307, doi: 10.1029/2004GL020296.

Turner, S.M., Bakker, D.C.E., Goldson, L.E., Messias, M.J., Nightingale, P.D., 2005. Considerations on the use of sulfur hexafluoride as a deliberate tracer in oceanic

biogeochemical lagrangian studies: lessons from EisenEx. In preparation for submission to Geophysical Research Letters.

Wanninkhof, R.H., 1992. Relationship between wind speed and gas exchange over the ocean. Journal of Geophysical Research 97, 7373-7382.

Wanninkhof, R., McGillis, W.R., 1999. A cubic relationship between air-sea CO_2 exchange and wind speed. Geophysical Research Letters 26 (13), 1889-1892.

Watson, A.J., Bakker, D.C.E., Boyd, P.W., Ridgwell, A.J., Law, C.S., 2000. Effect of iron supply on Southern Ocean CO_2 uptake and implications for glacial atmospheric CO_2. Nature 407, 730-733.

Watson, A.J., Messias, M.-J., Goldson, L., Skjelvan, I., Nightingale, P., Liddicoat, M.I., 2001. SF_6 measurements on EisenEx. Berichte zur Polar- und Meeresforschung 400, 76-81.

WDCGG, 2003. World Data Centre for Greenhouse Gases of the World Meteorological Organisation, Japan Meteorological Agency, Tokyo, Japan. Online data set, http://gaw.kishou.go.jp/wdcgg/wdcgg.html.

Acknowledgements

We thank the captain and the crew of R.V. *Tangaroa* and R.V. *Polarstern* for their enthusiastic support to SOIREE and EisenEx. The experiments were international, interdisciplinary projects with 29 and 56 participants, respectively, who all shared in the tasks related to the iron releases. We especially thank the chief scientists (Victor Smetacek (AWI), Phil Boyd, Rob Murdoch (NIWA)) and other participants (Ed Abraham, Uli Bathmann, Andy Bowie, Boris Cisewski, Peter Croot, Cliff Law, Harry Leach, Ulf Riebesell, Kim Tanneberger) for their contribution. Ute Schuster (UEA) assisted with the cruise preparations for SOIREE, while Anthony Kettle (UEA) gave valuable advice on the calculation of horizontal diffusion. We acknowledge the constructive comments by three reviewers. The work was supported by AWI, the National Institute of Water and Atmospheric Research, the European Community grants CARUSO (ENV4-CT97-0472) and ORFOIS (EVK-CT-2001-00100), NERC (Natural Environment Research Council) core funding to PML, the NERC SOIREE grant (NER/GR/A1431), and the New Zealand Foundation of Research, Science, and Technology.

Chapter 8

Summary and Perspectives

1. Summary

The investigations carried out during this thesis research focused on the biological pump operative in two very contrasting areas, yet intimately linked towards the same goal. This objective is to estimate the role of these two environments in the global carbon cycle, notably assess their potential sink of atmospheric CO_2 and the processes involved in this pump in the context of increasing atmospheric CO_2. On the one hand, the work carried out in the North Sea contributes to the global assessment of the role of coastal seas in the carbon cycle, attempted by different international programs. On the other hand, the iron enrichment experiment carried out in the Southern Ocean together with the results of other iron enrichment experiments, allowed us to assess the role of Fe limitation in the biological utilization of DIC and major nutrients, and evaluate the ensuing uptake of CO_2 from the atmosphere.

The continental shelf pump of CO_2 in the North Sea

The hypothesis of a "continental shelf pump" for uptake of CO_2 from the atmosphere with subsequent transport to the open ocean was assessed in a pilot study in the North Sea. The novel aspect of this work relies on the generation of a very comprehensive and accurate data set for the carbon dioxide system in the North Sea, based on four cruises of one month each, and carried out during four consecutive seasons. The major findings of this study allowed us to fulfill all the major scientific objectives elaborated in the project proposal.

For carbon, a completely new field database was established. The North Sea was successfully covered during four seasons by an adapted 1º by 1º grid corresponding to 97 stations. During late summer (Chapter 2), the bottom topography of the North Sea has a strong impact on the distributions of DIC and pCO_2. The surface distributions of these two parameters showed a clear boundary located around 54°N. South of this boundary the DIC and pCO_2 ranged from 2070 to 2130 μmol kg^{-1} and 290 to 490 ppm, respectively, whereas in the northern North Sea, values ranged between 1970 to 2070 μmol kg^{-1} and 190 to 350 ppm, respectively. The vertical profiles measured in the two different areas showed that the vertical mixing regime of the water column was the major factor determining the surface distributions. The entirely mixed water column of the shallow southern North Sea was heterotrophic, whereas the surface layer of the stratified water column in the deeper northern North Sea was close to metabolic balance. During late summer, the southern North Sea acts as a source of CO_2 for the atmosphere within a range of +0.8 to +1.7 mmol m^{-2} day^{-1}, whereas the northern North Sea absorbs CO_2 within a range of -2.4 to -3.8 mmol m^{-2} day^{-1}. The North Sea as a whole acts as a sink of atmospheric CO_2 of -1.5 to -2.2 mmol m^{-2} day^{-1} during late summer.

The delineation of regions of coastal seas that may, or may not, show summer stratification, as a critical indicator if the shelf acts as a CO_2 "pump" from the atmosphere,

is an important concept not previously highlighted in coastal seas. The North Sea is a unique open continental shelf where this can be shown. Here the large amount of data for the CO_2 system acquired during this thesis has allowed us to compare efficiently the southern to the northern North Sea. A parallel exists with the water column properties observed in different outer estuaries. In stratified (microtidal) estuaries, the organic carbon produced by primary production can escape from the surface layer down across the pycnocline and the CO_2 produced by degradation processes in the bottom is not readily available for exchange with the atmosphere (Borges, 2005). This is a similar process as in the northern North Sea and results in a sink of atmospheric CO_2 in such outer estuaries. On the other hand, in permanently well-mixed (macrotidal) estuaries, the decoupling between production and degradation of organic matter does not occur across the water column (Borges, 2005). This is similar to the southern North Sea, and implies that these systems are sources of CO_2 to the atmosphere or neutral, based on the data available to date. In open continental shelves and in outer estuaries, presence or absence of seasonal or permanent stratification appears to be a critical factor controlling air-water CO_2 fluxes.

The annual air-sea exchange of CO_2 for the whole North Sea calculated in chapter 3 was obtained from the ~22,000 surface measurement of pCO_2 obtained for each season, during the four consecutive cruises carried out during this thesis, thus constituting one of the most accurate estimates of the net annual air-sea flux of CO_2 for a coastal sea to date. As mentioned above, because of the absence of stratification during summer, the southern North Sea (south of 54 ºN) is an annual weak source of CO_2 for the atmosphere with a flux of 0.2 mol C m^{-2} yr^{-1}. The northern North Sea (situated between 54º and 61ºN) is a strong sink of CO_2 for the atmosphere with a flux of 1.7 mol C m^{-2} yr^{-1}. The North Sea as a whole is an annual sink of CO_2 for the atmosphere and takes up 1.4 mol C m^{-2} yr^{-1}, from which approximately 93% are then transported to the deeper layer of the North Atlantic Ocean. The overall North Sea thus acts as a highly efficient continental shelf pump for the absorption of CO_2 from the atmosphere.

In chapter 4, the seasonally resolved dataset of DIC, pCO_2 and inorganic nutrients was interpolated per month, to assess the abiotic and biological processes governing the monthly variations of DIC. The North Sea's regional variability was accounted for by using the 15-box scheme as proposed by the International Council for the Exploration of the Seas (ICES) (ICES, 1983). In the surface layer of the northern and central North Sea, autotrophy governs DIC changes from February to July and most of the organic carbon produced during this period is transported down into the deep layer and respired, mainly from April to July. During the remainder of the year, lateral and vertical advection and air-sea exchange of CO_2 govern the monthly DIC changes.

In the shallow southern North Sea, the biological processes govern the DIC variations during the whole year, with predominant autotrophy from February to July and predominant heterotrophy from August to January. The complete CO_2 system dataset allowed the first estimate of the Net Community Production based on inorganic carbon (NCP_C) in the different regions of the North Sea and chapter 4 highlights the regional variability for NCP_C. Taking into account this variability, an annual NCP_C of

4.3 ± 0.4 mol C m^{-2} yr^{-1} was estimated in the surface layer of the North Sea (513,000 km^2), which based on the latest estimate of Gross Primary Production (GPP) in the surface layer of the North Sea of 17.5 mol C m^{-2} yr^{-1} (Gazeau et al., 2004), accounts for 20 to 30% of the GPP. In this chapter 4, we also calculate for the whole North Sea the NCP_N based instead on utilization of inorganic nitrate. This was more than twofold lower because of the apparent overconsumption of carbon relative to nitrate and phosphate occurring in the central and the northern North Sea. This demonstrates that previous approaches in the central or whole North Sea, by NCP based on inorganic nutrient, seriously underestimated the NCP. For the whole North Sea as defined by ICES (513,000 km^2), the annual NCP_C is -0.10 ± 0.02 mol C m^{-2} yr^{-1}. This system is close to metabolic balance, predominantly heterotrophic, although it is a rather strong sink for atmospheric CO_2 as shown in chapter 3.

In chapter 5, a one box carbon budget has been established for the North Sea. This shows that the gross carbon budget is dominated by the exchange across the northern North Sea; the Atlantic Ocean supplying more than 98% of the carbon, mostly as DIC but also as DOC. The net carbon budget is dominated by the carbon inputs from the atmosphere, the Baltic Sea and rivers, which represent 29%, 40% and 31%, respectively, of the overall enrichment of the carbon content of the North Sea waters. The total enrichment is 2.73 10^{12} mol C yr^{-1}, which is approximately 2% of the initial carbon content. Dividing latter total carbon pool into an inorganic and organic pool, the inorganic pool is also increased by "internal" conversion of DOC to DIC as also discussed in chapter 3. This increase in DIC due to the internal conversion of DOC is in the same proportions as the DIC increase due to uptake of atmospheric CO_2. The one box carbon budget made in chapter 5 includes the Skagerrak area where community respiration exceeds gross primary production in the deep water column (Gazeau et al., 2004). The then 575,300 km^2 covered by the North Sea is a sink for organic carbon of -0.50 ± 0.2 mol C m^{-2} yr^{-1}, and thus can be characterized as a heterotrophic system.

The NCP_C estimates taking into account the regional variability of the North Sea proper (ICES area of 513,000 km^2) in Chapter 4 and the one-box full carbon budget estimates for the North Sea including Skagerrak (area of 575,300 km^2) in Chapter 5, show that these different areas are respectively, close to metabolism balance and heterotrophic. However, chapter 3 shows that these two areas are strong sink for atmospheric CO_2, which confirms that the CO_2 air-sea fluxes cannot be considered as a reliable indicator of the trophic state of an ecosystem.

In-situ iron enrichment in the Southern Ocean

The EisenEx experiment, demonstrated that iron is a limiting nutrient for phytoplankton growth in the Southern Ocean (Gervais et al., 2002). During this experiment, we managed to follow the evolution of DIC and inorganic nutrients under stormy spring conditions (chapter 6). The uptake of CO_2 and inorganic nutrients and the algal growth signal were well correlated, confirming that the biological pump was responsible for the

decrease in CO_2 in the surface waters of the patch compared to the outside control stations. We observed an uptake of CO_2 within five days after the first Fe-addition. This uptake was strongly influenced by the changes in mixed layer depth due to the succession of storms and calm weather during the experiment. A maximum uptake of DIC of 15 µmol kg^{-1} in a mixed layer of 80 meters depth occurred 20 days after the first Fe-infusion, and was concomitant with a maximum uptake of fCO_2 of 23 µatm and an increase in pH of 0.025 units. A similar uptake of silicate was observed inside and outside the patch. Since silicate consumption by diatoms growing under Fe-depleted conditions is higher than for diatoms growing under Fe-replete conditions (Takeda, 1998; Brzezinski et al., 2003; Timmermans et al., 2004, their Table 2), the presence of diatoms outside the patch is likely to be responsible for the substantial silicate uptake outside the patch. In the surface waters of the patch, we found values of 82, 5.9, 12, 2.9, and 0.5 for the ratios C/P, C/N, N/P, C/Si and N/Si, respectively. These values are in good agreement with values reported previously for diatom blooms in the Southern Ocean (Fanning, 1992; De Baar et al., 1997). Diatoms produce a large quantity of lipid material, which results in lower C/P and C/N ratios (Takahashi et al., 1985; Hedges et al., 2002) than the classical Redfield proportions. Further, under Fe-replete conditions, diatoms will consume more nitrate and less silicate than under Fe-deplete condition (Franck et al., 2003; Timmermans et al., 2004), thus resulting in a higher N/Si ratio in the surface water of the patch observed during EisenEx. Moreover, the sudden availability of iron in surface waters rich in major inorganic nutrients might have created a state of luxury consumption, as suggested by Droop (1973). The above low ratios calculated were attributed to such a state of luxury consumption in combination with the high growth of diatoms.

A preliminary computation of the overall consumption of carbon within the patch based on the DIC data set was attempted in chapter 6. In spite of the relatively modest observed changes in DIC, once integrated for the whole patch, these changes were equivalent to a significant uptake of 1.1×10^9 mol C after 20 days. We argued that the total C-uptake for the whole patch was larger than during previous Fe-fertilization experiments because of the large horizontal dispersion of the patch and the deep mixed layer in which the DIC uptake was observed. However, in collaboration with our colleagues from the different institutes involved in the EisenEx experiment, a more recent C-uptake budget based on the fCO_2 and SF_6 finalized dataset has been established for EisenEx (Chapter 7). The use of the finalized SF_6 dataset for this approach allowed us to evaluate the impact of the horizontal dispersion on the changes in DIC and thus establish a more accurate budget for the whole iron enriched patch. We compared it to the one of the SOIREE experiment calculated with a similar approach (Chapter 7). The iron-enriched waters in EixenEx absorbed four times more atmospheric CO_2 than in SOIREE between days 5 and 12, as a result of stronger winds enhancing the transfer coefficient for air-sea gas exchange. Since the SOIREE bloom was followed for only 13 days, results from the two experiments were compared on day 12. The total biological uptake of inorganic carbon across the patch was 1389 ton C (±10%) in SOIREE and 1433 ton C (±27%) in EixenEx after 12 days. In chapter 7 we argue that this similarity probably reflects the comparable size of the iron additions, as well as algal growth at a similar near maximum growth rate in these regions.

The findings imply that the overall larger patch size due to stronger mixing regime (both vertical and lateral) of EisenEx versus SOIREE, leads to similar overall biological carbon uptake 13 days after the iron-enriched waters. On the other hand, for EisenEx the preliminary C-uptake budget of 13 $\times 10^3$ ton C across the patch after 20 days calculated in chapter 6 exceeds by a factor four the one calculated in chapter 7 (2840 ton C) after 18 days. This demonstrates how difficult it is to quantify the short-term biological carbon uptake upon iron fertilisation during an intensive field campaign.

2. Perspectives

Coastal seas: Sink or source of CO_2 for the atmosphere?

In the first Land-Ocean Interaction in the Coastal Zone (LOICZ) report in 1995 (Kempe, 1995), Kempe concluded that the scientific community could not yet answer the question: "Do coastal seas act as source or sink of CO_2 for the atmosphere?". Since then, numerous studies have been carried out in many coastal seas of the world in order to answer this question (see Borges (2005) for overview). Our high spatial resolution study allowed derivation of one of the most accurate estimates of the net annual air-sea flux of CO_2 for a coastal sea to date. Several other investigations with sufficient spatial and temporal coverage demonstrated that open continental shelves such as the Barents Sea (Kaltin et al., 2002), Baltic Sea (Thomas and Schneider, 1999; Kuss et al., 2004) Gulf of Biscay (Frankignoulle and Borges, 2001) and the Marginal Seas of the Pacific Ocean (Chen et al., 2004a) absorb atmospheric CO_2. Moreover, all these coastal seas had an average uptake of CO_2 in the same range as the flux calculated in this thesis for the North Sea. It is common practice to place a regional study in wider or global context. An extrapolation of the flux calculated in chapter 3 for the North Sea to the 25.2×10^6 km^2 of continental margins, suggests that coastal seas would have a net CO_2 uptake of 0.4 Pg C $year^{-1}$, which is on the order of 20% of the global ocean's net annual uptake of anthropogenic CO_2 (1.95 Pg C $year^{-1}$ based on the cumulate uptake for the 1980-1999 period reported by Sabine et al. (2004). Similar global extrapolations have been made from direct pCO_2 measurement in the East China Sea and Gulf of Biscay (Tsunogai et al., 1999; Frankignoulle and Borges, 2001) and demonstrated a net annual uptake of atmospheric CO_2 and transport into the open ocean and provided strong support for the continental shelf CO_2 pump hypothesis.

Modelling studies suggest that the pump of CO_2 in open shelves would nowadays account for a net uptake of 0.6 Gt C yr^{-1} (Yool and Fasham, 2001), whereas the shelves were a source of CO_2 before the industrial revolution (Andersson and Mackenzie, 2004). In his latest assessment of the global carbon cycle, Chen (2004b) concluded, based on the overall direct pCO_2 measurement and mass balance approach, that taken together continental shelves are significant sinks for atmospheric CO_2, absorbing 0.36 Pg C yr^{-1}.

The increasing number of data in different coastal areas have made possible robust extrapolations for the entire coastal zone and has allowed the scientific community to

attempt answering the question formulated by Kempe (1995). The first goal of global extrapolations, and notably the one attempted in this thesis, is to yield robust estimates, in this case for the air-sea exchange of CO_2 in the coastal ocean, based on robust dataset and in agreement with the latest findings in the literature. The second goal of such extrapolations is also to point out significant results in order to stimulate the debate in the scientific community. The findings of this thesis together with others investigations (Walsh, 1991; Frankignoulle and Borges, 2001; Chen, 2004b; Ducklow and McCallister, 2005) have pointed out the significance of the coastal ocean, a biogeochemically highly active region of the biosphere, in the global CO_2 cycle. The aim of the worldwide scientific community involved in the investigations of the CO_2 cycle in the coastal ocean is to refine these extrapolations. The LOICZ was conceived to lead to a better understanding of the biogeochemical fluxes across the continental margins and coordinates the investigations of scientific groups working on different coastal ecosystems, thus resulting in numerous and frequent new findings. Recent investigations have demonstrated that, some coastal seas act as source of CO_2 to the atmosphere in a range of 1.0 to 2.5 mol C m^{-2} yr^{-1} (Cai et al., 2003; Borges, 2005; Zhai et al., 2005). Since then, the global extrapolation of a continental shelf pump has been discussed and some authors agued that the diversity and geographic situation of the coastal seas should be taken into account.

Recently, Borges (2005) compiled the annually integrated air-water CO_2 flux data in 44 coastal environments in order to answer the question: "Do we have enough pieces of the jigsaw to integrate CO_2 fluxes in the Coastal Ocean?". This study can be considered as the most complete evaluation of the CO_2 air-sea exchange in the coastal ocean to date, to which the North Sea study presented in this thesis contributes significantly. Borges (2005) argues that a rigorous up-scaling of air-water CO_2 fluxes in the coastal ocean is hampered by the poorly constrained estimate of the surface area of inner estuaries. Borges (2005) therefore considers two estimates, one excluding the estuaries and salt marshes, and a second one, which includes these ecosystems in the calculation. The first estimate, corresponds to an area of approximately 25×10^6 km^2 similar to the one used in the extrapolation presented in the chapter 3 of this thesis. Considering this area, the air to sea CO_2 flux in coastal ocean would be 0.37 Pg C yr^{-1} and would increase the oceanic uptake of 1.56 Pg C yr^{-1} calculated by (Takahashi et al., 2002) by 24%. This in good agreement with the extrapolation discussed in chapter 3 and above. In fact, when excluding the estuaries and marshes from the calculation the open shelves situated between 30º and 60º such as the North Sea, are mainly responsible for the absorption of CO_2 in coastal ocean with an air to sea CO_2 flux of 0.31 Pg C yr^{-1}. Moreover, open shelves situated between 60º and 90º absorb 0.16 Pg C yr^{-1}, whereas the open shelves between 30ºN and 30ºS have recently been reported to be a net source of CO_2 for the atmosphere, but responsible for a very small air to sea flux of 0.03 Pg C yr^{-1} for the area.

It appears nowadays evident that the coastal ocean, excluding estuaries and salt marshes, is a sink of CO_2 for the atmosphere since all latest and most robust estimates indicate a consistent pattern and a flux of 0.3 to 0.4 Pg C yr^{-1}. As mentioned by Borges (2005), the inclusion of estuaries leads to a reversal of the direction of air-water CO_2 fluxes in the coastal ocean and it appears critical to evaluate the surface area of inner and outer estuaries.

Iron Fertilization: Does it accelerate the ocean biological pump of CO_2?

While contributing to a global estimate of the air-sea CO_2 fluxes in the coastal North Sea, this thesis also aimed at testing the Fe limitation hypothesis of the Southern Ocean by an *in situ* Fe fertilization experiment. The Southern Ocean is among the major HNLC regions, together with the equatorial and subArctic Pacific Ocean constituting some 40% of the open oceans. The major results concerning the CO_2 system for the EisenEx experiment in which we took part in October-November 2000 have been detailed in chapters 6 and 7 and compared with the results from the SOIREE experiment previously carried out in the Southern Ocean and with the two pioneering experiments IronEx-1 and IronEx-2 carried out in the equatorial Pacific. Several more experiments have been carried out after the EisenEx experiment, starting by the Subarctic Pacific Iron Experiment for Ecosystem Dynamics Study (SEEDS) during summer 2001 (Tsuda et al., 2003). This was followed by the Southern Ocean Fe Experiment (SOFeX) in January –February 2002, during which two fertilizations were made in a north and south patch (Coale et al., 2004). During summer of the same year (July 2002), the Subarctic Ecosystem Response to Iron Enrichment Study (SERIES) was conducted at ocean station Papa (Boyd et al., 2004). Finally, the very recent Eifex experiment (2004) has been carried out in the Southern Ocean but results are not yet published. Here, I put in perspective the major conclusions from EisenEx presented in chapters 6 and 7 with the major findings from the latest Fe-fertilisations.

Implications of Fe-enrichment experiment. Overall, the experiments have three implications. Firstly they have shown that iron, as well as light, are the crucial co-limitations of these HNLC regions in the modern ocean. Secondly, in the ~420,000 years Vostok ice core record of glacial/interglacial oscillations, the glacial maxima of Fe dust input into the Antarctic region may, by enhancement of CO_2 utilization by algae, partly account for the glacial minima of atmospheric CO_2. Thirdly, it has been suggested that intentional large scale iron fertilization may, similarly, be an option for mitigation of anthropogenic CO_2, hence avoid the risk of future global warming.

1) Limitation of HNLC regions in the modern ocean - From the combination of 8 experiments it was demonstrated that the depth of the Wind Mixed Layer (WML), in regulating light availability, is the major factor controlling photosynthesis and therefore CO_2 uptake in the High Nutrient Low Chlorophyll (HNLC) regions of the ocean (de Baar et al., 2005). In that respect, as highlighted in chapters 6 and 7 of this thesis, the EisenEx experiment was conducted in the least favorable conditions with deep and variable WML with a maximum of 100 meters at the end of the experiment, thus resulting in a predominant light-limitation during this experiment. As a comparison, the other extreme case would be the SEEDS experiment, conducted in very calm weather and favorable conditions, which allowed a virtually complete removal of nitrate and silicate and uptake on day 13 accompanied by record decreases in fCO_2 (94 µatm) and DIC (61 mmol m^{-3}) in a 10 meters WML on the final day 13.

As mentioned (de Baar et al., 2005), a detailed comparison of carbon budgets among the 8 Fe experiments would be desirable, but the designs, implementations, weather conditions and actual evolution of these experiments have been quite different. Patch dilution has notably varied greatly and efforts to quantify this using the SF_6 tracer have proven difficult. This also explains why a preliminary C-uptake budget has been attempted in chapter 6 before the patch dilution could be quantified more precisely using the SF_6 tracer (chapter 7). Thus, the C budgeting efforts for various experiments have used different approaches. This makes the comparison difficult and yields different estimates depending on the assumptions made for the patch dilution, the depth of the WML in the edge of the patch and the observed DIC drawdown in the WML, as highlighted in chapter 7 by the comparison of the two budgets made in this thesis for EisenEx. The uncertainty in the values becomes even larger if proxies such as chlorophyll are used for estimating carbon uptake. Accurate quantification of carbon export is even more demanding (Gnanadesikan et al., 2003).

For EisenEx an effort has been made to evaluate the export of organic carbon into deeper waters (Riebesell et al., pers. comm.), by difference from the changes actually measured, larger terms in the budget. However, with export being only a small fraction of primary production and the changes in DIC and POC, and given the difficulty in assessing DOC and its changes, the calculated export signals hardly exceed the noise of the overall budget. For the SOFeX-north patch, the export of carbon as particles settling into deeper layers was determined to be significant by the ^{234}Th deficiency technique, but modest with respect to regular estimates in the region (Buesseler et al., 2004). The difficulty in determining deep carbon storage upon iron fertilization and the low efficiency of carbon export are fundamental obstacles for quantification of the net carbon storage.

As seen in chapters 6 and 7 of this thesis, the Antarctic Ocean is least favorable due to greater WML depths. However, only the Antarctic Ocean would yield long term CO_2 storage in deep waters by sinking of intermediate waters near the Subantarctic Front (Caldeira and Duffy, 2000; Bakker, 2004; Sabine et al., 2004). The Antarctic summation of SOIREE, EisenEx and SOFeX-South in high silicate high nitrate Antarctic waters yields an efficiency DIC/Fe = 4,347 (de Baar et al., 2005) and hinges largely on the most robust estimates presented in chapter 7 of this thesis. Assuming a 20% C-export (10% of primary production, the latter is twice the DIC removal), this would yield a C/Fe = 870 ratio for maximum conceivable uptake of CO_2 from the atmosphere (De Baar et al., 2005). Alternatively, a more favorable C export of C/Fe = 3,257 has been reported for SOFeX-South in austral summer (Buesseler et al., 2004).

2) Iron fertilization in the southern Ocean during the Last Glacial Maxima (LGM)- The implications of above DIC/Fe ratio values for the last deglaciation (17,000-11,000 y BP) are reported in detailed elsewhere (de Baar et al., in prep). Briefly, during the Last Glacial Maximum (LGM) the Fe dust input into the Antarctic region was 11-fold the modern dust flux (Edwards et al., 1998). After this dust flux terminated, the atmospheric CO_2 has risen initially with 80 µatm and eventually with 90 µatm to the pre-industrial value of 280 µatm. Taking an export efficiency C/Fe = 870 combined with a factor 10 in Fe dust flux, 30% wet deposition of which 14% dissolves, and a 3 month austral summer growth

season, yields an Fe fertilization effect which can account for only 0.5% of the observed rise of atmospheric CO_2. Taking the more favourable export ratio C/Fe=3257 after Buesseler et al. (2004), the Fe effect would be higher but still only 2% of the observed rate of atmospheric CO_2 increase. Hence, due to the low C/Fe efficiencies in the Antarctic Ocean, the termination of Fe dust input into the Antarctic region after the LGM may account for only 0.5% to 2% of the observed initial ~80 µtm rise of atmospheric CO_2 in the ice core record.

3) Intentional fertilization for mitigation of anthropogenic CO_2 - Extrapolation of the above export efficiency C/Fe = 870 to the current anthropogenic fossil fuel CO_2 emission rate of about 6.6 Petagram C per year ($0.55\ 10^{15}$ mol C yr^{-1}) (Sabine et al., 2004) would lead to a required Fe fertilization of 3×10^{12} mol yr^{-1} or 35×10^{9} kg yr^{-1}, i.e. 35 million tons Fe per year. This is 37-fold more Fe than originally hypothesized (i.e. ~2.2-fold 430,000 tons Fe to remove 3 PgC yr^{-1}, (Martin, 1990)). Alternatively, extrapolation of the most favourable C export of C/Fe = 3,257 for only SOFeX-South in austral summer (Buesseler et al., 2004) to the fossil fuel CO_2 emission rate would yield a lower required Fe fertilization of 0.17×10^{12} mol yr^{-1} or 9.3×10^{9} kg yr^{-1}. This is 9.3 million tons Fe per year, or 10-fold than originally hypothesized (Martin, 1990). Considering the cost of large scale Fe fertilization and the very low C/Fe efficiency, it is evident that continuous large scale Fe fertilization is not economically an option to reduce the atmospheric CO_2 concentration. Moreover accountability of the exact deep ocean storage of CO_2 is very poor.

From an environmental point of view, large scale Fe fertilization may have potential side effects that could even more alter the efficiency of such experiments. The increases in algal growth, carbon export, and remineralisation upon iron addition, would upon carbon export and sub-surface respiration, reduce oxygen levels in subsurface waters. Long-term or large-scale fertilization could create conditions with zero oxygen concentration ('anoxic conditions") at intermediate depth (Fuhrman and Capone, 1991; Sarmiento and Orr, 1991). In the modern ocean, the greenhouse gases nitrous oxide (N_2O) and methane, (CH_4), which, per molecule, are 275 and 62 times more potent greenhouse gases than CO_2 over a 20-year time scale (IPCC, 2001) are produced in anoxic regions. Low oxygen levels and anoxic conditions upon iron fertilization are likely to promote production of nitrous oxide and methane. In terms of greenhouse gas warming potential for these given gases, the negative effects of N_2O and CH_4 release to the atmosphere would counteract and possibly outweigh the benefits of the atmospheric CO_2 sequestration from iron addition (Fuhrman and Capone, 1991; Jin and Gruber, 2003). Iron fertilization may also modify the marine production of important gases, such as dimethylsulphide (DMS), halocarbons, and alkyl nitrates. Changes in the marine source of these gases following iron fertilization could have feedbacks on atmospheric chemistry and global climate (Fuhrman and Capone, 1991; Lawrence, 2002). Iron has a wide range of observed and potential side effects. These effects require further study before any Large-scale scheme is undertaken.

Taking into account the low efficiency of Fe fertilization in exporting carbon to deeper layer of the ocean, the side effects of such approach, and the ambiguity in quantifying the net export preventing accountable CO_2 credits bookkeeping, other venues are advisable. Thus, other approaches for mitigation would have to be considered, such as

direct injections of CO_2 in the deep ocean (Brewer, 2004) or engineering CO_2 sinks on land (Smith, 2004). However, rather than mitigation by seeking speculative storage modes, it would appear more feasible and economical to reduce CO_2 emissions. The more obvious and by far most economical approach would be to improve fuel economy.

3. Recommendations for future research

Analytical techniques

During this thesis research, the DIC measurements have been performed by the coulometric technique. Although the accuracy and precision of this technique have been particularly satisfactory and allowed us to acquire a very large dataset for this parameter, some improvement could be made. Thus, the time necessary per sample is ~ 7 minutes (~ 25 minutes for 3 replicates) and the machine requires constant attention from the analyst. Although reducing the measurement time for each sample seems difficult for the coulometric technique, developments towards a more automated technique would be necessary and would facilitate the work of the analyst. Very recently, developments towards faster analytical technique for the measurement of DIC have been published (Kaltin et al., 2005). These authors present a technique based on continuous gas extraction of acidified seawater that is pumped through an extraction chamber at a constant flow rate and a determination with a NDIR gas analyzer. This method allows 12 measurements per hour with similar accuracy and precision as the coulometric technique. Moreover, our laboratory has recently acquired a new extractor unit, which allows the determination of alkalinity and dissolved inorganic carbon from the same sample in parallel. In the future, these development of new methods will massively help the scientific community to acquire comprehensive data set for the carbon dioxide system with improve spatial and temporal resolution.

CO_2 in coastal seas

The large dataset acquired for the carbon system and related parameters in the North Sea during this thesis together with numerous other investigations in the coastal seas worldwide have been a major advancement for the assessment of the CO_2 air-sea exchange in the coastal ocean. However at a global scale, data on the coastal CO_2 system are still sparse for the lower latitude regions. Moreover, future research should concentrate on constraining air-ice CO_2 fluxes, which are currently assumed to be zero (Borges, 2005). The evaluation of the inter-annual variability of air-water CO_2 fluxes in coastal ecosystems in relation to El Niño-Southern Oscillation (ENSO) or North Atlantic Oscillation (NAO) will surely constitute one of the major tasks in future research. This will require a tremendous effort as for the shiptime and sampling, in that sense, the development of faster techniques to measure the CO_2 system parameters will be very helpful. Finally, recent efforts to acquire datasets for the CO_2 system in the coastal seas have been complemented

by the development of models, which are able to account for the high variability for the CO_2 system in coastal environments, notably in the North Sea (Gypens et al., 2004, Elkalay et al., 2005). The future improvement of these models will furthermore allow to assess the temporal variability of the coastal CO_2 air-sea fluxes as well as to implement the CO_2 air-sea fluxes in Global Circulation Models.

Iron fertilization experiments

The fertilisation experiments have allowed the scientific community to verify the observations made in bottles incubation and have led to significant results concerning the drivers and internal mechanisms of the plankton physiology and the associated CO_2 uptake. Indeed, the results obtained for the C utilization and storage efficiencies will now be used in ecosystem simulation models for HNLC regions in the present and past oceans. In this thesis, evidence has been provided that quantification of overall carbon uptake is difficult (chapters 6 versus 7). Advancements in the tracer techniques and budgeting the carbon export are necessary before attempting any large scale Fe-enrichment experiment. This would rely on more intensive sampling. Similar problems exists with the addition, budgeting, and fate of the iron fertilizer as discussed elsewhere (de Baar et al., 2005).

References

Andersson, A.J. and Mackenzie, F.T., 2004. Shallow-water oceans: a source or sink of atmospheric CO_2. Frontiers in Ecology and the Environment, 2(7): 348-353.

Bakker, D.C.E., 2004. Storage of Carbon Dioxide by Greening the Oceans? In: C.B. Field and M.R. Raupach (Editors), The global carbon cycle: integrating human, climate and the natural world. SCOPE, ISSN, Washington, D.C, pp. 453-467.

Borges, A.V., 2005. Do we have enough pieces of the jigsaw to integrate CO_2 fluxes in the Coastal Ocean? Estuaries, 28(1): 3-27.

Boyd, P.W., Law, C.S., Wong, C.S., Nojiri, Y., Tsuda, A., Levasseur, M., Takeda, S., Rivkin, R., Harrison, P.J., Strzepek, R., Gower, J., McKay, R.M., Abraham, E.R., Arychuk, M., Barwell-Clarke, J., Crawford, W., Crawford, D., Hale, M., Harada, K., Johnson, K., Kiyosawa, H., Kudo, I., Marchetti, A., Miller, W., Needoba, J., Nishioka, J., Ogawa, H., Page, J., Robert, M., Saito, H., Sastri, A., Sherry, N., Soutar, T., Sutherland, N., Taira, Y., Whitney, F., Wong, S.-K.E. and Yoshimura, T., 2004. The decline and fate of an iron-induced subarctic phytoplankto bloom. Nature, 428: 549-553.

Brewer, P.G., 2004. Direct Injection of CO_2 in the Ocean. In: C.B. Field and M.R. Raupach (Editors), The global carbon cycle: integrating human, climate and the natural world. SCOPE, ISSN, Washington, D.C, pp. 469-478.

Brzezinski, M.A., Dickson, M.-L., Nelson, D.M. and Sambrotto, R., 2003. Ratios of Si, C and N uptake by microplankton in the Southern Ocean. Deep-Sea Research II, 50: 619-633.

Buesseler, K.O., Andrews, J.E., Pike, S.M. and Charette, M.A., 2004. The Effects of Iron Fertilization on Carbon Sequestration in the Southern Ocean. Science, 304: 414-417.

Cai, W.-J., Wang, Z.A. and Wang, Y., 2003. The role of marsh-dominated heterotrophic continental margins in transport of CO_2 between the atmosphere, the land-sea interface and the ocean. Geophysical Research Letters, 30(16): 1849- doi:10.1029/2003GL017633.

Caldeira, K. and Duffy, P.B., 2000. The role of the Southern Ocean in uptake and storage of anthropogenic carbon dioxide. Science, 287: 620-622.

Chen, C.-T.A., Andreev, A., Kim, K.-R. and Yamamoto, M., 2004a. Roles of Continental Shelves and Marginal Seas in the Biogeochemical Cycles of the North Pacific Ocean. Journal of Oceanography, 60: 17-44.

Chen, C.-T.A., 2004b. Exchange of Carbon in the Coastal Seas. In: C.B. Field and M.R. Raupach (Editors), The global carbon cycle: integrating human, climate and the natural world. SCOPE, ISSN, Washington, D.C, pp. 341-351.

Coale, K.H., Johnson, K.S., Chavez, F.P., Buesseler, K.O., Barber, R.T., Brzezinski, M.A., Cochlan, W.P., Millero, F.J., Falkowski, P.G., Bauer, J.E., Wanninkhof, R.H., Kudela, R.M., Altabet, M.A., Hales, B.E., Takahashi, T., Landry, M.R., Bidigare, R., Wang, X., Chase, Z., Strutton, P.G., Friederich, G.E., Gorbunov, M.Y., Lance, V.P., Hilting, A.K., Hiscock, M.R., Demarest, M., Hiscock, W.T., Sillivan, K.F., Tanner, S.J., Gordon, R.M., Hunter, C.N., Elrod, V.A., Fitzwater, S.E., Jones, J.L.,

Tozzi, S., Koblizek, M., Roberts, A.E., Herndon, J., Brewster, J., Ladizinski, N., Smith, G., Cooper, D., Timothy, D., Brown, S.L., Selph, K.E., Sheridan, C.C., Twining, B.S. and Johnson, Z.I., 2004. Southern Ocean Iron Enrichment Experiment: Carbon Cycling in High- and Low-Si Waters. Science, 304: 408-414.

De Baar, H.J.W., Boyd, P.W., Coale, K.H., Landry, M.R., Tsuda, A., Assmy, P., Bakker, D.C.E., Bozec, Y., Barber, R.T., Brzezinski, M.A., Buesseler, K.O., Boyé, M., Croot, P.L., Gervais, F., Gorbunov, M.Y., Harrison, P.J., Hiscock, W.T., Laan, P., Lancelot, C., Levasseur, M., Marchetti, A., Millero, F.J., Nishioka, J., Nojiri, Y., van Oijen, T., Riebesell, U., Rijkenberg, M.J.A., Saito, H., Takeda, S., Timmermans, K.R. and Veldhuis, M.J.W., 2005. Synthesis of 8 Iron Fertilization Experiments: from the Iron age in the Age of Enlightenment. Journal of Geophysical Research (Oceans), in press.

De Baar, H.J.W., Van Leeuwe, M.A., Sharek, R., Goeyens, L., Bakker, K.M.J. and Fritsche, P., 1997. Nutrient anomalies in *Fragilariopsis kerguelenis* blooms, iron deficiency and nitrate/phosphate ratio (A.C Redfield) in the Antarctic Ocean. Deep-Sea Research II, 44(1-2): 229-260.

Droop, M.R., 1973. Some thoughts on nutrient limitation in algae. Journal of Phycology, 9: 264-272.

Ducklow, H.W. and McCallister, S.L., 2005. The biogeochemistry of carbon dioxide in the coastal oceans. In: A.R. Robinson and K.H. Brink (Editors), The Sea. Harvard University Press, in press.

Edwards, R., Sedwick, P.N., Morgan, V., Boutron, C.F. and Hong, S., 1998. Iron ice cores from Law Dome, East Antarctica: implications for past deposition of aerosol iron. Annals of Glaciology, 27: 365-370.

Elkalay, K., Thomas, H., Bozec, Y., Borges, A.V., Schiettecatte, L.-S., Heerdink, R., Ruardij, P. and De Baar, H.J.W., 2005. Biogeochemical 1D ERSEM ecosystem model applied to recent carbon dioxide and nutrient data in the North Sea. Submitted to Journal of Marine systems.

Fanning, K.A., 1992. Nutrients provinces in the sea: concentration ratios, reaction ratios and ideal covariation. Journal of Geophysical Research, 97: 5693-5712.

Franck, V.M., Bruland, K.W., Hutchins, D.A. and Brzezinski, M.A., 2003. Iron and zinc effects on silicic acid and nitrate uptake kinetics in three high-nutrient, low chlorophyll (HNLC) regions. Marine Ecology Progress Series, 252: 15-33.

Frankignoulle, M. and Borges, A.V., 2001. European continental shelf as a significant sink for atmospheric carbon dioxide. Global Biogeochemical Cycles, 15(3): 569-576.

Fuhrman, J.A. and Capone, D.G., 1991. Possible biogeochemical consequences of ocean fertilization. Limnology and Oceanography, 36(8): 1951-1959.

Gazeau, F., Smith, S.V., Gentili, B., Frankignoulle, M. and Gattuso, J.-P., 2004. The European coastal zone: characterization and first assessment of ecosystem metabolism. Estuarine, Coastal and Shelf Science, 60: 673-694.

Gervais, F., Riebesell, U. and Gorbunov, M.Y., 2002. Changes in the size-fractionated primary productivity and chlorophyll a in response to iron fertilization in the southern Polar Frontal Zone. Limnology and Oceanography, 47(5): 1324-1335.

Gnanadesikan, A., Sarmiento, J.L. and Slater, R.D., 2003. Effects of patchy ocean fertilization on atmospheric carbon dioxide and biological production. Global Biogeochem. Cycles, 17(2): 1050, doi: 1029/2002GB001940.

Gypens, N., Lancelot, C. and Borges, A.V., 2004. Carbon dynamics and CO_2 air-sea exchanges in the eutrophied coastal waters of the Southern Bight of the North Sea: a modeling study. Biogeosciences, 1: 147-157.

Hedges, J.I., Baldock, J.A., Gelinas, Y., Lee, C., Peterson, M.L. and Wakeham, S.G., 2002. The biochemical and elemental compositions of marine plankton: A NMR perspective. Marine Chemistry, 78: 47-63.

IPCC, 2001. The scientific basis. In: J.T. Houghton et al. (Editors), Contribution of Working Group I to the Third Assessment Report of the Intergovernmental Panel on Climate Change. Cambridge University Press, New York, USA, pp. 881.

ICES, 1983. Flushing times of the North Sea. ICES Cooperative Research Report. 123: 159 pp.

Jin, X. and Gruber, N., 2003. Offsetting the radiative benefit of ocean iron fertilization by enhancing N_2O emissions. Geophysical Research Letters, 30(24): 2249.

Kaltin, S., Anderson, L.A., Olsson, K., Fransson, A. and Chierici, M., 2002. Uptake of atmopsheric carbon dioxide in the Barents Sea. Journal of Marine Systems, 38: 31-45.

Kaltin, S., Haraldsson, C. and Anderson, L.G., 2005. A rapid method for the determination of total dissolved inorganic carbon in seawater with high accuracy and precision. Marine Chemistry, in press.

Kempe, S., 1995. Coastal seas: a net source or sink of atmospheric carbon dioxide? LOICZ/R&S/95-1, vi + 27 pp., LOICZ, Texel, The Netherlands.

Kuss, J., Nagel, K. and Schneider, B., 2004. Evidence from the Baltic Sea for enhanced CO_2 air-sea transfer velocity. Tellus, 56B: 175-182.

Lawrence, M.G., 2002. Side effect of oceanic iron fertilization. Science, 297: 1993.

Martin, J.-M., 1990. Glacial to interglacial CO_2 change: the iron hypothesis. Paleoceanography, 5: 1-13.

Sabine, C.L., Feely, R.A., Gruber, N., Key, R.M., Lee, K., Bullister, J.L., Wanninkhof, R., Wong, C.S., Wallace, D.W.R., Tilbrook, B., Millero, F.J., Peng, T.-H., Kozyr, A., Ono, T. and Rios, A.F., 2004. The Oceanic Sink for Anthropogenic CO_2. Science, 305: 367-371.

Sarmiento, J.L. and Orr, J.C., 1991. Three-dimensional simulations of the impact of Southern Ocean nutrient depletion on atmopsheric CO_2 and ocean chemistry. Limnology and Oceanography, 36(8): 1928-1950.

Smith, P., 2004. Engineered Biological Sinks on Land. In: C.B. Field and M.R. Raupach (Editors), The global carbon cycle: integrating human, climate and the natural world. SCOPE, ISSN, Washington, D.C, pp. 479-491.

Takahashi, T., Broecker, W.S. and Langer, S., 1985. Redfield ratio based on chemical data from isopycnical surfaces. Journal of Geophysical Research, 90(C4): 6907-6924.

Takahashi, T., Sutherland, S.C., Sweeney, C., Poisson, A., Metzl, N., Tilbrook, B., Bates, N.R., Wanninkhof, R., Feely, R.A., Sabine, C.L., Olafsson, J. and Nojiri, Y., 2002.

Global sea –air CO_2 flux based on climatological surface ocean pCO_2, and seasonal biological and temperature effects. Deep-Sea Research II, 49: 1601-1622.

Takeda, S., 1998. Influence of iron availability on nutrient consumption ratio of diatoms in oceanic waters. Nature, 393: 774-777.

Thomas, H. and Schneider, B., 1999. The seasonal cycle of carbon dioxide in the Baltic Sea surface waters. Journal of Marine Systems, 22: 53-67.

Timmermans, K.R., van der Wagt, B. and De Baar, H.J.W., 2004. Growth rates, half-saturation constants, and silicate, nitrate, and phosphate depletion in relation to iron availability of four large, open-ocean diatoms from the Southern Ocean. Limnology and Oceanography, 49(6): 2141-2151.

Tsuda, A., Takeda, S., Saito, H., Nishioka, J., Nojiri, Y., Kudo, I., Kiyosawa, H., Shiomoto, A., Imai, K., Ono, T., Shimamoto, A., Tsumune, D., Yoshimura, T., Aono, T., Hinuma, A., Kinugasa, M., Suzuki, K., Sohrin, Y., Noiri, Y., Tani, H., Deguchi, Y., Tsurushima, N., Ogawa, H., Fukami, K., Kuma, K. and Saino, T., 2003. A mesoscale iron enrichment in the western subarctic Pacific induces a large centric diatom bloom. Science, 300: 959-961.

Tsunogai, S., Watanabe, S. and Sato, T., 1999. Is there a "continental shelf pump" for the absorption of atmospheric CO_2? Tellus, 51B: 701-712.

Walsh, J.J., 1991. Importance of continental margins in the marine biogeochemical cycling of carbon and nitrogen. Nature, 350: 53-55.

Yool, A. and Fasham, M.J.R., 2001. An examination of the "continental shelf pump" in an open ocean general circulation model. Global Biogeochemical Cycles, 15(4): 831-844.

Zhai, W., Dai, M., Cai, W.-J., Wang, Y. and Hong, H., 2005. The partial pressure of carbon dioxide and air-sea fluxes in the northern South China Sea in spring, summer and automn. Marine Chemistry, in press.

Samenvatting

Sinds 1960 is de wereldbevolking gegroeid van 3 miljard tot nu meer dan 6 miljard mensen. Het verbruik van fossiele brandstoffen (aardolie, aardgas, steenkool) is nog sneller gestegen van 2 Petagram koolstof per jaar in 1960 tot nu bijna 7 Petagram koolstof per jaar (1 Petagram C = PgC = 10^{15} gram C). De 6 miljard mensen omvatten een biomassa (alleen de koolstof=C) van 'slechts' ~0.056 Pg. Elke wereldburger verbrandt dus ruim 100 maal haar/zijn eigen lichaamsgewicht aan fossiele brandstoffen per jaar. Dit is een gemiddelde, bewoners van rijke westerse landen zoals Nederland verstoken per persoon veel meer dan medeburgers in arme derde wereld landen. De wereldeconomie is dus een vooral op fossiele brandstoffen gebaseerde economie. Dit heeft echter wel grote gevolgen voor de biosfeer van onze planeet. Sinds het begin van de Industriele Revolutie in 1780 is het gehalte CO_2 in de lucht toegenomen van 0.028 % tot nu 0.038 %, ofwel van 280 10^{-6} atm naar 380 10^{-6} atm. Omdat CO_2 een belangrijk broeikasgas is (naast waterdamp en andere spoorgassen) kan dit leiden tot opwarming van de aarde. In 2001 concludeerde het Intergovernmental Panel of Climate Change (www.ipcc.ch) dat de CO_2 toename de meest plausibele verklaring is voor gemeten stijging sinds ~1860 van de gemiddelde temperatuur (voor ~1860 waren er nog geen betrouwbare thermometer reeksen van de lucht). Overigens spelen andere spoorgassen (H_2O, CH_4, N_2O, CFK's), stofdeeltjes en vele processen ook een rol, maar niemand twijfelt eraan dat de doorgaande stijging van het CO_2 gehalte in de lucht grote gevolgen heeft of zal hebben voor het klimaat op aarde.

De gemeten jaarlijkse toename van CO_2 in de lucht blijkt overigens maar ~60% van de jaarlijkse emissies van fossiele brandstoffen. De overige ~40% verdwijnt in de zeeen en oceanen. De opname van CO_2 in zee gaat langs tenminste twee routes of 'pompen'. De 'fysische pomp' is omdat het stijgende CO_2 gehalte hoger is dan het CO_2 gehalte in zeewater, dus gaat er een stofstroom lopen vanuit de lucht in de zee. Deze lucht/zee gas-uitwisseling is alleen in het oppervlaktewater, maar in de winter koelt het water in koude poolzeeen zo sterk af dat het iets zwaarder wordt en naar de diepzee zinkt. Aldus wordt de extra fossiele brandstof CO_2 naar de diepzee gepompt. De andere route is door fotosynthese. Algen die groeien in het oppervlaktewater nemen CO_2 op dat wordt aangevuld vanuit de lucht. De algen worden verder opgenomen in de voedselketen en soms vallen brokjes organisch materiaal naar beneden in de diepzee. Aldus komt er organisch vastgelegd koolstof in de diepzee terecht, en dat wordt daar grotendeels weer omgezet door bacterien naar CO_2. Van begin tot eind neemt de biologische pomp dus CO_2 op uit de lucht die tenslotte wordt opgeslagen in de diepzee.

Opname van kooldioxide door de Noordzee

De Japanse collega professor Tsunogai kwam in 1999 met een hypothese voor een variant van de biologische pomp: de CO_2-pomp op het continentale plat. In kustzeeen is vaak een onderstroom van oceaanwater dat in en dan weer uit de kustzee stroomt. Ondertussen zorgt de biologische pomp in het oppervlaktewater van die kustzee dat er steeds meer CO_2 wordt toegevoegd aan die onderstroom. Als gevolg bevat de uitgaande onderstroom meer CO_2 dan de ingaande, en is er een netto transport van CO_2, vanuit de lucht via algen en oppervlaktewater van de kustzee naar de diepe wateren van een naastgelegen oceaan. Promovendus Yann Bozec heeft samen met projectleider Helmut Thomas en collega Khalid Elkalay en vele anderen deze hypothese getoetst in de Noordzee. Van alle kustzeeen ter wereld is de Noordzee, temidden van ontwikkelde landen, de best bestudeerde kustzee ter wereld. Stromingen, voedingsstoffen stikstof (N) en fosfaat (P), algengroei waren in het algemeen goed bekend. Er loopt ook een onderstroom die vanuit de Atlantische Oceaan ten oosten van Schotland binnenkomt en na een rondreis langs de Noorse kust in een diepe geul weer terugstroomt in de diepe Noord Atlantische Oceaan. Echter over het CO_2 gehalte en transport in de Noordzee was vrijwel niets bekend. Vier expedities van telkens 1 maand werden uitgevoerd in 4 jaargetijden (vrij naar Vivaldi), namelijk augustus/september 2001, november 2001, februari/maart 2002 en tenslotte mei 2002. Per expeditie met eigen schip PELAGIA werd op 97 locaties ('stations') een verticaal profiel gemeten over een diepte varierend van 25-50 meter in de zuidelijke Noordzee tot 100-400 meter in de noordelijke Noordzee. Per station was het aantal meetpunten 12 op de diepe stations, wat minder in de ondiepe locaties. Terwijl het schip van station naar station voer werden onderweg tevens ~22,000 metingen uitgevoerd van het CO_2 gehalte in het oppervlaktewater. Daarnaast werden ook metingen van voedingsstoffen, algen biomassa enzovoorts uitgevoerd. Aldus werd verreweg de meest uitgebreide en nauwkeurige dataset ooit gerealiseerd voor een kustzee.

De meetresultaten stelden ons in staat te berekenen hoeveel CO_2 per jaar door deze continentaal-plat-pomp wordt opgenomen uit de lucht en tenslotte opgeslagen in de diepe Noord Atlantische Oceaan. Dit bleek 1.4 mol CO_2 per vierkante meter per jaar. Dit is veel hoger dan de jaarlijkse opname in de open oceaan. De reden is dat de fotosynthese in de Noordzee veel sterker is, want de daarvoor benodigede voedingsstoffen (N, P) zijn ruim beschikbaar. Integratie over de gehele Noordzee levert een jaarlijkse opname van fossiele brandstof CO_2 van 8.5×10^{12} gram C per jaar. Wanneer we dit zouden extrapoleren naar alle kustzeeen van de wereld (waar de Noordzee 2% van uitmaakt) dan zouden alle kustzeeen een opname van fossiele brandstof CO_2 hebben van 0.4 PgC per jaar. Dit zou ~20% zijn van de totale CO_2 opname door de wereldzeeen. Kustzeeen die samen maar 7% van het totale zee oppervlak zijn, nemen dus zeer efficient CO2 op; dit door ruime beschikbaarheid van voedingsstoffen voor fotosynthese zodat veel meer CO_2 wordt

vastgelegd dan in oppervlaktewater van de open oceaan waar vaak juist een gebrek aan voedingsstoffen is.

Het geleverde bewijs van de CO_2-pomp op het continentale plat, door interactie van biologische fotosynthese met chemische stoffen CO_2, N en P, en fysische onderstromen, was een doorbraak die in 2004 in het beroemde tijdschrift Science werd gepubliceerd. Dit leidde tot zeer veel aandacht, maar ook debat over de extrapolatie van de Noordzee (8.5×10^{12} gram C per jaar) naar alle kustzeeen van de wereld (0.4 Pg C per jaar). Echter recent zijn meer, zij het kleinere, studies van andere kustzeeen beschikbaar gekomen, en die leveren steeds sterker aanwijzingen dat alle kustzeeen samen inderdaad een flinke opname van fossiele brandstof CO_2 realiseren.

Effect van ijzer bemesting op CO_2 huishouding van de Antarctische Oceaan

Naast het CO_2 onderzoek in de Noordzee, is het proefschrift ook gericht op het testen van de ijzer hypothese voor de Antarctische Oceaan. Door gebrek aan opgelost ijzer in zeewater is de fotosynthese door microscopische algen niet optimaal in de Antarctische Oceaan. Dit enorme gebied, ~20% van het zee-oppervlak ofwel ~14% van het aardoppervlak heeft ondanks zijn Hoge concentraties Nutrienten fosfaat, nitraat en silicaat maar zeer Laag Chorofyl (de groene kleur van algen) in het oppervlaktewater. Deze "HNLC condities" zijn ook bekend als de Antarctische Paradox: hoe kan het dat er zo weinig algen groeien ondanks ruime beschikbaarheid van voedings-stoffen? In fotosynthese wordt met zonlicht (ingevangen door het groene chlorofyl) het opgeloste CO_2 vastgelegd in biomassa en aangevuld vanuit de lucht, door het ijzer-gebrek is deze biologische pomp voor CO_2 opname vanuit de lucht dus ook niet optimaal.

Tijdens een experiment EisenEx in november 2000 werd een gebied van ruim 50 vierkante kilometer driemaal verrijkt met opgelost ijzer vanaf de ijsbreker Polarstern. Tijdens de eerste ijzer toevoeging werd ook een kleine hoeveelheid sulfur-hexafluoride (SF_6) toegevoegd. Dit molecuul is zelfs in zeer lage concentraties nog meetbaar, en dient om de ijzer verrijkte plek steeds weer terug te kunnen vinden, en in kaart te brengen. De bedoeling was een groene oase van chlorofyl te realiseren in een verder diepblauwe oceaan. Het effect van toenemende fotosynthese en daarmee gepaard gaande extra opname van voedingsstoffen fosfaat, nitraat en silicaat, en kooldioxide, werd gedurende drie weken gevolgd. Reeds vijf dagen na de eerste ijzer-verrijking werd een afname van het CO_2 gehalte gemeten. Vervolgens werd door zware stormen de met ijzer verrijkte plek sterk verdund, zowel met onderliggend ijzer-arm water, als met ijzer-arme oppervlaktewateren van rondom. Het experiment en ons schip met opvarenden bevonden zich zonder meer in de 'roaring forties' die berucht zijn om de intensieve stormen. Aldus was na drie zware stormen de plek tot een diepte van ~100 meter doorgemengd, en in oppervlakte toegenomen van ~50 tot ~950 vierkante kilometer. Door de grote verdunning met onderliggend en

omringend water was het te meten effect van chlorofyl toename en afname van voedingsstoffen en kooldioxide navenant sterk verdund. Bovendien, door de diepe menging tot ruim 100 meter diepte, zitten de algen vaak in dieper, donker, water en krijgen zo onvoldoende zonlicht voor fotosynthese en CO_2 opname. Niettemin werd een maximale afname van 23 10^{-6} atm gemeten in het oppervlaktewater ten opzichte van de CO_2 druk in de lucht. Aldus ontstond er ook een bescheiden instroom van CO_2 vanuit de lucht in de zee. Het totale opgeloste CO_2 gehalte nam af met 15 millimolen per kubieke meter zeewater, en dit werd vergeleken met de gemeten afname van voedingstoffen fosfaat en nitraat in het zeewater. Tevens kon de verhouding worden berekend waarin de algen deze essentiele stoffen opnemen. Dit was C/P=82 en C/N=5.9 in vergelijking met klassieke literatuur waardes van C/P=106 en C/N=6.6 volgens de beroemde Redfield-verhoudingen. Een voorlopige budget berekening voor het gehele experiment kwam uit op een totale CO_2 opname van 13 duizend ton koolstof. De enorme verdunning van de oase met onderliggend water en omliggend oppervlaktewater is de oorzaak van grote onzekerheid in dit totale CO_2 budget. Daarom werd vervolgens een meer accurate schatting van deze menging en verdunning gemaakt. Dit is mogelijk op grond van de gemeten SF_6 gehaltes, die door de menging en verdunning steeds lager werden gedurende de drie weken van het experiment. Op grond van deze SF_6 afname kon de verdunning en menging worden verrekend in de CO_2 metingen. Dit leidde tot een viermaal lagere schatting van de CO_2 opname van 'slechts' 2840 ton koolstof gedurende de eerste 18 dagen van het experiment. De 4-voudige discrepantie met de eerdere schatting geeft aan hoe moeilijk het is om budgets te maken van een stormachtige oase in de Antarctische Oceaan.

Niettemin zijn beide schattingen van totale CO_2 opname nogal laag vergeleken met de originele ijzer hypothese door John Martin (1990). Dit heeft consequenties voor zowel het verleden als de toekomst. In het verleden blijken de lage CO_2 gehaltes in de lucht tijdens ijstijden samen te vallen met hogere gehaltes ijzer-rijk stof in het Antarctisch gebied. Dit werd gezien als aanwijzing dat een hogere ijzer toevoeging met ingewaaide stof zou hebben geleid tot meer fotosynthese van algen, dus een sterkere biologische pomp voor opname van broeikasgas CO_2 uit de lucht, et voila een ijstijd. De resultaten van ons experiment EisenEx (2000) en andere experimenten (SOIREE, 1999; SOFeX, 2002) in de Antarctische Oceaan zijn echter niet gunstig: per toegevoegde hoeveelheid ijzer wordt veel minder CO_2 opgenomen dan eerst was gedacht. Ook voor de toekomst was het voorstel gedaan om de Antarctische Oceaan met ijzer te bemesten, and zo het probleem op te lossen van het toenemende broeikasgas CO_2 door verbranding van fossiele brandstoffen. Echter de experimenten (EisenEx, SOIREE, SOFeX) laten zien dat per toegevoegde hoeveelheid ijzer veel minder CO_2 wordt opgenomen dan men had gedacht. Samenvattend blijkt ijzer dus wel degelijk de essentiele missende stof voor algengroei in de Antarctische Oceaan, maar opheffing van deze ijzer-armoede heeft weinig effect op het gehalte van broeikasgas CO_2 in de lucht.

Acknowledgements

This thesis is the outcome of four years of work carried out in my "cosy" office at the Royal Netherlands Institute for Sea Research and on the rough North Sea and Southern Ocean. During these 4 years spent away from home, I am grateful to a lot of people who have made this period of my life an invaluable experience, both from a professional and personal perspective.

My first word of thanks must go to my promotor Hein and supervisor Helmuth. Surely, when I think back to when I met these two people I could not have known how important they would become during the following 4 years. I met Hein in a hotel somewhere in downtown Capetown (SA) during the days preceding a long cruise. During the 6 weeks spent in the lab together on the Southern Ocean and the following 4 years, Hein has always been an invaluable source of knowledge on the different aspects of chemical oceanography and in providing motivation and help to ensure the completion of the different manuscripts within this thesis. Moreover, I have always enjoyed the friendly relationship and the great laughs we have shared during the past 4 years.

Helmuth and I met during one of the numerous cold and windy nights at the Potvis on Texel Island (North Holland). That was the beginning of a long collaboration and of many hours spent working together at the NIOZ, on the Research Vessel *Pelagia*, at Dalhousie University, during international meetings or defending the honour of the institute on the football pitch! I have been very fortunate to have a supervisor who always had the time to teach me all the details of the measurement of DIC and pCO_2 and to answer all my questions about the CO_2 system in seawater. Furthermore, all the chapters of this thesis are the result of long discussions with him and have all been greatly improved thanks to his detailed comments. I am sure this collaboration will continue in the future. I am grateful to Helmuth not only for helping me as a supervisor, but also for welcoming me at his home when I arrived during the cold winter on Texel or in Canada, and to Anna for often cooking some delicious meals which helped us to carry on working.

I am furthermore thankful to all the people from the CO_2 group at NIOZ, Michel Stoll, Patrick Laan, Elen Bowlens and Josje Snoek for helping me with the CO_2 instruments and software. I also thank Karel Bakker, Jan Van Ooijen and Evaline van Weerlee for performing the nutrient measurements during our cruises and Santiago Gonzalez for the DOC measurement. The CO_2 scientific community has been an exciting environment to work in during the past 4 years. I have benefited from and am thankful for the numerous collaborations of the NIOZ with other international institutes. I would particularly like to thank Dorothea Bakker for helping me a lot during my first cruise and for correcting my manuscripts. I also would like to thank Alberto Borges for his rigorous comments and for sharing his knowledge of the CO_2 chemistry in seawater.

For my research, I spent a couple of months at sea and I want to thank the crew of the research vessels *Pelagia* and *Polarstern* who have been of great assistance and support during the cruises. Thanks go also to the people who contributed to have such a nice atmosphere on the ship but particularly to Laure-Sophie, Helmuth, Alberto, Dorothea, Marie, Micha, and Santos.

During the past four years, I shared unforgettable moments with many friends on Texel and I am eternally grateful to them. Thanks go to all the players of the numerous football teams with whom I shared the defeats and glorious victory on Texel or on the mainland: "the Texelse Boys", "Texel 94", "ZDH", and of course the "Galacticos" from the "indoor NIOZ football team": the great keepers Wim and Cor, the rocks at the back "captain-chief" and Helmuth, the key all-round midfielders "Monsieur Scholesy", "Santi", Khalid and "Gattuso", and the scorers Leon, Bert, "Russky" and Beni. Warm thanks to Anne-Claire, Phil, Jerome, Isabel, Denis, Furu, Teresa, Beni, Luis, Mirja, Jasper, Ines, Micha, Khalid, Pedro, the 2 Thomas, Yvo, Sharyne, Neven, Kaï, Sanne, for the great atmosphere at NIOZ and of course for all the fiestas, barbecue, "Sunday dinners", "apero", "potvis football games", (long) coffee breaks etc… I would need much more pages to thank you all individually but I hope you all know how important you are for me. Special thanks go to "Bixente" for celebrating all the big wins of the French teams especially against the "rosbeef" of "Sholesy" and to Furu for supporting the terrible housemate I am (I see you smiling Phil!) and my numerous visits in her office. I would not be writing the final lines of my thesis if I would not have had the company of my two dear friends Phil and Anne-Claire. Even in french I could not express how important both of you are for me and how much I enjoy spending my time with you two. Simply thank you for being such great friends.

Quelques mots de remerciements en français…

Durant ces 4 années, j'ai eu l'opportunité de beaucoup voyager et je remercie Marie-Pierre et Antoine pour m'avoir souvent hébergé avant ou après mes longs voyages. Malgré tout, un breton a, évidemment, besoin de rentrer souvent au pays et j'ai par conséquent souvent emprunte les routes du Nord en direction de « la maison même! ». Je tiens donc à remercier la famille Baudoux pour m'avoir hébergé à Amiens dans la bonne humeur, pour la délicieuse cuisine picarde et les âpres discussions footballistiques qui me faisaient sentir proche de la maison.

Je remercie mes «potos bretons » Loïc, Mathieu, Olivier, Marco Fred, Morvan, souvent exilés, qui même loin m'ont toujours soutenus et qui font que c'est toujours un moment spécial de se retrouver en Bretagne avec les bretons fidèles ou d'adoptions, Elen et Arnaud, Julie, Mélanie, la famille Perrot, Eva, Marie etc…

Je tiens très sincèrement à remercier mes parents et ma famille pour m'avoir toujours encouragé durant mes longues années d'études et être toujours à mes cotés. Même si j'ai essayé de vous rendre visite aussi souvent que possible je sais que les bons moments passés ensemble ces dernières années ont souvent été trop cours mais sachez que j'ai toujours énormément pensé à vous. Merci à tous pour votre amour.

Je veux très spécialement remercier Carine, pour son amour et les merveilleux moments passés à mes cotés, pour avoir toujours été la dans les moments difficiles et supporté mes (nombreux) sauts d'humeurs. Tu as une énorme place dans mon cœur ma choupie.

Bibliography of the author (9/8//2005)

- Publications in peer-reviewed journals [8]:

Bozec Y., D.C.E. Bakker, C. Hartman, H. Thomas, R. Bellerby, U. Riebesell, H.J.W. de Baar, and A.J. Watson (2005). The CO_2 system in a Redfield context during an iron enrichment experiment in the Southern Ocean. *Marine Chemistry, 95, 89-105.*

Bozec Y., H. Thomas, K. Elkalay and H.J.W. de Baar (2005). The continental shelf pump for CO_2 in the North Sea-evidence from summer observation. *Marine Chemistry, 93, 131-147.*

De Baar H.J.W., P. Boyd, K. Coale, A. Tsuda, D.C.E. Bakker, Y. Bozec, M. Brzezinski, K. Buesseler, M. Boyé, P. Croot, F. Gervais, M. Gorbunov, P. Harrison, W. Hiscock, P. Laan, C. Lancelot, M. Levasseur, A. Marchetti, J. Nishioka, Y. Nojiri, T. van Oijen, U. Riebesell, S. Takeda, K. Timmermans and M. Veldhuis (2005). Synthesis of Eight in-situ Iron Fertilization in High Nutrient Low Chlorophyll waters Confirms the Control by Wind Mixed Layer Depth of Phytoplankton Blooms. *Journal of Geophysical Research, in press.*

Bakker D.C.E, Y. Bozec, P.D. Nightingale, L. Goldson, M.-J. Messias, H.J.W. de Baar, M. Liddicoat, I. Skjelvan, V. Strass, and A.J. Watson (2005). Storms influence inorganic carbon uptake upon iron enrichment experiment in the Southern Ocean. *Deep Sea Research Part I, 52, 1001-1019.*

Thomas H., Y. Bozec, H.J.W. de Baar, K. Elkalay, M. Frankignoulle, L.-S. Schiettecatte & A. V. Borges (2005). The Carbon budget of the North Sea. *Biogeosciences, 2, 82-96.*

Thomas H., Y. Bozec, K. Elkalay, and H.J.W. de Baar (2004). Enhanced open ocean storage of CO_2 from Shelf Sea pumping. *Science, 304, 1005-1008.*

Thomas H., Y. Bozec, K. Elkalay, and H.J.W. de Baar (2004). Reply to comments by Cai, W.-J. and Dai, M., on "Enhanced open ocean storage of CO_2 from Shelf Sea pumping" by H.Thomas, Y. Bozec, K. Elkalay, and H.J.W. de Baar, 2004. *Science, 406, 1477d.*

Guieu C., Y. Bozec, S. Blain, C. Ridame, G. Sarthou, and N. Leblond (2002). Impact of high Saharan dust inputs on dissolved iron concentrations in the Mediterranean Sea. *Geophysical Research Letter, 29(19), 1911-1914.*

- In revision or submitted in peer-reviewed journals [3]:

Bozec, Y., H. Thomas, L.-S. Schiettecatte, A.V. Borges, K. Elkalay and H.J.W. de Baar (2005). Processes controlling the seasonal variations of dissolved inorganic carbon in the North Sea. *In revision for Limnology and Oceanography.*

Thomas, H., Y. Bozec, K. Elkalay, H.J.W. de Baar, A.V. Borges, L.-S. Schiettecatte (2005). Variability of the surface water partial pressure of CO_2 in the North Sea. *Submitted to Biogeosciences.*

Elkalay, K., H. Thomas, Y. Bozec, A. V. Borges, , R. Heerdink, P. Ruardij, and H.J.W. de Baar (2005). Biogeochemical 1D ERSEM ecosystem model applied to recent carbon dioxide and nutrient data in the North Sea. *Submitted to Journal of Marine systems.*

- Book Chapters [1]:

Thomas, H., Y. Bozec, H.J.W. de Baar, K. Elkalay, M. Frankignoulle, W. Kühn, H.J. Lenhart, A. Moll, J. Pätsch, G. Radach, L.-S. Schiettecatte, and A. Borges (2005). Carbon and nutrient budgets of the North Sea. In: L. Atkinson, K.-K. Liu, R. Quinones, and L. Talaue-McManus, (eds) (2005). Carbon and nutrient fluxes in global continental margins, Springer, New York, *in press*.

Curriculum Vitae

Yann Bozec was born on the 27th December 1977 in Morlaix (Bretagne), north-west France. He was educated at the "Lycée Tristan Corbière" where he passed his Baccalauréat in 1995 before studying at the University of Bretagne Occidentale, in Brest. After 2 years of general education in science, he started to specialize in chemistry and received his Master degree in analytical and marine Chemistry with high honours in 2000. His graduation research was carried out at the "Institut Universitaire Européen de la Mer" in Plouzané under the supervision of Prof. Paul Tréguer, Prof. Stéphane Blain and Dr. Cécile Guieu, focusing on the "Measurement of dissolved iron by FIA-CL: Results from the PROSOPE cruise". In 2001, he began his PhD research at the Royal Netherlands Institute of Sea Research within the CARUSO and CANOBA programs. At the time of writing, he is preparing his "promotie" in his beautiful Bretagne and, in November 2005, will begin a post-doctoral position at the SCRIPPS institution of Oceanography in San Diego in the research group of Prof. Ralf Keeling.